

THE UNIVERSITY of EDINBURGH

This thesis has been submitted in fulfilment of the requirements for a Doctor of Philosophy at the University of Edinburgh.

Please note the following terms and conditions of use:

- This work is protected by copyright and other intellectual property rights, which are retained by the thesis author unless otherwise stated.
- A copy can be downloaded for personal, non-commercial research or study without prior permission or charge.
- This thesis cannot be reproduced or quoted extensively without first obtaining permission in writing from the author.
- The content must not be changed in any way or sold commercially in any format or medium without the formal permission of the author.
- When referring to this work, full bibliographic details, including the author, title, awarding institution and date of the thesis, must be given.

Net Zero electricity and hydrogen production with post-combustion CO_2 capture and storage

Daniel Thomas Mullen



THE UNIVERSITY *of* EDINBURGH

Thesis submitted for the degree of
Doctor of Philosophy

The University of Edinburgh
School of Engineering

Year of Submission 2024

Declaration

I declare that the thesis has been composed by myself and that the work has not been submitted for any other degree or professional qualification. I confirm that the work submitted is my own and that I am the first author in all the publications that comprise this thesis's five main chapters. For all publications, I have been in charge of or contributed to the Conceptualisation, Methodology, Software, Validation, Formal analysis, Investigation, Data Curation, Writing - Original Draft, Writing - Review & Editing, and Visualization. I confirm that appropriate credit has been given within this thesis where reference has been made to the work of others.

The work presented in Chapter 3 was previously published in the International Journal of Greenhouse Gas Control as "*On the cost of zero carbon hydrogen: A techno-economic analysis of steam methane reforming with carbon capture and storage*" by **Daniel Mullen**, Laura Herraiz, Jon Gibbins and Mathieu Lucquiaud. This study was conceived by all of the authors. I carried out Conceptualisation, Methodology, Software, Validation, Formal analysis, Investigation, Data Curation, Writing - Original Draft, Writing - Review & Editing, and Visualization.

The work presented in Chapter 4 was previously published in Energy Reports as "*On the cost of zero carbon electricity: A techno-economic analysis of combined cycle gas turbines with post-combustion CO_2 capture*" by **Daniel Mullen** and Mathieu Lucquiaud. This study was conceived by all of the authors. I carried out Conceptualisation, Methodology, Software, Validation, Formal analysis, Investigation, Data Curation, Writing - Original Draft, Writing - Review & Editing, and Visualization.

The work presented in Chapter 5 was previously published in to Frontiers in Energy Research as "*Thermodynamic Integration in Combined Fuel and Power (CFP) Plants Producing Low Carbon Hydrogen & Power with CCUS*" by **Daniel Mullen** and Mathieu Lucquiaud. This study was conceived by all of the authors. I carried out Conceptualisation, Methodology, Software, Validation, Formal analysis, Investigation, Data Curation, Writing - Original Draft, Writing - Review & Editing, and Visualization.

The work presented in Chapter 6 was previously published in Industrial & Engineering Chemistry Research as "*Monoethanolamine (MEA) degradation rates in post-combustion CO_2 capture plants with the capture of 100% of the added CO_2*" by **Daniel Mullen**, Lucas Braakhuis,

Hanna Katariina Knuutila, Jon Gibbins and Mathieu Lucquiaud. This study was conceived by all of the authors. I carried Conceptualisation, Methodology, Software, Validation, Formal analysis, Investigation, Data Curation, Writing - Original Draft, Writing - Review & Editing, and Visualization.

The work presented in Chapter 7 was previously published in Proceedings of the 17th Greenhouse Gas Control Technologies Conference as "*Flexibly Operated Capture Using Solvent Storage (FOCUSS) – Results*" by **Daniel Mullen**, Xiaomian Baxter, James Bowers, Harry Ellicott, Tom Ilett, Sam Atkinson, Mohamed Pourkashanian, Muhammad Akram, Abdulaziz Gheit, Mathieu Lucquiaud and Jonathan Gibbins. This study was conceived by all of the authors. I carried out Conceptualisation, Methodology, Software, Validation, Formal analysis, Investigation, Data Curation, Writing - Original Draft, Writing - Review & Editing, and Visualization.

Daniel Thomas Mullen

Abstract

Carbon Capture and Storage (CCS) systems are seen as a key technology for enabling the global imperative of arresting anthropogenic climate change. For this goal to be achieved, the global annual net change in atmospheric CO_2 must be reduced to zero, or below, within the next few decades. For CCS to be compatible with this target, residual, or uncaptured, CO_2 emissions from the process they decarbonise, and any downstream or upstream greenhouse gas (GHG) emissions must also be reduced to zero, or the equivalent amount of CO_2 recaptured within an appropriate timeframe.

Historically, CO_2 capture fractions from CCS systems of 90% have been targeted, citing exponentially increasing costs and energy demands as the barrier to achieving higher removal rates. This remaining 10%, or indeed 5%, as 95% CO_2 capture fractions have gained traction in recent years, is clearly incompatible with the goal of zero net change in atmospheric CO_2 (or net zero), let alone any aspirations for net CO_2 removal as is required by a growing number of climate models.

This thesis uses state of the art knowledge to investigate the thermodynamic, process and economic requirements to efficiently achieve ultra-high CO_2 capture fractions in post combustion capture (PCC) plants using a monoethanolamine (MEA) solvent. This revels the potential for PCC plants to operate at a CO_2 capture fraction resulting in no net addition of CO_2 to the atmosphere, termed 100% fossil CO_2 capture. This is completed by taking two standard and one novel, which was optimised as part of this work, energy conversion processes that will utilise CCS; combined cycle gas turbines (CCGT), for flexible and dispatchable power production, steam methane reforming (SMR), producing hydrogen as an option for fuel switching applications and the newly termed combined fuel and power (CFP) which combines the CCGT and SMR processes. Detailed process and economic models were developed that indicate that, if designed appropriately, the CCGT, SMR and CFP processes can achieve 100% fossil CO_2 capture with minimal process modification, commercially available technology and an approximately linear increase in production costs relative to CO_2 capture fraction.

For a CCGT, an additional 0.5%-point decrease in thermal efficiency (Lower Heating Value (LHV)) results from transitioning from 95% gross to 100% fossil CO_2 capture with an associated 4% increase in capital expenditure (CAPEX), while for the SMR a 1.9%-point decrease in thermal efficiency (Higher Heating Value (HHV)) and 5% increase in CAPEX is reported. For the CFP a 0.5% decrease and 3% increase for thermal efficiency (2nd Law) and

CAPEX is predicted, however a 4.4% increase in 2nd law thermal efficiency and a 17.3% decrease in CAPEX relative to operating the CCGT and SMR processes separately is seen. For the CCGT and SMR processes, the cost of recapturing upstream and downstream emissions using direct air capture (DAC) is also investigated. This results in a 9% (SMR) and 29% (CCGT) increase in production cost, for a median cost of DAC of 300 £/tCO_2 and global average natural gas supply chain emission rate of 1.5%, however high degrees of sensitivity are observed for both these variables.

The process conditions considered necessary to efficiently achieve 100% fossil CO_2 capture, namely increased solvent regeneration pressures (210 – 275KPa vs 170 – 190KPa), and therefore temperature (125 - 135°C vs 115 – 125°C), and increased exposure times to flue gases are thought to increase the degradation rate of CO_2 capture solvents. This is investigated through process modelling and the application of a newly developed monoethanolamine (MEA) degradation framework. This predicts that degradation rates increase by 24−138% when achieving 100% fossil CO_2 capture relative to a 95% gross CO_2 capture fraction, with absorber intercooling and minimising desorber sump residence times emerging as key plant parameters to minimise degradation. An economic assessment concludes that this increase would result in an increased operational expenditure (OPEX) of between 0.02−0.38 £/tCO_2.

Dynamic operations of CCS plants, particularly start up and shutdown (SUSD) events, pose a key operational challenge, particularly aiming to achieve ultra-high rates of CO_2 capture (+99%), as a constant flow of appropriately lean solvent is critical. Due to thermal inertia in the desorber, and indeed the availability of thermal energy during plant start up, it may not always be possible to produce lean solvent at the rate or quality required to enable high CO_2 capture fractions under dynamic operation. Through pilot scale test campaigns, start-up CO_2 capture fractions of greater than +97% are demonstrated though simulated start-up sequences when using an enhanced solvent storage scheme. While the procurement of operational data from a commercial CCGT demonstrates the availability of previously waste steam from the CCGT SUSD sequences that can be utilised to accelerated PCC start up times, reducing the required rich solvent capacity and additional solvent inventory from 350% of the base solvent inventory to just 50%, increasing the economic viability of CO_2 capture during SUSD.

The analysis presented in this thesis provides critical and novel evidence that will advise designers on the process and economic considerations required to efficiently develop projects that achieve net zero compatible CO_2 capture fractions in PCC plants.

Lay Summary

Carbon Capture, Utilisation, and Storage (CCUS), the permanent storage or reuse of CO_2 produced as part of industrial processes, is likely to be a key technology if we are to rapidly decarbonise our economy and avoid the worst effects of climate change.

Post-combustion Capture (PCC) separates the CO_2 from the downstream exhaust gases of an industrial process. It is a proven, well-tested technology that has been in operation for decades. Traditionally, PCC operates by mixing CO_2-rich exhaust gases (~ 2 – 25% CO_2) with an amine (ammonia derivative) mixed with water to form a CO_2 capture solvent in a packed "absorber" column. The amine in the solvent chemically bonds with the CO_2, removing the CO_2 from the flue gas, which is then released into the atmosphere. The bonded CO_2 is then heated to release the captured CO_2, which is then cleaned, compressed and transported for storage. The solvent then returns to the absorber to capture CO_2 again (this is illustrated in Figure 1 (A)).

Historically, CCUS plants have been designed to capture 90% of the CO_2 entering the absorber, but this 90% does not represent an upper limit on how much CO_2 can be captured. In a net zero economy, they will need to operate with zero greenhouse gas emissions. This thesis investigates how this 90% rate can be increased up to the point where no CO_2 produced in the plant is emitted to the atmosphere, i.e., 100% fossil CO_2 capture, an aspiration that, until recently, was considered economically infeasible.

I do this by taking two existing and critical energy-conversion processes, and one novel process, that will likely use CCUS to decarbonise: a natural gas-fired combined cycle gas turbine (CCGT) power plant for electricity; a steam methane reformer (SMR) for hydrogen production and the newly termed combined fuel and power (CFP) which combines the CCGT and SMR processes. Via rigorous design optimisation, modelling and pilot plant tests, I establish the process and economic conditions required to achieve ultra-high CO_2 capture (+99%) fractions using open-art and commercially available technology, demonstrating, for the first time, that when appropriately designed, minimal additional energy and operational/capital expenditure is required. Thus, I reach the novel conclusion that the capture of 100% of the CO_2 produced in the process can be made financially viable using the same financial mechanisms already in place to support CCUS.

This work goes one step further by estimating the lifecycle greenhouse gas emissions associated with the natural gas supply chain, CO_2 transport and storage network, and

construction/decommissioning for the CCGT and SMR processes. We propose and cost the recapture of these emissions using permanent negative emissions technologies, thus ensuring truly net-zero operation, this is illustrated in Figure 1 (B) where all the CO_2 generated, and the CO_2 equivalent of the remaining greenhouse gases, is returned to the subsurface.

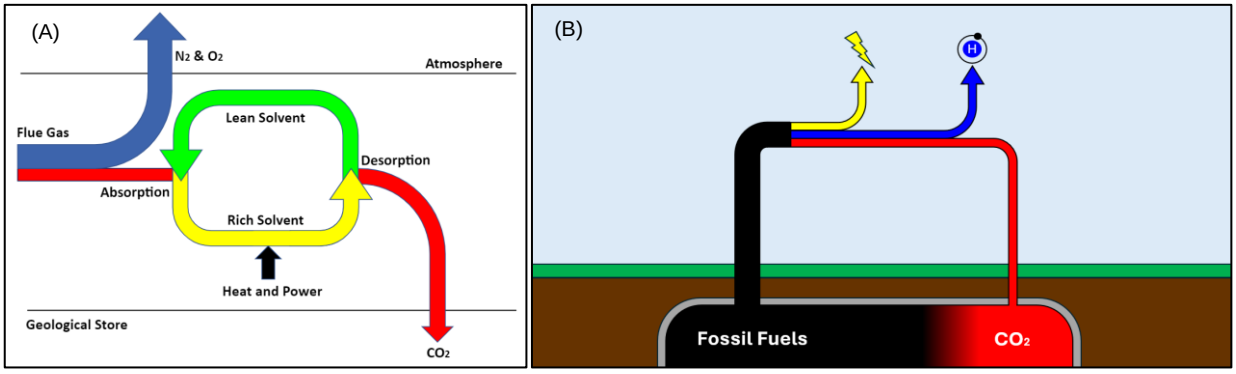


Figure 1: (A) Illustration of a post combustion CO_2 capture process using an amine solvent (B) Net Zero production of Electricity and Hydrogen with CCS by ensuring that all fossil Carbon extracted from the subsurface is returned for permanent storage.

Published Works

Journal articles:

1. **Mullen, D**., Braakhuis, L., Katariina Knuutila, H., Gibbins, J., & Lucquiaud, M. (2024). Monoethanolamine (MEA) degradation rates in post-combustion capture plants with 100% fossil CO2 capture. Ind. Eng. Chem. Res. 2024, 63, 31, 13677–13691.10.1021/acs.iecr.4c01525

2. **Mullen, D.,** & Lucquiaud, M. (2024). On the cost of zero carbon electricity: A techno-economic analysis of combined cycle gas turbines with post-combustion CO_2 capture. Energy Reports, 11, 5104-5124. 10.1016/j.egyr.2024.04.067.

3. **Mullen, D**., Herraiz Palomino, L., Gibbins, J., & Lucquiaud, M. (2023). On the cost of Zero Carbon Hydrogen: A Techno-Economic Analysis of Steam Methane Reforming with Carbon Capture and Storage. International Journal of Greenhouse Gas Control, 126(103904). 10.1016/j.ijggc.2023.103904

4. **Mullen, D**., & Lucquiaud, M. (2024). Thermodynamic integration in combined fuel and power plants producing low carbon hydrogen and power with CCUS. *Frontiers in Energy Research*, *12*. 10.3389/fenrg.2024.1511996

5. Cownden, R**., Mullen, D**., & Lucquiaud, M. (2023). Towards net-zero compatible hydrogen from steam reformation – Techno-economic analysis of process design options. International Journal of Hydrogen Energy, 48(39). 10.1016/j.ijhydene.2022.12.349

Conference proceedings:

1. **Mullen, D**., Baxter, X., Bowers, J., Ellicott, H., Ilett, T., Atkinson, S., Pourkashanian, M., Akram, M., Gheit, A., Lucquiaud, M., & Gibbins, J. (2024, October). Flexibly

Operated Capture Using Solvent Storage (FOCUSS[1]) – Results. 17th Greenhouse Gas Control Technologies Conference (GHGT-17).

2. **Mullen, D.** (2024, March 27). PCC - CARER: Post-Combustion Capture - Cost and Residual Emission Reduction (Presentation)). UKCCSRC Spring Conference.

3. Hua, W., **Mullen, D**., Wahid, A., Sitabkhan, K., & Mason, K. (2024). An Overview of Artificial Intelligence for Electric Vehicle Energy Systems Integration. Workshop on Artificial Intelligence for Sustainability, 178–186. https://doi.org/10.1007/978-3-031-50485-3_17

4. **Mullen, D**., Gibbins, J., & Lucquiaud, M. (2023, June). Towards a predictive tool for MEA degradation in post-combustion capture plants with ultra-high capture rates (Poster). 12th Trondheim Carbon Capture and Storage Conference .

5. **Mullen, D**., Herraiz, L., Gibbins, J., & Lucquiaud, M. (2022, October). On the cost of zero residual CO2 emission hydrogen: A techno-economic analysis of steam methane reforming with carbon capture and storage. Proceedings of the 16th Greenhouse Gas Control Technologies Conference (GHGT-16).

6. **Mullen, D**., Herraiz Palomino, L., & Lucquiaud, M. (2021). Advanced Thermodynamic Integration in Combined Fuel and Power (CFP) Plants Producing Low Carbon Hydrogen & Power with CCUS. 15th Greenhouse Gas Control Technologies Conference, 12. https://ssrn.com/abstract=3811367

7. **Mullen, D**., & Lucquiaud, M. (2022b). Zero Carbon Electricity with CCS: A Techno-Economic Analysis of Combined Cycle Gas Turbines. In 14th International Conference on Applied Energy (ICAE2022).

[1] FOCUSS (Flexibly Operated Capture Using Solvent Storage) was a project funded by the UK Department for Energy Security and Net Zero (DESNZ) under the Carbon Capture, Usage and Storage (CCUS) Innovation 2.0 Programme. It is an industry-led project managed and delivered by a consortium consisting of SSE Thermal (project lead), the University of Sheffield and AECOM. (https://www.gov.uk/government/publications/carbon-capture-usage-and-storage-ccus-innovation-20-competition-call-1-successful-projects)

8. **Mullen, D**., Herraiz, L., & Lucquiaud, M. (2021, October). Flue-Gas Sequential Combustion in Post Combustion Carbon Capture Applications (Presentation). 6th Post Combustion Capture Conference.

Project Deliverables

1. **Mullen, D**., Gibbins, J., & Van Os, P. (2023). WP1 (Predicting Degradation): D1.3.2 & D1.3.3. In ERA-NET Accelerating CCS Technologies (ACT2) - LAUNCH project[2] No. 299662.

2. Gibbins, J., Akram, M., **Mullen, D.,** Pokora, M., Pourkashanian, M., & Samson, A. (2022). PCC - CARER: Post-Combustion Capture - Cost and Residual Emission Reduction Final Report. In FLEXIBLE FUNDING CALL 2021. UKCCSRC

Miscellaneous

1. **Mullen, D**. (2022). WHY BINARY VIEWS SLOW ACTION ON CLIMATE CHANGE. In TEDxUniversityofEdinburgh.

2. **Mullen, D**., & Lucquiaud, M. (2022a). What is the cost of zero-carbon hydrogen with CCS? (S. C. C. & Storage, Ed.). Scottish Carbon Capture & Storage. https://www.sccs.org.uk/news-events/recent-news/700-blog-what-is-the-cost-of-zerocarbon-hydrogen-with-ccs

[2] LAUNCH (Lowering absorption process uncertainty, risks and costs by predicting and controlling amine degradation) was a three-year ACT2 funded project aimed at accelerating the implementation of CO_2 capture across the industry and enabling the development of novel solvents to support the widespread deployment CCUS. (https://climit.no/en/project/launch-lowering-absorption-process-uncertainty-risks-and-costs-by-predicting-and-controlling-amine-degradation/)

Acknowledgements

To Rosie, whom I met and married during this PhD, thanks for pretending to be interested in my graphs.

I would like to express sincere thanks to my primary supervisor turned informal supervisor/co-author/sounding board, Mathieu Lucquiaud, for his support during the highs and lows of this journey, Covid-19, painful publishing pathways and career moves (for both of us), I got there in the end, in no small part due to your knowledge, insights and commitment to CCS. And to my secondary supervisor turned primary, Hannah Chalmers, for picking up the baton during the aforementioned career moves.

A special shout-out must go to Jon Gibbins at the University of Sheffield. I learnt more about CCS from a phone call from you than any amount of research, even if I was mostly an innocent bystander for them. And to SSE Thermal and my manager Xiaomian Baxter for giving me the freedom to finish this PhD part-time and only a year behind when I said I would.

Finally, I would like to thank the School of Engineering at the University of Edinburgh for providing the funding for my PhD, without which I would have starved.

Table of Contents

1. Introduction 1

2. Literature review 7

3. On the cost of zero carbon hydrogen: A techno-economic analysis of steam methane reforming with carbon capture and storage 31

3.1 Discussion & Conclusions 33

3.2 Highlights 35

3.3 Limitations and Future Work 35

4. On the cost of Zero Carbon Electricity: A Techno-Economic Analysis of Combined Cycle Gas Turbines with post-combustion CO_2 capture 36

4.1 Conclusion 38

4.2 Highlights 39

4.3 Limitations and Future Work 39

5. Thermodynamic Integration in Combined Fuel and Power (CFP) Plants Producing Low Carbon Hydrogen & Power with CCUS 40

5.1 Abstract 40

5.2 Introduction 41

5.3 SMR and CCGT integration 44

5.4 Modelling Methodology 48

5.4.1 Gas turbine 49

5.4.2 Reformer furnace & Flue gas heat recovery 49

5.4.3 Steam cycle 50

5.4.4 Reforming Process 51

5.4.5 2nd Law (Exergy) Analysis 51

5.4.6 Technoeconomic Assessment 53

5.5 Results and Discussion 55

5.5.1 Thermal performance of the CFP plant 55

5.5.2 Performance with CO_2 Capture Integration 56

5.5.3 Exergy analysis 58

5.5.4 Technoeconomic analysis 59
5.6 Conclusion 60
5.7 Limitations and Future Work 61
6. Monoethanolamine (MEA) degradation rates in post-combustion capture plants with 100% fossil CO_2 capture 62
6.1 Conclusion 64
6.2 Highlights 66
6.3 Limitations and Future Work 66
7. Abatement of CO_2 emissions during start-up and shutdown of post-combustion capture plants 67
7.1 Conclusion 69
7.2 Highlights 70
7.3 Limitations and Future Work 70
8. Conclusions & Discussion 72
9. References 80
10. Appendix A – Chapter 5 Supporting information 94

List of Abbreviations

AMP	2-amino-2-methyl-1-propanol
BAT	Best Available Technology
BECCS	Bioenergy with CCS
CAPEX	Capital Expenditure
CCA	Cost of CO_2 Avoided
CCGT	Combined Cycle Gas Turbines
CCUS	Carbon Capture, Utilisation, and Storage
CFP	Combined Fuel and Power
CGTCP	Combined Global Temperature Change Potential
CO_2e	CO_2 equivalent
DACCS	Direct Air Capture and Storage
DPA	Dispatchable Power Agreement
EfW	Energy from Waste
EGR	Exhaust Gas Recirculation
EOR	Enhanced Oil Recovery
FGSF	Flue Gas Sequential Firing
GDT	Global Damage Potential
GHG	Greenhouse Gas
GTP	Global Temperature Change Potential
GWP	Global Warming Potential
HHV	Higher Heating Value
HP	High Pressure
HRSG	Heat Recovery Steam Generator
HRSG	Heat Recovery Steam Generator
IEA	International Energy Agencies
IP	Intermediate Pressure
IPCC	Intergovernmental Panel on Climate Change
IRR	Internal Rate of Return
LCOC	Levelised Cost of Capture
LCOE	Levelised Cost of Electricity
LCOH	Levelised Cost of Hydrogen
LHV	Lower Heating Value
LP	Low Pressure
MDEA	methyl diethanolamine
MEA	Monoethanolamine
NDC	Nationally Determined Contribution
NET	Negative Emission Technology
OPEX	Operational Expenditure
OTC	Once Through Cooler
PCC	Post-Combustion Capture
PFD	Process Flow Diagram
PSA	Pressure Swing Absorber
PZ	Piperazine
RP	Reformer Pressure
SMR	Steam Methane Reformation
SRD	Specific Reboiler Duty
SUSD	Start-Up and Shutdown
T&S	Transport and Storage
TIT	Turbine Inlet Temperature
VLE	Vapour-Liquid equilibrium

1. Introduction

Anthropogenic induced climate change, that is, the release of greenhouse gases (GHG) into the earth's atmosphere as a result of human activities, has already and continues to disrupt the normal climate cycles that have existed for millennia, posing an existential crisis to all life on this plant.

Virtually all human activity, either directly or indirectly, contributes to the increasing concentrations of atmospheric GHG's, primarily carbon dioxide (CO_2). If we are to avoid the worst effects of climate change, rapid decarbonisation of the global economy is required. There is however a competing obligation, to ensure that the societal benefits industrialisation has brought to the developed world are not sacrificed and continues to lift developing nations out of poverty.

Key among the boon's industrialisation has provided is access to affordable and reliable energy. However, the conversion of energy into useful forms (electricity, home/transport compatible fuels etc.) from readily available sources (fossil fuels) continues to be a significant emitter of GHG's. Recent decades have seen the laudable deployment of alternative sources of energy which produce electricity from renewable sources (wind, solar, hydroelectric etc.). However, the intermittency inherent in these sources proves a significant challenge to electricity grid operators whose remit is to provide affordable and, crucially, uninterrupted access to electricity. As a result, almost all predictions for regional and global energy networks predict some ongoing reliance on fossil fuels over the coming decades.

This continued reliance on fossil fuels poses a large risk to the decarbonisation Imperative, and if unavoidable, must be employed in such a way as to reduce the net emitted GHGs from their use to zero. Carbon Capture and Storage (CCS) technology, that is capture and geological storage of the CO_2 produced, can be leveraged to achieve this goal. The aim of CCS is to avoid the release of CO_2 from the use of carbon rich fuels by either removing the CO_2 from the fuel before use (pre combustion) or after use (post combustion). The CO_2 is then, instead of being released to the atmosphere, transported to a secure and geological storage site. CCS is a proven technology that has been in use for decades, although primarily for the removal of the CO_2 that is extracted alongside fossil fuels from geological reservoirs (gas sweetening) and not climate change mitigation.

Historically, CO_2 removal rates from CCS applications of 90% have been targeted as there was no economic incentive to achieve higher rates. This removal rate is clearly incompatible with long term climate change mitigation as this would still result in 10% of the CO_2 produced

in the process being emitted. This work aims to demonstrate the technical and economic feasibility of capturing 100% of the CO_2 generated (100% fossil CO_2 capture) within two fossil fuel-based energy-conversion processes: a combined cycle gas turbine (CCGT) and steam methane reformer (SMR), using an open-source and commercially available monoethanolamine (MEA) based post-combustion CO_2 capture technology.

To the knowledge of the author, Chapters 3 and 4 present the first comprehensive techno-economic assessments of a steam methane reformer (SMR) and combined-cycle gas turbine (CCGT) that demonstrates that operation with zero life-cycle emissions is economically achievable. This provides critical insights into the process conditions required to ensure that 100% fossil CO_2 capture is achieved with a minimal increase in specific energy demand. Detailed capital and operational expenditure models, developed for this work, demonstrate that the impact on the economics of the process is much lower than previous assessments have concluded. I quantify the non-process related lifecycle emissions using a cradle-to-gate assessment for the upstream, downstream, and embodied emissions, going as far as to include the recapture of these emissions using direct air capture (DACCS) in the financial model. This provides, for the first time, detailed cost estimates for the offset of the remaining lifecycle emissions once direct emissions are eliminated.

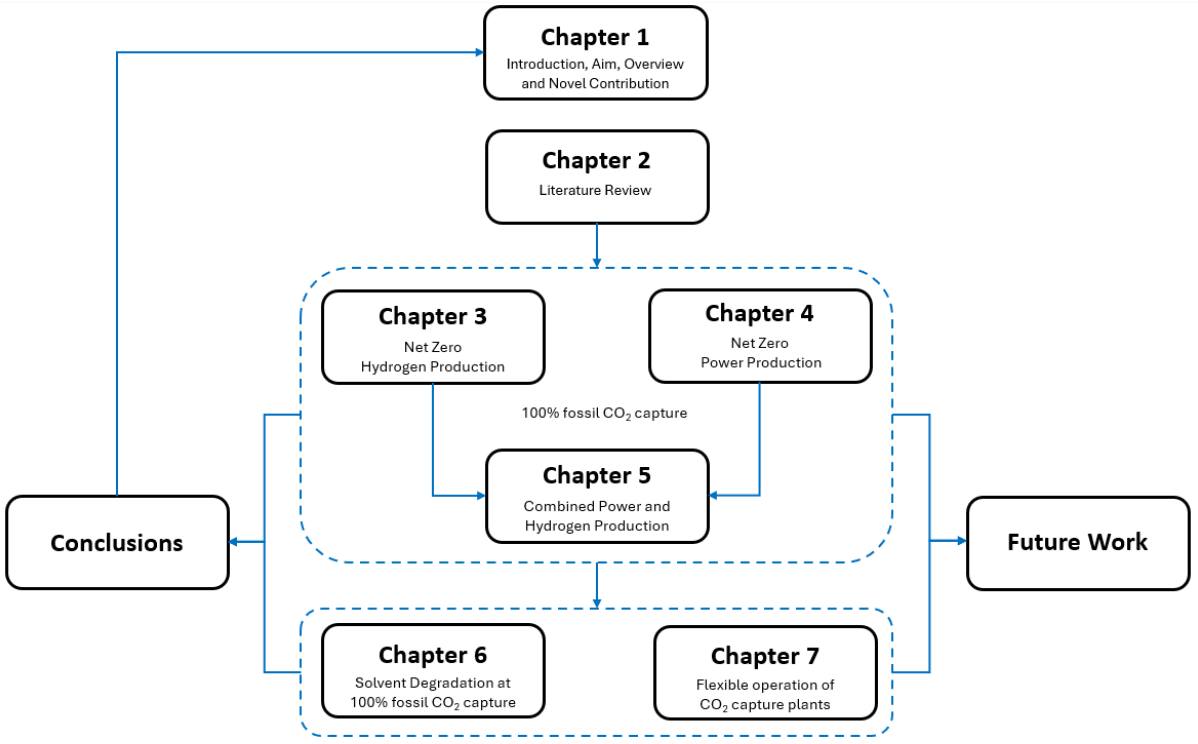


Figure 2: Thesis Overview

Chapter 5 presents the redesign of a novel plant configuration (operating at 100% fossil CO_2 capture) combining both the CCGT and SMR processes into a single "combined fuel and power" (CFP) plant. This not only takes advantage of the shared infrastructure both processes require but also provides a thermodynamic and capital expenditure benefit relative to both processes individually. This configuration is predicted to increase in the 2nd law thermal efficiency by 2.6% points over un-integrated processes (1.9% points over previous integration designs), decrease the effective specific reboiler duty by 5.5% and decrease plant CAPEX by 15.1 - 17.3%. This results in an estimated increase in the internal rate of return of 5.1 - 5.5% points over the base hurdle rate of 7.8%, highlighting the potential for substantial cost reductions presented by the CFP configuration.

Chapters 3 to 5 extensively detail the design parameters required to achieve 100% fossil CO_2 capture. However, in brief, in all cases, increasing CO_2 capture fractions from 90 – 95% gross to 100% fossil rates required three distinct but moderate design modifications[3]:

- **A minimum of 16 – 20m of absorber packing and up to 24m:** Exact value is dependent on the CO_2 concentration in the flue gas and lean loading utilised however this represents an increase of typically circa 4m over "standard designs". This increases the residence time of the solvent with the flue gas to be treated, ensuring sufficient absorption of CO_2 even at very low partial pressures. It's worth noting that this may not represent a substantial CAPEX increase if the same number of absorber beds can be maintained, i.e. 2 X 10m beds vs 2 X 8m.
- **Reduced lean solvent loadings:** Reducing lean loadings from 0.20 – 0.25 mol/mol to circa 0.10 – 0.16 mol/mol, in conjunction with any increased packing hight will ensure increased driving force of absorption in the upper portions of the absorber.
- **Increase Regeneration Pressures:** To efficiently achieve the required decrease in lean loading an increase in the operating pressure of the desorber will be required (210 – 275KPa vs 170 – 190KPa), with an associated and unavoidable increase in reboiler temperatures (125 - 135°C vs 115 – 125°C) which may impact solvent management requirements (ref Chapter 6).

When theses process modifications were implemented the increase in key process indicators; specific reboiler duty (SRD), capital (CAPEX) and operational (OPEX) expenditure, process efficiency and cost of production was found to increase in an approximately (or below) linear

[3] Results presented are for an open art 35% wt. MEA solvent however are expected to be broadly applicable to alternative solvents, noting that the absolute values will vary.

rate with increasing CO_2 capture fraction in contrast to the exponential increase that was previously assumed by the existing literature.

Chapters 3 and 4 identified solvent degradation at the process conditions required to achieve the thermodynamically efficient capture of 100% of the fossil CO_2 in Post Combustion CO_2 Capture (PCC) plants. These process conditions, namely increased solvent regeneration pressures (210 – 275KPa vs 170 – 190KPa), and therefore temperature (125 - 135°C vs 115 – 125°C) to generate lower lean loadings (0.1 mol/mol vs 0.20 - 0.25 mol/mol), and longer residence time in the absorber, as a knowledge gap in the existing literature. Chapter 6 provides the first body of evidence on this subject by using a newly developed solvent degradation framework (Braakhuis, Høisæter and Knuutila, 2022; Braakhuis and Knuutila, 2023) for MEA to compare the predicted solvent degradation rate for three industrial processes, an SMR, CCGT and Energy from Waste (EfW), operating at two distinct CO_2 capture fractions, 95% gross capture and 100% fossil capture, and different intercooling regimes. Not only quantifying the relative effect of increasing CO_2 capture fractions but also providing critical insights into effective process considerations for mitigating solvent degradation.

Finally, Chapter 7 presents analysis completed by the author as part of a project which was the first pilot plant test campaign to successfully demonstrate the use of solvent storage to achieve high levels of CO_2 capture (+97%) during a simulated plant start-up. Additionally, the author procured and analysed 17 start-up and 3 shutdown sequences from a commercial CCGT, demonstrating for the first time the quantity of previously waste steam available for acceleration of the PCC start-up sequence. This reduces the predicted solvent storage capacity requirements (and associated increase in solvent inventory) from 350% of the base inventory to just 50%. When early steam is employed but solvent storage is limited to the capacity of the absorber sumps the gross CO_2 capture fraction for a startup (defined as the period before the gas turbine load is above 99%) is predicted to be 72, 80 and 83% for a hot, warm and cold start respectively, a substantial increase over previous assumptions (Calvert and MacKenzie, 2020). However, achieving the ultra-high CO_2 capture fractions required for net zero operation was not possible without increased solvent storage.

Novel Contribution

Prior to commencement of this work a number of key gaps in the state of the field, i.e. utilising CCS as an effective climate change mitigation technology, were identified. These are summarised below:

- There was limited evidence detailing the effective process design for PCC plants operating at 100% fossil CO_2 capture fractions. This led to repeated predictions of rapidly increasing costs as capture fractions increase.
- The economic impacts of a mandate to recapture scope 2 and 3 GHG emissions from energy conversion processes had not been quantified.
- Combined fuel and power plants (CFP) had been proposed but with limited and inefficient integration.
- Increased MEA degradation rates due to the modified regeneration conditions and increased absorber residence time required to efficiently achieve 100% fossil CO_2 capture was often considered a barrier. However, no quantitative analysis had been completed.
- CO_2 capture during start-up and shutdown (SUSD) was considered impractical and costly. This would limit the effectiveness of decarbonised CCGTs to operate in a dynamic energy market while maintaining high net rates of CO_2 abatement.

The work presented in this thesis goes some way towards resolving these knowledge gaps, with a summary of the novel contributions and how they pertain those gaps detailed below:

- First comprehensive body of work detailing the process and economic conditions required to make 100% fossil CO_2 capture economically competitive, demonstrating that 100% fossil CO_2 capture is already economically incentivised in the UK. Provides clear and achievable design recommendations to do so.
- Scope 2 & 3 emissions are quantified and the recapture using direct air CO_2 capture (DACCS) is costed, providing evidence for the development of policy mechanisms to incentivise it.
- Clear process improvements to CFP plants are identified and costed. Demonstrating increased efficiency and profitability over independent generation.
- The effect increasing CO_2 capture fractions has on MEA degradation was predicted. Clear and apparently effective mitigation strategies were identified.
- Demonstrated a commercially available and cost-effective method to achieve high rates of CO_2 capture during SUSD through pilot plant test campaigns. The first body of evidence to propose, and quantify the benefit of, using of previously dumped steam

during the startup and shut down sequences for CO_2 capture, with the scope for substantial cost reductions and increased efficiency.

2. Literature review

Global Context

As of 2024, an estimated 50 billion tonnes of anthropogenic CO_2 equivalent (CO_2e) emissions are emitted every year (Climate Watch, 2024), with a cumulative addition in the region of 2600 $GtCO_2e$ since the start of the Industrial Revolution. This is a staggeringly large number but provides no context when taken in isolation. Perhaps it is more impactful to highlight the results of these activities.

In the last circa 150 years of human existence, CO_2 concentrations have increased from 280pmm to over 420pmm (Our world in data, 2024), a level not seen in the last 3 million years (Earth.org, 2024), leading to the warmest period globally in the last 100,000 years, or since the expansion of homo sapiens from our African cradle. The Intergovernmental Panel on Climate Change (IPCC) now considers it "likely" that warming will exceed 1.5^{o}C within the 21st century (Calvin *et al.*, 2023), with 2023 being the first year to break this limit (Poynting, 2024), albeit at least partially driven by an El Nino event.

At the current atmospheric CO_2 concentration, the IPCC (Intergovernmental Panel on Climate Change (IPCC), 2023b) attributes the following to anthropogenic induced climate change:

- Mass mortality events in plants and animals have been observed, driving the first known extinctions from anthropogenically induced climate change.
- The increasing frequency and intensity of droughts and heat waves have resulted in abrupt and possibly irreversible changes in some terrestrial and marine environments.
- The productivity of agricultural and food production has decreased in some regions, with the adverse effects of extreme climate events tripling over the last 50 years in Europe.
- The intensification of the global hydrological cycle has led to increased water scarcity and has exposed more people to water-related extreme events.
- Climate change-driven malnutrition in multiple regions has been observed.
- Higher temperatures, coupled with changes in land use, are expanding the areas conducive to the transmission of vector-borne diseases.

This is occurring while global temperature rise is still below the lower limit of 1.5^{o}C set by the Paris Agreement, an aspiration that now appears increasingly unlikely. Indeed, extrapolated trends from current policies are estimated to result in a median global warming of 2.4°C to

3.5°C by 2100 (Pathak *et al.*, 2023). The IPCC estimates that “cost-effective” mitigation pathways that have a >67% chance of limiting global warming to 2ºC, assuming immediate action is taken to increase nationally determined contributions (NDCs), are associated with a reduction in annual greenhouse gas (GHG) emissions from their current levels of circa 50-60 $GtCO_2e/y$ to 30-49 $GtCO_2e/y$ by 2030 and 14–27 $GtCO_2e/y$ by 2050.

When current NDCs are maintained up to 2030, it is considered impossible to limit global warming to 1.5ºC. Limiting warming to 2ºC, however, would require a 1.3–2.1 $GtCO_2e/y$ reduction in annual GHG emissions between 2030 and 2050 (Pathak *et al.*, 2023), a rate similar to the temporary and largely reversed reduction in global GHG emissions seen during the Covid-19 pandemic (Luterbacher *et al.*, 2021).

The conclusions are clear and, sadly, not new; the current pace of decarbonisation of our society is not likely to limit global warming to 1.5ºC or even 2°C. That being said, every fraction of a degree of warming avoided will reduce the fallout of anthropogenic-induced climate change. We must act with the utmost urgency to avoid the very worst effects of this self-induced crisis by rapidly deploying proven and effective solutions to the most CO_2e-intensive areas of our economies.

CCUS for GHG emission reduction

Carbon Capture, Utilisation, and Storage (CCUS) can be broadly defined as any process that separates CO_2 from a process stream containing other fluids, typically nitrogen, oxygen, and water, among other more dilute species. The aim of CCUS is to prevent or reduce the CO_2 entering the atmosphere as a result of the process that produced it, this is distinct from Direct Air Capture and Storage (DACCS) which proposes the direct removal of already emitted CO_2 from atmospheric air. This CO_2 can then be utilised in an industrial process to displace CO_2 that would otherwise be sourced by direct generation from fossil fuels or permanently stored in geological reservoirs, thus reducing the climate impact of that process by the net quantity of CO_2 utilised or stored.

The permanent storage of CO_2, typically cited as a minimum storage duration of 10,000 years, is achieved by direct injection into porous rock formations in the geological subsurface that are covered by one or more CO_2 impermeable “cap rocks”. Geological structures suitable for large scale CO_2 storage are typically separated into depleted oil and gas wells, or saline aquifers, with the former having the most operational experience due to the use of CO_2 in enhanced oil/gas recovery applications. A detailed review of CO_2 storage options is beyond the scope of this document however the reader is referred to Bashir et al. (2024).

The IPCC Sixth Assessment Report on Climate Change Mitigation (Pathak *et al.*, 2023) shows a heavy reliance on CCS in almost all climate change pathways assessed, with the median cumulative quantity of CO_2 stored via CCS approximately 500 Gt this century. In a special report by the IPCC on 1.5ºC, 3 out of 4 of the pathways included major use of CCS, with cumulative storage quantities of 348 - 1218 $GtCO_2$ (Delmotte *et al.*, 2022). Similarly, the International Energy Agencies (IEA) Net Zero Emissions by 2050 Scenario (Bouckaert *et al.*, 2021) includes 1.6 Gt of CO_2 captured and stored per year via CCS by 2030, a ~30-fold increase over the current capacity of 50 $MtCO_2$/y, rising to 7.6 $GtCO_2$/y by 2050.

Regional ambitions are increasing in an effort to meet these assessments. The UK has pledged to capture and store 20 - 30 $MtCO_2$/y by 2030, increasing to 90 – 170 $MtCO_2$/y by 2050 (UK Gov (D), 2023), while the EU aims to store 50 $MtCO_2$/y by 2030 (Global CCS Institute, 2023). In the Americas, Canada aims to store at least 15 $MtCO_2$/y by 2030, and assessments of the US Inflation Reduction Act estimate an additional 200-250 $MtCO_2$/y could be stored by 2030 as a result of the financial aid available (Global CCS Institute, 2023). Elsewhere, Japan is targeting 240 $MtCO_2$/y stored by 2050 and Saudi Arabia 44 $MtCO_2$/y by 2035, to name a few (Global CCS Institute, 2023).

In 2021, energy provision, be that heat and electricity for homes and businesses or fuel for transport or industry, accounts for 75.5% of global GHG emissions (Climate Watch, 2024). Of that, 33.8 $GtCO_2/y$ (~90%) was directly emitted CO_2, with the remaining 3.6 $GtCO_2e/y$ stemming from fugitive emissions of non-CO_2 GHGs, primarily methane (3.27 $GtCO_2e/y$). This makes the energy sector, by far, the main emitter of GHGs globally. CCUS is expected to play a major role in decarbonising this sector, with direct abatement of critical manufacturing industries such as steel (Tian *et al.*, 2018), cement (Heidelberg Materials, 2024) and chemical (Tata Chemicals, 2024), decarbonisation of distributed point source emitters by fuel switching to decarbonised fuel sources like ammonia (Mayer *et al.*, 2023), synthetic biofuels (Lindfeldt and Westermark, 2009; Johnson, Parker and Ogden, 2014; Mukherjee, Bruijnincx and Junginger, 2020) or hydrogen (Heap *et al.*, 2016; Joffe *et al.*, 2018). It is also expected to contribute to the ongoing decarbonisation of the electricity grid by providing decarbonised flexible and dispatchable electricity (NZT, 2024) when renewable generation does not meet grid demand. Although relevant to all of the above use cases, providing post-combustion technology is utilised, this work focuses on the decarbonisation of two key energy vectors. That of so-called “blue” hydrogen wherein a hydrocarbon fuel source is separated into, primarily, hydrogen and CO_2 and coupled with CCUS, and hydrocarbon-based flexible electricity generation from natural gas-fired combined cycle gas turbines (CCGT) with CCUS.

Hydrogen is seen as a pillar in many decarbonisation pathways as it produces zero CO_2 at the point of use, with the product of its oxidation simply water. This makes hydrogen potentially advantageous in decarbonising decentralised use cases, which traditionally emit CO_2. Potential applications include the provision of heat to industrial processes or domestic homes by fuel-switching from CO_2-intensive fuels, on-demand electricity production in hydrogen fuel cells or direct combustion for transport or grid support, chemical energy storage through electrolytic hydrogen production and storage at times of excess renewable generation or when combined with atmospheric CO_2, the production of sustainable liquid fuels (Heap *et al.*, 2016; Joffe *et al.*, 2018). Hydrogen is generally produced by separating the H_2 from either hydrocarbons or water by a variety of processes. For shorthand, methods of production are generally designated a colour to differentiate them.

The three main large-scale production methods for hydrogen are described below:

- Electrolytic hydrogen produced using dedicated or excess renewable electricity (green hydrogen)
- Hydrocarbon reformed hydrogen with CCUS (blue hydrogen)
- Hydrocarbon reformed hydrogen without CCUS (grey hydrogen)

Additional designations exist, such as pink hydrogen (electrolytic hydrogen from nuclear power) or white hydrogen (geological hydrogen); however, large-scale production via these processes is currently not envisioned (Ajanovic, Sayer and Haas, 2022; Yedinak, 2022). Both green and blue hydrogen can be produced in a low-carbon fashion, with the carbon intensity of the hydrogen product primarily dependent on the CO_2e of the electricity used in green hydrogen production and the CO_2 capture fraction achieved for blue hydrogen, along with the downstream and upstream GHG emissions (e.g., construction, fugitive emissions, transport and storage, etc.). However, it is technically feasible for both production methods to achieve zero carbon intensity. In the case of blue hydrogen this requires designing and operating a CO_2 capture process where all fossil CO_2 is prevented from entering the atmosphere, and where any residual atmospheric CO_2 from combustion air can return to the atmosphere. Chapter 3 provides a more detailed discussion and an investigation into a fully decarbonised blue hydrogen production facility.

Efforts to decarbonise the electricity grid in many parts of the world have had laudable results thus far, with the USA, Europe, China and the UK achieving a reduction in the CO_2 intensity of electricity supply of 32%, 24%, 25% and 51% respectively between 2000 and 2022 (Our World in Data, 2024). This reduction has primarily been driven by the deployment of renewable-based generation and fuel switching from coal and oil to natural gas. Globally, efforts have, however, been lagging, and unabated (without CCUS) fossil fuels remain the prime supplier of global electricity, with coal, oil, and gas providing 60.6%, down just 4% (from 64.6%) in 2000. Over the same period, the CO_2 intensity of electricity production decreased from 518 gCO_2e/KWh to 481 gCO_2e/KWh, a 6.2% decrease. It is clear that substantive efforts are required to reach a global net zero electricity system (defined here as zero GHG emissions on a life-cycle basis, either at the point of production or with the timely recapture and permanent storage of the equivalent quantity of GHG).

Under the assumption that consumers require the freedom to choose when to use electricity, it is an unavoidable conclusion that an electricity grid will require the capacity to match supply and demand irrespective of the instantaneous generation from intermittent power production

facilities (e.g., wind/solar). This can be achieved one of two ways, either through demand-side reduction, wherein consumers temporarily reduce their consumption to match the available supply, or through supply-side response, wherein additional electricity is supplied to the grid from a dispatchable source to meet demand. Although technically feasible, in only the most literal sense, complete reliance on demand-side reduction would expose the electricity grid to the risk of instability and the consumers to potentially mandated demand reduction to mitigate that instability. It is, therefore, reasonable to assume that some level of dispatchable electricity capacity will be required.

In the case of a net-zero electricity grid, this dispatchable electricity must itself be net-zero. Many technologies currently exist that, with the appropriate design, could provide this service; among them, energy storage systems are a prominent feature, such as electrolytic hydrogen production (with subsequent power generation via combustion in a gas turbine/internal combustion engine or used in a fuel cell), the compression, storage and subsequent expansion of air, pumped hydroelectric storage or large-scale batteries, to name a few. It is likely that these systems will form an important part of our energy grid going forward and are included in many published net zero policies (UK Gov (C), 2021b; European Commission, 2023). However, each of these systems are inextricably linked to renewable power generation and thus subject to the same intermittency. Designs where the dispatchable power requirement is served exclusively through renewable energy storage require the build-out of renewable generation capacity far in excess of peak demand and are not expected to provide the lowest cost decarbonisation pathway (Capros *et al.*, 2014; Dixon, Bell and Brush, 2022). Even if the daily dispatchable demand is met by renewable energy which has been stored, the scale of storage, and unavoidable losses, required to ensure energy security in the case of rare, but significant anticyclonic events (or other long duration weather events), where wind and/or solar generation is minimal, is staggering.

As previously mentioned, thermal power generation using hydrocarbon fuels currently accounts for 60.6% of global electricity generation. This method of electrical power generation, although CO_2 intensive, provides dispatchable power to virtually every electricity grid on the planet. Chapter 4 investigates utilising CCUS to fully decarbonise a natural gas-fired CCGT to provide on-demand, flexible power that is decoupled from the intermittency of renewable generation. This can be achieved by designing the CCUS process to capture of 100% of the process CO_2 emissions and the recapture of the CO_2 equivalent lifecycle GHG emissions via an appropriate negative emission technology, such as DACCS.

Hydrogen combustion in CCGT plants is often considered a viable source of dispatchable power generation, however if the hydrogen is provided via the “green route” (electrolytic production from renewables) it will be subject to the same intermittency constraints described above. Should the hydrogen be produced via the “blue route” a more truly, renewable decoupled, dispatchable source would be achieved. However, power generation in this manner suffers from poor round trip thermal efficiency. Chapter 3 predicts that a hydrogen production facility operating with no direct CO_2 emissions will have a thermal efficiency of 66.8% HHV, taking a highly conservative assumption of no transportation and storage losses/power demand or derating of the CCGT (63.5% LHV) a round trip LHV efficiency of 39.7% is predicted, comparing unfavourably to the 56.7% predicted by Chapter 4 for a fully decarbonised CCGT with CCS.

Both blue hydrogen and decarbonised CCGTs feature prominently in published governmental decarbonisation pathways (UK Gov (C), 2021b; European Commission, 2023). Both require similar infrastructure, such as access to a natural gas supply, CO_2 export capacity, cooling water, grid connection, and a skilled workforce. Therefore, it is likely that they will be deployed in geographically similar locations, as is the case in the UK cluster sequencing program (UK Gov (D), 2023). Chapter 5 investigates the potential benefit of sharing not only infrastructure but also the production of both blue hydrogen and decarbonised power in a single facility by introducing a novel “combined fuel and power” (CFP) process. The CFP process operates by supplementing the bottoming cycle of the CCGT, traditionally a Rankine cycle generating steam for supplementary electricity generation, for the steam methane reformation (SMR) cycle, which produces hydrogen. The supplementary firing of the O_2-rich exhaust gas from the gas turbine provides the high-grade heat required by the reforming cycle while reducing the CO_2/N_2 ratio entering the PCC, providing both thermal efficiency gains and capital expenditure reductions relative to both processes independently while capturing 100% of the CO_2 produced in the process.

Carbon Capture Technology

Theoretically, CCUS can be applied to any process that produces CO_2; however, it is typically limited to large centralised industrial emitters due to the infrastructure requirements for transporting the captured CO_2 and the scale of the capture technology, typical applications include:

- Heavy industry (e.g. cement and steel)
- Fuel production (e.g. hydrogen, ammonia and biomethane)
- Electricity generation (e.g. natural gas, coal and biomass)
- Waste treatment (incineration)

Although centralised in its nature, when applied to electricity or fuel production, CCUS can decarbonise decentralised systems, key examples being hydrogen for space heating and electricity for transport. Additionally, if the CO_2 is biogenic in nature as opposed to fossil-based, as is the case with biomass combustion, the capture and storage of that CO_2 would represent a net removal of CO_2 from the atmosphere, so-called negative emissions.

CCUS technologies broadly fall into three categories:

- Post-combustion: This encompasses any technology that separates CO_2 from a gas mixture downstream of an industrial process. Typically, this is a high-volume flow rate of flue gases at near atmospheric pressure containing mainly N_2, H_2O, and O_2, with dilute quantities of CO_2 (2 - 25% vol).
- Pre-combustion: A hydrocarbon fuel is first converted to a syngas containing primarily H_2, CO_2, CO and H_2O through exposure to high temperatures (typically >700^oC) in an O_2 or H_2O environment without (or with incomplete) combustion. The CO_2 is then separated from the syngas prior to use (Chen, 2022).
- Oxy-fuel combustion: Fuel is combusted in a pure oxygen environment, producing an exhaust stream containing primarily CO_2 and H_2O with small amounts of unburnt hydrocarbons, CO and O_2, and any impurities present in the fuel or oxygen source. The Allam cycle (Allam *et al.*, 2017) is an example of a commercial application of Oxy-fuel combustion in power generation.

Excluding Oxy-fuel, which only requires condensation of H_2O from the CO_2 stream, CO_2 capture, both pre and post-combustion, is completed via a number of mechanisms (Bukar & Asif, 2024), including, but not limited to:

- Cryogenic Separation: CO_2 separation via condensation or de-sublimation at cryogenic temperatures.
- Membrane Separation: CO_2 separation via diffusion through CO_2-selective materials.
- Solid Adsorption: The adsorption of CO_2 onto the surface of a CO_2-selective material in a reversible reaction.
- Chemical Looping: Reduction of metal oxides or carbonates with hydrocarbon fuel for oxy-fuel combustion; reduced material is re-oxidised/carbonated to restart the process.
- Carbonate Fuel Cells: Combined CO_2 capture and methane reforming using a molten carbonate electrolyte fuel cell.
- Liquid Absorption: The chemical bonding of CO_2 to a liquid solvent, typically to form carbamates or bicarbonates, in a reversible reaction; typical solvents are amine-based; however, potassium (Borhani *et al.*, 2015) and ammonia (Augustsson *et al.*, 2017) solvents have been proposed.

Liquid absorption, specifically amine-based, is the most technologically mature CO_2 capture technology having been used within the oil and gas industry for decades in “gas sweeting” applications. Outwith gas sweeting, amine-based PCC has been deployed at scale in a number of industrial applications, notably at Boundary Dam and Petra Nova (Mantripragada et al., 2019) representing the largest commercial scale application of CCS to power generation facilities. This trend of applying amine-based PCC capture to industrial applications appears set, at least in the near term, to continue. Five of the eight CO_2 capture projects chosen as part of the UK track one cluster sequence program plan to use this technology (DESNZ, 2023), with two out of the three remaining likely to use amine based pre combustion. Due to the technical and commercial maturity and over alternative CCS technologies, amine-based PCC is chosen as the focus of this work.

PCC by liquid absorption occurs when a solvent (typically amine-based) bonds the CO_2 in the exhaust (flue) gases of an industrial process in a reversible reaction. Absorption typically occurs in a packed bed absorber column close to atmospheric conditions; however, some solvents, such as potassium carbonate, may benefit from increased pressure and temperatures during absorption (Ayittey *et al.*, 2020) or, in the case of ammonia, lower temperatures (Augustsson *et al.*, 2017) .

Within this column, counter-current contact between the rising flue gas and descending CO_2 lean liquid solvent promotes the mass transfer of CO_2 from the vapour phase into the solvent. CO_2 lean flue gas leaves the top of the absorber column after emission control techniques (water (Morken *et al.*, 2014) and acid (Khakharia *et al.*, 2014) washes) minimise atmospheric emissions from the solvent, while CO_2-rich liquid solvent leaves the bottom of the column to be stripped of the captured CO_2.

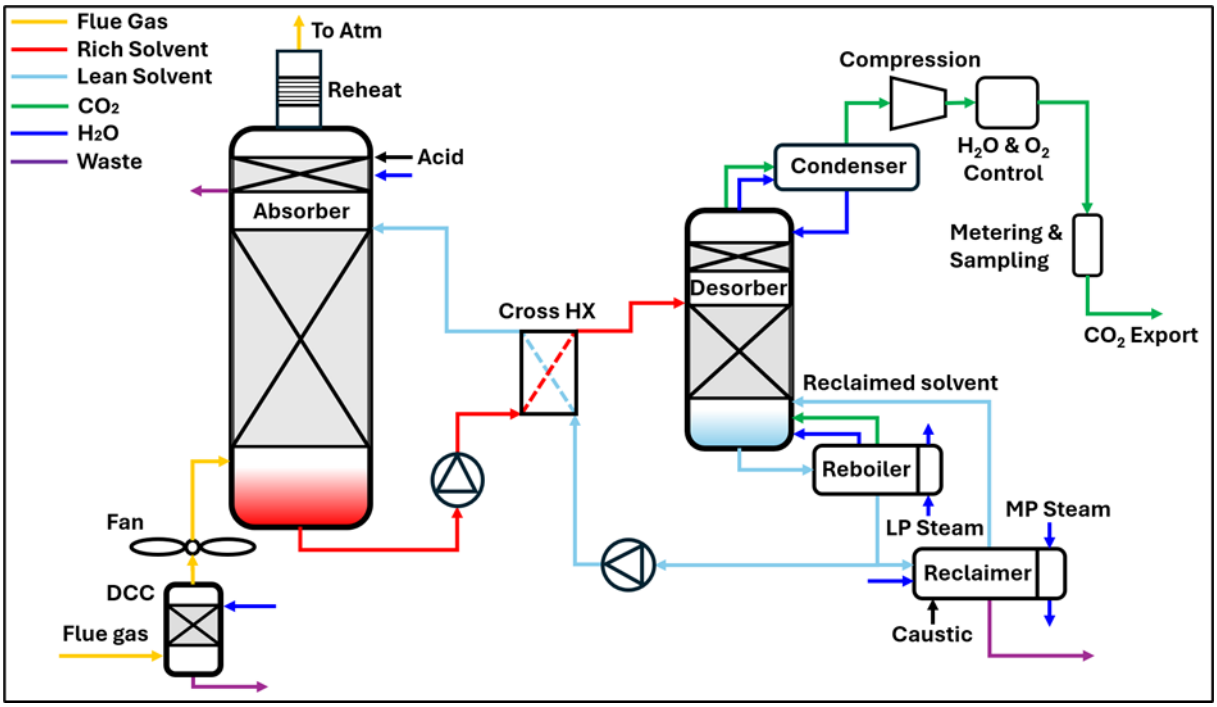


Figure 3 Process flow diagram for a typical amine-based post-combustion CO_2 capture plant

CO_2 stripping from the rich solvent occurs in a separate, often pressurised, desorber or "stripper" packed bed column; CO_2-rich solvent descends through the desorber, contacting rising steam, which has been generated at the bottom of the column by vaporising a portion of the H_2O content in the solvent in a heat exchanger known as a reboiler. This steam serves to promote the reverse reaction and liberate the CO_2 from the solvent by reducing the vapour phase partial pressure of CO_2 in the desorber and heating the solvent through condensation. CO_2/H_2O vapour leaves the top of the desorber column for drying, compression and conditioning for export while the now CO_2 lean solvent is cooled and returned to the absorber. Figure 3 shows a process flow diagram (PFD) for a typical amine-based post-combustion CO_2 capture plant, while detailed process descriptions can be found in Chapters 3 and 4.

Amines for CO_2 capture

Amines are ammonia (NH_3) derivatives where one or more of the hydrogen atoms are replaced by an organic group. When brought into contact with CO_2, amines will bond with the CO_2 to form a carbamate or bicarbonate (see Figure 4) compound in a temperature-reversible reaction, making them useful for CO_2 capture purposes.

Amines can be broadly characterised as primary (RNH_2), secondary (R_2NH), or tertiary (R_3N), depending on how many hydrogen atoms have been substituted by an organic group. Primary amines are highly reactive to CO_2 but have lower loading capacity than other amine groups. They are corrosive, have moderately high regeneration energies and degrade more rapidly, but are often lower cost than secondary or tertiary amines. Secondary amines have moderate reactivity to CO_2, lower regeneration energies and are more stable, but can create Nitrosamine and Nitramine-amines (N-amines collectively) directly when exposed to NO_X, which are potent carcinogens (Helgesen and Gjernes, 2016; PubChem, 2024). Tertiary amines have the lowest reactivity to CO_2 but have the highest loading capacity and the lowest regeneration energy and are the most stable (N.Borhani and Wang, 2019a).

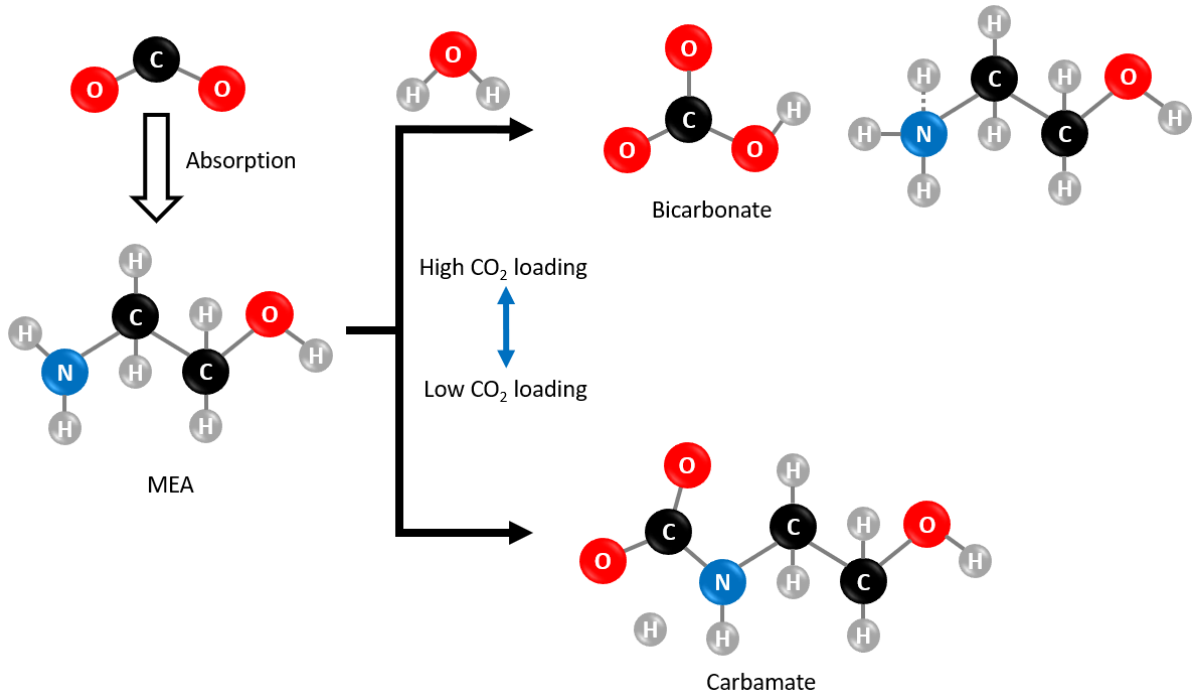


Figure 4: Absorption of CO_2 by monoethanolamine

The most commonly cited amines for use in post-combustion CO_2 capture are the primary amines monoethanolamine (MEA) and 2-amino-2-methyl-1-propanol (AMP), piperazine (PZ), a cyclic secondary amine and the tertiary amine methyl diethanolamine (MDEA). MEA (Sander and Mariz, 1992; CCS Institute, 2012) and MDEA (Romano, Chiesa and Lozza, 2010; Moioli

et al., 2017) have been used as binary solvents in CO_2 capture applications for decades. MEA for post-combustion processes with low-pressure and CO_2 lean flue gases, and MDEA for pre-combustion processes with higher-pressure and CO_2-rich gas streams. PZ has been proposed as a binary solvent (Gao and Rochelle, 2022) , or part of a blend solution, containing one or more additional amine compounds, notably CESAR1, an open-art solvent blend containing 27% wt. AMP and 13% wt. PZ.

The blending of different amines together in a solution to attempt to enhance the positive aspects of the component amines while mitigating the negatives is a common research theme (Knuutila, Rennemo and Ciftja, 2019; N.Borhani and Wang, 2019b; Vega *et al.*, 2020; Wanderley, Pinto and Knuutila, 2021). However, the efficacy of these blends relative to aqueous MEA solutions is a contentious and ongoing debate with no clear conclusion (Weir *et al.*, 2023). Due to its high reactivity, low cost and ease of reclamation relative to solvent blends (Flø *et al.*, 2017; Campbell *et al.*, 2022), MEA continues to serve as a viable solution for CO_2 capture from low-concentration CO_2 flue gases despite the purported benefits of alternative amine solvents. Stainless steel construction or carbon steel with corrosion inhibitors (DeHart *et al.*, 1999; Fytianos, Vevelstad and Knuutila, 2016; Udayappan and Veawab, 2022) can mitigate corrosion concerns, allowing higher-concentration solutions to be employed. At the same time, advanced configurations and control processes continually improve thermodynamic efficiency and limit amine loss and degradation rates. Due to the above points and the open-art nature of MEA allowing for unrestricted publication of the results, it has been used for this work.

Amine Degradation

Amines will degrade over time as they are exposed to the conditions present in the PCC plant, primarily oxygen-rich and or high temperatures environments; however, impurities in the flue gas or solvent such as NO_X (Fostås *et al.*, 2011; Chen and Rochelle, 2022), corrosion products (Goff, 2005; Morken *et al.*, 2019) or indeed amine degradation products themselves (Braakhuis, Høisæter and Knuutila, 2022) can also cause additional degradation or catalyse degradation reactions. Some degree of degradation, and by extension some quantity of circulating degradation products in the solvent, is unavoidable, but if not effectively controlled and allowed to accumulate, they can change the properties of the solvent, reducing CO_2 capture fraction and thermal efficiency, increasing equipment fouling and corrosion, increase atmospheric emissions and accelerate the degradation rate (Martin *et al.*, 2012), not only worsening all the former outcomes but incurring increased solvent replacement costs (Giannaris *et al.*, 2021).

MEA is highly reactive to oxygen (Braakhuis and Knuutila, 2023) and, when loaded with CO_2, is sensitive to thermal degradation (Braakhuis, Høisæter and Knuutila, 2022) within the operational temperature ranges proposed for CO_2 capture plants, i.e. 100-150°C. This has led to the emergence of multiple patented solvent blends (ACC, 2024; Basf, 2024; ION Clean Energy, 2024; MHI, 2024; Shell, 2024; UOP Honeywell, 2024) with suggested operational benefits over MEA through increased stability and reduced energy penalty. However, while the specific quantity of degradation may increase for MEA relative to alternative options (Weir *et al.*, 2023), MEA has a number of beneficial properties which may outweigh any potential increase in degradation. For one, thermal reclaiming, the process of separating undegraded and degraded solvent through distillation, has been shown to be very effective for MEA with near total removal of degradation products (Flø *et al.*, 2017), while solvent blends (such as CESAR1) have not been able to demonstrate the same level of removal (Campbell *et al.*, 2022). As a primary amine, MEA cannot directly form N-amines, with N-amine formation only possible from secondary reactions of degradation products, which, if kept low though effective thermal reclaiming, should be minimal (Flø *et al.*, 2017). This allows MEA to tolerate higher levels of NO_X in the flue gas and reduces the environmental impact of the plant, as N-amines have been shown to be potent carcinogens (Helgesen and Gjernes, 2016; PubChem, 2024). Any volatile emissions from MEA operations have been shown to be effectively controlled by established emission control techniques, such as water and acid washes (Khakharia *et al.*, 2014; Morken *et al.*, 2014). Finally, MEA is low-cost relative to alternative solvents (Weir *et al.*, 2023), meaning that, from a purely economic basis for solvent replacement costs, the economically acceptable degradation rate is linearly related to the relative difference in the

cost of two solvents, i.e., a solvent that is half the price can degrade twice as much for the same OPEX.

Nonetheless, it is important to quantify the magnitude of solvent degradation expected within a process and to identify any design parameters which may aid in controlling degradation rates. Particularly in operational conditions with limited or no operational experience, such as those required to efficiently achieve very high CO_2 capture fractions i.e., those greater than 99% of the CO_2 entering the absorber, this is explored in detail in Chapter 6.

Increasing CO_2 capture fractions

Under the assumption that the current GHG-intensive global energy system must progress to a zero GHG system, any CO_2 capture plants operational within that system must not increase the level of anthropogenic GHG emissions at any stage in their life cycle or, alternatively, recapture and permanently store any emitted GHGs (or CO_2 equivalent values) within an appropriate timeframe.

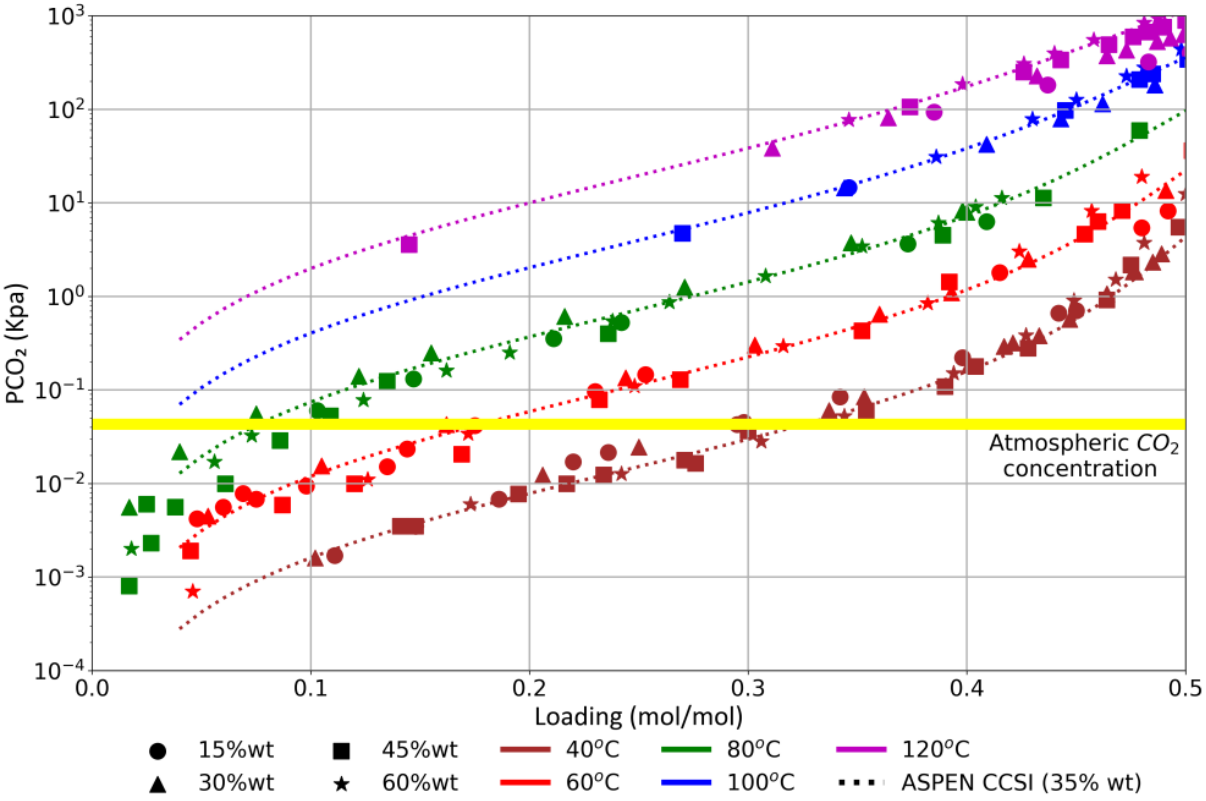


Figure 5: Experimental CO_2 Vapour-Liquid equilibrium (VLE) data for loaded MEA solutions at varying concentrations (Aronu et al., 2011). Dotted lines represent extracted VLE from the open source CCSI ASPEN Plus model used in this work (ASPENtech, 2022).

A key factor in the CO_2 intensity of any product produced with a CO_2 capture plant installed is the CO_2 capture fraction achieved, i.e. the mass of CO_2 exported divided by the mass of CO_2 entering the CO_2 capture plant. Historically, CO_2 capture fractions of 90% were the generally accepted target (Brandl *et al.*, 2021), which would indeed represent a large reduction in the CO_2 intensity of a product. However, as noted above, under calls for net zero, this assumption no longer appears tenable. Thankfully, there is no thermodynamic limit to the amount of CO_2 that can be captured from a gas stream other than, of course, 100%.

Indeed, it is unclear how this 90% target emerged as the standard design point. The earliest reference quoting a 90% CO_2 capture fraction is found in Booras and Smelser in 1991 (Booras and Smelser, 1991), who describes the Fluor Ecoamine FG process, capturing 90% of the CO_2 using an MEA solution from a pulverised coal plant, but even this early reference does not specify why 90% was chosen. Indeed, a follow-up publication a year later (Sander and Mariz, 1992) states that "Recoveries between 85% and 95% of the CO_2 present in atmospheric pressure flue gases are achievable" for the Fluor Ecoamine FG process.

Regardless of where it arose, the idea that CO_2 capture fractions above 90% are uneconomical is not supported by current research. Chapter 4 provides a critical review of the available literature on ultra-high CO_2 capture fractions, defined as CO_2 capture fractions greater than 95%. Achieving increased capture fractions can be challenging because, as the capture fraction increases, the resultant partial pressure of CO_2 at the outlet of the absorber decreases. For a given solvent at a given lean loading this will result in a decreased driving force of absorption, requiring higher and higher residence times in the absorber to increase capture fractions. This often leads researchers to conclude that substantial increases in absorber packing heights are required to achieve very high rates of CO_2 capture (Danaci et al., 2021). However, an alternative route is to decrease the solvent lean loading to retain or enhance the driving force of absorption at the top of the absorber, even at substantially increased CO_2 capture fractions.

This is illustrated in (Figure 5) where experimental CO_2 Vapour-Liquid equilibrium (VLE) data for loaded MEA solutions at varying concentrations is presented (Aronu et al., 2011). Taking the lean loadings often cited in modelling studies of 0.2 - 0.3 mol/mol (Danaci et al., 2021) and typical absorber exit temperatures (~50°C). Figure 5 demonstrates that CO_2 capture fractions that result in a CO_2 concentration at the absorber exit of less than circa 400 – 2000 ppm will be challenging due to the limited or absent driving force. However, at loadings below circa 0.16 mol/mol the experimental data indicate that there is sufficient driving force to achieve capture fractions with a resultant CO_2 concentration at the absorber exit at or below current atmospheric CO_2 levels.

Although at the time of writing there is no published experimental data available demonstrating this rate of CO_2 capture for MEA, recent pilot plant campaigns at Niederaussem (Moser et al., 2024) achieved absorber exit CO_2 concentrations of 321 ppm with a specific reboiler duty (SRD) of 3.85 GJ/tCO_2 using a CESAR1 solvent.

In studies where this requirement for lower lean loadings is recognised, sub-optimal regeneration conditions are typically employed, increasing the required heat input to achieve the lower lean loadings and decreasing energy efficiency.

Michailos and Gibbins (Michailos and Gibbins, 2022) describe what they term the “inflection point” phenomenon for solvent regeneration. As the desorber reboiler produces lower lean loadings, the energy of regeneration required to produce that lean loading is relatively constant until a distinct point or “inflection point”, where the energy input needed to achieve a lower lean loading increases exponentially. The process modelling predicts that this is due to an increased rate of production of steam in the reboiler relative to CO_2 release from the solvent. This steam production rate eventually exceeds the capacity of the desorber column to condense, resulting in increased heat rejection in the reflux condenser. The same process modelling indicates that this steam production can be suppressed by increasing the desorber operating pressure. This allowed lower lean loadings (circa 0.12 mol/mol) to be achieved with specific reboiler duty similar to that of traditional lean loadings at the cost of higher reboiler operating temperatures and increased exergy of reboiler steam. Michailos and Gibbins predict that, when increased regeneration pressures are used to suppress this inflection point, increasing the CO_2 capture fraction from 95% to 99% increases the thermal energy requirement by just 7.7% (3.50 to 3.77 GJ/tCO_2) for a 35 %wt. MEA solvent solution and a CCGT flue gas.

This thesis, above all else, was produced to explore the thermodynamic, process, and economic conditions needed to allow post-combustion CO_2 capture plants to operate with net-zero GHG emissions. Paramount among these is the need to increase CO_2 capture fractions up to their economic limit. The CO_2 capture fraction this entails is tied, inextricably, to the lowest cost permanent negative emission technology (NET). The economic optimum CO_2 capture fraction for any CO_2 capture plant operating under a net zero obligation is the point at which the marginal cost of CO_2 capture, that is, the cost of increasing the CO_2 capture fraction above its current level, is higher than the cost of the recapture of the emitted CO_2. This is a moving goalpost and is not only process, project and geologically specific but also temporally variable as the cost of negative emissions decreases into the future.

Nevertheless, an indicative point must be chosen, and the point at which no additional CO_2 is added to the atmosphere from direct operations seems like a pertinent choice for evaluation. Again, this is process-specific, as the gross CO_2 capture rate across the absorber that results in zero fossil CO_2 being emitted (i.e. circa 420ppm in the flue gas leaving the absorber)

depends on the ratio of atmospheric CO_2 entering the boundary of the plant to the amount of fossil CO_2 generated in the process (Equation 1).

$$\frac{Mass\ CO_{2_{Fuel^*}}}{Mass\ CO_{2_{Fuel^*}} + Mass\ CO_{2_{Atmospheric}}} = \frac{Mass\ CO_{2_{Captured}}}{Mass\ CO_{2_{Flue\ Gas}}} = CO_2\ capture\ \%_{Gross} \qquad (1)$$

* Assuming complete combustion

For a typical CCGT with a CO_2 concentration of 4-5% in the flue gas, a gross CO_2 capture fraction across the absorber of 99 to 99.2% is required, increasing to 99.6 - 99.7% for a Biomass, EfW or coal-fired power plant and 99.8% for an SMR. Due to the varying nature of this gross CO_2 capture fraction, the term 100% fossil CO_2 capture is used hereafter.

Techno-economic analysis of an SMR and CCGT operating with 100% fossil CO_2 capture are presented in Chapter 3 & Chapter 4, respectively. Chapter 5 presents the novel CFP plant configuration operating at 100% fossil CO_2 capture.

Model Validation

Two key modelling software packages are used to predict the performance of the processes described in Chapters 3, 4 & 5.

For any plant upstream of the flue gas fan i.e. CCGT, SMR and CFP processes, gPROMS Process Builder (gPROMS, 2021) was utilised. gPROMS is a process modelling platform that allows the creation of bespoke unit models for each specific plant operation (i.e. gas turbine, superheater, pumps etc.), with the user defining the equations that govern the unit performance. gPROMs uses the Peng-Robinson equation of state for gas mixtures and the Scientific Formulation IAPWS-95 for water and steam. Where available, the performance of a unit was validated and tuned against published performance information. For example, the GE 9HA.01 gas turbine developed in gPROMs was validated against published performance (General Electric, 2017) in open cycle mode and tuned to key plant performance data i.e. turbine exit temperature, thermal efficiency, flue gas flow rate etc. to achieve the best possible fit to the data. Where unit level performance was not available, i.e. HRSG tube banks, a system validation was completed. Net plant efficiency and power output was tuned to published performance data while remaining within allowable engineering limits i.e. HRSG pinch and flue gas exit temperatures. In each case, this validation was completed prior to the integration of PCC to allow validation against OEM performance data.

Table 1: CCSI Validation range vs Range investigated in this work

		This Work	2014 Campaign	2017 Campaign
Lean Loading	mol/mol	0.04 – 0.30	0.06 – 0.40	0.14 – 0.34
CO_2 Concentration	Vol %	4.7 – 19.5 (wet)	8.2 – 11.6 (dry)	7.6 – 11.7 (dry)
CO_2 capture Fraction	% Gross	90 – 99.8	54 – 99.9	51.7 – 97.5
MEA Concentration	% wt. unloaded	35	27 – 33	29 - 32
Desorber Pressure	Kpa	180 – 440	179 – 185	179 - 191

The process modelling of the CO_2 capture plant is conducted using an open-source MEA model funded by the US Department of Energy and developed by the Carbon Capture Simulation for Industry Impact (CCSI) in ASPEN PLUS (ASPENtech, 2022). This model is validated against pilot-scale data from two dedicated test campaigns comprising of 23 (Morgan et al., 2018) and 29 (Morgan *et al.*, 2020) data sets obtained from MEA test campaigns at the

US National Carbon Capture Centre (NCCC). The CCSI model reports good accuracy against the experimental data, predicting CO_2 capture efficiency with an average uncertainty of 2.6 ± 0.5%.

However, as this work investigates previously unexplored areas of PCC operation, the validation data used in the development of the CCSI model does not extend entirely to the ranges investigated here. Notably lower lean loadings, higher desorber pressures and low CO_2 concentrations in the CCGT flue gases. This is detailed in Table 1. This introduces a degree of uncertainty into the analysis as there is a reliance on extrapolation from the experimental data. However, this is mitigated somewhat by the fact that the CCSI model appears to match experimental VLE data well, even at low lean loadings (ref Figure 5). At the time of writing this uncertainty is unavoidable as there is no alternative model available that is validated at the ranges investigated, highlighting the need for further work.

The interface between the gPROMs and CCSI models is managed manually, by passing flue gas data from the gPROMs model to CCSI and the resultant auxiliary power and steam demand from the CCSI model back to gPROMs to resolve for the updated demand, this is iterated until convergence.

Life Cycle GHG emissions

While direct CO_2 emissions from plant operations make up a large portion of the lifecycle GHG emissions of an energy vector decarbonised with CCUS, a non-trivial quantity occurs down and upstream of the process. Upstream, supply chain emissions dominate, which, in the case of natural gas-powered processes, primarily occur during the extraction, processing, and transport of said natural gas. Downstream emissions can occur in the CO_2 transport and storage network and have been quantified as 19.2 $kgCO_2e/tCO_2$ captured (or 1.92%) by Paulillo et al. (Paulillo *et al.*, 2024). Emissions attributed to the construction and decommissioning of a plant must also quantified. Paulillo et al. (Paulillo *et al.*, 2024) provide an estimate of 0.85 $kgCO_2e/tCO_2$ captured for the CO_2 capture plant. Spath and Mann provide lifecycle analysis for both SMR (Spath and Mann, 2001) and a CCGT (Spath and Mann, 2000), attributing 41 $gCO_2e/Kg\ H_2$ and 2 $kgCO_2e/MWh$ to the construction and decommissioning of the SMR and CCGT plants, respectively.

Bauer et al. (Bauer *et al.*, 2022) completed a review of global natural gas supply chain emissions; while large spatial and temporal variability is observed, they concluded that a mid-range value emission rate of 1.5% mass of CH_4 emitted per mass of natural gas is appropriate for lifecycle assessments, attributing an additional 9.5 gCO_2e/MJ (HHV) to non-methane leakage-related GHG emissions such as energy demand, transport and storage infrastructure, and flaring. Additionally, the UK's low carbon hydrogen standard (UK Gov (C), 2022b) advises the use of an emission factor of 6.29 gCO_2e/MJ (LHV) for the UK natural gas supply chain.

The climate's response to the emission of methane gas is different to that of CO_2. While the radiative efficiency of atmospheric methane is greater than that of CO_2 ($5.7 \pm 1.4 \times 10^{-4}$ vs $0.133 \pm 0.16 \times 10^{-4}\ Wm^{-2}ppb^{-1}$) it is much shorter lived (11.8 ± 1.8 years vs centuries to millennia) (Intergovernmental Panel on Climate Change (IPCC), 2023a). In an effort to account for these two competing properties, short-lived GHGs are often reported in CO_2 equivalent values (CO_2e) using some GHG emission metric, the most common of which is Global Warming Potential (GWP), although others exist, including Global Temperature Change Potential (GTP), Global Damage Potential (GDP), and notably, GWP*. GWP values represent the average radiative forcing of a pulse emission of a GHG over a defined time horizon (primarily 20 or 100 years) (Balcombe *et al.*, 2018) and, although convenient in its application, has faced much criticism in recent years. This is primarily based on the need to pick a time horizon of interest, which, for short-lived GHG like methane, can have a large impact on the value of the metric (82.5 vs 29.8 gCO_2/gCH_4 for GWP20 and GWP100, respectively) and the fact that it is based on a single pulse emission, giving no indication of the effect of a sustained

emission source. As methane emissions from natural gas supply chains are not single-pulse emissions but rather sustained emissions over a given period, the use of GWP is inappropriate. Alternatively, for time series emissions of short-lived GHGs, the latest IPCC report (AR6) (Intergovernmental Panel on Climate Change (IPCC), 2023a) suggests that the use of new metrics (combined GTP (CGTP) or GWP*) more closely matches the climate effect of these scenarios.

GWP*, proposed by Allen et al. (Allen *et al.*, 2018) (Equation 2), relates the current or forecasted methane emissions from a source to historical values, and a net change in atmospheric CO_2e for that year is predicted; a detailed analysis of methane emissions under the GWP* model is available in Chapter 3.

$$CO_2\mathrm{e(t)} = \mathrm{GWP100} * [4.53 * \mathrm{E_{CH4}\,(t)} - 4.25 * \mathrm{E_{CH4}(t-20)}] \quad (2)$$

Where t is the year under analysis, $CO_2e(t)$ is the equivalent CO_2 emissions resulting from methane emissions in year t (tCO_2e/pa), GWP100 is the global warming potential value of methane over 100 years, and $ECH_4(t)$ is the total annual methane emissions in year t (tCH_4/y).

Using GWP* and an assumed 25-year operational life of an asset, the emission factor presented by Bauer et al.(Bauer *et al.*, 2022), i.e. 1.5%, results in a mid-term climate impact (>50 years) from methane leakage in the supply chain of 2.3 gCO_2e/MJ (HHV).

In order for industrial processes to be net zero, these life cycle emissions will need to be reduced as far as reasonably practical in the first instance, with the remainder recaptured and permanently stored using some form of NET, i.e., afforestation, advanced weathering, or soil management, assuming that permanence of storage can be assured, or CCS-enabled NETs such as bioenergy with CCS (BECCS) or DACCS. The techno-economic implications of the recapture of residual life cycle emissions from an SMR and CCGT are explored in Chapters 3 and 4 respectively.

Flexible operation

In a dynamic energy system, the production rate of a given energy vector may be required to change to match the demand or available storage capacity, meaning that the associated CCUS plant may see frequent changes in the quantity or composition of flue gas to process. This is particularly prominent for power generation with CCUS, as these plants are expected to play a large role in grid stabilisation and energy security, responding dynamically and frequently to match supply with demand as the generation output from the renewable energy fleet varies, with hundreds of start-up sequences per year not uncommon for a mid-merit CCGT (Calvert and MacKenzie, 2020). Indeed, in the UK, the main funding mechanism for power CCUS projects, the dispatchable power agreement (DPA) (UK Gov (A), 2022a), requires the generator to demonstrate a time averaged CO_2 capture fraction within 5% of the design value, for which 95% is considered the best available technology (BAT) (Gibbins and Lucquiaud, 2021), under all operational modes, inclusive of start-up, shut-down and load changes.

Historically, CCUS plants have been designed to operate primarily under steady-state conditions, experiencing minimal load changes and infrequent start-up and shut-down (SUSD) sequences. Therefore, operating under dynamic conditions while ensuring a high level of CO_2 capture (>95%) poses a novel challenge to designers. Critical to ensuring high CO_2 capture fractions in a PCC plant is ensuring that the flue gas in the absorber is always matched with sufficient quantities of lean solvent at the appropriate loading. During load changes, this poses a challenge, as the desorber, in which the lean solvent is generated, is slow to respond due to thermal inertia in the system. This is exacerbated during a start-up sequence as, in the early stages of the process, no or low levels of steam are available, curtailing the ability to generate lean solvent for CO_2 capture.

The question then becomes, how can the absorber be supplied with lean solvent with the appropriate loading in sufficient quantities to maintain high levels of CO_2 capture at all times? An engineered solution is to generate and store sufficient quantities of lean solvent in advance of a start-up sequence, which allows for the capture of CO_2 independent of the desorbers current capacity to generate lean solvent (Calvert and MacKenzie, 2020). The rich solvent generated during this process is then stored until sufficient steam is available to regenerate it.

Chapter 7 presents analysis completed by the author as part of a project[4] which investigated, through process modelling, pilot-scale testing, and data from an operational CCGT, the combination of solvent storage with an optimised CCGT and CO_2 capture plant start-up sequence to achieve CO_2 capture fractions in excess of 97% during a simulated start-up event. Of particular note is the use of operational data from a commercial CCGT to explore the use of "early" and "late" steam available during SUSD events. This is the primary novel contribution of the author although he provided technical input to all aspects of the project.

The above chapter provides context to the need to reduce GHG emissions from facilities operating with CO_2 capture down to zero, summarises the state of the art in post combustion CO_2 capture and analyses the existing literature that pertains to ultra-high CO_2 capture fractions and lifecycle GHG emissions, highlighting the strengths and weaknesses. The following chapters detail the authors novel contributions to the field as part of this doctoral degree.

[4] FOCUSS (Flexibly Operated Capture Using Solvent Storage) was a project is funded by the UK Department for Energy Security and Net Zero (DESNZ) under the Carbon Capture, Usage and Storage (CCUS) Innovation 2.0 Programme. It is an industry-led project managed and delivered by a consortium consisting of SSE Thermal (project lead), the University of Sheffield and AECOM. (https://www.gov.uk/government/publications/carbon-capture-usage-and-storage-ccus-innovation-20-competition-call-1-successful-projects)

3. On the cost of zero carbon hydrogen: A techno-economic analysis of steam methane reforming with carbon capture and storage

As hydrogen has increasingly been considered a critical component of the net zero transition (Joffe *et al.*, 2018), it is imperative that it is produced in a low and eventually zero-carbon fashion. It is currently foreseen that large scale low carbon hydrogen will be produced using one of two production methods:

- Electrolysis using dedicated or excess renewable electricity (green hydrogen): Hydrogen is produced via the electrolytic separation of water into hydrogen and oxygen using surplus or dedicated renewable electricity. The carbon intensity of production is a function of the CO_2 intensity of the electricity used and the lifecycle CO_2 intensity of the equipment, with Valente et al. (Valente, Iribarren and Dufour, 2017) estimating the Global Warming Potential (GWP) of electrolytic hydrogen produced via wind power at 0.16 – 2.02 $kgCO_2/kg\ H_2$.
- Hydrocarbon reforming with CO_2 capture and storage (CCS) (blue hydrogen): The separation of a hydrocarbon into hydrogen and organic molecules (typically CO_2 and CO) with subsequent capture and storage of the produced CO_2. Global production of hydrogen via Hydrocarbon reforming is dominated by the steam reformation of methane (CH_4) in steam methane reformers (SMRs). When coupled with CCS achieving a 90% CO_2 capture fraction, direct CO_2 emissions are of the order of 1.03 $kgCO_2e/kg\ H_2$, however this excludes lifecycle emissions.

This work presents a model of a 1000 MWh_{th} (Higher Heating Value (HHV)) SMR produced in gPROMS Process Builder (gPROMS, 2021) coupled with an open-source steady-state post combustion capture (PCC) model (Morgan *et al.*, 2020) using a 35% wt. monoethanolamine (MEA) solution. Three distinct CO_2 capture fractions are analysed: 90% (or 10% residual emissions) present for context with historical studies, 95% (or 5% residual emissions) as the current best available technology (BAT) for PCC plants in the UK (Gibbins and Lucquiaud, 2021), and the capture of 100% of the fossil CO_2 produced in the process, nominally 99.8% of the CO_2 entering the CO_2 absorber. Driving force of CO_2 absorption is maintained in the absorber, even at increased CO_2 capture fractions, via the use of low lean loadings (0.16 mol/mol), 20m of absorber packing and intercooling to reduce the bulk temperature and promote CO_2 absorption. Efficient regeneration of the solvent to the low lean loading is

achieved by increasing the CO_2 stripping pressure to 210Kpa and temperature to 125^oC, a value historically thought to limit thermal degradation (Elliott, 2022) of MEA solvents.

Greenhouse Gas (GHG) emissions from the natural gas supply chain, CO_2 transport and storage network, and plant construction/decommissioning are estimated from the available literature. Their recapture using permanent negative emissions is proposed as a method of ensuring zero lifecycle emissions production of hydrogen, with direct air CO_2 capture and storage (DACCS) with an estimated cost of 100-1000 £/tCO_2 serving as the highest cost scenario.

The output of a bespoke multi-level factorial cost model predicts the plant capital expenditure (CAPEX) and operational (OPEX) expenditure feeds a comprehensive economic analysis and sensitivity study, estimating the levelised cost of hydrogen (LCOH) and levelised cost of capture (LCOC) for each CO_2 capture fraction and the net zero case, where lifecycle CO_2 capture emissions are recaptured, while the cost of CO_2 avoided is calculated for the counterfactual, natural gas combustion, advising the natural gas price that would make blue hydrogen competitive with both green hydrogen and natural gas combustion with recapture using direct air capture.

International Journal of Greenhouse Gas Control 126 (2023) 103904



Contents lists available at ScienceDirect

International Journal of Greenhouse Gas Control

journal homepage: www.elsevier.com/locate/ijggc





On the cost of zero carbon hydrogen: A techno-economic analysis of steam methane reforming with carbon capture and storage

Daniel Mullen [a,*], Laura Herraiz [a], Jon Gibbins [b], Mathieu Lucquiaud [b]

[a] School of Engineering, The University of Edinburgh, Edinburgh, United Kingdom
[b] Department of Mechanical Engineering, The University of Sheffield, Sheffield, United Kingdom

ARTICLE INFO

Keywords:
Carbon capture and storage
Zero carbon hydrogen
Net zero
CCUS
Blue hydrogen
Techno-economics

ABSTRACT

This article challenges the view that zero carbon hydrogen from steam methane reforming (SMR) is prohibitively expensive and that the cost of CO_2 capture increases exponentially as residual emissions approach zero; a flawed narrative often eliminating SMR produced hydrogen as a route to net zero. We show that the capture and geological storage of 100% of the fossil CO_2 produced in a SMR is achievable with commercially available post-combustion capture technology and an open art solvent. The Levelised Cost of Hydrogen (LCOH) of 69£/MWh_{th} HHV (2.7£/kg) for UK production remains competitive to other forms of low carbon hydrogen, but retains a hydrogen lifecycle carbon intensity of 5 gCO_2e/MJ (LHV) due to natural gas supply chain and embodied greenhouse gas (GHG) emissions. Compensating for the remaining lifecycle GHG emissions via Direct Air Capture with geological CO_2 Storage (DACCS) increases the LCOH to 71–86 £/MWh_{th} HHV (+3–25%) for a cost estimate of 100–1000 £/tCO_2 for DACCS and the 2022 UK natural gas supply chain methane emission rates. Finally, we put in perspective the cost of CO_2 avoidance of fuel switching from natural gas to hydrogen with long term price estimates for natural gas use and DACCS, and hydrogen produced from electrolysis.

1. Introduction

Hydrogen is increasingly being recognised globally as a useful component of a net zero greenhouse gas (GHG) economy, since no CO_2 is produced at the point of use. It is a potential energy vector for decarbonising decentralised emission sources such as home heating and heavy goods vehicles (HGV), or industries where electrification or direct CO_2 capture is impractical (Joffe et al., 2018).

The need for rapid scale up of low GHG emission hydrogen production has been reflected in the Sixth Carbon Budget (Stark et al., 2020), issued by the UK Committee on Climate Change, and the 2021 UK hydrogen strategy (UK Hydrogen, 2021). This report suggests that 250–460TWh HHV (Higher Heating Value) of hydrogen will be needed in the UK annually by 2050, making up 20–35% of total energy consumption. For comparison, 27 TWh HHV of hydrogen was produced in the UK in 2016 (Heap et al., 2016), primarily for industrial processes such as ammonia production. The UK has recently set a target of installing up to 10GW of low carbon hydrogen production capacity by 2030 (Beis 2022) in order to meet the goals set out in the Sixth Carbon Budget.

Large-scale low carbon hydrogen production in the UK is expected to be mainly accomplished by a combination of the following methods:

- Electrolysis using dedicated or excess renewable electricity (green hydrogen): Hydrogen produced in this fashion provides one route to low carbon hydrogen with a direct CO2 intensity of 0.1 gCO_2e (equivalent)/MJ H2 Lower Heating Value (LHV). However, currently Levelised Costs of Hydrogen (LCOH) in excess of 109£/MWh_{th} HHV are reported by the UK Department for Business, Energy and Industrial Strategy (BEIS) due to high capital costs, low load factors and limited availability of surplus electricity (UK Hydrogen, 2021; Hydrogen production costs 2021).
- Methane reforming with CO_2 capture and storage (blue hydrogen): This includes a Carbon Capture & Storage (CCS) system, which separates the CO_2 produced during the process for permanent geological storage. This process may be done in a Steam Methane Reformer (SMR) or an Autothermal Reformer (ATR). The carbon intensity of the hydrogen produced varies depending on the CO_2 capture fraction applied. Typical reported values lie between 0 – 21.4 gCO_2e/MJ H2 (LHV) (UK Hydrogen, 2021). In the past, lower capture fractions (~90%) have been assumed for SMR+CCS and higher values (~95%) for ATR+CCS (e.g. see (Hydrogen production costs

* Corresponding author.
E-mail address: D.T.Mullen@sms.ed.ac.uk (D. Mullen).

https://doi.org/10.1016/j.ijggc.2023.103904
Received 7 November 2022; Received in revised form 29 April 2023; Accepted 5 May 2023
Available online 10 May 2023
1750-5836/© 2023 The Author(s). Published by Elsevier Ltd. This is an open access article under the CC BY license (http://creativecommons.org/licenses/by/4.0/).

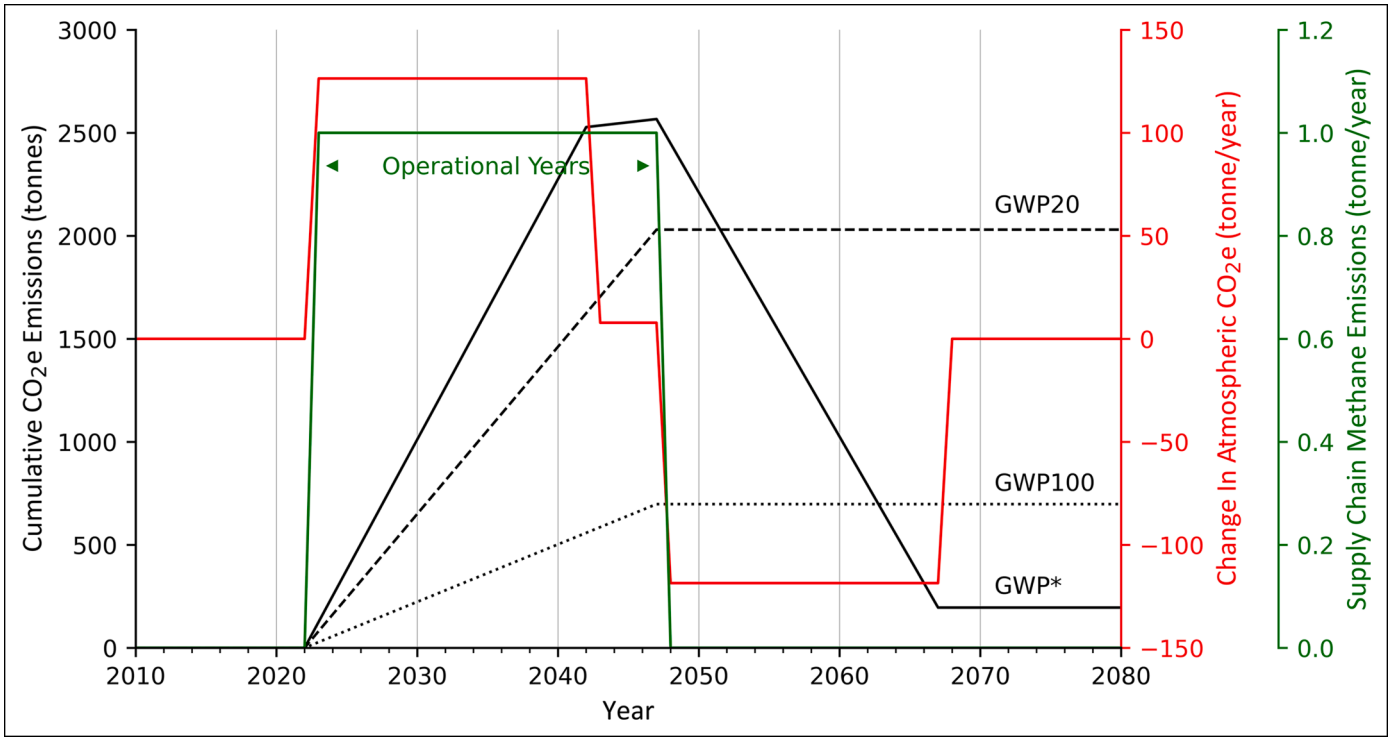


Fig. 1. Comparison of GWP*, GWP100 & GWP20 when evaluating cumulative CO_2e emissions resulting from a sustained methane emission rate of 1 tonne per annum over a 25 year period. The green line represents annual methane emission's while the red line shows net change in atmospheric CO2e per year as predicated by GWP*.

2021)). In a recent UK study LCOH for SMR+CCS production with a natural gas price of 19–46£/MWh_{th} HHV are reported at 39–73 £/MWh_{th} HHV with a direct CO2 intensity of 8.7 $gCO_2e/MJ\ H_2$ (LHV)(Hydrogen production costs 2021).

As noted above, for blue hydrogen production the amount of CO_2 captured relative to the amount of CO_2 produced (CO_2 capture fraction) in SMRs is often assumed to be 90% and, with the assumed future increases in CO_2 emission costs, this will lead to significant escalation in the predicted cost of hydrogen production using SMR+CCS. It is clear that 10% residual emissions, if truly unavoidable, cast doubt on the viability of SMR+CCS produced blue hydrogen as a climate mitigation technology in the context of an energy system compatible with net zero GHG ambitions.

Indeed this is the case in a recent article published by Howarth and Jacobson (Howarth and Jacobson, 2021) claiming that uncaptured CO_2 emissions from the SMR process, coupled with the energy required to drive the CO_2 capture process and the upstream methane emission result in a carbon intensity of blue hydrogen of 88–91% that of an SMR with no CO_2 capture. The assumptions made by Howarth and Jacobson are widely criticized by Romano et al. (Romano et al., 2022). As an illustration, the SMR model proposed by Howarth and Jacobson assumes a net CO_2 capture fraction of just 61%, an average capture fraction of 76% is applied to the SMR with no allowance for the capture of the CO_2 generated due to the additional energy requirement imparted by CO_2 capture, a critical oversight. Despite the low CO_2 capture fraction, a thermal energy consumption rate in the CO_2 capture plant of 6.25 GJ/tCO_2 captured is implicit in the analysis. This is assumed to be supplied via the combustion of additional methane with no thermal integration to the SMR plant or supplementary electricity generation, as such, the thermal energy used is high grade and a poor application of the 2nd law of thermodynamics. This represents a dramatic deviation from the low grade thermal energy, typically low pressure steam, requirement reported in operational plants. Nessi et al. (Nessi; et al., 2021) recently completed a review of 37 PCC plants in or previously in operation worldwide. 25 plants had sufficient data available in the public domain and reported an achieved specific thermal energy requirement for CO_2 capture of between 2.1–3.7GJ/tCO_2, with CO_2 capture fractions ranging from 45% in one case to up to 98%, with circa 90% being typical.

This article extends on Romano et al. (2022) to add evidence on the integration, design, operation and costs of hydrogen production with 100% CO_2 capture, and the added costs of permanent offsetting to achieve zero lifecycle carbon intensity. It is timely with a growing body of research on ultra-high CO_2 capture operation, and timely with regulatory developments pushing for increasing capture fractions in the permitting of new CCS facilities.

Recent UK guidance by the UK Environment Agency (Gibbins and Lucquiaud, 2021; Gibbions and Lucquiaud, 2021) notably considers a 95% CO_2 capture fraction as the current Best Available Technology (BAT) for post-combustion CO_2 capture from biomass and gas-fired thermal power plants, while a 95% or above capture fraction for SMR+CCS is considered by Curtis et al. in a recent BAT review on hydrogen production methods (Curtis, 2022). The National Energy Technology Laboratory, in a report for the US Department for Energy, found that transitioning from an unabated SMR to operating with a 96% capture fraction increased the LCOH from 1.06 $/kg H_2 to 1.64 $/kg H_2 (Comparison of commercial 2022). The UK low carbon hydrogen standard published in 2022 considers 20 $gCO_2e/MJ\ H_2$ (LHV) the maximum net carbon intensity (inclusive of all supply chain and construction emissions) threshold for acceptance as low carbon hydrogen (UK 2022). As this standard proposes the functional unit of CO_2 intensity of hydrogen to be $gCO_2e/MJ\ H_2$ (LHV) it will be reported as such in this study for comparative purposes.

The growing body of evidence suggesting that ultra-high capture fractions, defined here as CO_2 capture fractions equal to or higher than 99%, can be technically and economical feasible is reported in Feron et al. (2019); Danaci et al. (2021); Michailos and Gibbins (2022); Gao et al. (2019); Ismail Shah et al. (2021); Hirata et al. (2019). Feron et al.

reported that increasing the CO_2 capture fraction of a post-combustion solvent-based system (30%wt MEA) from 90% to a zero residual emission level would give a 1.5 percentage point reduction (34.5% to 33%) in thermal efficiency on a LHV basis for a ultra-supercritical coal fired power plant, and a 2.2 percentage point reduction for a natural gas fired combined cycle (48.6% to 46.4% LHV) (Feron et al., 2019). Work completed by Danaci et al. reported that, for a representative flue gas flow rate of 500 kg/s, a 30%wt MEA solvent and flue gas CO_2%vol concentrations of 4%, 10% and 20%, transitioning from 90% to 99% CO_2 capture results in an increase in total capture cost of 7%, 10% and 13% respectively (Danaci et al., 2021). A process modelling study of CO_2 post-combustion capture from a combined cycle gas turbine power plant by Michailos and Gibbins reported that transitioning to 99% CO_2 capture from 95% can be achieved with a moderate increase of 7.7% in the specific thermal energy input to the reboiler (specific reboiler duty) of the CO_2 capture process for a 35%wt solvent solution, providing the absorber is sufficiently sized and the desorber pressure is high enough to avoid excessive water vapour in the product CO_2 at the reduced lean loading required (Michailos and Gibbins, 2022). Pilot scale tests at the National Carbon Capture center (NCCC) completed by Gao et al. find that increasing the CO_2 capture fraction of a coal-fired power plant from 90% to 99% resulted in an increase in specific reboiler duty of lower than 5% with a 5 m piperazine (PZ) solvent solution (Gao et al., 2019). Tests completed at Technology Centre Mongstad show that, with 24 m of packing, 35 - 37%wt monoethanolamine (MEA) solvent and a CO_2% vol of 3.9–4.2%, 99% CO_2 capture can be achieved with a specific reboiler duty of 3.8 GJ/tCO_2 compared to 3.6 GJ/tCO_2 for a 90% CO_2 capture fraction (Ismail Shah et al., 2021), approximately a 6% increase. Hirata et al. working with Mitsubishi Heavy Industries Engineering, Ltd using a proprietary solvent (KS-1™) investigated 99.5% CO_2 capture fraction for a reference 650 MW_e coal fire power plant and predicted that near zero emissions could be achieved with a 3% increase in the total annualised cost of CO_2 Capture ($/t$CO_2$) (Hirata et al., 2019).

When considering the life cycle emissions of hydrogen production from natural gas, it is also essential to account for all aspects of the hydrogen supply chain; venting, flaring and pipeline natural gas emissions are potentially large contributors to the carbon intensity of blue hydrogen.

While methane is a more potent greenhouse gas than CO_2, it is shorted lived in the atmosphere with an estimated perturbation residence time of 11.8 ± 1.8 years (Masson-Delmotte et al., 2021) and, as such, does not accumulate in the in the same way. If, for example, methane emissions from the previous decade were equal to current emissions virtually no additional contribution to the rate of warming would have occurred because the level of atmospheric methane remains approximately constant. Research completed by Oxford University (Smith et al., 2021; Cain et al., 2019) suggests that the use of Global Warming Potential (GWP) values consistently overestimates the warming effect of methane in scenarios where global methane emissions are constant or reducing and recommends the use of an alternative metric called GWP*. This metric relates current or forecasted annual methane emissions to historical values and a CO_2e value for the net change in atmospheric methane is predicted. CO_2e values under GWP* are calculated as shown in Eq. (1). Climate modelling (Smith et al., 2021; Cain et al., 2019) studies suggest that GWP* correlates with global temperature response to methane emissions to a much higher degree of accuracy than GWP.

$$CO_2e(t) = GWP_{100} * [4.53 * E_{CH_4}(t) - 4.25 * E_{CH_4}(t-20)] \quad (1)$$

Where t is the year under analysis, CO_2e(t) is the equivalent CO_2 emissions resulting from methane emissions in year t, GWP_{100} is the global warming potential value of methane over 100 years and E_{CH4}(t) is the total annual methane emissions at year t.

Fig. 1 shows the predicted cumulative CO_2e emissions resulting from a sustained 1 tonne of annual methane emissions over a 25 year period when calculated using GWP*, GWP100 and GWP20. Fig. 1 illustrates that the GWP100 and GWP20 metrics fail to capture the short lived nature of methane emissions and assume that the resulting CO_2e emissions remain present in the atmosphere indefinitely. GWP*, however, shows a spike in CO_2e emissions in excess of that predicted by GWP100 & 20 in the first 20 years of operation. The rate of emissions then drops off in the final 5 years of operation and, as the historical methane emissions oxidise. A rapid decline in cumulative atmospheric CO_2e is seen once methane emissions cease, eventually returning to a net change in atmospheric CO_2e of 195tCO_2e, much lower than the 678 & 2030 tCO_2e predicted by GWP100 & 20 respectively. For simplicity GWP* assumes all oxidation of atmospheric CH_4 occurs at year 20, in reality there is an exponential decrease in of the quantity of atmospheric CH_4 over time, the end result being a reduction in the peak atmospheric CO_2e presented in Fig. 1. Fig. 1 illustrates how GWP100 and GWP20 (as used by Howarth and Jacobson (Howarth and Jacobson, 2021)) can overestimate the long term net climate impact of methane emissions, hence GWP*, as a more accurate metric, is used in this work.

It is worth noting that, although the net cumulative CO_2e predicted by GWP* eventually falls to 195tCO_2e per tonne of sustained methane emissions over 25 years, temporary driving of global warming in excess of what could be attributed to this long term value will occur in the period of elevated atmospheric CO_2e i.e. during and immediately after cessation of methane emissions. This temporary warming rate increase requires consideration during the environmental impact assessment of a proposed project and highlights the importance of efforts to reduce fugitive methane emissions from supply chains.

A recent review on the climate impacts of blue hydrogen by Bauer et al. (Bauer et al., 2022) characterises global natural gas supply chain emission rates as "grams of CH_4 emitted per gram of natural gas delivered". Large variability is noted on both spatial and temporal bases, with the emission rate and measurement accuracy also varying considerably based on the producer in question. Near zero emissions of 0.1% is reported in regions such as Norway and Qatar while emission factors of over 6% are reported in areas such as Libya and Iraq. Bauer et al. used a factor of 1.5% for a mid-range value in their life cycle assessments. Additionally, the recent low carbon standard issued by the UK BEIS advises using an average carbon intensity of natural gas supply of 6.29 gCO_2e/MJ (LHV) (calculated using GWP100) for the UK natural gas supply chain (UK 2022), which corresponds to an emissions rate of 1.04%. In a net zero economy, where any remaining life cycle emissions will have to be compensated for via the use of Carbon Dioxide Removal Technologies (CDRs), as the likely lowest cost option these supply chain emissions will need to be reduced as far as reasonably practicable, a goal echoed by the recent COP26 pledge to reduce global methane emissions by 30% by 2030 (Cop26, 2021).

An important concept in CDRs is the permanence of CO_2 storage away from the atmosphere. Climate change is likely to be a millennium spanning challenge due to the very long lifetime of CO_2 in the atmosphere and the inertia of the climate response to rising atmospheric CO_2 concentrations, and thus any negative emission technology must be consistent with a long term mitigation strategy. Nature-based negative emissions via e.g. reforestation, soil management have uncertain permanence compared to the use of engineered technologies such as Bioenergy with CCS (BECCS) and Direct Air Capture (DACCS) that place the CO_2 in secure geological storage with expected retention of over 10,000 years (Alcalde et al., 2018). For the purposes of this paper DACCS is used as the CDR technology for comparisons, since it is less dependant on finite ecosystem limitations than BECCS. Since DACCS has a higher reported cost than most other CDR technologies (Fuss et al., 2018), this also sets a cap on the premium for permanently compensating for indirect emissions in the hydrogen production chain. Due to limited commercial deployment to date, evidence-based cost estimates for future DACCS are currently unavailable. A recent review by McQueen et al. investigates the current state of the art in DACCS technology (Mcqueen et al., 2021). They place the near-term cost of commercial DACCS (excluding transport and geological storage costs) at

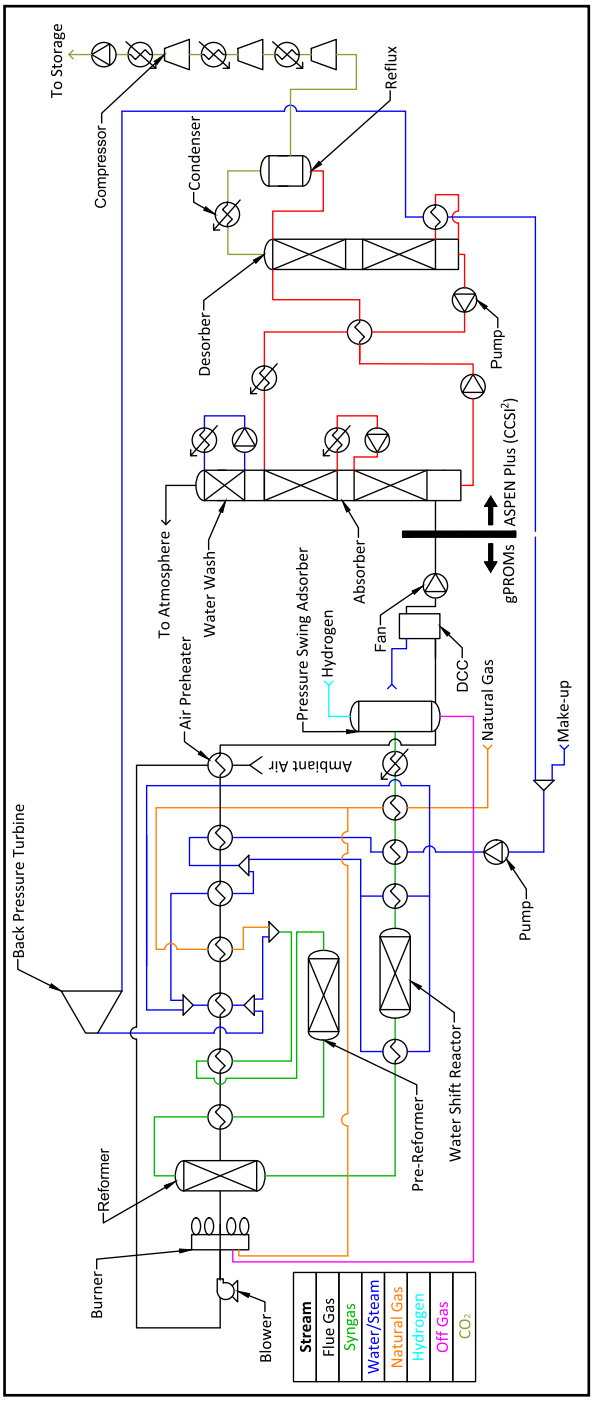


Fig. 2. Steam methane reformer with post combustion carbon capture configuration.

350–400£/tCO_2 and conclude that prices are expected to fall as DACCS deployment increases and the "learn by doing" effect is realised. A cost range of 100–1000£/tCO_2 with a median value of 300£/tCO_2 is used in this paper; it is considered to cover a band consistent with values reported by the International Energy Agency (Direct Air Capture 2022).

The techno-economic analysis of a conventional steam methane reformer (SMR) in this paper includes three post-combustion capture (PCC) plant options that are designed and optimised for distinct CO_2 capture fractions:

- Net 90% CO_2 capture with 10% residual emissions, corresponding to a production carbon intensity of 8.6 $gCO_2e/MJ\ H_2$ (LHV). It is included to provide comparable evidence with previous studies.
- Net 95% CO_2 capture with 5% residual emissions, corresponding to a production carbon intensity of 4.3 $gCO_2e/MJ\ H_2$ (LHV). This is included to keep in line with recent regulatory developments in the UK for the permitting of post-combustion capture units.
- Zero residual emissions, i.e. 100% capture of the fossil carbon entering the boundaries of the hydrogen plant, with a production carbon intensity of 0.0 $gCO_2e/MJ\ H_2$ (LHV). It corresponds to an overall CO_2 capture fraction of 99.8% in the CO_2 capture plant, once atmospheric CO_2 entering the boundaries of the plant in the combustion air is accounted for.

A design of a PCC plant for ultra-high capture fractions from SMR flue gas is presented for the first time, drawing on state of the art research (Feron et al., 2019; Danaci et al., 2021; Michailos and Gibbins, 2022; Gao et al., 2019; Ismail Shah et al., 2021; Hirata et al., 2019), front end engineering design (FEED) studies (Elliott, 2022; Bechtel 2019; Nexant 2016; Bechtel 2018) and computational modelling (Morgan et al., 2020). Results from this PCC model are coupled with a SMR model to establish the additional thermodynamic penalty associated with transitioning to zero residual emission operation.

The output of a detailed multi-level factorial cost model used to predict plant capital expenditure (CAPEX) and operational expenditure (OPEX) feeds a comprehensive economic analysis estimating the Levelised Cost of Hydrogen (LCOH), Levelised Cost of Capture (LCOC) and Cost of CO_2 Avoided (CCA). The cost of producing zero carbon hydrogen on a life cycle basis, with DACCS with geological storage compensating for natural gas supply chain emissions, embodied carbon in construction and CO_2 transport and storage emissions is presented. A sensitivity study establishes to what degree variation in key economic and operational factors effects the LCOH, providing a clear pathway for further cost reductions and de-risking of investments.

2. Methodology

2.1. Modelling methodology for a steam methane reformer (SMR) with post combustion CO_2 carbon capture (PCC)

A model of a 1000 MWh_{th} HHV SMR is produced in gPROMS Process Builder (gPROMS products 2021), a process modelling platform that allows the creation of bespoke unit models for each specific plant operation, Peng-Robinson & IAPWS-95 are used as the gas mixture and steam/water thermodynamic models respectively. The flue gas and low pressure steam conditions is feed into an open source steady state MEA based PCC model (Morgan et al., 2020). This model (Morgan et al., 2020) was created by the Carbon Capture Simulation for Industry Impact ($CCSI^2$) partnership (Ccsi 2022) in Aspen Plus (Aspentech 2022), which was developed using pilot scale data provided by the US National Carbon Capture Centre (NCCC) (National 2021). The output from the PCC model, namely thermal and electrical energy requirements, is then feed back into the SMR model and an iterative design optimisation process is completed.

The SMR with PCC process is illustrated in Fig. 2, the technical and operational parameters are based on a conventional SMR with post-

combustion CO_2 capture in a report commissioned by the IEA Greenhouse Gas R&D Programme (IEAGHG) in 2017 (Collodi et al., 2017). A detailed list of plant parameters are available in Appendix A.

2.2. Flue gas path

The incoming ambient air is preheated to 150–170°C using residual heat from the furnace exhaust flue gas. The preheated air then enters the burners where a mixture of natural gas and off-gases from the pressure swing adsorber is used to raise the flue gas temperature up to 1800–1900°C, whereupon it passes over the reformer tubes to provide heat to an endothermic reforming reaction converting natural gas to hydrogen and carbon monoxide. The flue gas leaves the reformer at ~950°C and the remaining heat is used to reheat process synthesis gas (syngas) and generate steam at 42 bar and 400°C for the reforming process, power generation and thermal energy input to the CO_2 capture plant for solvent regeneration. As noted above, the remaining low grade heat is then used to preheat the incoming ambient air before being sent to the post-combustion CO_2 capture plant for CO_2 removal.

The flue gas exits the air preheater in Fig. 2 and initially passes through a direct contact cooler, cooling the flue gas to saturated conditions at 40°C. A booster fan then increases the flue gas pressure sufficiently to overcome the pressure drop through the absorber train. The flue gas then enters the bottom of a counter current packed bed absorber while CO_2 lean MEA solvent (lean solvent) enters the top. The ratio of lean solvent to flue gas flow rate is often referred to as the liquid to gas ratio or L/G ratio and is set to achieve the required CO_2 capture fraction in the absorber, in conjunction with other process parameters. As the flue gas passes up through the solvent-laden packing, CO_2 transfers to the liquid solvent and reacts exothermically, heating the flue gas and solvent. The CO_2 depleted flue gas leaves the top of the CO_2 capture packing and then goes through a water wash section, to remove residual MEA prior to release to the atmosphere. The now CO_2 rich solvent (rich solvent) leaves the bottom of the absorber to be stripped of CO_2.

If we were to assume constant CO_2 partial pressure in a flue gas, for illustrative purposes only as this is not possible in actuality, the driving force for absorption would decreases as the solvent absorbs CO_2, resulting in a decreased mass transfer rate. When the CO_2 partial pressure in the flue gas is equal to the CO_2 equilibrium pressure above the solvent, the flue gas and the solvent are considered in equilibrium and no further mass transfer will occur. All other things being equal, equilibrium at the bottom of the absorber would result in the minimum thermal energy input for solvent regeneration, i.e. minimum specific reboiler duty, as CO_2 uptake would be maximised while sensible and latent heat addition to the water content of the solvent mixture is minimised. However, due to the decreased driving force of absorption as the system approaches equilibrium, an infinitely large absorber would be required. Specific reboiler duties are expected to always be reduced at higher rich loadings (Michailos and Gibbins, 2022), however, as the packing height increases, the rate of reduction in specific reboiler duty tends to decrease, leading to diminishing returns as the rich loading approaches equilibrium. To the knowledge of the authors, there is no universally accepted criterion to determine absorber height independent of project specific constraints, as it is trade-off between OPEX and CAPEX burden.

The redistribution of liquid in an absorber typically takes place every 20 theoretical stages, corresponding to 8m of Mellapak 252.Y packing, to ensure uniform solvent distribution, with 25 theoretical stages, or 10m of Mellapak 252.Y packing, serving as a realistic upper limit (Ausner, Iija "Maximum packed bed height Mellapak 252.Y" (pers. comm., February 28, 2022)). As a result, a limit of 10m of packing per absorber bed is used in this analysis, although in practice this limit varies according to the packing used and must be properly accounted for during the design phase. In order to reduce CAPEX at higher CO_2 capture fractions, a limit of two absorber beds, or a total of 20m packing, is set as a maximum design constraint. This is supported by evidence from the process models developed as part of this study that predict a marginal reduction in reboiler duty for increases in packing height above 20m.

For capture fractions resulting in zero residual emission configurations, given the lean loading values used in this study, an intercooler is found to be required between the two packed beds of the absorber. This extracts the MEA solvent from the absorber for cooling, thus increasing the capacity of the solvent to absorb CO_2. The solvent passing through the intercooler is cooled down to a pre-set temperature using cooling water before re-admitting it to the absorber. This ensures that sufficiently high rich loadings are achieved.

The rich solvent leaving the bottom of the absorber is pumped to the CO_2 desorber. Prior to the desorber, sensible heat from the hot lean solvent leaving the desorber at ca. 120–130°C is transferred to the rich solvent in the cross-flow heat exchanger. Heat is transferred to the reboiler by condensing low pressure steam extracted from the power cycle associated with the SMR. The heat input required is referred to as the reboiler duty and is usually reported in specific terms, as defined by Eq. (2) (Soltani et al., 2017).

$$q_{reg} = \frac{H_{reboiler}}{\dot{m}_{CO_2}} = q_{sen} + q_{vap,H_2O} + q_{abs,\ CO_2} \quad (2)$$

Where $q_{reg}$is the specific reboiler duty for solvent regeneration, $H_{reboiler}$ is the total thermal input to the reboiler, $\dot{m}_{CO_2}$ is the mass of CO_2 extracted from the solvent, $q_{sen}$is the sensible energy necessary to heat the solvent, q_{vap,H_2O} is the energy associated with evaporating water leaving with the CO_2, and $q_{abs,\ CO_2}$ is the thermal energy associated with CO_2 desorption from the solvent.

The contribution of these three components to the specific reboiler duty varies with solvent rich and lean loadings and, by extension, with the CO_2 capture fraction. Sensible energy is the thermal energy input required to raise the rich solvent temperature from the outlet of the cross-flow heat exchanger to the desorber operating temperature. It is primarily a function of heat exchanger pinch temperatures and solvent flow rates (noting that the lean solvent mass flow rate is inherently lower than the rich solvent mass flow rate). The energy contribution to water evaporation is a function of the desorber pressure and the CO_2 exit temperature at the top of the desorber column plus the water/MEA/CO_2 vapour-liquid equilibrium (VLE). This determines the amount of unrecoverable latent heat of vaporisation of H_2O, which then has to be removed during subsequent condensation and H_2O removal from the CO_2 stream. The third component is the CO_2 desorption energy requirement, which depends on the specific enthalpy of absorption/desorption of the solvent.

As MEA degradation rates increase with temperature, a maximum desorber temperature of 125 °C applied to all cases. This is currently considered appropriate for MEA (Michailos and Gibbins, 2022; Elliott, 2022; Bechtel 2019; Léonard et al., 2015). According to the model predictions, this allows a lean loading of 0.16 mol CO_2/mol MEA to be achieved at a pressure of 210 kPa without increasing specific reboiler duty due to excessive water vapour in the CO_2 exiting the desorber. Higher desorber operating pressures, and hence temperatures, would facilitate achieving lower lean loadings, which may lead to a more economical CO_2 capture process; further research is, however, required to quantify MEA degradation rates at temperatures above 125 °C and also as a function of lean loading and other plant-specific parameters. For example, Braakhuis et al. (2022) recently published MEA thermal degradation data suggesting that reducing lean loading may partially or entirely offset the increase in thermal degradation associated with higher operational temperatures (Braakhuis et al., 2022) as thermal degradation in MEA appears to be rate limited by CO_2 concentration in the solvent.

After leaving the desorber, the lean solvent enters the solvent heat exchanger for cooling prior to entering the top of the absorber while the CO_2/H_2O mixture leaves the top of the desorber and the water is condensed to achieve a CO_2% vol of ca. 95%. The CO_2 rich stream is then

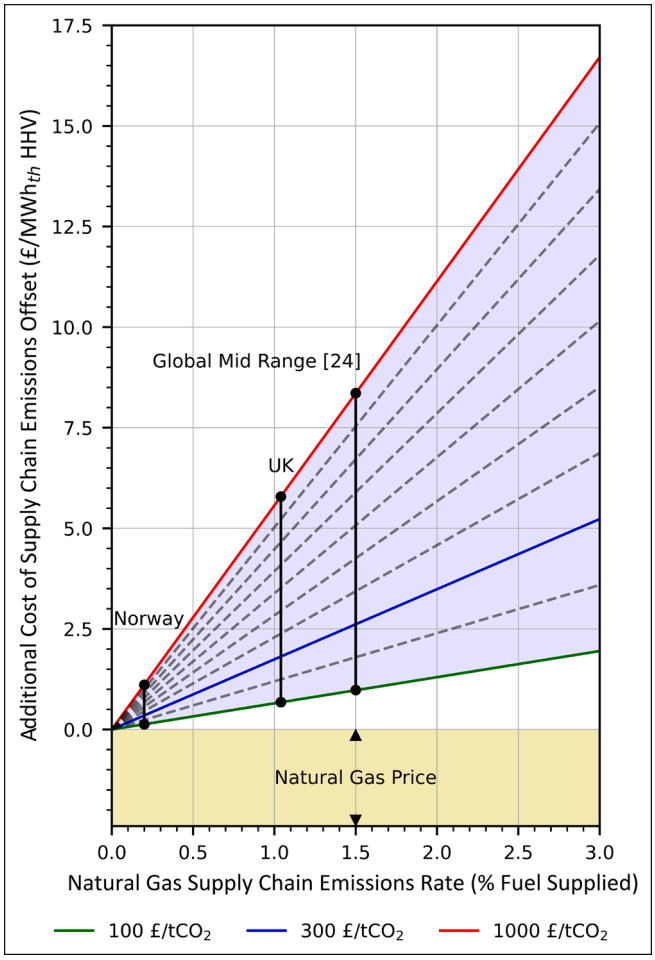


Fig. 3. The additional cost to natural as price to offset supply chain emissions, for a range of supply chain emissions and costs of direct air capture under GWP*.

assumed to be compressed in this study using a three-stage compressor with intercooling (where most of the remaining water is removed) to above the critical pressure of 73.8 bar, where it may be liquefied and pumped up to the required pressure (assumed to be 110 bar in this study) for transport and storage, with a CO_2 purity of ca. 99.9%. No additional heat recovery techniques to reduce the energy penalty are included in this model.

When CO_2 capture fractions are increased, the total quantity of CO_2 absorbed by the solvent per second increases. Ultra-high capture fractions in excess of 99% can be achieved by two means, which can be combined: increasing the solvent flow rate, and by extension q_{sen}, or by increasing the difference between lean and rich solvent loadings, and thus increasing the solvents capacity to absorber CO_2 per kg (which in practice means reducing the lean loading by reducing the partial pressure of CO_2 at the base of the desorber). An increase in absorber packing height relative to that for a lower CO_2 capture fraction may also be necessary to achieve sufficiently high rich loadings and minimise specific reboiler duty at ultra-high capture fractions.

Additionally, and depending also on the lean loading used, the location along the absorber and absolute quantity of heat released by the exothermic absorption reaction may change at ultra-high capture fractions due to the shift in the CO_2 mass transfer profile. This can cause the temperature profile along the absorber to change compared to a 90% capture fraction and, for a given lean loading, mass transfer limiting temperature peaks can become more prominent in the absence of intercooling.

2.3. Natural gas reforming and power generation

High pressure steam and preheated natural gas feedstock at 400°C and 34 bar are mixed, further heated to 500°C and enter a pre-reformer, which is an adiabatic reactor that converts 100% of the C_2+ hydrocarbons and olefins present in the feedstock into CO and H_2. The ratio of steam to natural gas is controlled to give a steam to carbon ratio of 2.5 mol H_2O/mol Carbon in the reformer. After pre-reforming the syngas is re-heated to 600°C prior to entry to the catalyst-filled reformer tubes where two concurrent reactions occur to form a syngas consisting of equilibrium proportions of CH_4, H_2O, H_2, CO_2 and CO at ca. 91 °C. The Steam-Methane reforming reaction as described by the equilibrium shown in Eq. (3) and the Water-Gas shift reaction as described by Eq. (4). Less than 100% methane conversion in the reformer is expected due to process pressure and temperature limitations and a 85% methane conversion rate is calculated for the for the above process conditions; this unreacted methane is typically known as 'methane slip'.

$$CH_4 + H_2O \leftrightarrow CO + 3H_2 \quad \Delta H_r = 206 \frac{\text{kJ}}{\text{mol}} \tag{3}$$

$$CO + H_2O \leftrightarrow CO_2 + H_2 \quad \Delta H_r = -41 \frac{\text{kJ}}{\text{mol}} \tag{4}$$

This syngas is cooled to 320°C via an evaporator prior to entry into the water gas shift reactor (WGSR), where further conversion of CO occurs (ca. 72%) via the Water-Gas shift reaction, a 7%, 10% and 5% pressure drop is assumed for the pre-reformer, reformer and water gas shift reactor respectively.

The remaining useful heat in the syngas stream is used to pre-heat the natural gas and the water condensate in the power cycle. Final cooling and condensation of the syngas to 35°C is completed before entering a pressure swing absorber (PSA), which is modelled as a "black box" and wherein it is assumed that 90% of the H_2 (Collodi et al., 2017) is separated out at 25 bar for export. The off gas, consisting of the remaining H_2, unreacted CH_4, H_2O, CO and the CO_2, is mixed with additional natural gas for combustion in the burners of the SMR furnace. Due to the high grade heat requirement of the reforming process, the flue gas has useful energy in excess of that useable for natural gas reformation; this is employed to raise steam, some of which is fed to the reformer, with any surplus steam diverted to a steam turbine for power generation, with an assumed isentropic efficiency of 90%, or simply exported for off-plant use, depending on site specific conditions. In CCS applications, surplus steam would be typically be diverted to a back pressure turbine with an exhaust pressure suitable for the supply of thermal energy to the CO_2 capture plant at constant temperature, in this case 3.7 bar. For the capture fractions used in this study the thermal requirement of the CO_2 capture process is shown to be in excess of the low pressure steam available in an unabated SMR. As a result additional steam production is required, necessitating an increase in supplementary fuel and ambient air intake.

2.4. Supply chain emissions

As a potent greenhouse gas, any methane emissions in the natural gas supply chain need to be compensated for via some form of negative emission technology in order for hydrogen production to achieve zero life cycle greenhouse gas emissions. The specific carbon intensity of natural gas supply ranges from 1.1 to 16.4 kgCO_2eq/MWh$_{th}$ (HHV) of natural gas for the emission rate range of 0.2 to 3% when calculated using GWP* for a 25 year operational life. For the purpose of this analysis, we assume that the necessary installed capacity of DACCS is

Table 1
Embodied and CCS upstream CO_2 emissions.

Emission source	Unit	Value
Post Combustion CO_2 Capture Plant Operation (Herraiz Palomino et al., 2022)	gCO_2e/ KG CO_2 Captured	19.2
Post Combustion CO_2 Capture Plant Construction (Herraiz Palomino et al., 2022)	gCO_2e/ KG CO_2 Captured	0.85
Steam Methane Reformer Construction (Spath and Mann, 2001)	gCO_2e/ KG H_2 Produced	41

commercially available and independent of the H_2 producer. A cost range of 100–1000£/tCO_2 is considered to cover a range of estimates consistent with values reported in the literature (Mcqueen et al., 2021; Direct Air Capture 2022) while CO_2 transport and storage cost for the resulting additional captured CO_2 are set at 19 £/tCO_2 (Assessing the Cost 2018) and the natural gas price set at 28£/MWh_{th} HHV (Review of next generation 2022).

The cost of offsetting supply chain emissions can be directly allocated to fuel prices in LCOH calculations by attributing an additional cost per unit of fuel supplied. This is shown in Fig. 3 as an additional fuel price premium for a range of emission rates and DACCS costs. A DACCS cost of 300£/tCO_2 and a UK natural gas supply emission rate of 1.04% is used as the median estimate for LCOH analyses, resulting in a 6% (1.8 £/MWh_{th} HHV) increase in fuel costs. Increasing the long term fuel cost assumed in this study of 28£/MW_{th} to 29.8 £/MW_{th} HHV. A DACCS price of 300 £/tCO_2 is consistent with a report by the US National Academy of Science and Engineering (Negative Emissions 2019) and at the upper end of estimates by the International Energy Agency (IEA) for plants built using current technology at 125–335$/t$CO_2$ (Direct Air Capture 2022).

A best case scenario is also included in this study, where methane emissions from the supply chain are reduced to be broadly in line with leaders Norway and Qatar (Bauer et al., 2022) and an average emission rate of 0.2% is assumed.

2.5. Embodied carbon and CCS fugitive emissions

Estimated values for the embodied carbon emissions associated with the construction of both the SMR and PCC plant, along with downstream emissions associated with CO_2 transport and storage, are detailed in Table 1. A lifecycle assessment (LCA) on natural gas steam reforming completed by the National Renewable Energy Laboratory (NREL) (Spath and Mann, 2001) provides the estimation for embodied CO_2 in the SMR construction, while Herraiz et al. provides a detailed LCA on the capture plant construction and operational chain (Herraiz Palomino et al., 2022).

The embodied CO_2 emissions from construction are distributed over the construction period of the plant while the CO_2 emissions associated with operation of the CO_2 capture plant and infrastructure are considered to occur annually. All embodied CO_2 emissions are recaptured with DACCS and permanent geological storage. It represents a realistic order of magnitude estimation and demonstrates that the effect on the LCOH is of the order of 1.0–8.6£/MWh_{th} HHV for DACCS costs in the range of 100–1000 £/tCO_2. Of note is the high contribution of reclaimer bottoms disposal to the embodied carbon value (circa 6 gCO_2 eq/$kgCO_2$ captured); Herraiz et al. assume that this waste product is disposed of via incineration with no associated CCS. This is unlikely to be consistent with net zero commitments, and as such the embodied CO_2 emission value used here is likely to be a conservative estimate in the long term. Additionally, as the respective industries involved in SMR & PCC construction (steel, concrete, transport etc.) and MEA production decarbonise, as well as improved solvent management procedures develop it can be expected that the total embodied CO_2 value would decrease proportionally leading to a reducing LCOH penalty over time.

Table 2
Economic model parameters.

Parameter	Unit	Value
Discount rate (Review of next generation 2022)	%	7.8
Interest Rate (Elliott, 2022)	%	4.0
Productive lifetime (Collodi et al., 2017)	Years	25
Base year	–	2023
Year operational	–	2026
Build Time (Collodi et al., 2017)	Years	3 Years
CAPEX expenditure curve (Collodi et al., 2017)	%	20/45/35
Load Factor (Collodi et al., 2017)	%	95%
Transport and storage cost (Assessing the Cost 2018)	£/tCO_2	19
Natural Gas Fuel price (Review of next generation 2022)	£/MWh	28
Electricity selling price (Mullen and Lucquiaud, 2022)	£/MWh	105
Chemical Engineering Plant Index (CEPCI) (THE CHEMICAL ENGINEERING 2022)	–	816.3
International Construction Cost Index [Netherlands/UK/Texas] (Arcadis 2020)	–	100/138/97
USD to GBP exchange rate (2020) (Rates, 2023)	£/$	0.82
Equipment Tax/Insurance/Freight (Elliott, 2022; Donald, 2007)	%	10
Civil Works factorial cost (Elliott, 2022; Bechtel 2019; Bechtel 2018)	%	21
Utilities factorial cost (Elliott, 2022; Bechtel 2019; Bechtel 2018)	%	18
Electrical factorial cost (Elliott, 2022; Bechtel 2019; Bechtel 2018)	%	30
Project management (Elliott, 2022; Bechtel 2019; Bechtel 2018)	%	21
Contractor Fee (Donald, 2007)	%	3
Project Contingency (Elliott, 2022; Bechtel 2018)	%	10
Owners Costs (Review of next generation 2022)	%	7
Start-up & Spares (Review of next generation 2022)	%	5
Utility Connections (Review of next generation 2022)	%	1
Consulting Fee (Review of next generation 2022)	%	1
Maintenance (CCS) (Assessing the Cost 2018)	%/Year	1.5
Maintenance (SMR) (Assessing the Cost 2018)	%/Year	3.0
Labour (Assessing the Cost 2018)	£/Employee/Year	69,810
Insurance/Tax/Admin (Review of next generation 2022)	%/Year	1.5
Regulatory (Review of next generation 2022)	%	2.0
MEA (Michailos and Gibbins, 2022)	£/t	940
Caustic (Evaluating the Costs of Retrofitting 2017)	£/t	34
Reclaimer disposal (Michailos and Gibbins, 2022)	£/t	500
Working Capital (Assessing the Cost 2018)	–	1 Months Consumables

Table 3
Post combustion CO_2 capture plant engineering, procurement & construction (EPC) cost estimates.

Item	Zero residual emissions (M£)	5% residual emission (M£)	10% residual emission (M£)
Absorber	58	47	45
Regeneration	66	59	55
Heat Exchangers	47	44	42
Compression	39	37	37
Miscellaneous	21	22	22
Tax & Freight	23	21	20
Total Plant Cost	256	230	220
Civil	54	48	46
Utility	46	41	40
Electrical	77	69	66
Project Management	91	82	78
Bare Module Cost	523	470	450
Contractor Fee	16	14	14
Contingency	52	47	45
Engineering, procurement & construction	591	531	509

Table 4
Total Plant CAPEX Estimates.

Item	Zero residual emissions (M£)	5% residual emission (M£)	10% residual emission (M£)
PCC EPC	591	531	509
SMR EPC	605	605	605
Connections	12	11	11
Start-up/ Commissioning/ Spares	60	57	56
Regulatory Costs	24	23	22
Owners Costs	84	79	78
Consultation Costs	12	11	11
Interest during construction	103	97	96
Total CAPEX	1489	1415	1387

2.6. Levelised cost of hydrogen (LCOH)

The Levelised Cost of Hydrogen (LCOH) is the discounted lifetime cost of building and operating a hydrogen production asset, expressed as a cost per energy unit of hydrogen produced (£/MWh_{th} HHV) (Hydrogen production costs 2021). It covers all costs to the producer including, CAPEX, OPEX, fuel, waste disposal and financing costs. LCOH is expressed as a net present cost, as shown by Eq. (5). Although LCOH cannot be used to establish business model strike prices, it is considered a viable metric for comparing different hydrogen generation technologies. The economic values used to develop the LCOH model are detailed in Table 2.

$$LCOH = \frac{NPV\ Costs}{NPV\ Hydrogen} \tag{5}$$

$$NPV\ Costs = \sum_{i=1}^{n} \frac{CAPEX_i + OPEX_i - Power\ Generation\ Revenue_i}{(1 + Discount\ Rate)^i} \tag{6}$$

$$NPV\ Hydrogen = \sum_{i=1}^{n} \frac{Hydrogen\ Production_i}{(1 + Discount\ Rate)^i} \tag{7}$$

$(n = time\ period)$

Where NPV is the net present value of the expense or revenue in question.

Table 5
Operational cost estimates.

Item	Zero residual emissions (M£)	5% residual emission (M£)	10% residual emission (M£)
Net annual OPEX	499	481	472
Natural Gas	371	361	357
Solvent Regeneration	50	46	43
Fixed OPEX	56	54	52
CO_2 Transport and Storage (T&S)	44	41	38
Debt Financing	2	2	2
Power Generation Revenue	−25	−22	−21

2.7. Capital expenditure (CAPEX)

A detailed multi-level factorial cost model, shown in Eq. (13) and provided in the supplementary material is used to calculate the required CAPEX, with an estimated accuracy of +35%/−15% corresponding to an American association of cost engineers (AACE) Class 4 estimate (Christensen, 2005), which is considered sufficient for project feasibility studies. The capital cost estimates are presented in Table 4 and details of the parameters for the cost model and there sources are presented in Table 2.

Engineering, Procurement and Construction (EPC) cost for an SMR is estimated using Eq. (8) with the reference cost obtained from a report issued by the BEIS (Hydrogen production costs 2021). Hydrogen production capacity is used as the scaling parameter and the scaling exponent is set at 0.79 as per Sinnott and Towler (Sinnott and Towler, 2020).

$$SC_t = RC * \left(\frac{SP}{RP}\right)^{Exp} * \left(\frac{CEPCI_t}{CEPCI_{ref}}\right) * \left(\frac{ICCI_t}{ICCI_{ref}}\right) * \left(Exchange\ Rate_{ref}\right) \tag{8}$$

Where *Exp* is the Scaling Exponent, *RC* is the reference plant cost, *RP* is the reference plant parameter, *SP* is the scaled plant parameter, *SC* is the scaled plant cost, CEPCI is the chemical engineering plant cost index, ICCI is the international construction cost index, T is the current year and ref is the reference year.

Reference costs and scaling parameters for each post combustion CO_2 capture plant item along with installation and tax & freight factors are taken from Sinnott and Towler, Woods (Donald, 2007) and the available FEED studies (Elliott, 2022; Bechtel 2019; Bechtel 2018) and converted to UK 2023 prices using the chemical engineering plant index (CEPI) (THE CHEMICAL ENGINEERING 2022), historical currency exchange rates and the international construction cost index (ICCI) (Arcadis 2020). A physical module cost (PMC) for each piece of equipment is evaluated using Eq. (9) while the total plant cost (TPC) is the summation of the PMC for each piece of equipment (Eq. (10)).

$$Physical\ Module\ Cost\ (PMC) = SC * \left(1 + f_{installation} + f_{tax\ \&\ freight}\right) + I \tag{9}$$

$$Total\ Plant\ Cost\ (TPC) = \sum PMC \tag{10}$$

Where $f_{installation}$ is the installation cost relative to the equipment purchase cost and specific to each type of equipment however it is usually between 2 and 7. $f_{tax\ \&\ freight}$ is the cost of delivery of a piece of equipment to site and is set at 10% of the purchase cost and I is the specific equipment instrumentation cost.

Factors for civil works, utility installation, electrical equipment and project management are estimated from the front end engineering design (FEED) studies available in the public domain (Elliott, 2022; Bechtel 2019; Bechtel 2018) and applied to the TPC for each major PCC plant item to get a Bare Module Cost (BMC) as shown in Eq. (11).

$$Bare\ Module\ Cost\ (BMC) = \left(1 + f_{project\ management}\right) * \left[\left(1 + f_{civil} + f_{utility} + f_{electrical}\right) * TPC\right] \tag{11}$$

Table 6
Sensitivity study parameters and ranges.

Item	Lower	Base	Upper
Natural Gas price (HHV)	5 £/MWh	28£/MWh	100 £/MWh
Electricity Price	0 £/MWh	105 £/MWh	200 £/MWh
CAPEX	−15%	As evaluated	+35%
OPEX	−30%	As evaluated	+30%
Discount Rate	5%	7.8%	20%
Carbon Price	0 £/tCO_2	0 £/tCO_2	200 £/tCO_2
Load Factor	0.6	0.95	1
T&S Cost	10 £/tCO_2	19 £/tCO_2	50 £/tCO_2
DACCS Price	100 £/tCO_2	300 £/tCO_2	1000 £/tCO_2
Natural Gas Supply Chain Emissions	0.2%	1.04%	3.0%

A 3% contractor fee as per Woods (Donald, 2007) and a 10% contingency consistent with common FEED study practice is applied to the BMC to get the total EPC cost.

$$Engineering,\ Procurement\ and\ Construction\ (EPC) = \left(1 + f_{contractor\ fee} + f_{contingency}\right) * BMC \tag{12}$$

Total CAPEX burden is then found by adding owner's, and regulatory costs to the total EPC value while including any additional capital requirement for connections to natural gas, CO_2 and electricity networks, start-up/spares costs, consultancy fees and interest repayments accrued during the construction period as per Eq. (13). As working capital is assumed to be recovered at the end of the operational life of the plant, it is not included in the total CAPEX burden. The debt associated with working capital is serviced annually for the duration of the plant life wherein it is released.

$$CAPEX = (EPC_{SMR} + EPC_{PCC}) * \left(1 + f_{owners} + f_{regulatory} + f_{spares\ \&\ start-up} + f_{connections} + f_{consultancy}\right) + Interest\ during\ construction \tag{13}$$

A breakdown of the PCC EPC costs for both the zero, 5% and 10% residual emissions cases are shown in Table 3 while Table 4 shows the total plant CAPEX burden.

3. Operational expenditure (OPEX)

OPEX comprises any ongoing costs related to normal operations of a plant and includes fuel, consumables, labour and maintenance costs as well as the cost of CO_2 transport and storage, emissions penalties (i.e. carbon tax), waste disposal and insurance or taxes. Any revenue from the sale of power is subtracted from total annual costs to provide a net annual cost value as per Eq. (6). An MEA consumption rate of 2 kg/tCO_2 is assumed based on estimations by Elliott et al. (Elliott et al., 2021) for a desorber operating at 2.4 bar and 130 °C, resulting in an annual solvent replacement cost of 3.8–4.3M£ while the price of disposing of the reclaimer bottoms is assumed to be 500£/t, adding an additional 2.0–2.3M£ per annum. It is assumed that 60 permanent staff members will be required to maintain and operate the SMR and PCC plant. An additional 1.5% of the EPC cost is assumed to cover annual insurance, taxes and overheads. The natural gas prices presented in this report are based off projected wholesale fossil fuel costs for 2025, available at (Fossil fuel price assumptions 2022), while the average electricity price is taken as the levelised cost of electricity for zero residual emission electricity produced using a combined cycle gas turbine (Mullen and Lucquiaud, 2022) using the same natural gas price of 28£/MWh_{th} HHV and serves as a best estimate for long term uninflated values. Table 5 presents the results for the OPEX analysis; no carbon price is assumed in this instance.

3.1. Cost of CO_2 avoided (CCA)

The cost of CO_2 avoided (CCA) expresses a technology-independent cost of reducing CO_2 emissions from a given activity per tonne of CO_2e (£/tCO_2e).

The CCA for the end use cost of fuel switching from natural gas to hydrogen i.e. gas-to-blue is described by Eq. (14) (Rehl and Müller, 2013).

$$Cost\ of\ CO_2 Avoided_{gas\ to\ blue} = \frac{LCOH - Natural\ Gas\ Price}{Natural\ Gas\ lifecycle\ emissions - Hydrogen\ lifecycle\ emissions} \tag{14}$$

Where LCOH is the levelised cost of hydrogen (£/MWh_{th}), natural gas price is the wholesale cost of natural gas (£/MWh_{th}) while hydrogen and natural gas emissions is the lifecycle CO_2 equivalent emissions resulting from the supply of one unit of heat via hydrogen or natural gas respectively (tCO_2e/MWh_{th}). For the purpose of this work gas-to-blue CCA is reported on both a HHV and LHV as the appropriate metric is dependant on end use of the H_2 product. A large portion of the applications for fuel switching from natural gas to hydrogen require high grade heat, i.e. open cycle gas turbines, furnaces or domestic/industrial boilers, where the latent heat of H_2O vaporisation is typically not recovered. For applications such as this a CCA reported on a LHV basis

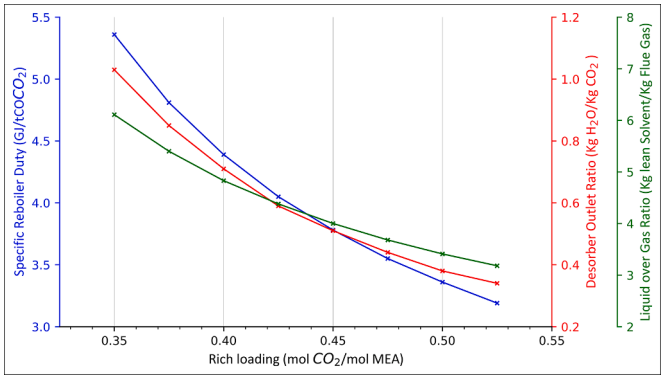


Fig. 4. Effect of increasing rich loading on specific reboiler duty for a constant lean loading of 0.16 mol CO_2/mol MEA and 20% v/v flue gas CO_2 concentration and 100% fossil CO_2 capture.

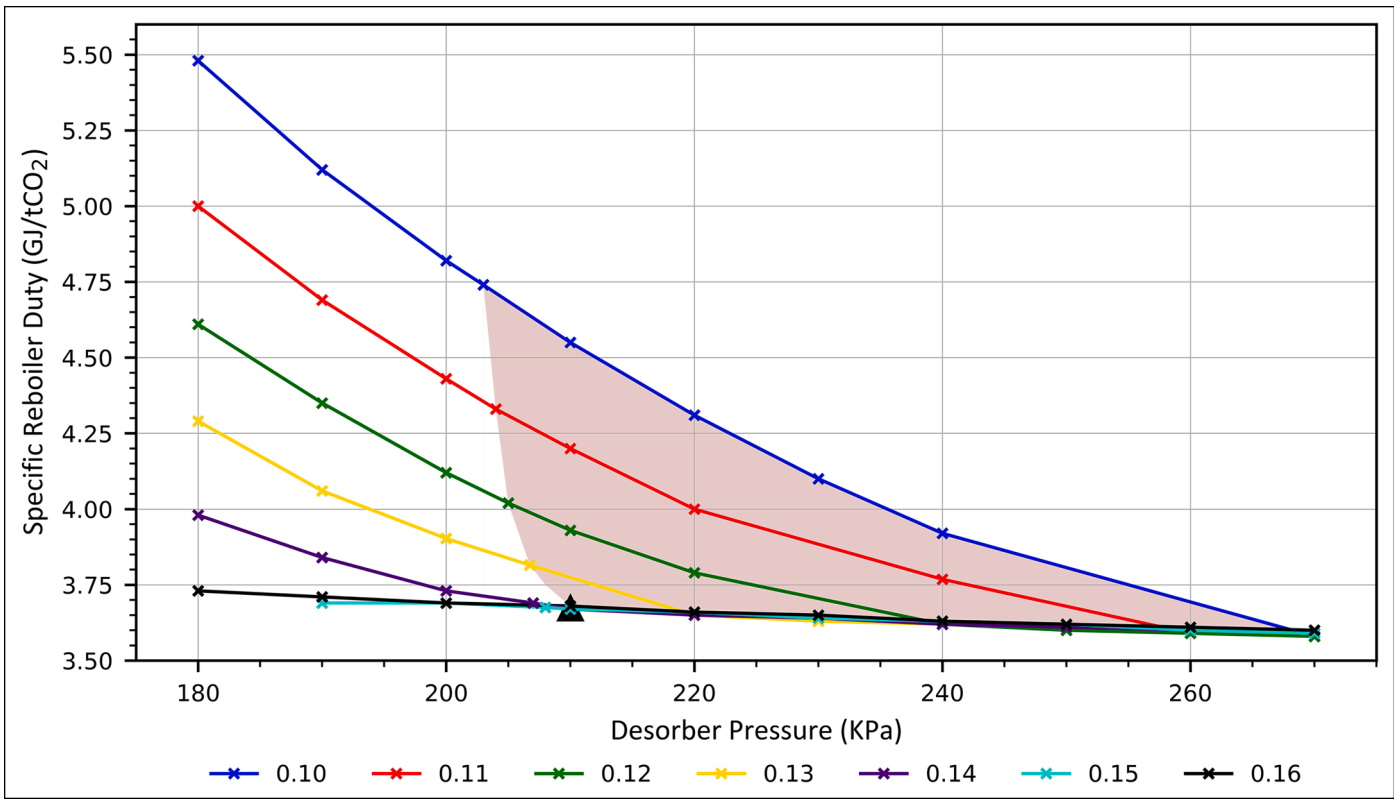


Fig. 5. Effect of desorber operating pressure on the specific reboiler duty for a range of lean solvent loadings (mol CO_2/mol MEA) for a rich loading of 0.47 mol CO_2/mol MEA. Shaded zone represents operational range where reboiler temperature is above 125 °C.

may be more representative, however for applications where the latent heat of H_2O vaporisation is recovered such as condensing boilers HHV may be more appropriate.

3.2. Levelised cost of capture (LCOC)

The Levelised Cost of Capture (LCOC) is the discounted lifetime cost of building and operating a CO_2 capture asset and is expressed as a cost per tonne of CO_2 captured £/tCO_2 and defined by Eq. (15) (Review of next generation 2022). The LCOC is typically presented without including transport and storage costs, and as such that convention is maintained in this study.

$$LCOC = \frac{NPV\ Costs}{Total\ discounted\ lifetime\ CO_2 captured} \quad (15)$$

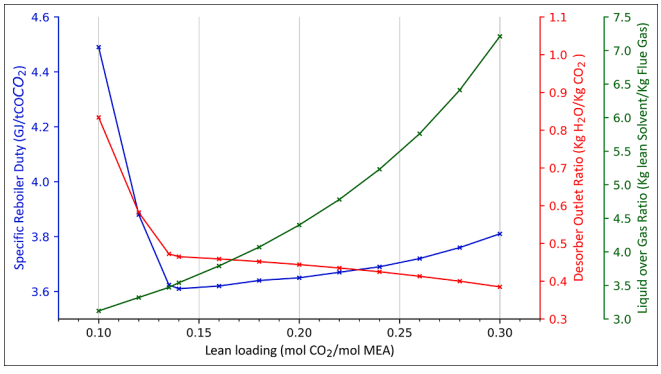


Fig. 6. Reboiler Duty, L/G and desorber outlet ratio for constant rich loading of 0.47 mol CO_2/mol MEA and desorber operating pressure of 210kpa.

3.3. Sensitivity study

Upper and lower estimates of ten key operating and economic parameters are investigated and the impact on the LCOH presented. Table 6 details the bounds of the sensitivity study.

4. Results and discussion

4.1. Zero residual emissions

The results presented in this section show that, for the assumptions used, the ultra-high capture fractions required to achieve zero residual emissions from SMR+CCS plants can be achieved economically through optimisation of the post combustion CO_2 capture plant design. The thermal efficiency of H_2 production decreases by just 1.9 percentage points while total plant CAPEX and OPEX are increased by 5.3% and 4.3% respectively, relative to the 5% residual emissions case.

4.2. Design of a post combustion CO_2 capture plant for ultra-high capture fraction

Optimisation of the post combustion CO_2 capture plant design for ultra-high capture fractions necessitates using lean solvent loadings, in this case 0.16 mol CO_2/mol MEA, lower than those typically reported in the literature for a 90% capture fraction (circa 0.2–0.25 mol CO_2/mol MEA). This ensures that the driving force for CO_2 absorption at the top of the absorber remains sufficient to allow effective utilization of the available absorber packing when intercooling is also employed. Under these conditions an additional 6 m of absorber packing is also required to reach reasonably high rich loadings, limiting the increase in thermal energy requirement to just 1.6%. A strong relationship between desorber pressure and specific reboiler duty is observed, indicating that increased desorber pressure, and hence also increased reboiler

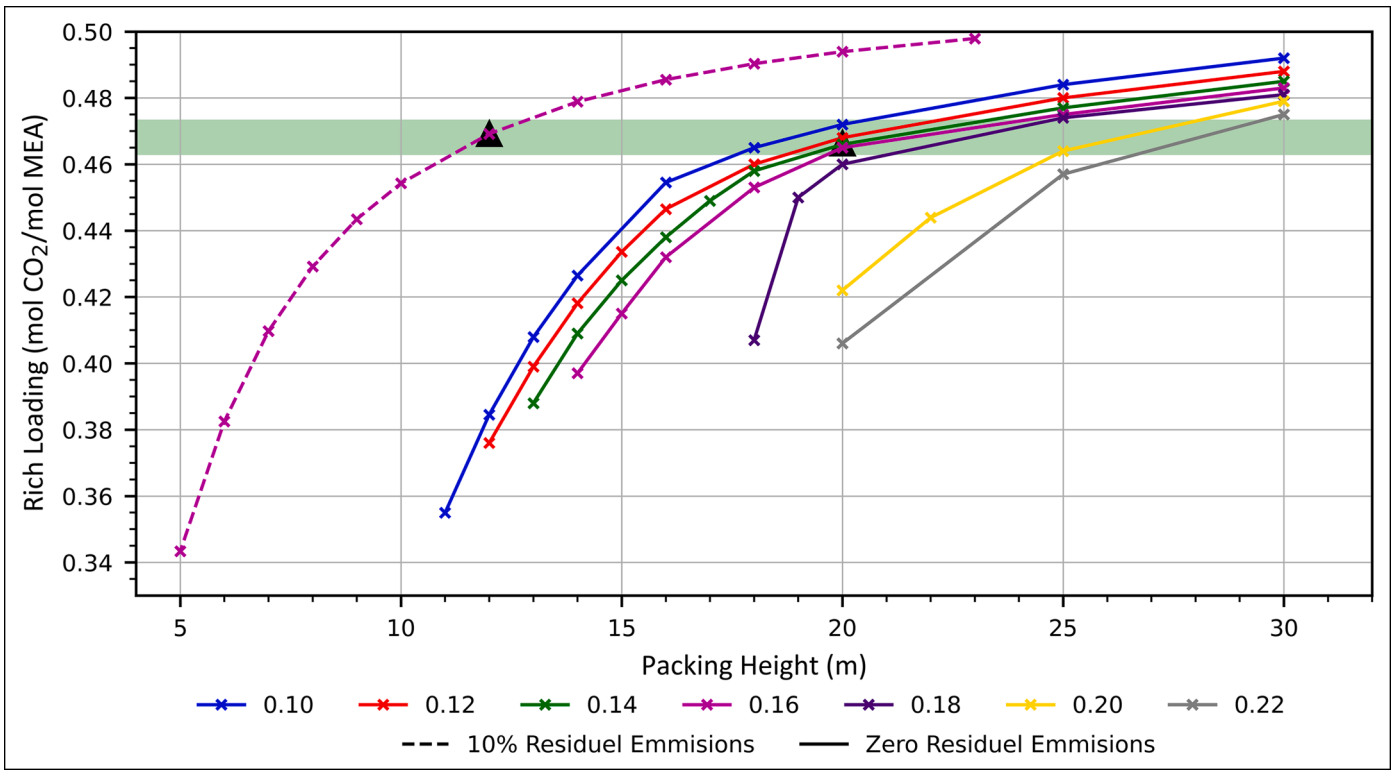


Fig. 7. Effect of packing height on rich solvent loading for a range of lean loadings. The green horizontal bar represents 86.5–88.5% of rich loading equilibrium while the black triangles represent chosen design points. Flue gas CO_2 concentration is 20 vol%.

Table 7
Design and operating parameters of the CO_2 capture plant.

Parameter	Unit	Zero residual emissions	5% residual emission	10% residual emission
[§]Flow Rate (Flue Gas)	*kg/s*	275	262	256
Inlet Temperature	*°C*	40	40	40
CO_2 Concentration	*Mole Frac*	19.4	19.9	20.2
Absorbers	–	1	1	1
Packing Stages	–	2	2	2
Packing Height	*m*	20	14	12
Diameter	*m*	12	12	12
Packing Volume	m^3	2262	1583	1357
Solvent Return Temp	*°C*	38	35	35
Intercooler Return Temp	*°C*	25	–	–
Absorber Flooding	*%*	78	79	79
Rich/Lean HX approach temperature	*°C*	10	10	10
Lean Loading	*mol* CO_2/ mol *MEA*	0.16	0.16	0.16
Rich Loading	*mol* CO_2/ mol *MEA*	0.466	0.469	0.469
Operating Pressure	*KPa*	210	210	210
Reboiler Temperature	*°C*	125	125	125
Specific Reboiler Duty	GJ/tCO_2	3.67	3.62	3.60

temperatures, may be required at low lean loading levels in order to limit the increase in specific reboiler duty.

Fig. 4 shows how, for a constant lean loading and CO_2 capture fraction, an increasing rich loading at the bottom of the absorber decreases specific reboiler duty, this analogous of increasing the total packing height. As rich loading increases the CO_2 absorbed per unit of

Table 8
Performance assessment of a SMR plant with zero, 5% and 10% residual emission PCC.

Parameter	Unit	Zero residual emissions	5% residual emission	10% residual emission
H_2 Export (HHV)	MW_{th}	1000	1000	1000
H_2 Export	kg/s	7	7	7
House Load	MW_e	−26	−24	−23
Net Power Output	MW_e	33	30	28
Supplementary fuel	kg/s	8.7	7.9	7.5
Feedstock	kg/s	20	20	20
Total Fuel	kg/s	29	28	28
Total Fuel (HHV)	MWh_{th}/s	0.416	0.404	0.400
H_2 Production Eff (HHV)	%	66.8	68.7	69.6
CO_2 Export	kg/s	76	71	67
Specific carbon intensity of H_2	gCO_2e/ MJ LHV	5.0	9.0	13.2

Table 9
LCOH, LCOC, CCA and CAC for Zero, 5% and 10% residual emission operation.

Case	LCOH (£/MWh_{th})	LCOC (£/tCO_2)	CCA (gas-to-blue) (£/tCO_2e) HHV	CCA (gas-to-blue) (£/tCO_2e) LHV
No CO_2 abatement	44.2	–	–	–
10% residual emissions	65.3	64.2	254.6	289.7
5% residual emissions	66.4	63.3	240.9	271.9
Zero residual emissions	68.8	64.7	237.5	265.9

Table 10
LCOH for Zero, 5%, 10% residual and no CO_2 abatement operation with a range of carbon tax applied.

Carbon Tax (£/tCO_2)	Zero residual emissions	5% residual emissions	10% residual emissions	No CO_2 abatement
0	68.8	66.4	65.3	44.2
100	68.8	67.7	67.9	69.5
200	68.8	69.0	70.6	94.7
300	68.8	70.3	73.2	119.9
500	68.8	71.6	75.8	145.2

Table 11
LCOH breakdown: No Carbon pricing.

		Zero residual emissions	5% residual emission	10% residual emission
Fuel	£/MWh_{th}	41.9	40.7	40.2
CAPEX	£/MWh_{th}	17.9	17.0	16.7
OPEX	£/MWh_{th}	6.7	6.4	6.3
CO_2 Transport and storage	£/MWh_{th}	5.3	4.9	4.6
Power Generation Revenue	£/MWh_{th}	−3.0	−2.7	−2.5
Total	£/MWh_{th}	68.8	66.4	65.3

solvent increases proportionately; this reduces the sensible heat addition required to heat the solvent to the desorption temperature decreases (see Eq. (2)) as the quantity of water contained in the solvent mixture per unit of CO_2 captured decreases. Concurrently the water VLE at the top of the desorber changes with rich loading, as represented by the H_2O to CO_2 desorber outlet ratio. This tends to further decrease the specific reboiler duty at higher rich loadings.

For a 35% wt MEA solvent and rich loading of 0.47 mol CO_2 a strong effect of varying desorber pressure, and by extension reboiler temperature, is observed for lean solvent loadings at the lower end of the investigated range 0.10 – 0.14 mol CO_2/mole MEA, as illustrated in Fig. 5. This is because the VLE of H_2O at the bottom of the desorber was found to be highly dependant on both desorber pressure and CO_2 loading, a relationship that tends to result in increased vaporisation of H_2O at lower pressures and CO_2 loadings, leading to a rise in required thermal input. This is illustrated in detail in Fig. 6 for a desorber operation pressure of 210KPa. The effect becomes less significant for lean loadings equal or higher than 0.15 mol CO_2/mol.

The 125°C solvent temperature ceiling imposed in this study limits the minimum lean loading to 0.15 mol CO_2/mole MEA at a desorber pressure of 210 KPa (as per Fig. 5) if excessive specific reboiler duties values are to be avoided; a slightly higher value of 0.16 mol CO_2/mol MEA was chosen as the default lean loading in all cases to allow for operational flexibility.

Since lean loadings in the 0.10 – 0.14 mol CO_2/mole MEA range are likely to be required to achieve economical capture of 100% of the fossil CO_2 from flue gases with lower CO_2 concentrations than SMR's, as shown by Michailos and Gibbins (Michailos and Gibbins, 2022), increased desorber pressures, and hence increased reboiler operating temperatures, will be required to limit the increase in specific reboiler duty in these applications. Such low lean loadings may also have advantages for SMR PCC, e.g. avoiding the need for intercooling or facilitating reduced packing heights. This may result in an increase in MEA consumption per tonne of CO_2 captured due to increased thermal degradation but the impact on the cost of CO_2 capture could be minimal given the MEA replacement costs of 2.3$/$tCO_2$ estimated by Elliott et al. in 2021 for a desorber operating at 240KPa and 130 °C (Elliott et al., 2021)

Table 12
LCOH for various natural gas supply chain emissions rates over the range of DACCS cost estimates.

Case	Natural Gas supply chain emission rate (% fuel supplied)	LCOH £/MWh_{th} HHV (DACCS Cost = 100–1000 £/tCO_2)	Increase in fuel cost (%) (Natural gas to H_2)	CCA (HHV) (£/tCO_2e)	CCA (LHV) (£/tCO_2e)
Low	0.20%	70–79	150–182	223–272	248–300
UK	1.04%	71–86	153–208	222–302	247–332
High	3.00%	73–103	160–266	220–367	244–401

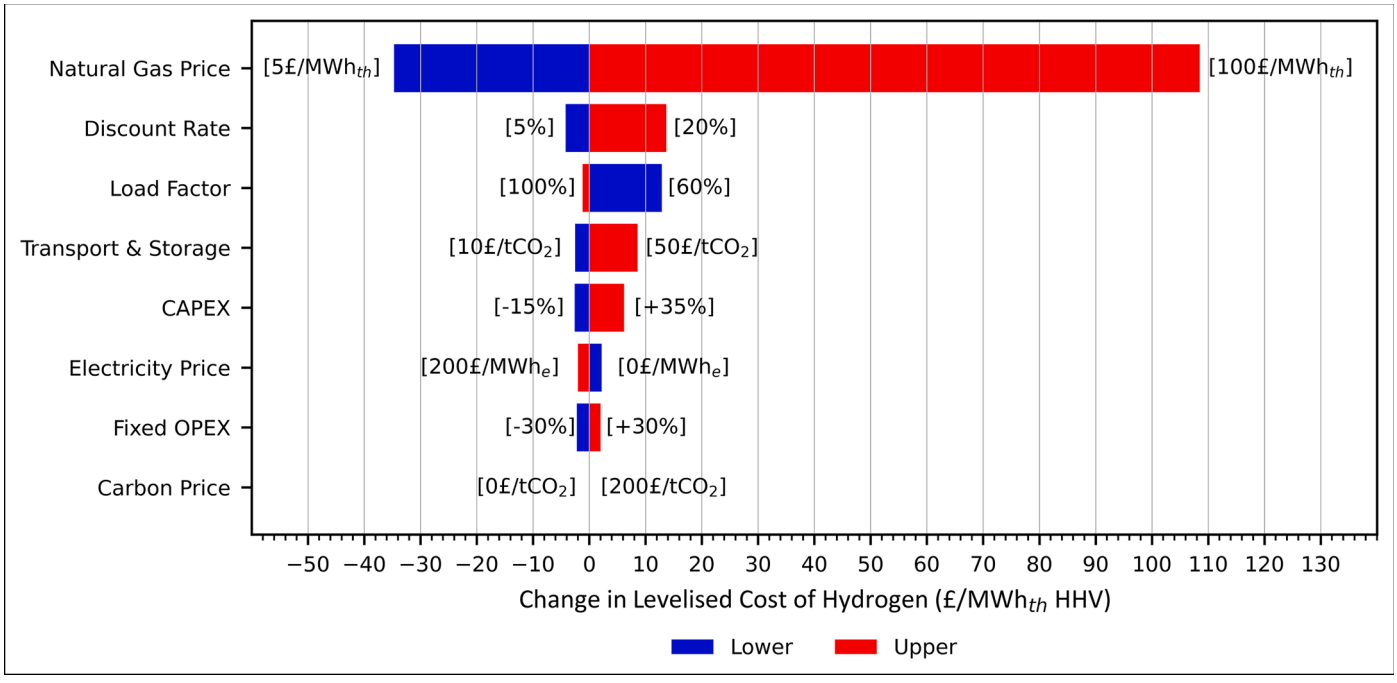


Fig. 8. Effect of techno-economic parameters on the LCOH for zero residual emission operation sensitivity study.

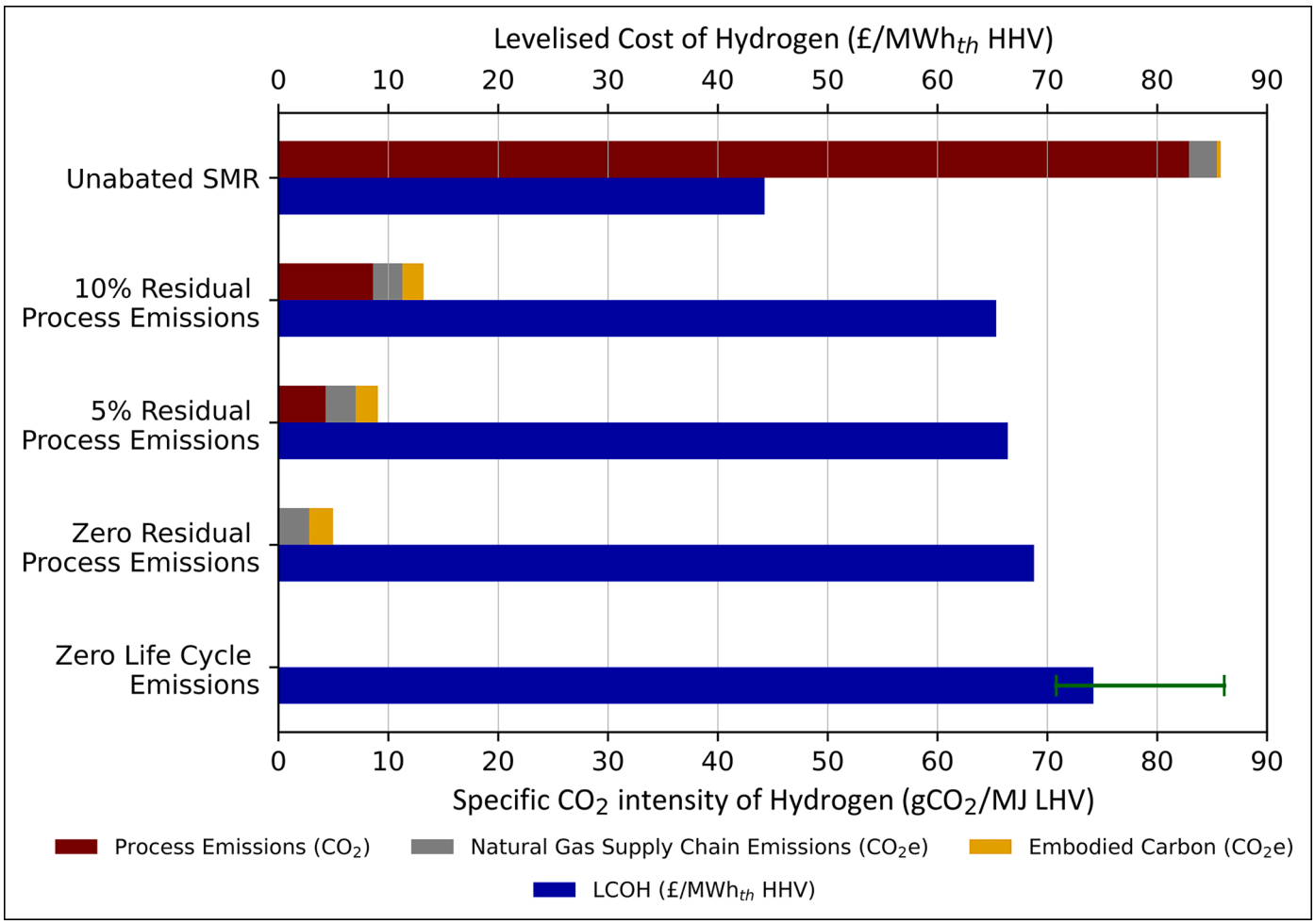


Fig. 9. CO_2 intensity of H_2 production vs LCOH for a UK case (1.04% natural gas supply chain emissions and DACCS at 100 - 1000£/tCO_2). Green bar represents the change in LCOH over the range of DACCS costs analysed.

Fig. 7 illustrates the effect of increasing the absorber packing height on rich loading over a range of solvent lean loadings for both a zero residual and 10% residual emission configurations. In general, operating at lower lean loadings and appropriately lower L/G ratios leads to reduced packing height while still achieving sufficiently high rich loadings. In this study, the packed bed CO_2 absorber is designed so that the rich solvent loading approaches 87.5% of the absolute value of solvent loading at equilibrium at the bottom of the absorber (ca. 0.47 mol CO_2/mol MEA). It is believed that this may represent a reasonable trade-off between CAPEX-related absorber packing height and OPEX-related specific reboiler duty.

The 10% residual emission case requires less packing height to achieve rich loadings of or above 87.5% of equilibrium and can do so at higher lean loadings, should that be required. This is primarily due to the increased partial pressure of CO_2 at the top of the absorber relative to the zero residual emissions case. 12 and 14m of packing is used for the 5 and 10% residual emission cases respectively and is broadly in line with what is reported in the literature. A FEED study completed by Bechtel, for a CO_2 capture retrofit to a coal fired power plant for 90% CO_2 capture with a flue gas concentration of 11.2% vol, considers two packed beds of 7.5m each (Bechtel 2018). Another FEED study, completed by Nexant, for a pilot scale CO_2 capture plant for installation on a natural gas combined cycle with a flue gas concentration of 3.8% vol for 85% CO_2 capture, assumes a packing height of 22m (Nexant 2016). As required packing height decreases with increasing flue gas concentration for a given CO_2 capture fraction, 12 and 14m of packing for an SMR PCC application with 20% vol CO_2 in the flue gas appears to be an acceptable estimate.

It is worth noting that the rich loading achieved for the zero residual emissions configuration is slightly below that of the 5 and 10% residual emissions cases at 0.466 vs 0.469 mol CO_2/mol MEA. This is a marginal compromise to meet the 20 m packing height constraint discussed in section 2.1; increasing packing height further would require a third bed and impart a step change in absorber CAPEX.

Exact optimum points for absorber design are hard to quantify as they will be dependant on project specific constraints i.e. CAPEX availability, OPEX impacts, access to heat for solvent regeneration, land availability, maximum absorber height restraints etc. As such absorber design should be assed and optimised on a project specific basis.

4.3. Performance assessment of the effect of increased CO_2 capture fractions on an SMR plant with PCC

Table 7 provides a summary of the design and operating parameters of the PCC plant for the 5%, 10% and zero residual emissions configurations.

The lean solvent temperature entering the top of the absorber and the intercooling return temperature have a larger effect on the CO_2 absorption rate throughout the absorber column for higher CO_2 capture fractions and thus these temperatures have been optimised for the zero residual emissions case. Solvent return temperature optimisation and intercooling are found to have a minimal effect for both the 5 and 10% residual emission cases and as such are not included. As similar rich and lean loadings are achieved in all cases, specific reboiler duty is also

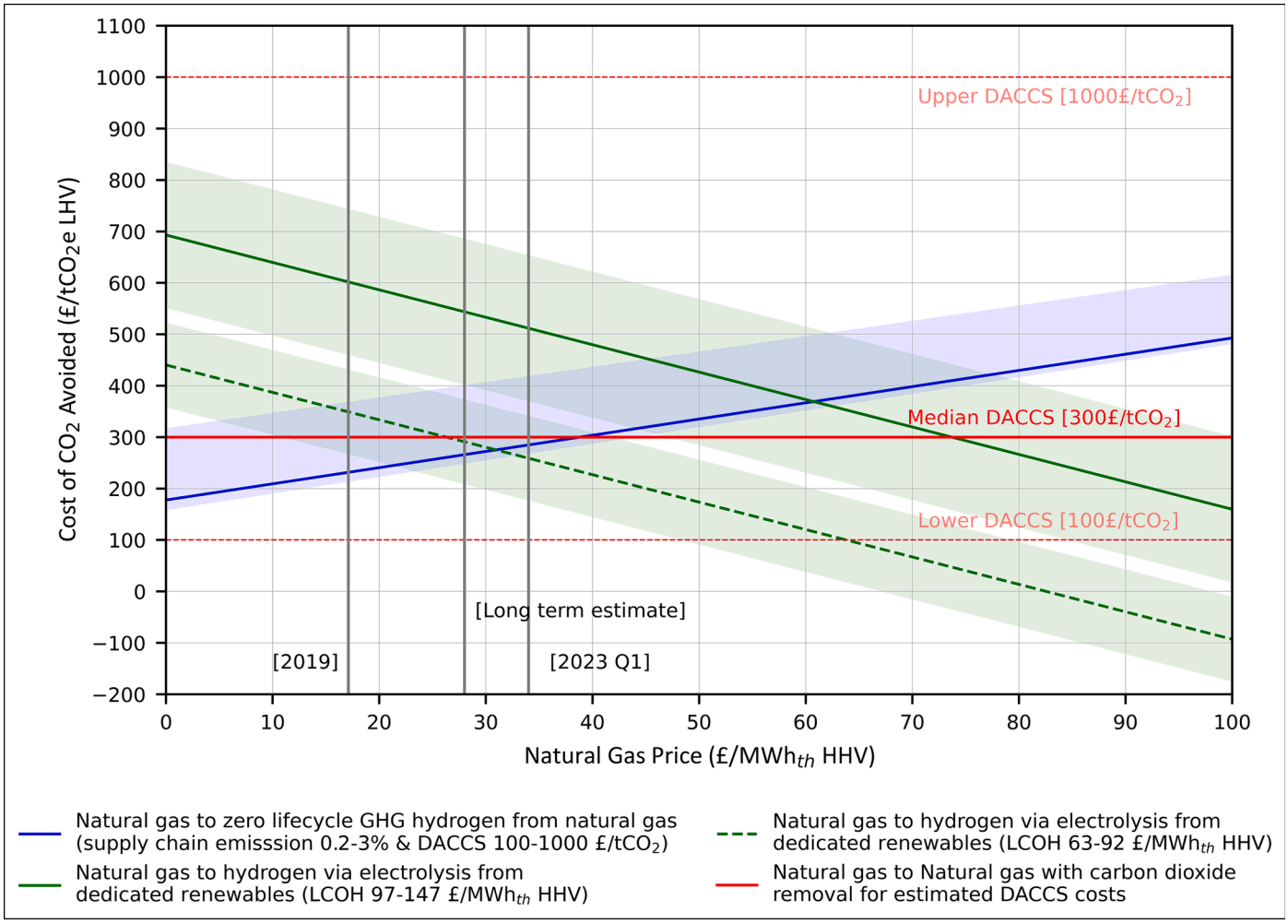


Fig. 10. A cost of CO_2 avoided comparison of fuel switching options for a range of natural gas prices on a LHV basis, including 2019, 2023 and long term estimate prices. Shaded regions indicated upper and lower bounds.

similar. Due to the increase in the absolute quantity of heat input to the reboiler at higher capture fractions, as the total amount of CO_2 captured per unit of H_2 produced increases, the quantity of ambient air and combustion fuel needed increases proportionately in order to supply sufficient steam for solvent regeneration. This leads to the increased flue gas flow rate and decreased flue gas CO_2% vol (primarily due to the increased nitrogen content of the flue gas per unit of hydrogen exported with the additional intake of ambient air) detailed in Table 7.

Table 8 shows the performance of the SMR operating with zero residual emissions compared to 5% and 10%.

The additional steam for solvent regeneration required to increase the CO_2 capture fraction to zero residual emissions results in an increase in the consumption of natural gas in the burner, causing a marginal shift in the H_2 to Power production ratio. A 1.9% point difference in H_2 production efficiency (HHV) is noted between the 5% residual and zero residual emissions cases. House load increases with increases CO_2 capture fraction, primarily due to the higher CO_2 flow rate to the compressors. No other process modifications are required to reach this increased CO_2 capture fraction.

4.4. Levelised cost of hydrogen production

An economic analysis predicting the levelised cost of hydrogen (LCOH), levelised cost of capture (LCOC) and cost of CO_2 avoided (CCA) is shown for zero, 5% and 10% residual emissions operation of a 1000 MW capacity SMR when no carbon pricing is applied, the results are detailed in Table 9 and Table 11. Under these conditions zero residual emission operation is shown to be just 5.3% and 3.6% more costly than hydrogen produced with 10% and 5% residual emissions respectively. When a carbon tax is introduced, as in Table 10, the situation changes, as cases with residual emissions will be penalised when a carbon tax is present a breakeven point occurs. Table 10 shows that for a carbon tax of just 100£/tCO_2 all CCS enabled hydrogen production is more cost effective than an unabated SMR. At 200£/tCO_2 zero residual emission operation is the most cost effective option of the configurations analysed.

However, the primary reason for the mass production of hydrogen is to decarbonise a carbon intensive energy vector, likely natural gas, and as such cost is not the only metric of value. The cost of CO_2 (CCA) avoided allows for the direct comparison of H_2 production methods per unit of CO_2 avoided, it can be used to form a holistic view of all options available to determine the least cost option for moving away from a carbon intensive energy vector. When the CCA (direct emissions only) of switching from natural gas to hydrogen is considered (assuming combustion as the final use), zero residual emission production was found to be the lowest cost option with a value of 238 £/tCO_2e on a HHV bases and 266 £/tCO_2e on a LHV bases and a natural gas price of 28£/MWh_{th} (HHV), this conclusion remains true for all natural gas prices analysed as part of this study.

Table 9 shows that the LCOC and CCA follows a non-linear relationship to capture fraction; this is tentatively attributed to non-linear CAPEX relationships, increase fuel requirements and varying specific

Table 13
Detailed Process parameters for a Zero Direct Emission SMR.

Parameter	Unit	Value
Reformer Operating Pressure	Bar	32
Reformer Reaction Temperature	°C	913
Methane Conversion Efficiency (Reformer)	%	85
Steam to Carbon Ratio (Reformer)	–	2.5
Pre-Reformer Reaction Temperature	°C	500
Carbon Monoxide Conversion Efficiency (WSR)	%	72
WSR Reaction Temperature	°C	410
Flue gas flow rate	Kg/s	275
Flue gas CO_2 concentration	% Vol	20
Turbine Inlet Pressure	Bar	42
Turbine Outlet Pressure	Bar	3.7
Turbine Inlet Temperature	°C	400
Turbine Isentropic Efficiency	%	90
Pump Isentropic Efficiency	%	70
Fan Isentropic Efficiency	%	70
Generator Efficiency	%	99
Mechanical efficiency (Turbine)	%	99
Mechanical efficiency (Pump & Fan)	%	95
CW water supply temperature	°C	8
CW return temperature	°C	25
Economizer steam side ΔP	%	1
Superheat steam side ΔP	%	2
Heat Recovery gas side ΔP	%	0.1
Pre-reformer ΔP	%	7
Reformer ΔP	%	10
WSP ΔP	%	5
Minimum Pinch Temp (Heat recovery)	°C	10
Minimum Flue gas Oxygen concentration	% vol	1
Solvent (MEA composition)	% wt	35
Specific reboiler duty	GJ/tCO_2	3.67
Lean/Rich HX minimum approach temperature	°C	10
Minimum Solvent return temperature	°C	35
Minimum Intercooler return temperature	°C	25
Absorber Flooding point	%	80
Lean Solvent loading	Mol/Mol	0.16
Desorber operating pressure	KPa	210
Structured Packing ΔP	mbar/m	2
Desorber packing	–	MELLAPAK 252Y
Absorber packing	–	MELLAPAK 252Y
Maximum Reboiler Temperature	°C	125
Rich Loading Target	% VLE	85
Gas Mixture Thermodynamic Model	-	Peng-Robinson
Steam/Water Thermodynamic Model	-	IAPWS-95

Table 14
Natural Gas composition.

Species	% vol	Species	% vol
Methane	89.00	Propane	1.00
Ethane	7.00	Nitrogen	0.89
Carbon Dioxide	2.00	Butane	0.11

reboiler duty as detailed in Table 11.

5. Sensitivity study

The results from the LCOH sensitivity study completed using the range of parameters described in Table 6 are shown in Fig. 8; each parameter is varied in turn while the remaining parameters are kept constant. The LCOH is shown to be highly sensitive to the natural gas price and moderately sensitive to discount rate and load factor. Variation in CAPEX has a less prominent effect with a −15% to +35% swing resulting 3.1% variance in LCOH.

5.1. Compensating for supply chain emissions & embodied carbon

As shown in Table 9, In all cases the CCA of zero residual operation is found to be the lowest cost decarbonisation option for SMRs, as a result the authors consider 100% fossil CO_2 capture in the CO_2 capture process as likely to be the preferred pathway to achieving zero life cycle CO_2 emission hydrogen from natural gas in SMRs. The results presented in this section consider a zero residual emission SMR as the hydrogen production method.

Given the uncertainty in both future DACCS prices and natural gas supply chain emissions, LCOH values for three cases are presented in Table 12 for zero life cycle CO_2 emissions hydrogen production using steam methane reforming with zero residual emission CO_2 capture.

The first case is an optimistic outlook wherein global natural gas supply chain emissions fail in line with current best practices and achieve an average global rate of 0.2%. The second cases represents a mid-range estimate where current UK natural gas supply chain emission rates are used (1.04%). The final case represents a pessimistic outlook where global natural gas supply chain emissions, at 3%, are twice the median value of 1.5% assumed by Bauer et al. Total embodied carbon is estimated at 1.4MtCO_2e, which is offset via additional DACCS. Construction emissions are offset during the construction period and CCS fugitive emissions are offset annually. Estimations for the LCOH of zero lifecycle CO_2 emissions hydrogen production range from 70£/MWh_{th} HHV on the low end to 103£/MWh_{th} HHV in the most pessimistic scenario, representing a 2–50% increase in LCOH as a result of offsetting supply chain and embodied carbon. For the UK case with a mid-range estimate for the price of DACCS of 300/tCO_2 the LCOH of zero lifecycle CO_2 emissions hydrogen is 74£/MWh_{th} HHV, an 8% increase.

Fig. 9 shows the life cycle CO_2e emissions and associated LCOH for five representative cases for large scale hydrogen production in the UK using SMR technology. As would be expected the cost of H_2 production increases as the degree of decarbonisation increases, this is primarily due to the increase CAPEX and OPEX of the CCS plant on an absolute basis. However when considered on a specific decarbonisation basis, with metrics such as CCA, it is clear that, for the assumptions detailed in this paper, the least cost decarbonisation pathway trends towards increasing CO_2 capture rates.

5.2. Sensitivity study

Both natural gas emission rates and DACCS prices are expected to vary both spatially and temporally, highlighting the importance of case by case assessments, spatially due to varying natural resources, financial incentives and infrastructure between regions, and temporally as pledges to reduce natural gas supply chain emissions come into effect and DACCS technology matures.

For fuel switching to hydrogen to be economical the LCOH must be such that the CCA (as per Eq. (14)) is lower than the current cost of DACCS, otherwise, recapturing natural gas emissions via DACCS is the least cost option. In practice, as the presented values include only the relative fuel supply costs, the breakeven LCOH that would make hydrogen competitive with direct natural gas use with DACCS is somewhat lower than shown in Fig. 10. This is due to the costs of conversion of the distribution system and end use facilities from natural gas to hydrogen. However a detailed examination of this is beyond the scope of this paper.

Fig. 10 illustrates how the CCA of fuel switching from natural gas to blue hydrogen is sensitive to natural gas prices. Should natural gas prices return to those seen prior to 2020 at circa 17£/MWh_{th} HHV (50p/therm) the CCA for switching to zero lifecycle emission hydrogen from natural gas would reduce to below 213–368£/tCO_2 on a LHV basis for the UK. However, should that not be the case and natural gas prices remain at the levels encountered at the time of writing (i.e. the first half of 2023) of 34.1 £/MWh_{th} HHV (100p/therm (Ofgem 2022)) the CCA for gas-to-blue switching would be 268–419£/tCO_2. A long term estimate for natural gas wholesale price of 28£/MWh_{th} HHV (82p/therm) (Review of next generation 2022) results in a CCA of 248–401£/tCO_2.

Of note is the fact that no allowance is made for cost reductions in the post combustion carbon capture system over time in this analysis, and

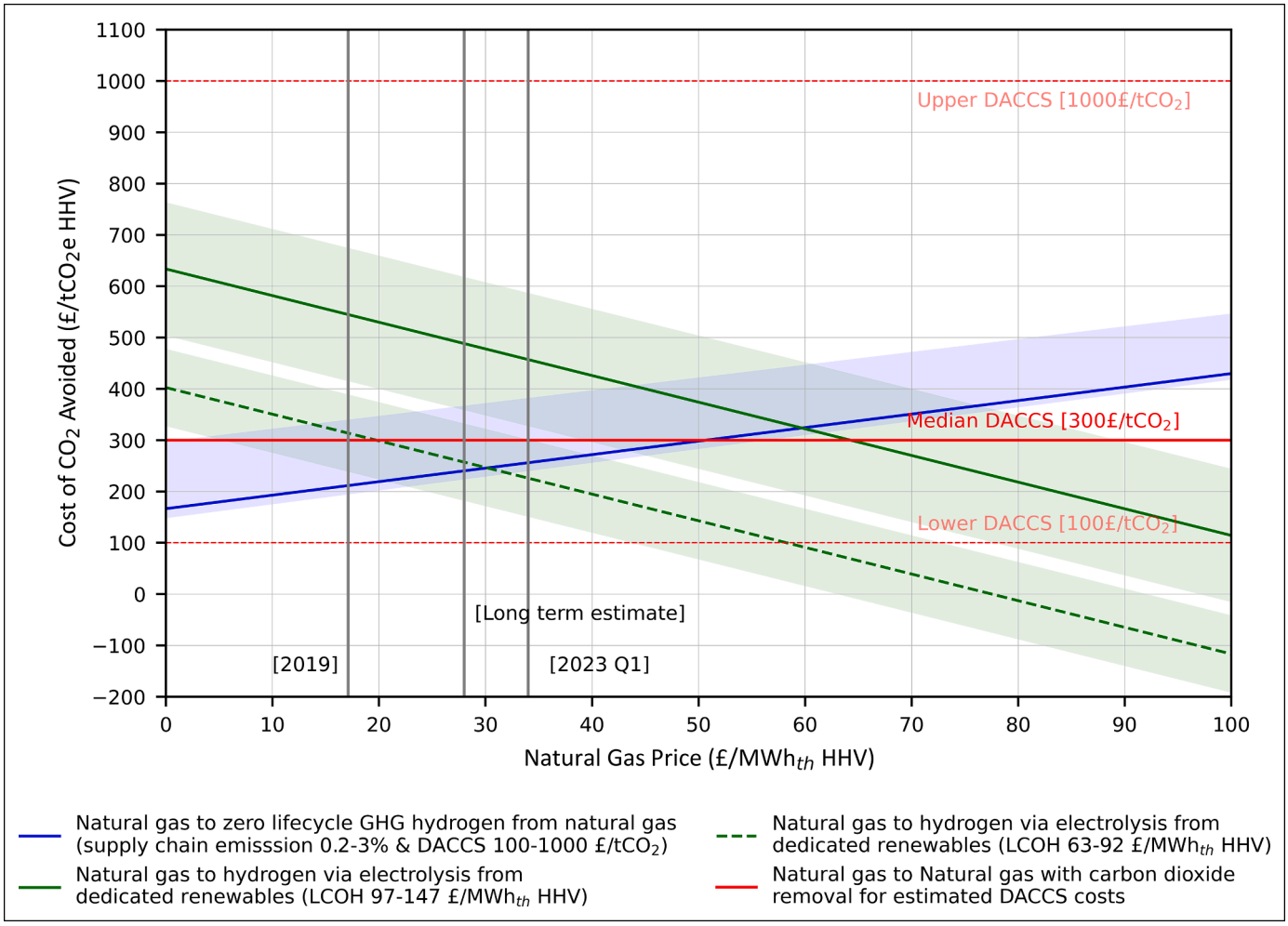


Fig. 11. LCOH of Zero life cycle emission H_2 vs Natural Gas Emissions rates and DACCS Cost.

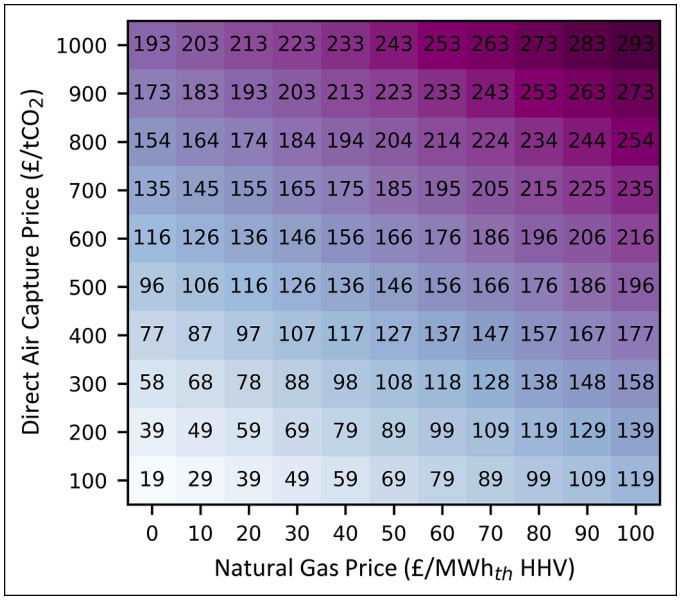


Fig. 12. A cost of CO_2 avoided comparison of fuel switching options for a range of natural gas prices on a LHV basis, including 2019, 2023 and long term estimate prices. Shaded regions indicated upper and lower bounds.

that the costs presented here represent first of a kind status. Learning as deployment increases and the technology approaches N_{th} of a kind status will reduce the CCA of fuel switching. Estimated LCOH values in 2025 (97–147£/MWh_{th} HHV) and 2050 (63–92£/MWh_{th} HHV) for hydrogen production via electrolysis with dedicated renewable energy (green hydrogen) published by BEIS (Hydrogen production costs 2021) are shown for illustrative purposes as the shaded green regions in Fig. 10. Implicit in the assumption of the above LCOH values for green hydrogen is that no capacity to export power to the national grid is present. This means the value of that power is independent from the national grid and as such is unaffected by peaks in the wholesale electricity price. Should that not be the case the LCOH of green hydrogen would be linked to the wholesale electricity price, and by extension, given the current market structure, the wholesale natural gas price. All other factors being equal this would result in an increase in the CCA of green hydrogen. Fig. 10 also assumes zero life cycle emissions from green hydrogen production. This will likely result in an under estimation of the CCA, quantification of the life cycle emissions from green hydrogen production is, however, beyond the scope of this paper.

6. Conclusions

We show, for the first time, that transitioning to zero life-cycle CO_2 emission hydrogen production from natural gas involves a minor increase in costs relative to the traditionally assumed CO_2 capture fraction of 90–95% and a reduction in the cost of CO_2 avoided (CCA). This leads the authors to the novel conclusion that 100% fossil CO_2 capture in the

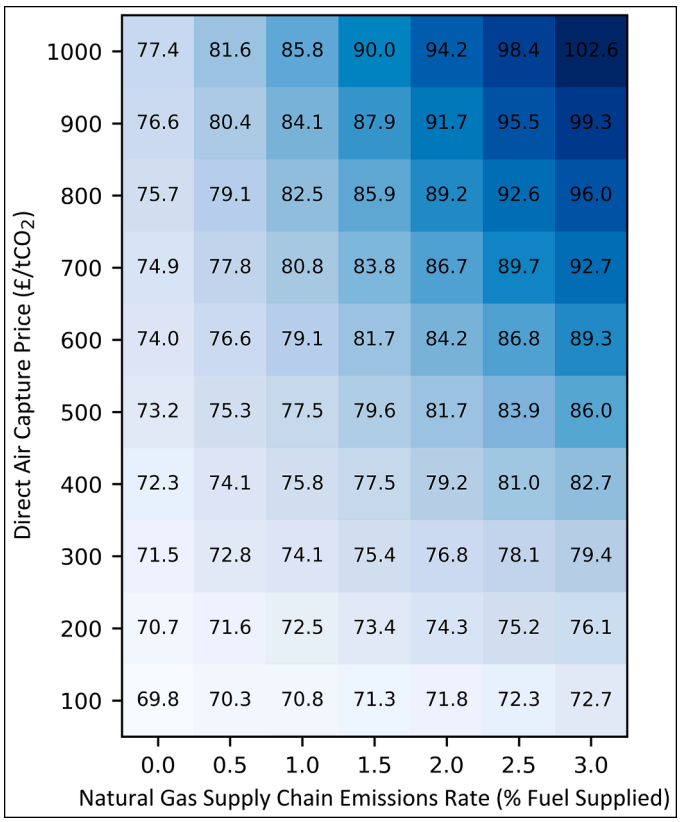


Fig. 13. Maximum economic levelised cost of net zero hydrogen for a range of natural gas and DACCS prices. Analyses is independent of hydrogen production method.

CO_2 capture process is likely to be the preferred pathway to achieving zero life cycle CO_2 emission hydrogen from natural gas in SMRs

The first step is to achieve zero residual emissions from the production process. This would require the industry and blue hydrogen project developers to design plants that are capable of capturing 100% of fossil CO_2 emissions, a technological requirement believed to be, based on the studies referenced and results presented in this paper, achievable with commercially available technology and open art solvents. We combine insights from our process modelling with a multi-level financial assessment tool developed to inform a techno-economic model describing a steam methane reformer (SMR) equipped with post-combustion CO_2 capture capable of 100% of fossil CO_2 capture.

The PCC plant design proposed in this study differs from conventional PCC design only due to the increase in packing height (14 m to 20 m) and reduced solvent lean loadings (0.16 from circa 0.20–0.25 mol CO_2/mol MEA). This is necessary to limit CO_2 capture thermal energy use to a minimal increase of 1.6% per tonne of CO_2 captured. The additional gas input needed to increase CO_2 captured per unit of H_2 produced lowers hydrogen production efficiency by 1.9% point HHV, from 68.7 to 66.8%. This, coupled with the use of an open art solvent (35%wt MEA), leads to the conclusion that zero residual emission operation of an SMR can be achieved using currently available technology and at a much lower efficiency impact than previously thought.

Additionally, it is estimated that capital and operating costs increase by, respectively, 5.3% and 4.3% for a 1000 MW HHV hydrogen facility, compared to hydrogen produced with 5% residual CO_2 emissions. The Levelised Cost of Hydrogen with zero residual emissions is 69£/MWh_{th} HHV (2.7£/kg) for 2023 UK capital costs and a long term natural gas price of 28 £/MWh_{th} HHV, this represents a 4% increase in the LCOH relative to operating with 5% residual emissions and a 55% increase from an SMR with no CO_2 abatement.

The second step towards zero-carbon hydrogen requires using carbon-dioxide removal (CDR) technologies to recapture greenhouse gas emissions across the whole hydrogen supply chain, including emissions associated with the supply of natural gas and embodied CO_2 emissions in the construction and operation of the SMR and the CCS infrastructure. Recent pledges at COP26 to reduce global methane emissions by 30% by 2030 are a partial step to make blue hydrogen more climate compatible, but current best practices will need to be implemented globally to reduce global average emission rates in the natural gas supply chain from 1.5% to 0.2% or below.

At 0.2% supply chain methane emission rate, and with a cost of DACCS with geological CO_2 storage of between 100 and 1000 £/tCO_2 (based on the lower and upper end of long-term estimates in the literature), the Levelised Cost of Hydrogen for an assumed natural gas cost of 28 £/MW_{th} HHV and electricity price of 105£/$MWh_e$with zero life cycle greenhouse gas emissions ranges from 70 to 79£/MWh_{th} HHV (2.8 - 3.1 £/kg). This is well within the range of the cost estimates for other forms of low carbon hydrogen production in the UK, with production costs for electrolysis with dedicated renewable generation estimated at 97–147 £/MWh_{th} HHV (3.8 – 5.8£/kg) for projects commissioning in 2025, falling to 63–92£/MWh_{th} HHV (2.5 - 3.6£/kg) in 2050 (Hydrogen production costs 2021).

DACCS costs have been identified as a factor in net-zero hydrogen production but they also determine whether or not it is desirable to use hydrogen in preference to natural gas. As Fig. 10 shows, at the median DACCS cost of 300 £/tCO_2 the greater natural gas use involved in blue hydrogen production means that gas+DACCS is competitive at natural gas prices above circa 40 £/MWh_{th} HHV. However, because system and end use conversion costs have not been included, the actual gas price that would make blue hydrogen unattractive at this DACCS cost would be somewhat lower. At the minimum DACCS cost considered, 100 £/tCO_2, blue hydrogen is never competitive at any gas price. However no allowance has been made for capital and operational cost reductions in the blue hydrogen production process due to learning, with assumed learning being a factor in the lower DACCS cost estimates.

We note that analogous studies of methods to achieve zero-carbon hydrogen using other hydrogen production technologies could also be undertaken and that these might offer advantages over the SMR+CCS route. It is, however, a significant finding that at least one zero-carbon hydrogen route has been demonstrated and that this is for the SMR+CCS route, which, anecdotally, is often currently assumed to offer inferior capture performance to autothermal reactor (ATR) routes. It is our hope that this study can form a basis for future research and policy decisions and help inform a more rounded discussion on hydrogen and the energy system as a whole.

Finally, the authors would like to note that this study serves not as an advocation for blue hydrogen over green hydrogen, or even for the propagation of a hydrogen economy. Rather it is an attempt to provide much needed balance to the discussion. If indeed society decides to progress the hydrogen economy, what truly matters is that this is achieved at the lowest societal and environmental cost possible. To this end we believe that blue hydrogen can play an integral part in achieving this goal; with crucial emphasis on *part*. What is becoming abundantly clear is that an equitable and timely transition to a net zero GHG economy will require every viable lever available to us, regardless of shade.

CRediT authorship contribution statement

Daniel Mullen: Conceptualization, Methodology, Software, Validation, Formal analysis, Investigation, Writing – original draft, Writing – review & editing, Visualization, Data curation. **Laura Herraiz:** Writing – review & editing, Investigation. **Jon Gibbins:** Writing – review & editing, Investigation. **Mathieu Lucquiaud:** Conceptualization, Supervision, Project administration, Writing – review & editing, Investigation, Resources, Funding acquisition.

Declaration of Competing Interest

The authors declare that they have no known competing financial interests or personal relationships that could have appeared to influence the work reported in this paper.

Data availability

I have attached the CAPEX model as supplementary information, any additional data required can be made avalible.

Acknowledgements

Daniel Mullen would like to acknowledge the School of Engineering at the University of Edinburgh for providing the financial support for this work. For the purpose of open access, the authors have applied a Creative Commons Attribution (CC BY) license to any Author Accepted Manuscript version arising.

Supplementary materials

Supplementary material associated with this article can be found, in the online version, at doi:10.1016/j.ijggc.2023.103904.

Appendix A

Table 13.
Table 14.

Appendix B

Fig. 11.
Fig. 12 and Fig. 13.

References

Alcalde, J., Flude, S., Wilkinson, M., Johnson, G., Edlmann, K., E Bond, C., et al., 2018. Estimating geological CO2 storage security to deliver on climate mitigation. Nat. Commun. 9 https://doi.org/10.1038/s41467-018-04423-1.

Arcadis, 2020. International Construction Costs 2020. The Organisation. https://connect.arcadis.com.

Aspentech. ASPEN PLUS V10 [internet]: the orginisation; 2022 [Available from: https://www.aspentech.com/en/products/engineering/aspen-plus.

Assessing the Cost, 2018. Reduction Potential and Competitiveness of Novel (Next Generation) UK Carbon Capture Technology. Amec Foster Wheeler Group. https://www.gov.uk. Report No.: 13333-8820-RP-001.

Bauer, C., Treyer, K., Antonini, C., Bergerson, J., Gazzani, M., Gencer, E., et al., 2022. On the climate impacts of blue hydrogen produciton. Sustain. Energy Fuels 6. https://doi.org/10.1039/D1SE01508G.

Bechtel, 2018. Retrofitting an Australian brown coal power station with post-combustion capture - a conceptual study. Bechtel Infrastruct. Power Corp.

Bechtel. CO2 capture facility at kårstø, norway: front-end engineering and design (FEED) study report. Feed Study. GASSNOVA; 2019 3 Aprial 2019. Report No.: 25474-000-30R-G04G-00001.

Beis, 2022. British Energy Security Strategy. Prime Minister's Office, 10 Downing Street. www.gov.uk.

Braakhuis, L., Høisæter, K.K., Knuutila, H.K., 2022. Modeling the formation of degradation compounds during thermal degradation of MEA. Ind. Eng. Chem. Res. 61 (7), 2867–2881. https://doi.org/10.1021/acs.iecr.1c04496.

Cain, M., Lynch, J., Allen, R., Fuglestvedt, M.S., Frame, J.J., Macey, D.H., 2019. A. Improved calculation of warming-equivalent emissions for short-lived climate pollutants. Clim. Atmos. Sci. 2 https://doi.org/10.1038/s41612-019-0086-4.

Ccsi. WELCOME TO THE CARBON CAPTURE SIMULATION FOR INDUSTRY IMPACT (CCSI2) [Internet]: the Orginisation 2022 [Available from: https://www.acceleratecarboncapture.org/.

Christensen, P.D., Larry. cost estimate classification system – as applied in engineering, procurement, and construction for the process industries aace; 2005. Report No.: 18R-97.

Collodi, G., Azzaro, G., Ferrari, N., 2017. Techno-Economic Evaluation of SMR Based Standalone (Merchant) Hydrogen Plant with CCS. Int. Energy Agency Greenhouse Gas.

Comparison of commercial, 2022. State-of-the-art, Sossil-Based Hydrogen Production Technologies. National Energy Technology Laboratory. Report No.: DOE/NETL-2022/3241.

Cop26, P. World leaders kick start accelerated climate action at COP26 ukcop26.org: COP26 Press; 2021 [Available from: https://ukcop26.org/world-leaders-kick-start-accelerated-climate-action-at-cop26/.

Curtis, C. Review of Best Available Techniques (BAT) for Hydrogen Production from Methane and Refiner Fuel Gas with Carbon Capture. Costain; 2022. Report No.: 7415737-001 REV A1.

Danaci, D., Bui, M., Petit, C., Dowell Mac, N., 2021. En route to zero emissions for power and industry with amine-based post-combustion capture. Environ. Sci. Technol. 55 (15) https://doi.org/10.1021/acs.est.0c07261.

Direct Air Capture. Paris: International Energy Agency; 2022.

Donald, R.W., 2007. Rules of Thumb in Engineering Practice. Wiley VCH.

Elliott, W., Benzb, A., Gibbins, J., Michailos, S., 2021. An open-access, detailed description of post-combustion CO2 capture plant. In: Proceedings of the 15th International Conference on Greenhouse Gas Control Technologies. Abu Dhabi.

Elliott, W.R. Front-end engineering design (FEED) study for a carbon capture plant retrofit to a natural gas-fired gas turbine combined cycle power plant (2 2 1 Duct-Fired 758-MWe facility with F Class Turbines). https://www.energy.gov/: Bechtel; 2022 March 2022.

Evaluating the Costs of Retrofitting, 2017. CO2 Captured in an Integrated Oil Refinery: Technical Design Basis and Economic Assumptions. IEA Greenhouse Gas R&D Programme. Report No.: 2017-TR5.

Feron, P., Cousins, A., Jiang, K., Zhai, R., Hla, S.S., Thiruvenkatachari, R., Burnard, K., 2019. Towards zero emissions from fossil fuel power stations. Int. J. Greenhouse Gas Control 87, 188–202. https://doi.org/10.1016/j.ijggc.2019.05.018.

Fossil fuel price assumptions [Internet] https://www.gov.uk/: department for Business, Energy and Industrial Strategy; 2022 [Available from: https://www.gov.uk/government/collections/fossil-fuel-price-assumptions.

Fuss, S., F Lamb, W., Callaghan, M.W., Hilaire, J., Creutzig, F., Amann, T., et al., 2018. Negative emissions - Part 2: costs, potentials and side effects. Environ. Res. Lett. 13 (6) https://doi.org/10.1088/1748-9326/aabf9f.

Gao, T., Selinger, J.L., Rochelle, G.T., 2019. Demonstration of 99% CO2 removal from coal flue gas by amine scrubbing. Int. J. Greenhouse Gas Control 83, 236–244. https://doi.org/10.1016/j.ijggc.2019.02.013.

Gibbins, J., Lucquiaud, M., 2021. Post-combustion Carbon Dioxide capture: Best Available Techniques (BAT). UK Goverment. https://www.gov.uk. Contract No.: Guidance and support.

Gibbions, J..Lucquiaud, M. BAT Review for New-Build and Retrofit Post-Combustion Carbon Dioxide Capture Using Amine-Based Technologies for Power and CHP Plants Fuelled by Gas and Biomass as an Emerging Technology under the IED for the UK. https://ukccsrc.ac.uk: UKCCSRC; 2021 July 2021.

gPROMS products: gPROMS PROCESSBUILDER [Internet] 2021 [Available from: https://psenterprise.com/products/gproms/processbuilder.

Heap, R., Jackson, N., Bance, P., Gammer, D., 2016. Potential Role of Hydrogen in the UK Energy System. Energy Research Partnership.

Herraiz Palomino, L., Su, D., Muslemani, H., Struthers, I., Thomson, C., Chalmers, H., Lucquiaud, M., 2022. A preliminary assessment of negative CO2 emissions in the European waste sector. In: Proceedings of the 2nd International Conference on Negative CO2 Emissions. Göteborg, Sweden.

Hirata, T., Tsujiuchi, T., Kamijo, T., Kishimoto, S., Inui, M., Kawasaki, S., et al., 2019. Near-zero emission thermal power plant using advanced KM CDR processtm. Int. J. Greenhouse Gas Control 92, 102847.

Howarth, R.W, Jacobson, M.Z., 2021. How green is blue hydrogen? Energy Sci. Eng. 9 (10), 1676–1687. https://doi.org/10.1002/ese3.956.

Hydrogen production costs, 2021. Department for business. Energy Ind. Strat. https://www.gov.uk/.

Ismail Shah, M., Silva, E., Gjernes, E., Åsen Ingvar, K., 2021. Cost reduction study for MEA based CCGT post-combustion CO2 capture at technology center Mongstad. 15th Greenhouse Gas Control Technol. Conf. 15–18. Abu dhabi: SSRN.

Joffe, D., Livermorey, S., Hemsley, M. Hydrogen in a low-carbon economy. Committee on Climate Change; 2018 22 November 2018.

Léonard, G., Crosset, C., Toye, D., Heyen, G., 2015. Influence of process operating conditions on solvent thermal and oxidative degradation in post-combustion CO2 capture. Comput. Chem. Eng. 83, 121–130. https://doi.org/10.1016/j.compchemeng.2015.05.003.

Masson-Delmotte, V., Pirani, A., Chen, Y., Matthews, J.B.R., Yelekçi, O., Lonnoy, E., et al., 2021. Climate Change 2021: The Physical Science Basis. Cambridge University Press: IPCC.

Mcqueen, N., Vaz Gomes, K., Mccormick, C., Blumanthal, K., Pisciotta, M., Wilcox, J., 2021. A review of direct air capture (DAC): scaling up commercial technologies and innovating for the future. Prog. Energy 3 (3). https://doi.org/10.1088/2516-1083/abf1ce.

Michailos, S..Gibbins, J. A modelling study of post-combustion capture plant process conditions to facilitate 95–99% Co2 capture levels from gas turbine flue gases frontiers in energy research. 2022;10. 10.3389/fenrg.2022.866838.

Morgan, J.C., Chinen, A.C., Anderson-Cook, C., Tong, C., Carroll, J., Saha, C., et al., 2020. Development of a framework for sequential Bayesian design of experiments: application to a pilot-scale solvent-based CO2 capture process. Appl. Energy 262. https://doi.org/10.1016/j.apenergy.2020.114533.

Mullen, D., Lucquiaud, M., 2022. Zero carbon electricity with CCS: a techno-economic analysis of combined cycle gas turbines. In: Proceedings of the 14th International Conference on Applied Energy (ICAE2022). Germany. Bochum.

National Carbon Capture Center [Internet] 2021 [Available from: https://www.nationalcarboncapturecenter.com/.

Negative Emissions, 2019. Technologies and Reliable Sequestration: A Research Agenda. The National Academies Press: National Academies of Sciences, Engineering, and Medicine, Washington, DC.

Nessi;, E., Papadopoulos;, A.I., Seferlis, P., 2021. A review of research facilities, pilot and commercial plants for solvent-based post-combustion CO2 capture: packed bed, phase-change and rotating processes. Int. J. Greenhouse Gas Control 111. https://doi.org/10.1016/j.ijggc.2021.103474.

Nexant, 2016. Pre-Feasibility Study for Establishing a Carbon Capture Pilot Plant in Mexico. World Bank. https://www.gob.mx.

Ofgem. Gas Prices: forward Delivery Contracts - Weekly Average (GB) ofgem.gov.uk 2022 [Available from: https://www.ofgem.gov.uk/energy-data-and-research/data-portal/wholesale-market-indicators.

Rates, E., 2023. US Dollar to British Pound Spot Exchange Rates for 2020 [Internet]. Exchange Rates. Available from: https://www.exchangerates.org.uk/USD-GBP-spot-exchange-rates-history-2020.html.

Rehl, T., Müller, J., 2013. CO2 abatement costs of greenhouse gas (GHG) mitigation by different biogas conversion pathways. J. Environ. Manage. 114, 13–25. https://doi.org/10.1016/j.jenvman.2012.10.049.

Review of next generation, 2022. carbon capture technology for industrial, waste and power sectors. www.GOV.UK. Dep. Bus. Energy Ind. Strat.

Romano, M.C., Antonini, C., Bardow, A., Bertsch, V., Brandon, N.P., Brouwer, J., et al., 2022. Comment on "How green is blue hydrogen? Energy Sci. Eng. 10 (7), 1944–1954. https://doi.org/10.1002/ese3.1126.

Sinnott, R., Towler, G., 2020. Chemical Engineering Design. Elsevier.

Smith, M.A., Cain, M., Allen, M.R., 2021. Further improvement of warming-equivalent emissions calculation. Clim. Atmos. Sci. 4 https://doi.org/10.1038/s41612-021-00169-8.

Soltani, S.M., Fennell, P.S., Mac Dowell, N., 2017. A parametric study of CO2 capture from gas-fired power plants using monoethanolamine (MEA). Int. J. Greenhouse Gas Control 63, 321–328. https://doi.org/10.1016/j.ijggc.2017.06.001.

Spath, P.L., Mann, M.K., 2001. Life Cycle Assessment of Hydrogen Production Via Natural Gas Steam Reforming. National Renewable Energy Laboratory. Report No.: NREL/TP-570-27637.

Stark, C., Mike, T..Joffe, D. The sixth carbon budget: the UK's path to net zero. Committee on Climate Change; 2020 9 December 2020.

THE CHEMICAL ENGINEERING, 2022. PLANT COST INDEX [Internet] Chemengonline. Com. Chemical Engineering. Available from: https://www.chemengonline.com/pci-home.

UK Low carbon hydrogen standard. www.gov.uk: Crown copyright; 2022.

UK Hydrogen, 2021. Strategy. www.gov.uk: department for business. Energy Ind. Strat.

3.1 Discussion & Conclusions

This study provides critical insights into the process conditions required to operate a SMR that captures 100% of the fossil CO_2 produced in the process. It demonstrates that through the following relatively minor process modifications:

- Increased absorber packing height from 14 to 20m.
- Reduction in lean loading from the traditional levels of circa 0.20-0.25 to 0.16 mol CO_2/mol MEA.
- Increased desorber pressure and temperature from circa 180Kpa and 120°C to 210Kpa and 125°C.

The driving force in the absorber can be maintained, achieving approximately stable rich loadings (0.47 mol CO_2/mol MEA) as CO_2 capture fractions increase. As high-rich loadings are key to reducing specific reboiler duties (SRD), this allows 100% fossil CO_2 capture to be achieved with an SRD of 3.67 GJ/tCO_2, compared to 3.62 and 3.60 GJ/tCO_2 with 5% and 10% residual emissions respectively. This results in a 1.9% point drop in HHV thermal efficiency in hydrogen production when moving from 5% residual emissions (68.7%) to 100% fossil CO_2 capture (66.8%) and 2.8% from 10% residual emissions (69.6%).

A detailed techno-economic model estimates the LCOH production, which captures 100% of the fossil CO_2, at 68.8 £/MWh$_{th}$ HHV (2.7 £/kg) just 5.3% (65.3£/MWh$_{th}$ HHV) and 3.6% (66.4 £/MWh$_{th}$ HHV) more costly than hydrogen produced with 10% and 5% residual emissions, respectively and a 55% (44.2 £/MWh$_{th}$ HHV) increase from an SMR with no CO_2 abatement. This, coupled with the use of an open art solvent (35 %wt. MEA), leads to the conclusion that 100% fossil CO_2 capture can be achieved for the SMR process using currently available technology and at a much lower efficiency impact than previously thought, with a carbon penalty of circa 200 £/tCO_2 making it the most economical option.

Nonetheless, this does not mean zero carbon hydrogen is achieved. This work proposes that CO_2e emissions from methane leakage, CO_2 transport and storage network and the construction & decommissioning of the plant be recaptured using permanent negative emission technology (NET). As likely the most expensive form of NET, DACCS with an

estimated cost of 100 – 1000 £/tCO_2 is used in this study. This increases the cost of hydrogen production to 70 – 103 £/MWh_{th} HHV (2.8 – 4.1 £/kg).

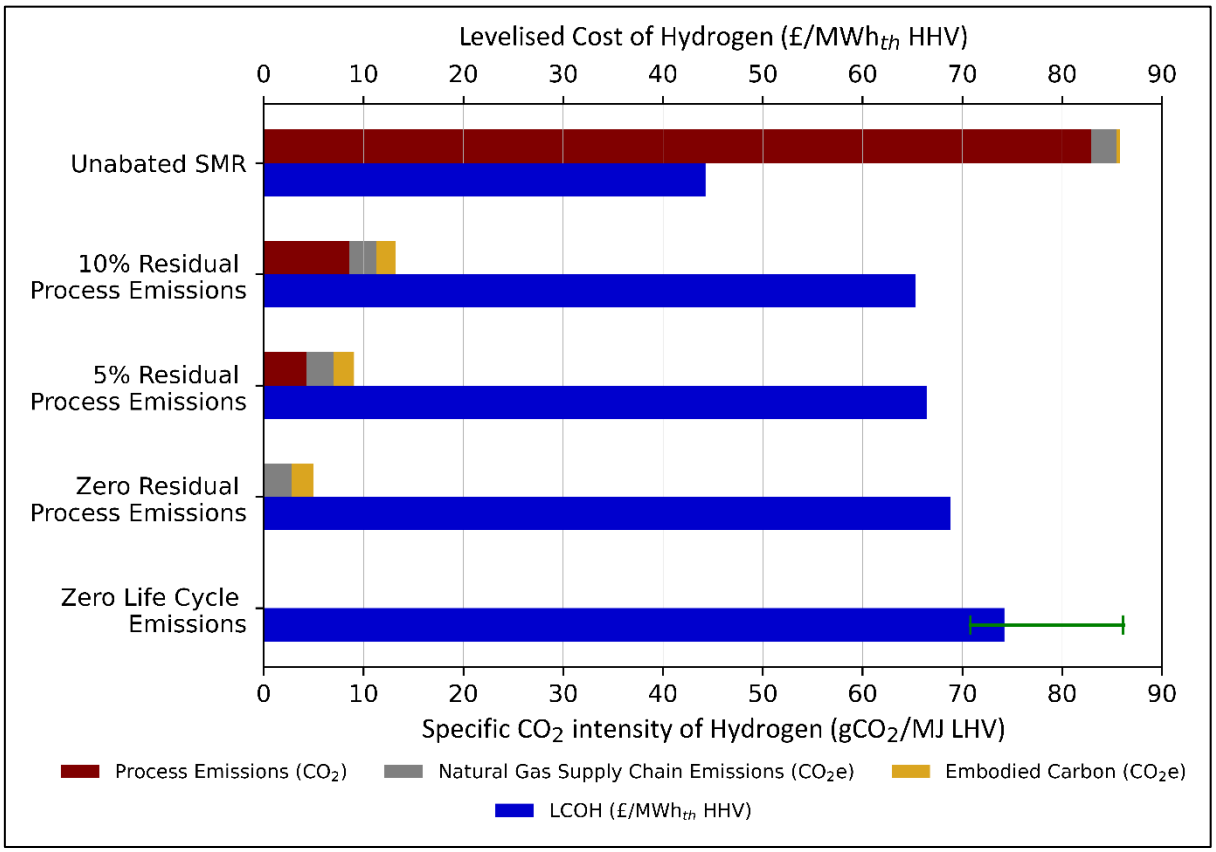


Figure 6: On the cost of zero carbon hydrogen: A techno-economic analysis of steam methane reforming with carbon capture and storage - Graphical Abstract

---

When compared to the counterfactual for hydrogen use (combustion of natural gas), assuming combustion of hydrogen as the use case. The cost of CO_2 avoided (CCA) was found to be 265.9 £/tCO_2e on a lower heating value (LHV) basis for the 100% fossil CO_2 capture case and 248-401 £/tCO_2e when lifecycle emissions were included, with a median value of 273 £/tCO_2e (1.5% natural gas supply chain emissions and DACCS costs at 300 £/tCO_2). The lowest cost permanent NET was identified as a critical factor in the viability of hydrogen to serve as an economic CO_2 reduction pathway. In order to be economical, the CCA using the appropriate counterfactual must be lower than the cost of the recapture of the emissions from said counterfactual.

3.2 Highlights

- Zero carbon blue hydrogen can be achieved economically with commercially available technology.
- 100% fossil CO_2 capture increases capital and operational costs 5% and 4%.
- Permanent fugitive emission offset increases hydrogen costs by 2 to 25% in the UK.
- Global warming potential metric GWP* indicates lower climate impact of methane.
- Fuel switching CO_2 avoidance costs range from 223 to 367 £/tCO_2e (HHV).

3.3 Limitations and Future Work

The following limitations were identified for the work described in this chapter; any future work should endeavour to resolve these limitations:

- The GWP of leaked hydrogen from the production facility and downstream supply chain was not included in this study due to the high degree of uncertainty around leakage rates and the atmospheric effect of hydrogen.
- The cost and CO_2e emissions from the construction and operation of a hydrogen supply chain were not included, which would increase the cost of CO_2 avoided from the counterfactual of natural gas combustion.
- This lifecycle study is limited to the GHG effect of the atmospheric methane and CO_2 equivalent emissions; additional GHGs such as NO_2 and SF_6 are not included. Likewise, non-GHG-related environmental considerations are out of scope.
- The lean loading in the post-combustion plant was limited to 0.16 mol CO_2/mol MEA. This was due to concerns around detrimental increases in MEA degradation rates at higher regeneration temperatures, which are required to efficiently produce lower lean loadings. Emerging research conducted as part of this thesis (ref Chapter 6) has indicated that this may not be as large of an issue as previously thought; should that be the case, it's likely an increase in thermal efficiency of hydrogen production would be possible with reduced lean loadings.

.

4. On the cost of Zero Carbon Electricity: A Techno-Economic Analysis of Combined Cycle Gas Turbines with post-combustion CO_2 capture

Any functioning electricity grid requires the ability to match the supply of electricity with the demand from consumers. When instantaneous generation or stored energy from intermittent renewable generators (e.g., wind/solar) is below demand, and demand cannot be reduced sufficiently the marginal generation source must be a dispatchable source.

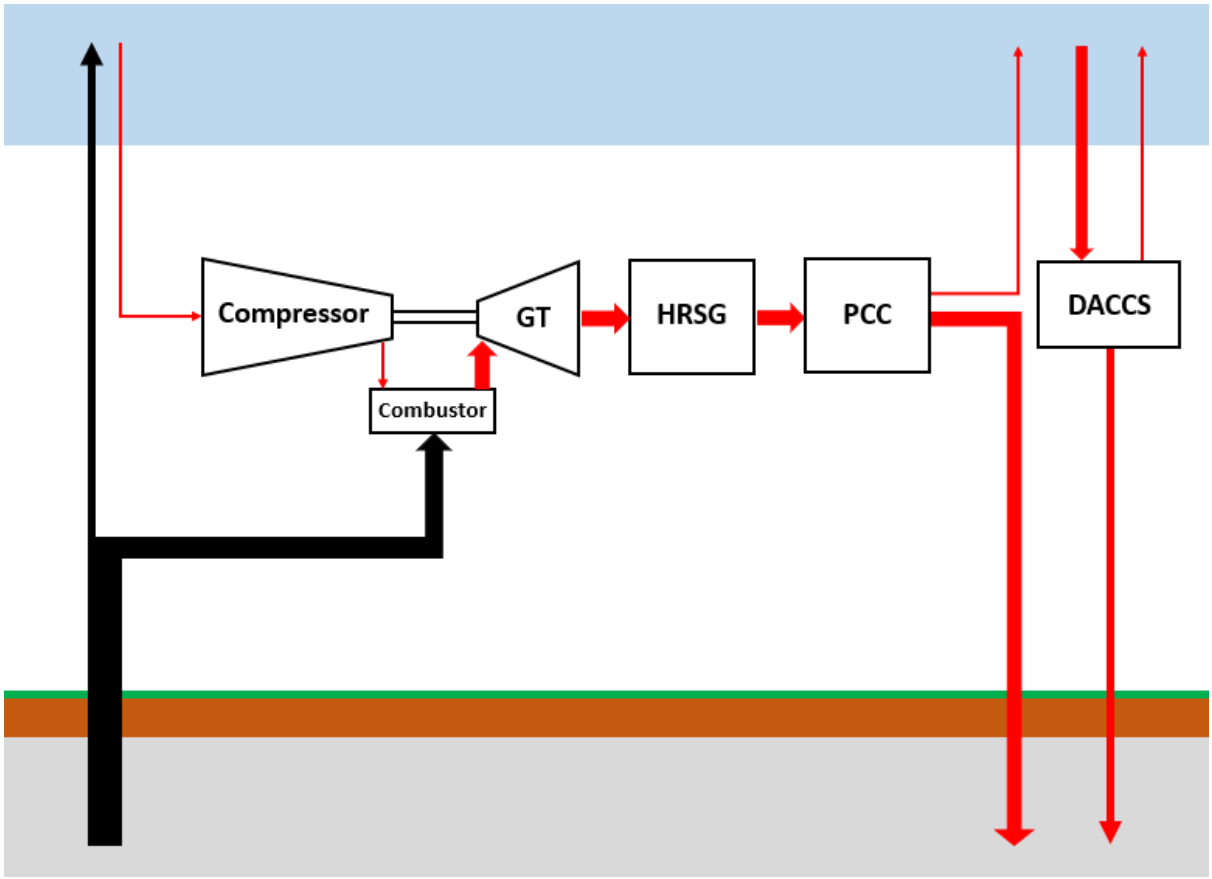


Figure 7: Illustration of a route to zero carbon electricity from CCGTs using post combustion CO_2 capture coupled with direct air capture. CO_2 (Red), Fossil Carbon (Black)

In many modern electricity grids, particularly those on the European continent, this capacity is typically provided by the highly efficient natural gas fired combined cycle gas turbines (CCGT). This study investigates how, in a net zero compatible electricity grid, CCGTs can continue to meet this critical role while being fully decarbonised via a combination of post combustion carbon capture (PCC) achieving CO_2 capture fractions that remove all of the CO_2 produced in the process i.e., 100% fossil CO_2 capture (equivalent to a 99.2% gross CO_2 capture fraction

in CCGTs) and direct air CO_2 capture and storage (DACCS) (or equivalent negative emissions technology (NET)) to recapture any upstream or downstream greenhouse gas (GHG) emissions.

A bespoke model of a GE H-Class 1 X 1 combined cycle gas turbine (GE 9HA.01) with a rated thermal efficiency of 63.5% lower heating value (LHV) was created in gPROMS Process Builder (gPROMS, 2021) while the PCC using a 35% wt. (Monoethanolamine) MEA solution was modelled using an open-source steady-state PCC model (Morgan *et al.*, 2020). State of the art understandings of the solvent regeneration process was utilised as part of the analysis to demonstrate the thermally efficient capture of 100% of the CO_2 generated in the process. This provides evidence that this can be achieved with comparable specific energy requirements to those required to achieve a 95% CO_2 capture fraction. A new model (Braakhuis, Høisæter and Knuutila, 2022) describing the mechanisms governing the thermal degradation of MEA is employed to estimate the increase in specific solvent thermal degradation that results from the increased solvent regeneration temperatures required to efficiently achieve the ultra-high CO_2 capture fractions proposed. The cost of recapture of all upstream and downstream greenhouse gas (GHG) emissions using DACCS is estimated from the available literature as between 100-1000 £/tCO_2 with 300£/tCO_2 as the median value.

A detailed techno economic analysis is completed to assess the cost completeness of net zero CCGTs when compared to the counterfactual of 95% CO_2 capture fraction, with the UK dispatchable power agreement (DPA) serving as a case study.

Energy Reports 11 (2024) 5104–5124

Contents lists available at ScienceDirect

Energy Reports

journal homepage: www.elsevier.com/locate/egyr

Research Paper

On the cost of zero carbon electricity: A techno-economic analysis of combined cycle gas turbines with post-combustion CO_2 capture

Daniel Mullen [a,*], Mathieu Lucquiaud [b]

[a] School of Engineering, University of Edinburgh, Edinburgh, United Kingdom
[b] Department of Mechanical Engineering, University of Sheffield, United Kingdom

ARTICLE INFO

Keywords:
Carbon capture and storage
Net-zero
Climate mitigation technologies
Combined-cycle gas turbine
Post Combustion CCS

ABSTRACT

To achieve a sustainable electricity grid, affordable and dispatchable power capacity that supports grid stability and does not increase atmospheric CO_2 levels will be required. Combined cycle gas turbines (CCGTs) with post-combustion CO_2 capture (PCC) can meet these requirements by capturing and permanently storing all combustion CO_2 emissions and, coupled with negative emissions technologies, any remaining life-cycle emissions. For the first time, we present a comprehensive analysis of the technical and financial challenges of producing zero-carbon electricity from CCGTs on a life-cycle basis. We conclude that when the design is optimised, fossil CO_2 capture fractions can be increased from 96% to 100% with minimal process modification, commercially available technology and an additional 0.5% decrease in thermal efficiency. This represents a significant 60–70% reduction in the additional efficiency penalty required to reach zero CO_2 emission operation. The Cost of CO_2 Avoided of 100% fossil CO_2 capture is just 128 £/tCO_2, a 3 £/tCO_2 increase over the 95% gross CO_2 capture fraction required to permit PCC projects in the UK. Indeed, within the bounds of the UK power CCS business model, we show that 100% fossil CO_2 capture maximises both variable and capacity payments to the producer, resulting in a 2% decrease in the cost of power produced. For zero-carbon electricity on a life-cycle basis, the recapture and permanent geological storage of all remaining life-cycle CO_2e emissions from plant construction & decommissioning, CO_2 T&S network operation and the natural gas supply chain (operational CO_2e emissions and methane leakage) increases the median Cost of CO_2 Avoided to 178 £/tCO_2 (130–371 £/tCO_2), leading to the novel conclusion that a market mechanism equating to a CO_2 price of over 178£/tCO_2 is likely sufficient to incentivise the development of truly CO_2-neutral CCGTs.

1. Introduction

An electricity grid compatible with the 2050 climate commitments requires retaining existing capacity or installing new capacity to dispatch on-demand power to ensure a stable electricity supply to consumers during fluctuations in intermittent power production facilities. Implicit in the assumption of a net zero electricity grid is that this dispatchable power capacity is itself net-zero, with life-cycle greenhouse gas (GHG) emissions eliminated or recaptured and permanently stored. Many potentially low-carbon technologies could provide this service, including zero-carbon energy storage, increased interregional grid connections, and thermal power generation with carbon capture and storage (CCS).

When instantaneous generation or stored energy from intermittent renewable generators (e.g. wind/solar) is below demand, and demand cannot be reduced sufficiently, the marginal generation source must be a

Abbreviation: CCS, Carbon Capture and Storage; CCGT, Combined Cycle Gas Turbine; PCC, Post Combustion Capture; DEZNZ, Department for Energy Security and Net Zero; LCOE, Levelised Cost of Electricity; LCOC, Levelised Cost of Capture; CCA, Cost of CO_2 Avoided; BAT, Best Available Technology; LHV, Lower Heating Value; HHV, Higher Heating Value; NCCC, National Carbon Capture Centre; MEA, Monoethanolamine; CAPEX, Capital Expenditure; OPEX, Operational Expenditure; GHG, Greenhouse Gas; DACCS, Direct Air Carbon Capture and Storage; T&S, Transport and Storage; CCSI, Carbon Capture Simulation Initiative; L/G, Liquid over Gas ratio; FEED, Front-End Engineering Design; GWP, Global Warming Potential; LCA, Life Cycle Analysis; NPV, Net Present Value; EPC, Engineering, Procurement and Construction; EOP, Electricity Output Penalty; SRD, Specific Reboiler Duty; CEPI, Chemical Engineering Plant Index; ICCI, International Construction Cost Index; NREL, National Renewable Energy Laboratory; NET, Negative Emission Technology; EGR, Exhaust Gas Recycle; EfW, Energy From Waste; DPA, Dispatchable Power Agreement.

* Corresponding author.
E-mail address: d.t.mullen@sms.ed.ac.uk (D. Mullen).

https://doi.org/10.1016/j.egyr.2024.04.067
Received 17 December 2023; Received in revised form 18 March 2024; Accepted 30 April 2024
Available online 10 May 2024
2352-4847/© 2024 The Authors. Published by Elsevier Ltd. This is an open access article under the CC BY license (http://creativecommons.org/licenses/by/4.0/).

dispatchable source. It follows that, in the case where a future electricity grid fails to supply 100% of its power from non-dispatchable sources, the cost of providing dispatchable power is a critical factor in the overall cost of electricity grid decarbonisation and furthermore that dispatchable power generation assets must be decarbonised. In many parts of the world, these assets are fossil fuel based and increasingly combined cycle gas turbines (CCGT). A fully decarbonised CCGT provides the ability to dispatch on-demand power decoupled from renewable generation and may eliminate the need to deploy excess renewables and extensive energy storage facilities.

This decarbonisation pathway is echoed by the sixth carbon budget issued by the UK Committee on Climate Change (Stark et al., 2020), which expects demand for low-carbon electricity to double from today's 300 TWh/pa to between 550 and 680 TWh/pa by 2050, with dispatchable generation making up 6–15% (43–83 TWh) of the energy mix. This report suggests that CCS-enabled CCGTs are expected to play a pivotal role by supplying a predicted 30 TWh/pa of UK demand. This represents 5% of total power demand. However, it is indispensable for maintaining grid stability thanks to its swift response capabilities, significant rotational inertia and availability thanks to the long-term storage capability of natural gas.

Although commercially available and operational globally on coal-

Table 1
Review of published data on CO_2 capture fractions over 95%.

Reference	Solvent	Data source	Lean Loading (mol/mol)	CO_2%vol	Flue gas source	CO_2 capture fraction (%)	SRD	CCA	LCOC
Feron et al. (2019)	30%wt MEA	Modelling	0.20[a]	13.4	Coal	99–99.7	3.35 – 3.7 GJ/tCO_2	54.8–58.3 €/tCO_2	-
						95	3.64 GJ/tCO_2	55.2 €/tCO_2	-
				4.2	CCGT	99–99.1	4.2–4.4 GJ/tCO_2	85.5–87.1 €/tCO_2	-
						95	3.6 GJ/tCO_2	78.6 €/tCO_2	-
Danaci et al. (2021)	30%wt MEA	Modelling	0.27	4	Not Specified	99	-	-	57.5 – 99.3 $/t$CO_2$
						95	-	-	53.0 – 84.4 $/t$CO_2$
				8		99	-	-	46.6 – 69.7 $/t$CO_2$
						95	-	-	44.6 – 62.5 $/t$CO_2$
				12		99	-	-	43.3 – 60.6 $/t$CO_2$
						95	-	-	42.0 – 55.8 $/t$CO_2$
				21		99	-	-	40.2 – 52.2 $/t$CO_2$
						95	-	-	39.4 – 49.4 $/t$CO_2$
Michailos and Gibbins (2022)	35%wt MEA	Modelling	0.12	4	CCGT	99	3.77 GJ/tCO_2	-	-
			0.13–0.19			95	3.5 GJ/tCO_2	-	-
Gao et al. (2019)	5 M piperazine	Pilot Plant	0.2–0.27	10.6–12.3	Coal	99.1	2.3 GJ/tCO_2	-	-
						95	2.2 GJ/tCO_2	-	-
Shah et al. (2021)	35–37%wt MEA	Pilot Plant	0.21 – 0.26	3.9–4.2	CHP	97–98	3.7–4.0 GJ/tCO_2	-	-
						91	3.6 GJ/tCO_2	-	-
Hirata et al. (2019)	KS-1™	Pilot Plant	-	13.5	Coal	99.5	+2%[b]	+3%[b]	
Mullen et al. (2023)	35%wt MEA	Modelling	0.16	19.4	SMR	99.8	3.67 GJ/tCO_2	265.9 £/tCO_2e[d]	64.7 £/tCO_2
				19.9		95	3.62 GJ/tCO_2	271.9 £/tCO_2e[d]	63.3 £/tCO_2
Su et al. (2023)	35%wt MEA	Modelling	0.16	11.1	EfW	99.7	3.72 GJ/tCO_2	-	-
						95	3.59 GJ/tCO_2	-	-
Cownden et al. (2023)	30%wt MEA	Modelling	0.26	16.4	SMR	99	-	89 $/t$CO_2$[e]	-
						95	-	80 $/t$CO_2$[e]	-
Brandl et al. (2021)	30%wt MEA	Modelling	0.05–0.30	4	CCGT	98–99	-	-	120–190 $/t$CO_2$
						95	-	-	70–100 $/t$CO_2$
				8	CCGT (EGR)	98–99	-	-	80–100 $/t$CO_2$
						95	-	-	65–80 $/t$CO_2$
				12	Coal	98–99	-	-	70–85 $/t$CO_2$
						95	-	-	60–70 $/t$CO_2$
Moser et al. (2021)	CESAR1	Pilot Plant	-	15.2[c]	Coal	98	3.24 GJ/tCO_2	-	-
						95	3.00 GJ/tCO_2	-	-
Benquet et al. (2021)	CESAR1	Pilot Plant	-	3.5	CHP	98	3.2 GJ/tCO_2		
Hume et al. (2021)	CESAR1	Pilot Plant	0.10	5	CHP	98	3.61 GJ/tCO_2		
This Work	35%wt MEA	Modelling	0.10	4.9	CCGT	99.2	3.67 GJ/tCO_2	128 £/tCO_2e	108.8 £/tCO_2e
						95	3.52 GJ/tCO_2	125 £/tCO_2e	105.4 £/tCO_2e

[a] Assumed,
[b] Percentage change relative to the base case of 90% CO_2 capture,
[c] Dry basis,
[d] Based on natural gas fuel switching,
[e] Based on "grey H_2" abatement

fired power generation facilities (Steyn et al., 2022), the deployment, demonstration, and application of post-combustion capture (PCC) to the global CCGT fleet has yet to be realised as the low CO_2 concentration in CCGT flue gases increases the cost per unit of CO_2 captured compared with more concentrated sources (Danaci et al., 2021).

For CCS applications, a CO_2 capture fraction of 85–90% has been historically used throughout the literature (Brandl et al., 2021) and Front-End-Engineering-Design studies funded by governments for commercial projects (Elliott, 2022; Bechtel, 2019, 2018). This range of capture fractions and the associated residual stack emissions is rapidly becoming outdated. For example, the UK Best Available Technology (BAT) guidance recommends that PCC plants are designed to achieve a minimum net 95% CO_2 capture fraction annually. Although this is a welcome development, on the scale of decarbonisation required, this 5% rate of residual stack emissions is not trivial and is incongruous with net zero commitments. In the UK, the importance of providing and incentivising decarbonised fossil-based power generation has been illustrated by the Dispatchable Power Agreement (DPA) (Dispatchable Power Agreement business model summary, 2022) which details the business model for CCS-enabled power generation. Within this agreement is the concept of "clean power", whereby a facility's bankable power generation capacity is the net power output multiplied by the achieved CO_2 capture fraction over a specified period of time, i.e. the power paid for is decarbonised power. This simple calculation rewards a higher CO_2 capture fraction so long as the resulting decrease in abated power output is not more than 1% per every additional 1% point increase in CO_2 capture fraction.

There are increasing examples in the literature of capture fractions over 95% being technologically achievable and, in some cases, economically viable. An overview of the current literature on ultra-high CO_2 capture fractions, defined as CO_2 capture fractions greater than 95%, is detailed in Table 1.

Feron et al. report that transitioning to 99–99.1% from 95% CO_2 capture for an amine-based post-combustion system (30%wt MEA) impacts a 1.4–1.8% point decrease in thermal efficiency for a CCGT. This represents a significant deviation from the 0.5% reported in this work. The differences in MEA concentration will partly explain this discrepancy. However, no evidence of lean loading optimisation is presented in Feron et al.; therefore, we must assume that it has not been completed. Indeed, this appears to be supported by the increase in the liquid-to-gas ratio, i.e. from 0.92 to 1.07–1.22. This represents a 16–32% increase in solvent flow rate for a 4% increase in CO_2 capture fraction. This inefficiency must be born from an un-optimized lean loading leading to compromised rich loadings and inflated specific reboiler duties. Fig. 9 in Feron et al. indicates that this study may have used a lean loading of 0.20 mol/mol. However, this cannot be verified. As demonstrated, this is likely insufficient for achieving ultra-high CO_2 capture fractions in a CCGT while ensuring adequate driving force of absorption in the absorber column.

Danaci et al. showed that for a demonstrative flue gas flow rate of 500 kg/s with flue gas $CO_{2\%}$vol concentrations of 4%, 8%, 12% and 21% and using a 30%wt MEA solvent, transitioning from 90% to 99% CO_2 capture results in increases in the total capture costs of 12–26%, 6–16%, 4–12%, 3–7% respectively (Danaci et al., 2021). However, as with Feron et al., a lean loading optimisation was not completed, and a fixed value of 0.27 mol/mol was used. Section 3 of this manuscript explains how lean loadings above 0.14 mol/mol limit the driving force of absorption throughout the absorber column for CCGT flue gas when operating at ultra-high CO_2 capture fractions. It can then be inferred that the fixed lean loading assumed by Danaci et al. results in an unnecessarily high OPEX & CAPEX burden on the capture plant at low CO_2 concentrations and high CO_2 capture fractions. Similarly, this was the case in Cownden et al., who used a lean loading of 0.26 mol/mol for a 30%wt MEA solution. This was sufficient for lower rates of CO_2 capture due to the high CO_2 concentration in a steam methane reformer flue gas; however, it led to exponential increases in the cost of hydrogen production at capture fractions above circa 95%.

Brandl et al. present a model that attempts to predict the levelised cost of capture for a range of CO_2 flue gas concentrations and CO_2 capture fractions. Their results show that the levelised cost of capture increases from 70 to 100 \$/tCO_2 at 95% CO_2 capture for CCGT flue gases to 120 to 190 \$/tCO_2 at 98–99% CO_2 capture. Unlike the previous studies mentioned, lean loading optimisation has been completed by Brandl et al. However, the consent reboiler pressure of 159KPa assumed in this study is unlikely sufficient to avoid the inflection phenomenon described in Section 2.2 of this manuscript and will lead to an exponential increase in specific reboiler duty at low lean loadings. This would explain the rapidly increasing OPEX cost, which proposes a near doubling of OPEX for a 4% increase in CO_2 capture fraction in the most extreme case.

Michailos and Gibbins present a comprehensive process modelling study for a CCGT operating at ultra-high CO_2 capture fractions, optimising for lean loading and regeneration pressure. They show that transitioning to 99% CO_2 capture from 95% is achievable with a modest increase of 7.7% in the thermal energy input to the CO_2 capture process for a 35%wt MEA solvent solution (from 3.50 to 3.77 GJ/tCO_2). However, the analysis presented is limited to the thermodynamics of the CO_2 capture plant and does not consider the effect on the CCGT or the impact on the cost of electricity produced; as such, the studies ability to inform policy decisions is limited. A holistic assessment is required.

Su et al. and Mullen et al. also recognised the importance of low lean loadings and the benefits of increased desorber pressure. However, they limited the lean loading to at or above 0.16 mol/mol due to concerns relating to MEA degradation at increased regeneration temperatures. However, the application of recent work by Braakhuis et al (Braakhuis et al., 2022). presented in this manuscript indicates that the reduced carbamate concentration in lean amine solutions may partially or entirely offset any increase in thermal degradation due to increased regeneration temperatures (see Section 3.3). This was sufficient to achieve acceptable rich loadings in steam methane reformer and energy from waste flue gases due to the higher concentration of CO_2 but is unlikely to be suitable for a CCGT.

Gao et al., Shah et al., Hirata et al., Benquet et al., Hume et al. and Moser et al. present results from various pilot-scale plant operations where ultra-high CO_2 capture fractions of between 95 – 99.5% have been achieved with SRD values ranging from 3.0 – 4.0 GJ/tCO_2 for four different solvent formulations, one proprietary (KS-1™) and three open-art (MEA, Piperazine & CESAR1).

Gao et al. showed that increasing the CO_2 capture fraction of a coal-fired power plant from 90% to 99% increased the thermal input to the reboiler by less than 5%. Shah et al. demonstrated that 99% CO_2 capture can be achieved with a specific reboiler duty of 3.8 GJ/tCO_2, compared to 3.6 GJ/tCO_2 for a 91% CO_2 capture fraction. Hirata et al. calculated that achieving 99.5% CO_2 capture could be achieved with a 3% increase in the cost of CO_2 capture compared to 90%. Both Menquet et al. and Hume et al. present results from test campaigns at Technology Centre Mongstad completed using the CESAR1 solvent. Both presented findings for CO_2 capture fractions of 98%, with Benquet reporting an SRD of 3.2 GJ/tCO_2 for a 3.5% vol CO_2 flue gas with 24 m packing and Hume reporting an SRD of 3.61 GJ/tCO_2 for 5% vol CO_2 and 18 m of packing. Finally, Moser et al. found that specific reboiler duty increased from 3 GJ/tCO_2 to 3.24 GJ/tCO_2 for CO_2 capture fractions of 95 and 98%, respectively. Although these pilot plants are unlikely to have been designed or optimised for ultra-high CO_2 capture fractions, they nonetheless have been achieved with increases in energy and cost requirements that appear closer to a linear relationship to CO_2 capture fraction rather than exponential, a conclusion that appears to be solvent independent.

Of particular relevance are those CO_2 capture fractions resulting in zero residual stack emissions at the point of generation, where 100% of combustion CO_2 produced as part of the plant operation is captured, hereafter referred to as 100% fossil CO_2 capture. The effective CO_2

capture fraction required to achieve 100% fossil CO_2 capture varies between applications depending on the ratio of excess air used in combustion and, by extension, the ratio of fossil CO_2 to atmospheric CO_2 present in the flue gas. For a typical CCGT with a CO_2 concentration of 4–5% in the flue gas, a CO_2 capture fraction of 99–99.2% is required, increasing to 99.7% for a coal-fired power plant and 99.8% for a steam methane reformer (Mullen et al., 2023).

Yet, for electricity produced from natural gas to have zero life-cycle emissions, GHG emissions from the natural gas supply chain and embodied CO_2 in the construction and operation of the CCGT and CCS infrastructure must be recaptured.

Mullen et al (Mullen et al., 2023). propose that the cost of recapturing natural gas supply chain emissions is directly allocated to fuel prices in the LCOE calculations by attributing an additional operating cost per unit of energy supplied. The cost premium to be added depends on the current cost of DACCS and the carbon intensity of the natural gas supply chain.

The recapture of the embodied carbon from construction can correspond to an increase in CAPEX, with the recapture occurring during the construction period. Upstream emissions from the CCS T&S system are recaptured continually, representing an increase in OPEX costs.

To the authors' knowledge, this study presents the first comprehensive and optimised techno-economic analysis of a CCGT fitted with post-combustion CO_2 capture operating with a scope 1 carbon intensity of 0.0 gCO_2e/kWh. This is achieved by designing the PCC plant to achieve a gross capture fraction of 99.16% in the absorber column. This represents the capture of 100% of fossil CO_2 entering the boundaries of the power plant when the excess air used for combustion has been accounted for. Plant performance and costs are consistently compared to those of unabated CCGT and those of a CCGT with a scope 1 carbon intensity of 15.1 gCO_2e/kWh, corresponding to gross CO_2 capture fraction of 95% (96% fossil CO_2 capture), as per current UK guidelines for the permitting of post-combustion capture facilities. Both configurations are compared on the basis of thermal efficiency, levelised cost of electricity (LCOE), levelised cost of capture (LCOC) and cost of CO_2 avoided (CCA).

We go one step further in our analysis and present the added cost to electricity production required to achieve genuinely net zero operation of a CCGT, with the recapture and permanent storage of all life-cycle emissions with negative emission technologies (NET), as illustrated in Fig. 1. Including scope 2 and scope 3 emissions in electricity generation from CCGTs with CO_2 capture for the first time.

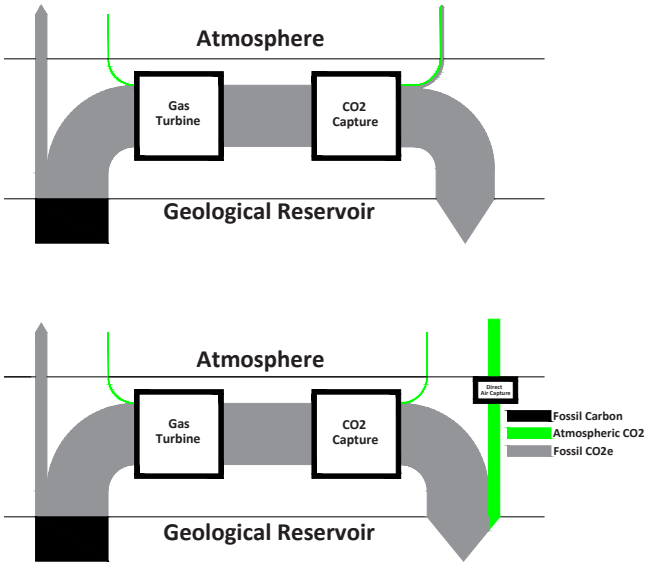


Fig. 1. Representation of pathways for a CCGT operating with 5% stack emission (top) and zero stack emission and fugitive emission recapture with DACCS (bottom). Atmospheric CO_2 (as represented by the green line) passing through the plant is 0.82% of the CO_2 leaving the CO_2 capture plant.

2. Methodology

2.1. Modelling methodology

A GE H-Class 1 ×1 combined cycle gas turbine (GE 9HA.01) with a rated thermal efficiency of 63.5% (LHV) is chosen here due to the availability of operational parameters in the public domain (Ge-Power, 2017, 2016; Smith et al., 2000; Matta et al., 2000). This is modelled using gPROMS Process Builder (gPROMS products: gPROMS PROCESSBUILDER, 2021), a flowsheet-based process modelling platform that allows the creation of high-fidelity custom models of processes for each specific plant operation. These units are built using first-principles mathematical models, defining the engineering relationships governing the process (i.e. reaction kinetics, thermodynamics) with the advanced solver simultaneously solving all equations from all the other units in the flowsheet. Peng-Robinson & IAPWS-95 are used as the gas mixture and steam/water thermodynamic models, respectively. Process modelling for the design and optimisation of the CO_2 capture plant is conducted using an open-source model developed by the Carbon Capture Simulation for Industry Impact (CCSI) in ASPEN PLUS (Morgan et al., 2020). This open-source model has been validated against pilot-scale data from the US National Carbon Capture Centre (NCCC) (National Carbon Capture Center, 2021). Fig. 2 shows a process flow diagram of the electricity generation and CO_2 capture processes. A detailed list of plant parameters is available in Appendix A. The CCGT process is identical to a GE H-Class 1 ×1 CCGT (GE 9HA.01) except for the LP steam extraction from the LP/IP crossover, which supplies steam to the CO_2 capture plant, and hot LP condensate return from the desorber reboiler. The flue gas exiting the LP economiser is separated into two streams and cooled down to saturated conditions at 40 °C; booster fans are then used to overcome the pressure drop through parallel CO_2 absorbers, each processing half the flow.

The flue gas enters the bottom of a counter-current packed bed absorber while the CO_2 lean MEA solvent (lean solvent) enters the top. The lean solvent to flue gas flow rate ratio is often called the liquid-to-gas ratio (L/G ratio). It is set to achieve the required CO_2 capture fraction in the absorber in conjunction with other process parameters. As the flue gas passes through the solvent-laden packing, CO_2 is transferred to the liquid solvent and reacts exothermically, heating the flue gas and solvent. The CO_2-depleted flue gas leaves the top of the CO_2 capture packing and then passes through a water wash and acid wash section to reduce residual MEA and amine degradation products down to environmentally acceptable levels before its release into the atmosphere. CO_2-rich solvent (rich solvent) leaves the bottom of the absorber to be stripped of CO_2.

Redistribution of liquid is typically required every 20 theoretical stages, corresponding to 8 m of Mellapak 252.Y packing, to ensure uniform solvent distribution in absorption columns (Ausner, Iija "Maximum packed bed height Mellapak 252.Y" (pers. comm., February 28, 2022)), while maximising bed height reduces absorber CAPEX per m^3 of additional packing as the need for additional column internals is minimised. To ensure maximum utilisation of CAPEX, 20 m of packing is used for a CCGT operating with 96% fossil CO_2 capture, and 24 m is used to achieve 100% fossil CO_2 capture. This is similar to the packing height requirements of other CO_2 capture applications (see Fig. 5 for a sensitivity study). A FEED study completed by Bechtel investigating the retrofitting of CO_2 capture to a coal power plant for 90% CO_2 capture with a flue gas concentration of 11.2% v/v CO_2 advised a packing height of 15 m (Bechtel, 2018). Shah et al. show that for tests completed at Technology Center Mongstad on flue gas CO_2 concentrations of 3.6–4.0% v/v CO_2 with MEA, 18 m of packing is sufficient to achieve favourable specific reboiler duties at 90% CO_2 capture. In comparison, 24 m is required to achieve CO_2 capture fractions over 98% (Shah et al.,

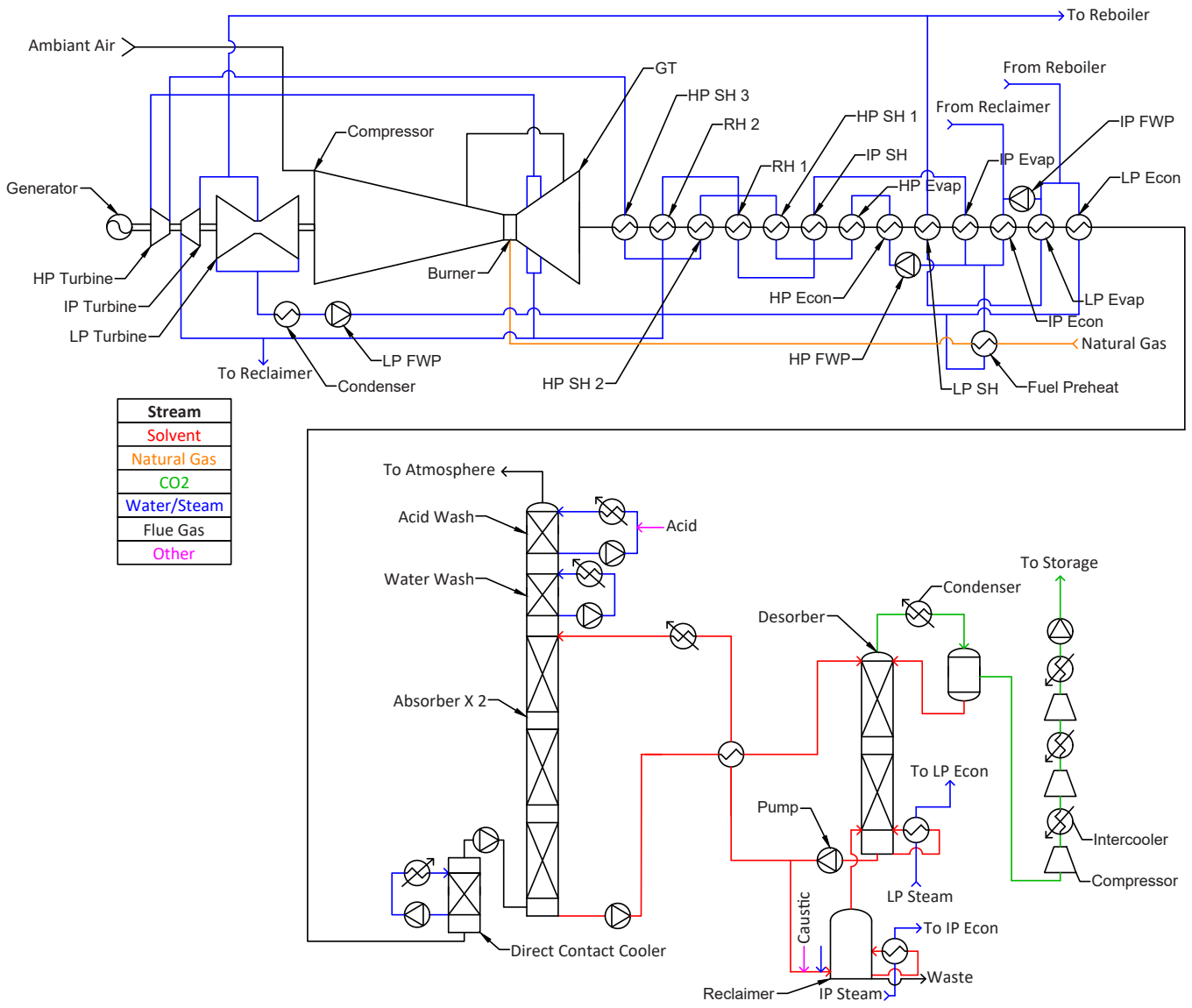


Fig. 2. Process flow diagram of a conventional combined cycle gas turbine fitted with post combustion carbon capture.

2021). Due to the low partial pressure of CO_2 at the top of the absorber when 100% fossil CO_2 capture is achieved, a lean loading of 0.14 mol CO_2/mol MEA or below was found to be required, i.e., lower than typical values of 0.2–0.3 mol CO_2/mol MEA found in the literature for 90% capture. 24 m of packing ensures that the energy released from the exothermic absorption reaction is spread more evenly throughout the height of the absorber, avoiding a mass-transfer pinch and the use of absorber intercooling.

The rich solvent leaving the bottom of the absorber is pumped to the CO_2 desorber. Before the desorber, sensible heat from the hot lean solvent leaving the desorber at ca. 120–140 °C is transferred to the rich solvent in the lean/rich heat exchanger. As the rich solvent travels down the counter-current desorber column, the stripping steam generated in the reboiler liberates the stored CO_2 from the solvent, which exits the top of the desorber column to be cooled, dried, and compressed. The final specification of the CO_2 to be delivered to the pipeline is project-specific; however, this study considers dense-phase CO_2 at 110 bar. Heat is transferred to the reboiler by condensing low-pressure steam extracted from the power cycle.

2.2. Desorber inflection point

Michailos and Gibbins and Mullen et al. both describe what has been termed the "inflection point" phenomenon within the desorber column of an amine-based PCC plant. As the desorber reboiler produces lower lean loadings, the energy of regeneration required to produce that lean loading is relatively constant until a distinct point or "inflection point", where the energy input needed to achieve lower lean loading increases exponentially. The results from the process modelling by Michailos and Gibbins indicate that this is due to the increased production of steam in the reboiler, which exceeds the capacity of the desorber column to condense, resulting in increased heat rejection in the reflux condenser. The same process modelling indicates that this steam production can be suppressed by increasing desorber operating pressure, allowing for decreased lean loadings to be achieved with specific reboiler duty similar to that of traditional lean loadings (0.2–0.3 mol/mol) at the cost of higher reboiler operating temperatures and increased exergy of reboiler steam. Due to the low partial pressure of CO_2 at the top of an absorber when operating at ultra-high CO_2 capture fractions, a low lean loading is likely to be required to maintain the driving force of absorption. For this study, all the desorber operating conditions presented are designed to operate at the inflection point for a given lean loading,

resulting in variable desorber operating temperatures and pressures for each lean loading.

2.3. Solvent consumption rates

MEA will degrade when exposed to oxygen-rich atmospheres (oxidative degradation) (Goff and Rochelle, 2004) or high temperatures (thermal degradation) (Davis and Rochelle, 2009). Unless effectively controlled, solvent degradation can reduce CO_2 capture performance, increase atmospheric emissions and operational costs and accelerate equipment corrosion (Martin et al., 2012).

While MEA has been used in industrial settings for decades (Steyn et al., 2022), however, the rate of MEA degradation is often not reported due to commercial sensitivity, while pilot scale campaigns are often not long enough to quantify degradation rates. Where available, Table 2 details the total MEA consumption rate (which is a combination of process losses and solvent degradation) observed over various pilot plant test campaigns, representing a range of 0.17 – 1.5 kg/tCO_2 captured. The wide range seen is indicative of the sensitivity of MEA consumption rates to operational procedures (effective atmospheric emission control) and conditions (flue gas composition, regeneration conditions, equipment residence times) as well as solvent management techniques (solvent reclaiming).

As detailed throughout this manuscript, thermally efficient capture of 100% of the fossil CO_2 from a CCGT flue gas will required solvent regeneration at 130–140 °C, which is higher than those presented in Table 2 at 117 – 123 °C. It was history expected that this would dramatically increase thermal degradation rates (Davis and Rochelle, 2009). However a new model presented by Braakhuis et al (Braakhuis et al., 2022). describing thermal degradation in a loaded MEA solution shows that the formation of degradation compounds is strongly related to carbamate concentration within the solution (CO_2 loading), indicating that as loading decreases, the rate of thermal degradation will also decrease. Table 3 summarises the degradation pathways of CO_2-loaded MEA due to thermal degradation as presented by Braakhuis et al.

This work applies the Braakhuis model to the higher regeneration temperatures and low lean loadings (see Section 3.3) required for ultra-high CO_2 capture. The results indicate that the reduced carbamate concentration in lean amine solutions partially or entirely offsets the expected increase in thermal degradation rate caused by higher reboiler temperatures. This implies that the reboiler temperature and pressures required to regenerate very lean amine solutions efficiently may not substantially increase MEA degradation rates. This is further investigated in Section 3.

Further work by Braakhuis et al (Braakhuis and Knuutila, 2023). presents an oxidative degradation model for MEA. They find that, although natural gas-based flue gases (such as a CCGT) have higher O2 concentrations than those found in Coal or waste-to-energy (WtE) plants, the lower temperatures in the absorber due to the decreased rate of reaction between the solvent and CO_2 lean flue gas limits oxidative degradation. Braakhuis et al. predict that the resulting specific oxidative degradation rate of MEA will be similar or lower for natural gas-based combustion than for Coal or WtE flue gases. Nonetheless, MEA degradation rates at the conditions required for ultra-high CO_2 capture remain an open question and require long-term test campaigns to quantify.

In any case, the overall cost implications of a moderate increase in MEA consumption rate are likely minimal due to the low purchase cost of MEA. Elliott et al (Direct Air Capture, 2022). present results from a FEED study completed by Bechtel for Panda Energy; they estimate MEA consumption at 2 kg/tCO_2 captured when solvent regeneration is completed at circa 130°C. The MEA supply price of 1.15 $/kg listed by Elliott et al. results in a cost of 2.3 $/t$CO_2$ captured. The sensitivity of the levelised cost of electricity is further investigated in Section 3.3.

2.4. Life cycle emissions

Mullen et al. provide the effect of supply chain methane emissions on product life-cycle emissions (Mullen et al., 2023). Although natural gas is a more potent GHG than CO_2, it is shorter-lived in the atmosphere (11.8 ± 1.8 years) (Masson-Delmotte et al., 2021) and, as such, does not accumulate in the same way. Global warming potential (GWP) is a metric traditionally used for comparing the climate impact of different GHGs by equating the rates of each species with an equivalent emission rate of CO_2. However, Cain et al. and Smith et al (Smith et al., 2021; Cain et al., 2019). show that GWP consistently overestimates the warming effect of methane emissions in scenarios where the global methane emission rate is constant or reducing. This article uses the alternative metric proposed by Cain et al., GWP*, which determines CO_2-equivalence based on both the current rate of methane emissions and the change in emission rate (Eq. 1).

$$CO_2e(t) = GWP_{100} * [4.53 * E_{CH4}(t) - 4.25 * E_{CH4}(t-20)] \quad (1)$$

Where t is the year under analysis, CO_2e(t) is the equivalent CO_2 emissions resulting from methane emissions in year t (tCO_2e/pa), GWP100 is the global warming potential value of methane over 100 years, and $E_{CH4}(t)$ is the total annual methane emissions in year t (tCH_4/pa).

Mullen et al. state, "If methane emissions from the previous two decades were equal to current emissions, virtually no additional contribution to the rate of warming would have occurred because the level of atmospheric methane remains approximately constant."

Fig. 3 from Mullen et al. shows the predicted cumulative atmospheric CO_2e emissions resulting from an increase of 1 tonne per year in annual methane emissions sustained for a 25-year operational period (then returning to zero) when calculated using three different CO_2 equivalent metrics (GWP*, GWP100, and GWP20). As GWP100 and GWP20 assume no oxidation of atmospheric methane, the long-term net change in

Table 2
MEA consumption rates at pilot plant facilities.

Plant	Flue Gas	MEA % wt.	Desorber P (bara)	Desorber T (°C)	Duration	Solvent Consumption Rate (kg/tCO_2)	Reclaiming
Esbjerg (Knudsen et al., 2007)	12.4% CO_2 (Coal)	30	1.89	120.5	550 Hrs	1.4	No
Niederaussem (Moser et al., 2011)	14.2% CO2 (Coal) 3.9% O_2	30	1.75	117	5000 Hrs	0.3	No
Tiller (Aronu et al., 2019)	13.4% CO2 (BECCS) 6.5% O_2	30	1.8–1.9	120–123	706 Hrs	0.56	No
Niederaussem (Weir et al., 2023)	14.2% CO_2 (Coal) 5.0% O_2	30	1.75	117	270 Days	0.35	No
Niederaussem (Weir et al., 2023)	14.2% CO_2 (Coal) 5.0% O_2	30	1.75	117	100 Days	0.17	Yes
TCM (Faramarzia et al., 2016)	3.7% CO_2	30	1.9	120	8 Weeks	1.5	No
Huaneng Changchun (Feron et al., 2016)	11.59% CO_2 4.53% O_2	17.7–20.5	-	120	1063 Hrs	0.82	No

Table 3
MEA thermal degradation pathways as presented by Braakhuis et al.

Reaction	Degradation Product	CAS registry	Reaction	Reaction law	Rate Constant (k) [m^3/mol.s]	Activation energy (kJ/mol)
R_1	HEEDA	111–41–1	2MEA -> HEEDA + H_2O	k[MEA][CO_2]	1.599e-11	151.1
R_2	TRIMEA	1965–29–3	MEA + HEEDA -> TRIMEA	k[HEEDA][CO_2]	1.117e-10	121.5
R_3	HEIA	3699–54–5	HEEDA + CO_2 -> HEIA	k[HEEDA][CO_2]	3.054e-10	142.6
R_4	AEHEIA	1402137–23–8	TRIMEA + CO_2 -> AEHEIA	k[TRIMEA][CO_2]	2.839e-10	136.2
R_5	BHEU	15438–70–7	2MEA -> BHEU + H_2O	k[MEA][CO_2]	1.281e-12	Not provided

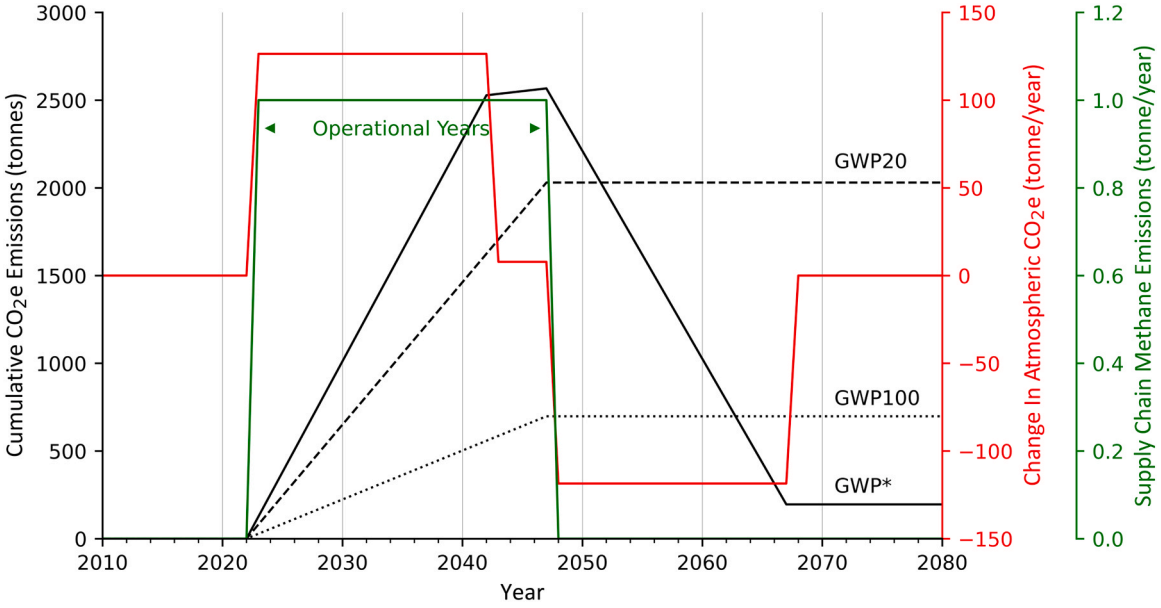


Fig. 3. Comparison of GWP*, GWP100 and GWP20 when evaluating cumulative CO_2e emissions resulting from a sustained methane emission rate of 1 tonne per annum over a 25-year period. The green line represents annual methane emissions while the red line shows the net change in atmospheric CO_2e per year as predicated by GWP* (extracted from Mullen et al (Mullen et al., 2023).).

atmospheric CO_2e emissions predicted by these metrics fails to capture the methane emissions' and overestimates the long-term climate result. GWP*, however, shows a spike in CO_2e emissions over that predicted by GWP100 & 20 in the first twenty years of operation before declining the final five years of operation. Cumulative atmospheric CO_2e declines rapidly once methane emissions cease, settling at a net change in atmospheric CO_2e of 195tCO_2e, much lower than the 678 and 2030 tCO_2e predicted by GWP100 & 20, respectively.

It is worth noting that, although the net cumulative change to atmospheric CO_2e predicted by GWP* eventually falls to 195tCO_2e per tonne of sustained methane emission over the 25 years considered, temporary driving of global warming over what could be attributed to this long-term value will occur in the period of elevated atmospheric CO_2e, i.e. during and immediately after cessation of methane emissions. This temporary warming rate increase requires consideration during the environmental impact assessment of a proposed project and emphasises the urgent need to reduce fugitive methane emissions from supply chains. GWP* has been shown to track the global temperature response to methane emissions to a much higher degree of accuracy than GWP (Masson-Delmotte et al., 2021) and, as such, is used throughout this work.

Additional challenges lie in quantifying the rate of fugitive methane emissions in natural gas supply chains. A recent review on the climate impacts of blue hydrogen by Bauer et al (Bauer et al., 2022). notes large spatial and temporal variability in fugitive emissions of methane from the supply chain. Near-zero emissions of 0.1% are reported in regions such as Norway and Qatar, whereas leakage rates of over 6% are reported in areas such as Libya and Iraq. Bauer et al. recommend a mid-range value of 1.5% for life-cycle assessments, system boundaries for this study include natural gas extraction, gathering and processing as well as and high-pressure transmission. Additionally, the recent low carbon standard issued by the UK DEZNZ (formally BEIS) advises using an average carbon intensity of natural gas supply of 6.29 gCO_2e/MJ (LHV) (calculated using GWP100) for the UK natural gas supply chain (UK Low Carbon, 2022), which corresponds to an emissions rate of 1.04%. The CO_2e emission intensity of natural gas supply due to leakage ranges from 0.3 to 4.6 gCO_2e per MJ (HHV) for a supply chain emission rate range of 0.2–3.0% when calculated using GWP* over a 25-year operational life. Bauer et al. attributes a further 9–10 gCO_2e per MJ (HHV) to non-methane leakage related GHG emissions such as energy demand, transport and storage infrastructure and flaring. Therefore, this cradle-to-gate assessment leads to total natural gas supply chain carbon intensity of 9.3 – 14.6 gCO_2e per MJ (HHV).

Values for the embodied GHG equivalent emissions associated with the construction and decommissioning of a CCGT plant are estimated using a life-cycle assessment (LCA) completed by the National Renewable Energy Laboratory (NREL) (Spath and Mann, 2000) and set at 2 kgCO_2e/MWh produced. Herraiz et al. provide a detailed LCA on the CO_2 capture plant construction & decommissioning, estimating embodied GHG equivalent emissions of 0.85 kgCO_2e/tCO_2 and attributes operational emissions from the transport and storage network as 19.2 kgCO_2e/tCO_2 captured (Herraiz Palomino et al., 2023).

In a net zero economy, these life-cycle emissions will need to be reduced as far as reasonably practical, a goal echoed by the recent COP26 pledge to reduce global methane emissions by 30% by 2030 (Cop26, P., 2021). The remainder will need to be compensated for via the use of Negative Emission Technologies (NET), such as afforestation, soil management, bioenergy with CCS (BECCS), and direct air CO_2

capture and storage (DACCS). As climate change is likely to be a millennium-spanning challenge due to the lifetime of atmospheric CO_2, any NET must be consistent with a long-term mitigation strategy. This paper uses DACCS with permanent geological storage of over 10,000 years (Knudsen et al., 2007) as the primary NET. Since DACCS has higher reported costs than any other NET (Fuss et al., 2018), this sets a cap on the premium to compensate for indirect emissions in the production chain. Due to limited commercial deployment, accurate cost estimates for DACCS are currently unavailable. A recent review by Mc Queen et al. investigates the current state-of-the-art DACCS technology (Mcqueen et al., 2021). A cost range of 100–1000 £/tCO_2 is considered to cover a range of estimates consistent with values reported by the International Energy Agency (Direct Air Capture, 2022) and considers a long-term cost of commercial DAC (excluding transport and geological storage costs) of 300 £/tCO_2 based on Mc Queen et al. For the purpose of this work it is assumed that the cost of DACCS represents a net CO_2 removal cost and no additional life cycle emissions are attributed to the power producer.

This study is limited to the greenhouse gas effect of the atmospheric methane and CO_2 equivalent emissions from the following sources:

- Natural gas supply chain, from extraction to combustion in the gas turbine
- Construction and decommissioning of the CCGT, CCS plant and CO_2 T&S network
- Operation of the CO_2 T&S network

The following is beyond the scope of this study:

- Additional GHGs such as NO_2, SF_6 etc
- Power transmission network construction and losses
- Non GHG related environmental considerations

2.5. Economic parameters

2.5.1. Levelised cost of electricity (LCOE)

LCOE is the discounted lifetime cost of building and operating an asset divided by the discounted lifetime electricity production (Eqs. 2 to 4). It includes all costs incurred by the producer, including CAPEX, OPEX, fuel, waste disposal and financing costs. The economic values used to develop the model are detailed in Table 4.

$$LCOE = \frac{NPV\ Costs}{NPV\ Electricity}\# \tag{2}$$

$$NPV\ Costs = \sum_n \frac{CAPEX_n + OPEX_n}{(1 + Discount\ Rate)^n}\# \tag{3}$$

$$NPV\ Electricity = \sum_n \frac{Electricity\ Production_n}{(1 + Discount\ Rate)^n}\# \tag{4}$$

$(n = time\ period)$

Where NPV is the net present value of the expense or revenue in question.

Eqs. 7 to 9 detail the multi-level factorial cost model used to calculate plant CAPEX with an estimated accuracy of +35%/-15% (AACE Class 4) (Christensen and Larry, 2005).

Engineering, Procurement and Construction (EPC) cost for a CCGT is estimated from a report issued by BEIS (Assessing the Cost Reduction Potential and Competitiveness of Novel Next Generation UK Carbon Capture Technology, 2018). Total PCC EPC cost is evaluated on an equipment level using Eq. 7 & 8. Due to the corrosivity of MEA and wet CO_2 streams, all equipment in direct contact with these substances is assumed to be stainless steel (SS 304). Reference costs and scaling parameters for each PCC plant item, along with installation, tax, and freight factors, are taken from Sinnott and Towler (Sinnott and Towler, 2020), R. Woods (Donald, 2007) and the available FEED studies (Elliott,

Table 4
Economic Model Parameters.

Parameter	Unit	Value
Discount rate (Review of next generation carbon capture technology for industrial, 2022)	%	7.8
Interest Rate (Elliott, 2022)	%	4.0
Productive lifetime (Collodi et al., 2017)	Years	25
Base year	-	2023
Year operational	-	2026
Build Time (Collodi et al., 2017)	Years	3 Years
CAPEX expenditure curve (Collodi et al., 2017)	%	20/45/35
Load Factor (Collodi et al., 2017)	%	85%
Transport and storage* cost (Assessing the Cost Reduction Potential and Competitiveness of Novel Next Generation UK Carbon Capture Technology, 2018)	£/tCO_2	19
Natural Gas Fuel price (Review of next generation carbon capture technology for industrial, 2022)	£/MWh	28
Chemical Engineering Plant Index (CEPCI) (THE CHEMICAL ENGINEERING PLANT COST INDEX, 2022)	-	816.3
International Construction Cost Index [Netherlands/UK/Texas] (Arcadis, 2020)	-	100/138/97
USD to GBP exchange rate (2023) (Rates, 2020)	£/$	0.82
Equipment Tax/Insurance/Freight (Elliott, 2022; Donald, 2007)	-	1.10
Civil Works factorial cost (Elliott, 2022; Bechtel, 2019, 2018)	-	1.21
Utilities factorial cost (Elliott, 2022; Bechtel, 2019, 2018)	-	1.18
Electrical factorial cost (Elliott, 2022; Bechtel, 2019, 2018)	-	1.30
Project management (Elliott, 2022; Bechtel, 2019, 2018)	-	1.21
Contractor Fee (Donald, 2007)	-	1.03
Project Contingency (Elliott, 2022; Bechtel, 2018)	-	1.10
Owners Costs (Review of next generation carbon capture technology for industrial, 2022)	-	1.07
Start-up & Spares (Review of next generation carbon capture technology for industrial, 2022)	-	1.05
Utility Connections (Review of next generation carbon capture technology for industrial, 2022)	-	1.01
Consulting Fee (Review of next generation carbon capture technology for industrial, 2022)	-	1.01
Maintenance (CCS) (Assessing the Cost Reduction Potential and Competitiveness of Novel Next Generation UK Carbon Capture Technology, 2018)	%/Year	1.50
Labour (Assessing the Cost Reduction Potential and Competitiveness of Novel Next Generation UK Carbon Capture Technology, 2018)	£/Employee/ Year	69,810
Insurance/Tax/Admin (Review of next generation carbon capture technology for industrial, 2022)	%/Year	1.50
Regulatory (Review of next generation carbon capture technology for industrial, 2022)	-	1.02
MEA (Michailos and Gibbins, 2022)	£/t	940
Caustic (Evaluating the Costs of Retrofitting et al., 2017)	£/t	34
Reclaimer disposal (Michailos and Gibbins, 2022)	£/t	500
Working Capital (Assessing the Cost Reduction Potential and Competitiveness of Novel Next Generation UK Carbon Capture Technology, 2018)	-	1 Months Consumables

* Defined as the cost charge by CO_2 network operator to dispose of export CO_2 from the boundary of the plant to permanent geological storage

2022; Bechtel, 2019, 2018) and converted to UK 2023 prices using a chemical engineering plant index (CEPI) of 816.3, historical currency exchange rates and an international construction cost index (ICCI) for the UK of 138 (Arcadis, 2020).

$$SC = RC * \left(\frac{SP}{RP}\right)^{Exp} \# \tag{5}$$

$$EPC = \left(f_{contractor\,fee} + f_{contingency}\right) * \left\{ \begin{array}{c} f_{project\,management} * \\ \left(f_{civil} + f_{utility} + f_{electrical}\right) * \\ \sum\left(I + \left(f_{installation} + f_{\frac{tax}{freight}}\right) * SC\right) \end{array} \right\} \# \tag{6}$$

$$CAPEX = \left(EPC_{SMR} + EPC_{PCC}\right) * \left(\begin{array}{c} 1 + f_{owners} + f_{regulatory} + f_{spares\&start-up} + \\ f_{connections} + f_{consultancy} \end{array}\right) \# + Intrest\ during\ construction \tag{7}$$

Where *Exp* is the Scaling Exponent, *RC* is the reference plant cost, *RP* is the reference plant parameter, *SC* is the scaled plant cost, *SP* is the scaled plant parameter, f_i represents a factorial cost, and I is the equipment instrumentation cost.

2.5.2. Cost of CO_2 avoided (CCA)

The Cost of CO_2 Avoided (CCA) compares a plant with CCS to a reference plant operating without CCS (an unabated CCGT) to establish the average cost of avoiding 1 ton of CO_2 emissions (Rubin, 2012). CCA is calculated using Eq. 8.

$$\frac{LCOE_{ccs} - LCOE_{ref}}{Residual\ Emissions_{ccs} - Residual\ Emissions_{ref}} \# \tag{8}$$

Where LCOE is the levelised cost of electricity for the CCS-enabled and reference plant (£/MWh_{th}) and Residual Emissions are the atmospheric CO_2 emissions for the CCS-enabled and reference plant (tCO_2/MWh_{th}). The unit of CCA is £/tCO_2.

2.5.3. Specific primary energy consumption for CO_2 avoided (SPECCA)

The Specific primary energy consumption for CO_2 avoided (SPECCA) provides a measure of the primary energy consumption required to avoid 1 ton of CO_2 emissions and is defined by Eq. 9.

$$SPECCA = \frac{3600 * \left(1/\eta_{ccs} - 1/\eta_{ref}\right)}{Residual\ Emissions_{ccs} - Residual\ Emissions_{ref}} \# \tag{9}$$

Where η_{ccs} & η_{ref} is the thermal efficiency for the CCS-enabled and reference plant (MWh_e/MWh_{th}) and Residual Emissions are the atmospheric CO_2 emissions for the CCS-enabled and reference plant (tCO_2/MWh_{th}). The unit of SPECCA is GJ/tCO_2.

2.5.4. Levelised cost of capture (LCOC)

Similar to LCOE, the LCOC is the discounted lifetime cost of building and operating an asset (see Eqs. 10 to 12), in this case, the CO_2 capture plant, divided by the discounted lifetime production rate of the product, in this case CO_2. One of the main OPEX costs in the LCOC calculation is the cost of steam for solvent regeneration and parasitic electricity load. Lost generation due to steam extraction and parasitic electricity load was costed at the LCOE of the abated CCGT as per Table 8.

$$LCOC = \frac{NPV\ Costs}{NPVCO_2} \# \tag{10}$$

$$NPV\ Costs = \sum_n \frac{CAPEX_n + OPEX_n}{(1 + Discount\ Rate)^n} \# \tag{11}$$

$$NPVCO_2 = \sum_n \frac{CO_2 Production_n}{(1 + Discount\ Rate)^n} \# \tag{12}$$

$(n = time\ period)$

Where NPV is the net present value of the expense or revenue in question.

2.6. Sensitivity study

Upper and lower estimates of 14 key operating and economic parameters are investigated, and the impact on the LCOE is presented. Table 5 details the bounds of the sensitivity study, and each parameter was varied in turn while the remaining parameters were maintained at the base value.

3. Results and discussion

3.1. 100% Fossil CO_2 capture

The driving force of CO_2 absorption into a solvent can be calculated by comparing the partial pressure of CO_2 vapour that would be in equilibrium with a solvent at a given concentration, loading and temperature with the actual CO_2 partial pressure above the same solvent.

Equilibrium CO_2 pressure for a range of solvent states is extracted from the open-source model developed by the Carbon Capture Simulation for Industry Impact (CCSI) in ASPEN PLUS (Morgan et al., 2020). It is then compared to flue gas CO_2 concentrations along the height of an absorber for a range of inlet solvent lean loadings and a CO_2 capture fraction of 99.16%, resulting in 100% fossil CO_2 capture. An idealised absorber would have zero driving force at the top and bottom of the column, with a large driving force in the middle. The maximum rich loading would be achieved with the maximum CO_2 capture fraction for a given lean loading. This would, however, require an infinitely tall absorber as the driving force for mass transfer rate decreases as the solvent approaches equilibrium with the flue gas CO_2 concentration. Fig. 4 presents the ratio of the partial pressure of CO_2 to the equilibrium pressure of CO_2 in the solvent at distinct points along the absorber packing for a range of lean loadings and 100% fossil CO_2 capture. A ratio of 1 would mean that equilibrium between the two fluids has been achieved. As the lean loading value decreases, the bottom of the absorber approaches the equilibrium state, maximising the rich loading leaving the absorber, increasing solvent capacity and lowering the

Table 5
Sensitivity study parameters and ranges.

Item	Lower	Base	Upper
Natural Gas Price (£/MWh HHV)	5	28	100
CAPEX (%)	-15	As evaluated	+35
OPEX (%)	-30	As evaluated	+30
Discount Rate (%)	5	7.8	20
Load Factor (-)	0.2	0.85	1
T&S Cost (£/tCO_2)	10	19	50
MEA consumption rate (kg/tCO_2)	0	2	10
MEA price (£/tMEA)	500	940	2000
DACCS Price (£/tCO_2)	100	300	1000
Natural Gas Supply Chain (% of CH_4 Leakage)	0.2	1.5	3.0
Natural Gas Supply Chain (non-Leakage related) (gCO_2/MJ HHV)	0	9.5	20
PCC operational emissions (gCO_2e/kg CO_2)	0	19.2	100
PCC construction embodied CO_2 (gCO_2e/kg CO_2)	0	0.852	10
CCGT construction embodied CO_2 (gCO_2e/MWh)	0	2	10

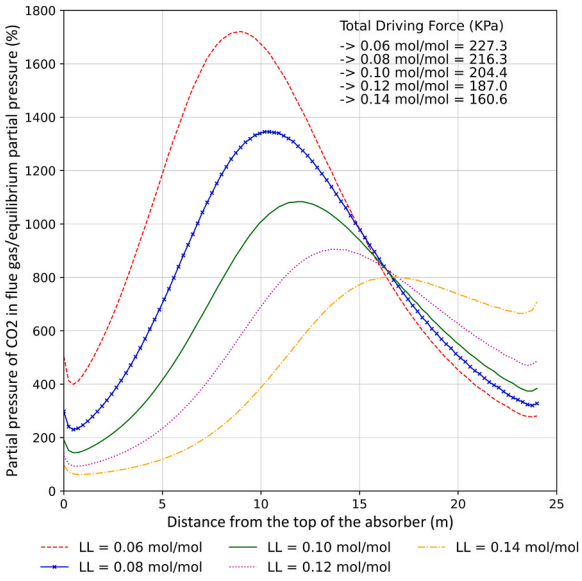


Fig. 4. Driving force profile of a 24 m absorber for a range of inlet lean loadings (LL) for CCGT flue gas with 100% fossil CO_2 capture. The total driving force shown in the top RHS is calculated as per Eq. 9.

contribution of sensible heat addition to the specific reboiler duty, as per Equation 13.

$$q_{reg} = \frac{H_{reboiler}}{\dot{m}_{CO_2}} = q_{sen} + q_{vap} + q_{abs,CO_2}\# \tag{13}$$

Where $q_{reg}$is the specific reboiler duty for solvent regeneration, $H_{reboiler}$is the total thermal input to the reboiler, $\dot{m}_{CO_2}$ is the mass of CO_2 extracted from the solvent, q_{sen} is the sensible energy necessary to heat the solvent to regeneration conditions q_{vap} is the thermal energy leaving the top of the desorber with the H_2O/CO_2 vapour mixture, and q_{abs,CO_2} is the thermal energy associated with CO_2 desorption from the solvent.

$$Total\ Driving\ force(KPa) = \int_{0m}^{24m} (Partial\ pressure\ of\ CO_2 in\ flue\ gas - Equlibium\ partial\ pressure)\# \tag{14}$$

Eq. 16 provides a metric to quantify how effectively an absorber is utilised for a given L/G ratio and CO_2 capture fraction by taking the integral of the driving force along the length of the absorber packing. A value of 0 would result in no mass transfer, while an infinite value could be expected for the idealised absorber described above. Fig. 4 shows that the total driving force of absorption in the absorber at 0.06 mol/mol is circa 40% higher than that at 0.14 mol/mol. All else being equal, this results in a higher amount of mass transfer per unit mass of solvent.

However, to determine the result on the cost of electricity produced, the OPEX and CAPEX implications of achieving a given lean loading needs to be understood. This is shown in Fig. 5, which presents key performance indicators for distinct plants optimised for the given lean loading, absorber packing heights and CO_2 capture fraction. Due to the inflection point phenomenon described in Section 2.2, producing low lean loadings while minimising the specific reboiler duty requires increased desorber pressure and reboiler temperature. As a result, the extraction pressure of the low-pressure steam increases to maintain the pinch temperature in the reboiler between the condensing steam and solvent, see Fig. 5(g). Although the specific reboiler duty decreases at lower lean loadings, see Fig. 5(e). This causes the electrical energy penalty of steam extracted per unit of mass of steam to increase due to the increased exergy of higher enthalpy steam, eventually offsetting any further reduction in specific reboiler duty, see Fig. 5(d). This increased electrical penalty is partially, but not entirely, offset by a decreased CO_2 compression duty caused by the higher desorber operational pressure, see Fig. 5(h) while auxiliary power develops a U-shaped curve as lower lean loadings require higher pumping pressure to avoid 2 phase flow in the hot rich line however when mass transfer is limited at higher lean loadings solvent flow rates increase causing auxiliary power requirements to increase, see Fig. 5(f). Each factor in the EOP combines to make up the total EOP of the plant, and a minimum is seen; see Fig. 5(b). It is worth noting the sensitivity of EOP to lean loading for the 100% fossil CO_2 capture cases when compared to the 96% fossil CO_2 case. This high degree of sensitivity indicates that tight control over the lean loading will be much more critical for the efficient operation of PCC plants at ultra-high CO_2 fractions than for those at lower capture fractions.

An additional parameter available to designers to increase rich loading (reducing specific reboiler duty) is the packing height within the absorber itself; however, this comes with increased CAPEX that may outweigh the gain in thermal efficiency, see Fig. 5(c). As can be seen from Fig. 5(a), the net thermal efficiency of a 100% fossil CO_2 capture plant peaks at 0.06–0.12 mol/mol over the range of packing heights considered, although the specific reboiler duty does not present a minimum. A 0.25% point reduction in plant efficiency from using 24 m packing vs. 30 m results in a 1.6% saving in plant CAPEX.

Fig. 6 shows the LCOE and CCA results for the cases that are presented in Fig. 5 and compares them to the Net plant output. While plant output is at a maximum when 30 m of packing is used, the additional CAPEX required offsets the financial benefit, resulting in a marginally higher LCOE. The reverse is seen for 20 m of packing; CAPEX reductions are not sufficient to offset the increased plant output until very low lean loadings are used. This indicates that 24 m of packing for a CCGT operating at 100% fossil CO_2 capture serves as an approximate optimum for the assumptions detailed in this manuscript. Furthermore, for the 24 m packing case, an approximate and shallow optimum between 0.04 and 0.10 mol/mol (±0.15 £/MW_e) is shown in Fig. 6. As a lean loading of 0.10 mol/mol is thought to result in this range's lowest MEA consumption rate (see Fig. 8), it has been chosen as the optimised design case for the remainder of this study. A similar trend is seen for the 96% fossil CO_2 capture case therefore, 0.10 mol/mol is also taken as the design case. As was the case in Fig. 5, in both the 20 and 24 m cases, a high degree of sensitivity to lean loading is seen for the LCOE and CCA, again highlighting the importance of tight control over operational parameters.

The process and economic modelling results for the optimised design cases described in Fig. 5 and Fig. 6 are shown in Table 6 to Table 10. Transitioning from 96% to 100% fossil CO_2 capture requires the installation of an additional 4 m of packing in each of the two absorbers. This limits the increase in specific reboiler duty to 4.2%, minimises the reduction in thermal efficiency to 0.53% point (LHV), and results in a net increase in energy penalty of 8.2% (from 70.2 to 76.0 MW).

While both CO_2 capture fractions investigated increase CAPEX and OPEX of the CCGT considerably relative to an unabated plant (as per Table 7), the relative difference between 96% and 100% fossil CO_2 capture is limited to an increase of 4.0% and 0.8% respectively, noting that this allows a 4% increase in CO_2 capture fraction.

An LCOE of 104 £/MWh_e is reported in Table 8 for the 100% fossil CO_2 capture case, a 2.8 and 41.0 £/MWh_e increase over the 96% fossil

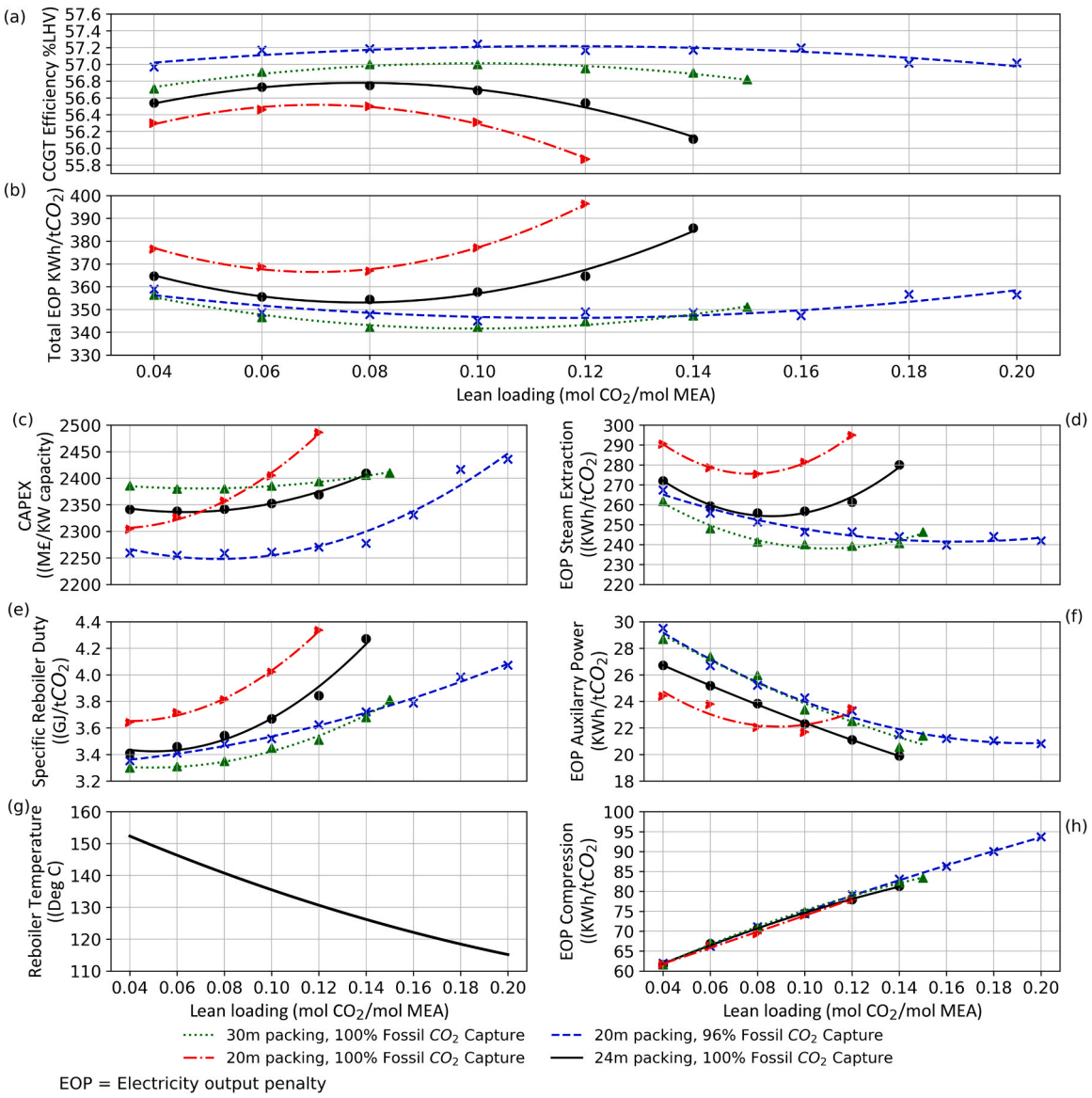


Fig. 5. Effect of lean loading and packing height for a CCGT operating with 100% and 96% fossil CO_2 capture.

CO_2 capture and no CO_2 capture cases, respectively. A breakdown of the contribution of each cost to the LCOE is available in Table 9. In all cases, fuel costs dominate the LCOE, accounting for 53–77% of the total cost, a dominance that is illustrated in the sensitivity study completed in Section 2.6. For CCS cases, CAPEX increases from 17% to 29–30% due to the added CAPEX burden of the CCS plant, while fixed OPEX increases from 7% to 10–11%, namely due to increased staffing and solvent-related costs. Comparing the 96% and 100% fossil CO_2 capture cases. The contribution of CAPEX and fixed OPEX to LCOE increased by 4.9 and 4.1%, respectively, which is proportionate to the increase in CO_2 capture fraction, while fuel costs increase by 0.9%.

CCA is reported at 128 £/tCO_2 for the 100% fossil CO_2 capture case, marginally higher than 125 £/tCO_2 for the 96% fossil CO_2 capture case, a similarly marginal increase in SPECCA is observed (from 2.2 to 2.3 GJ/tCO_2). The marginal CCA of transitioning from 96% to 100% fossil CO_2 capture is 184£/tCO_2

3.2. CO_2 Capture fraction and decarbonised power

A sensitivity study to compare CO_2 capture fraction and LCOE and CCA is shown in Fig. 7. As would be expected, as CO_2 capture fractions increase, Net power output decreases as more CO_2 is captured and the LCOE and CCA increase. This is because there is no financial incentive (carbon tax, etc.) for increasing CO_2 capture fractions included in this model, and as such, due to the energy and CAPEX demands, capturing more CO_2 will always result in an increased financial burden. In the UK, the Dispatchable Power Agreement (DPA) (Dispatchable Power Agreement business model summary, 2022) details the business model for CCS-enabled power generation and utilises the concept of “clean” or “decarbonised” power to provide this incentive. Within the DPA, the bankable power capacity of a facility is the net power output multiplied by the achieved CO_2 capture fraction over a specified period of time, i.e. the power paid for is decarbonised power. This simple calculation incentives higher CO_2 capture fraction so long as the resulting decrease in abated power output is not more than 1% per every additional 1% point increase in CO_2 capture fraction. This is clearly illustrated in Fig. 7. For both the 24 and 20 m packing cases, as the CO2 capture fraction increases, the “decarbonised power” output of the plant increases. This maximises the available revenue for a plant operator under the UK system. However, increasing CO_2 capture fractions comes with an increased CAPEX burden that is not captured in the net plant output calculation. To incorporate this, an LCOE calculation was completed

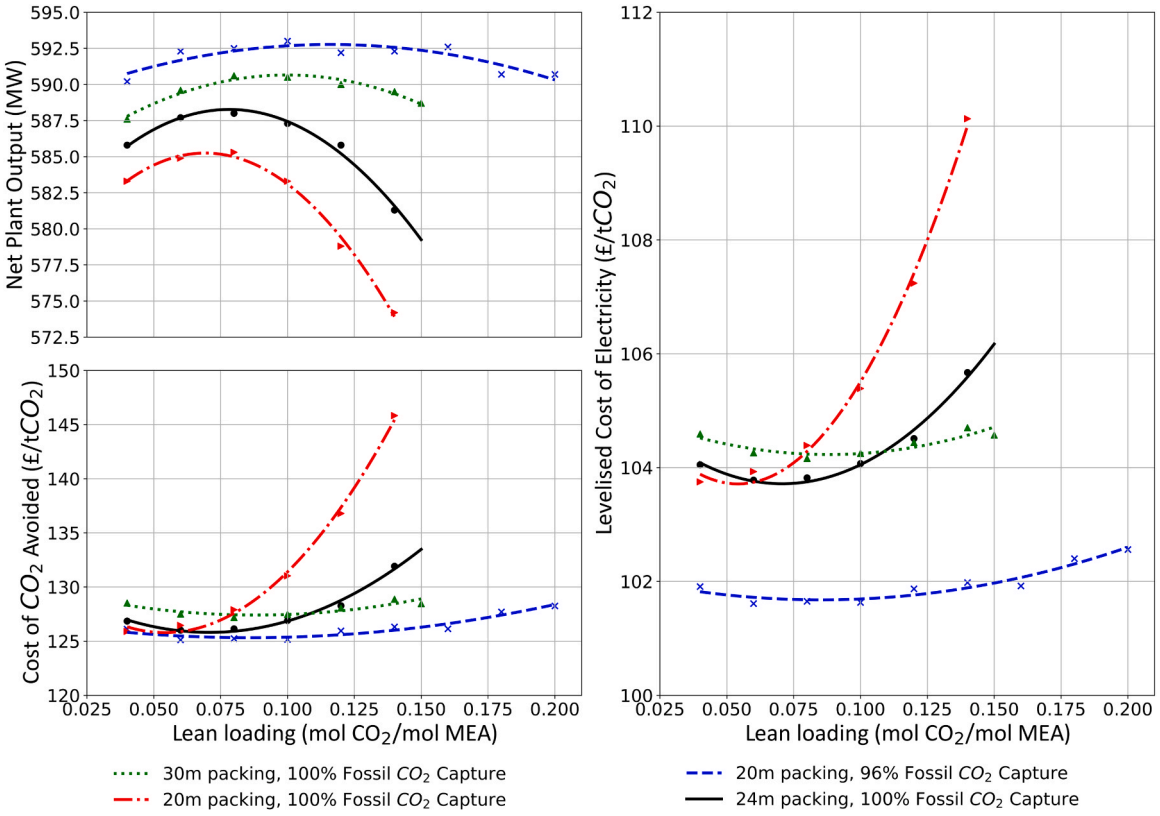


Fig. 6. Net plant output, CCA and LCOE as a function of lean loading for various packing heights and CO_2 capture rates.

Table 6
Plant performance for 100% fossil CO_2 capture, 96% fossil CO_2 capture and a no CO_2 capture case.

Parameter	Unit	100% fossil CO_2 capture	96% fossil CO_2 capture	No CO_2 Capture
Scope 1 specific carbon intensity	gCO_2e/kWh	0.0	15.1	320.5
Fossil CO_2 Capture fraction	%	100	95.8	0
Gross CO_2 Capture fraction	%	99.16	95	0
Net Output	MW_e	587.5	593.0	663.3
Natural Gas (HHV)	MWh_{th}/s	0.319	0.319	0.319
Thermal Efficiency (LHV)	%	56.7	57.2	64.0
Specific Reboiler Duty	GJ/tCO_2	3.67	3.52	-
CO_2 Export	kg/s	59.0	56.6	-
CO_2 Stack Emissions	kg/s	0.5	3.0	59.5
[a] Flue Gas Flow Rate	kg/s	792	792	792
CO_2 Concentration	*Mole Frac*	4.9	4.9	4.9
Absorbers	-	2	2	
Packing Stages	-	3	2	
Packing Height	m	24	20	
Diameter	m	11.4	11.3	
Absorber Flooding	%	<80	<80	
Lean Loading	*mol CO_2/ mol MEA*	0.10	0.10	
Rich Loading	*mol CO_2/ mol MEA*	0.44	0. 46	
L/G	*kg/kg*	0.88	0.81	
Reboiler Temp	^oC	136	136	

[a] Saturated at 40 °C

using the decarbonised power output of the plant as the denominator in Eq. 4. This gives a levelised cost of decarbonised electricity or LCODE. As can be seen in Fig. 7, the LCODE decreases as CO_2 capture fractions increase for both cases, however, for the 20 m packing case, a minimum

Table 7
Capital & Operational cost estimates.

Item	100% fossil CO_2 capture	96% fossil CO_2 capture	No CO_2 Capture
Total CAPEX	**1394**	**1341**	**523**
CCS EPC	699	657	-
CCGT EPC	420	420	420
Interest during construction	96	92	36
Additional CAPEX	179	172	67
Annual OPEX	**319**	**317**	**262**
Fixed OPEX	48.8	47.3	21.0
Variable OPEX	271	269	241
Abatement CAPEX increase	**167%**	**156%**	
Abatement OPEX increase	**22%**	**21%**	

Table 8
CCA, LCOC, SPECCA & LOCE results (Carbon Tax = 0 £/tCO_2).

Parameter	Unit	100% fossil CO_2 capture	96% fossil CO_2 capture	No CO_2 Capture
Cost of CO_2 Avoided (CCA)	£/tCO_2	128	125	-
Levelised cost of Capture (LCOC)	£/tCO_2	109	105	-
Specific primary energy consumption for CO_2 avoided (SPECCA)	GJ/tCO_2	2.3	2.2	-
Levelised cost of Electricity (LCOE)	£/MWh_e	104	102	63

Table 9
Breakdown of LCOE (Carbon Tax = 0 £/tCO$_2$).

LCOE Contribution	Unit	100% fossil CO_2 capture	96% fossil CO_2 capture	No CO_2 Capture
Fuel	£/MWh_e	54.7	54.1	48.4
CAPEX	£/MWh_e	31.3	30.0	10.4
Debt finance	£/MWh_e	0.4	0.4	0.3
Fixed OPEX	£/MWh_e	11.2	10.7	4.3
T&S	£/MWh_e	6.9	6.5	0
TOTAL	£/MWh_e	104	102	63

is presented at 97–98% CO_2 capture, whereas with 24 m of packing, the LCODE is minimum is present from 98 – 99.16% CO_2 capture fractions (i.e. 100% fossil CO_2 capture). This leads the authors to the novel conclusion that, under the UK system, providing the absorber is sufficiently sized, it pays to capture more CO_2 with a modelled 2% decrease in the LCODE when operating at 100% fossil CO_2 capture compared to 96%. Indeed, even when the packing height appears not to be optimised (i.e. 20 m), a financial benefit can still be achieved by increasing CO_2 capture fractions, with an apparent optimum of 97–98% but even 100% fossil CO_2 capture providing a decrease in LCODE.

3.3. Solvent consumption rates

A lean loading of 0.10 mol CO_2/mol MEA is considered in this study based on a desorber pressure of 2.75 bar and reboiler temperature of 136 °C to minimise energy consumption. Higher reboiler temperature than proposed in prior FEED studies (Bechtel, 2018; Pre-Feasibility Study for Establishing, 2016) and pilot scale test campaigns (Knudsen et al., 2007; Moser et al., 2011; Aronu et al., 2019; Weir et al., 2023; Faramarzia et al., 2016; Feron et al., 2016) is thought to lead to higher rates of MEA thermal degradation, although this may be mitigated by operation at lower lean loadings. The Braakhuis model of MEA thermal degradation (see Table 3) is implemented in Python 3.9 as part of this work to investigate the effect of lean loading and regeneration temperature on thermal degradation within the reboiler of a PCC plant. A representative 20-minute residence time in the reboiler and 5000 regeneration cycles, corresponding to approximately the number of regeneration cycles required to achieve steady-state conditions, is considered for a 35%wt. MEA solvent solution and a constant rich loading of 0.46 mol/mol. The MEA consumption rate due to thermal degradation in the reboiler is calculated as per Eqs. 15, 16 and 17 for a range of lean loadings and reboiler temperatures consistent with thermally efficient operation (see Section 2.2) and listed in Table 11. Fig. 8 details the results of this investigation.

Table 10
LCOE results over a range of carbon tax.

Parameter	Unit	100% fossil CO_2 capture	96% fossil CO_2 capture	No CO_2 Capture
100	£/MW_e	104.1	103.1	95.5
200	£/MW_e	104.1	104.6	127.5
300	£/MW_e	104.1	106.2	159.6
400	£/MW_e	104.1	106.2	191.6
500	£/MW_e	104.1	106.2	223.7

Table 11
Solvent regeneration conditions for the range of lean loadings in this study.

Lean Loading (mol CO_2/mol MEA)	Reboiler P (bara)	Reboiler T (°C)
0.04	4.37	153.3
0.06	3.65	145.5
0.08	3.14	140.0
0.10	2.75	135.1
0.12	2.48	131.4
0.14	2.18	126.8

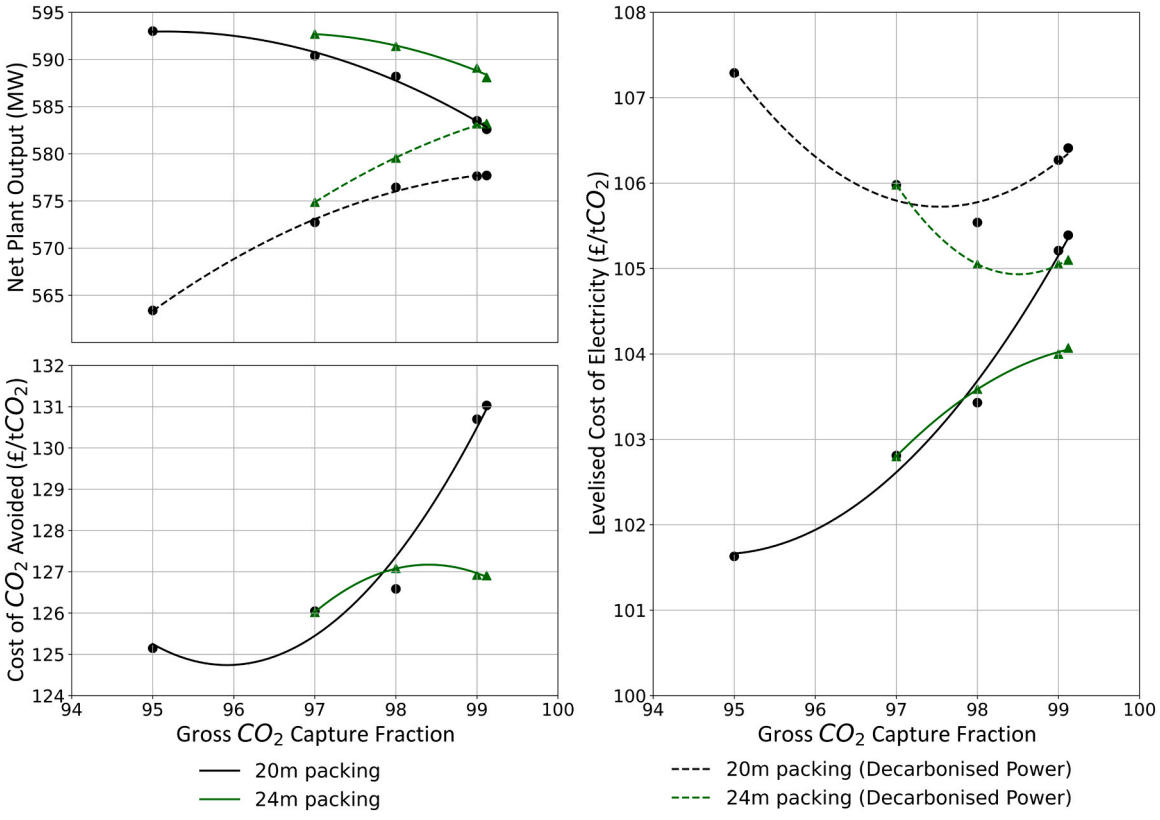


Fig. 7. Net Power, CCA and LCOE as a function of CO_2 Capture Fraction.

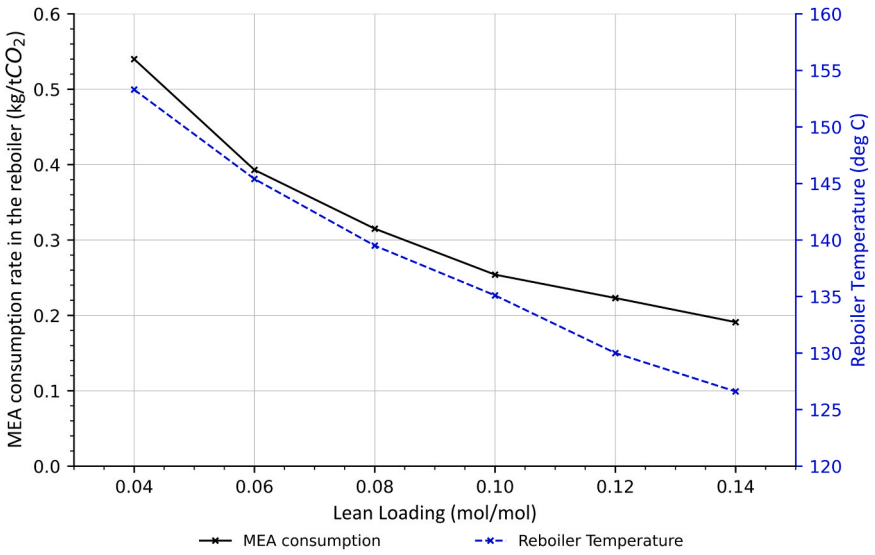


Fig. 8. Application of thermal degradation model for loaded MEA proposed by Braakhuis et al. for a range of lean loadings, 20 min residence time in the reboiler, 5000 regeneration cycles and a 35% wt. MEA solvent solution with a constant rich loading of 0.46 mol/mol. Range for lean loadings between 0.20 and 0.30 mol/mol with a reboiler temperature of 120 °C is 0.14–0.36 (kg/tCO$_2$).

$$MEA\ consumed_{regeneration\ cycle} = \sum_{t=0}^{residence\ time} MEA\ consumed_{R(1-5)_t}\# \tag{15}$$

to the reboiler and did not consider the effect of reducing lean loading on the rest of the PCC plant, as thermal degradation elsewhere in the plant will also be impacted by lean loading, albeit to a lower degree due to the reduced temperatures and residence time. A holistic view of the entire

$$CO_2Captured_{regeneration\ cycle} = (rich\ loading - lean\ loading) * MEA\ concentration_{t_0}\# \tag{16}$$

$$MEA\ consumption\ rate = \frac{\sum_{n=1}^{5000} MEA\ consumed_{regeneration\ cycle}}{\sum_{n=1}^{5000} CO_2Captured_{regeneration\ cycle}}\# \tag{17}$$

Where $MEA\ concentration_{t_0}$ is the initial molar concentration of MEA in the solvent i.e. 35%wt, $MEA\ consumed_{R(1-5)_t}$ is the MEA consumed due to reactions 1–5 (as per Table 3) at the reboiler temperature, MEA concentration, loading and degradation compound concentrations in the solvent at time t. Residence time is the residence time of the solvent in the reboiler, and n is the number of regeneration cycles.

Fig. 8 indicates that although thermal degradation does seem to increase with reducing lean loading, the rate may be much less than previously assumed, and for lean loadings over 0.07 mol/mol may be comparable to or less than the 0.14–0.36 kg/tCO$_2$ range that is seen for lean loadings in the 0.2–0.3 mol/mol range. The critical factor being the decrease in lean loading, decreasing carbamate concentration and thus the reaction rate, coupled with the increase in regeneration temperature. Increasing regeneration temperatures at higher loadings would lead to excessively high degradation rates. From a thermal degradation perspective, it follows that thermal degradation will be minimised for a given regeneration temperature and pressure at the lowest feasible lean loading, which is limited by the presence of the "inflection point" described in Section 2.2, as the energy required to further lower lean loadings increase exponentially past a specific loading for a given regeneration pressure. Therefore, for ultra-high CO$_2$ capture fractions, optimising lean loading and regeneration conditions is critical to minimise energy requirements and thermal degradation rates.

It is important to note that the analysis presented in Fig. 8 is limited

CO$_2$ capture process is required to definitively state the effect of lean loading on solvent consumption rates; however, this is beyond this paper's scope and needs further work. A total (oxidative and thermal degradation as well as atmospheric emissions) MEA consumption rate of 2 kg/tCO$_2$, which is less than the highest reported value in pilot test campaigns (ref Table 2), is assumed, and a sensitivity study detailing the effect of MEA consumption rates on the LCOE is completed.

3.3.1. Sensitivity study

Achieving sufficient desorption of CO$_2$ from the MEA solvent to meet the required lean loading requires operating the desorber at 2.75 bar and 136 °C. Considerable uncertainty around the MEA consumption rates at these reboiler conditions is noted, and the applied consumption rate of 2 kg/tCO$_2$ represents a best-guess estimate. However, a sensitivity study has been completed and is shown in Fig. 9. Doubling the assumed MEA consumption rate to 4 kg/tCO$_2$ at the 2023 MEA wholesale price of 940 £/t increases the LCOE by just 1 £/MWh$_e$ (approximately 1%). An MEA consumption rate of this magnitude is not supported by the evidence presented in this manuscript; even so, the effect on LCOE is minimal due to the low purchase cost of MEA, a situation which may not be comparable for other solvents reporting a lower consumption rate and a possibly much higher purchase price.

The results from an LCOE & CCA sensitivity study completed using the parameters described in Table 5 are shown Fig. 10; each parameter is varied in turn while the remaining parameters are kept constant. The LCOE is highly sensitive to the natural gas price and load factor and moderately sensitive to the discount rate. Variation in CAPEX has a less prominent effect with a -15% to +35% swing, resulting in a -5 to +11 £/MWh$_e$ variance in LCOE. Load factor is shown to dominate the sensitivity of CCA, with a reduction from 85% to 20%, tripling the CCA.

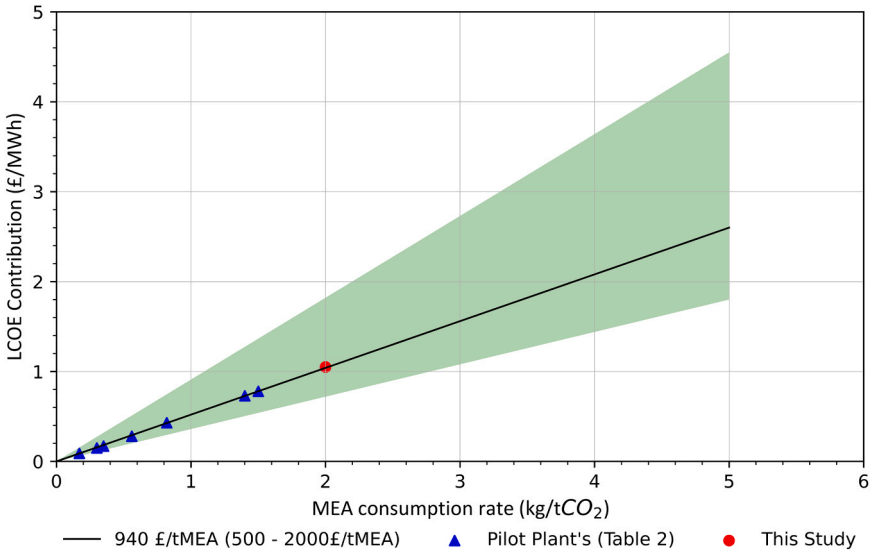


Fig. 9. MEA consumption rate vs increase in LCOE of a CCGT operating with 100% fossil CO_2 capture, a 2 kg/tCO_2 consumption rate is assumed for this study.

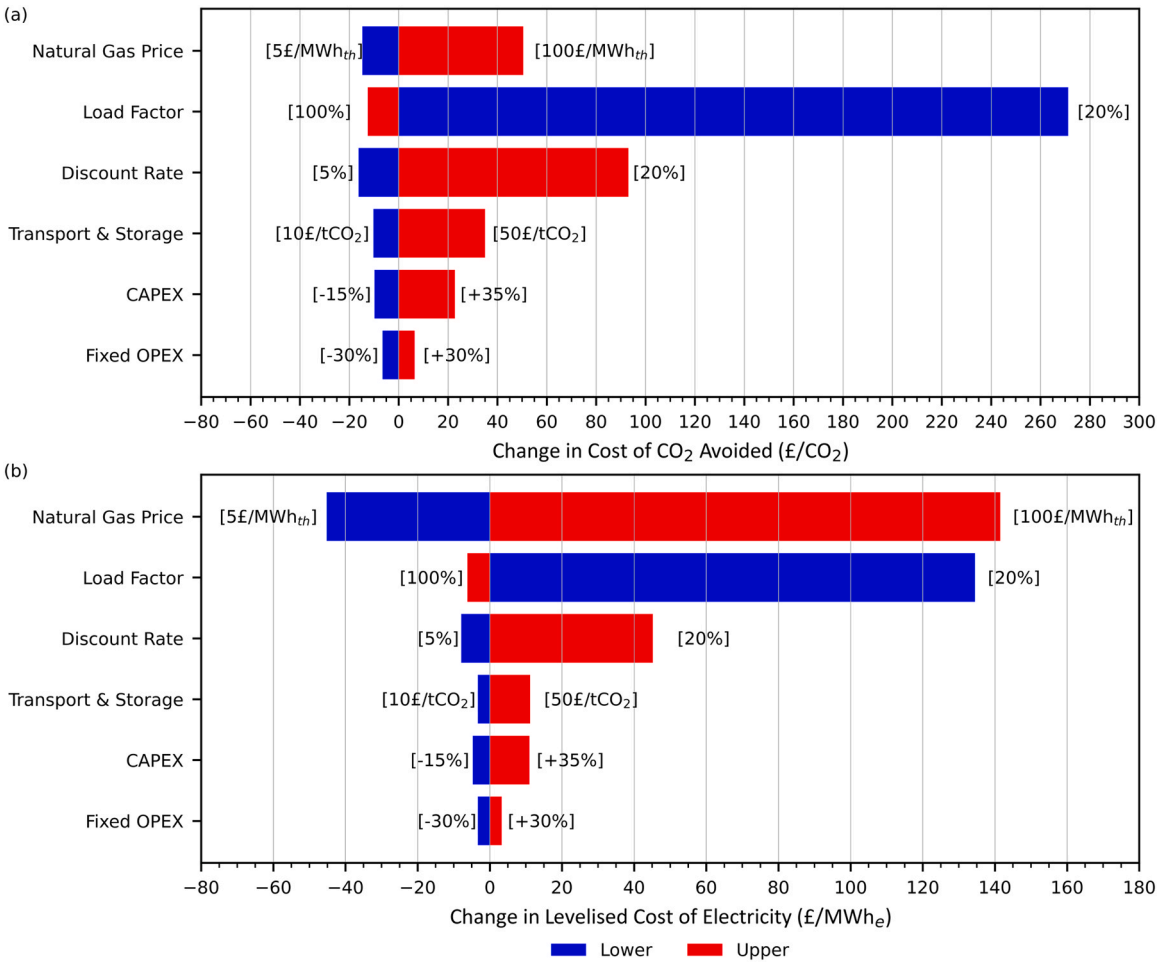


Fig. 10. Effect of techno-economic parameters on the Cost of CO_2 avoided (a) and the levelised cost of electricity (b) for net zero stack emission operation sensitivity study.

Table 12
Embodied and CCS upstream CO_2 emissions.

Emission source	Value	Unit	LCOE increase (DACCS = 100 £/tCO_2)	LCOE increase (DACCS = 300 £/tCO_2)	LCOE increase (DACCS = 1000 £/tCO_2)
PCC Operation (Herraiz Palomino et al., 2023)	19.2	gCO_2e/KG CO_2 Captured	0.83	2.22	7.08
PCC Construction (Herraiz Palomino et al., 2023)	0.85	gCO_2e/KG CO_2 Captured	0.08	0.20	0.65
CCGT Construction (Spath and Mann, 2000)	2.0	gCO_2e/KWh Produced	0.66	1.77	5.65
Total	9.5	gCO_2e/KWh Produced	1.57	4.19	13.38

Table 13
LCOH for various natural gas supply chain emissions rates over the range of DACCS cost estimates.

Case	Natural Gas supply chain emission rate	LCOE increase £/MWh_e(DACCS = 100–1000 £/tCO_2)
Low	0.2%	8–70
UK	1.04%	9–79
Global	1.5%	10–84
High	3.0%	12–101

This is primarily due to the CAPEX intensity of the PCC plant contributing more to the relative difference in LCOE between abated and unabated plants at low load factors. CCA was less sensitive to natural gas prices due to the relative nature of the metric, i.e., an increase in natural gas price increases the LCOE of abated and unabated plants, albeit not at the same rate for the latter.

3.4. Zero life cycle emissions

Transitioning from 100% fossil CO_2 capture to zero life-cycle emissions requires the recapture of supply chain fugitive GHG emissions, embodied CO_2 from construction, and upstream CO_2 transmission and storage (T&S) emissions via the use of Negative Emission Technologies, and in this paper, DACCS with permanent geological storage.

Values for the embodied carbon emissions associated with the construction of a CCGT are estimated using a life-cycle assessment (LCA) completed by the NREL. At the same time, Herraiz et al. provide a detailed LCA on the capture plant construction and operational chain (Herraiz Palomino et al., 2023). Total lifetime embodied carbon emissions are estimated at 1.04 $MtCO_2$ for a CCGT operating with 100% fossil CO_2 capture. The effect on LCOE of recapturing these emissions is detailed in Table 12 and found to contribute to an increase in LCOE of between 1.6–13.4 £/MWh_e over the range of DACCS costs investigated. Appendix B presents a sensitivity study highlighting the effect uncertainty in these figures has on the LCOE.

As can be seen from Table 13, LCOE increases by a further 8 – 101 £/MWh_e when the natural gas supply chain emissions are recaptured. Non leakage related CO_2e emissions from the natural gas supply chain are set at 9.5 gCO_2e/MJ HHV as per Bauer et al.

Combining the results from Table 12 and Table 13 corresponds to an LCOE for net-zero electricity of 114–218 £/MWh_e and an associated CCA of 130 – 371 £/tCO_2. For the global median case of 1.5% natural gas supply chain emissions and a median DACCS price of 300 £/tCO_2, the LCOE and CCA are 135 £/MWh_e and 178 £/tCO_2, respectively. Further sensitivity studies can be found in Appendix B

4. Conclusion

This article presents a first assessment of the cost of zero life-cycle greenhouse gas emission electricity from a zero stack CO_2 emission combined cycle gas turbine (CCGT), with negative emission technologies (NET) used to recapture residual life-cycle emissions.

In the first part of this study, we assess the technical and commercial implications of increasing the CO_2 capture fraction of an amine-based post-combustion carbon capture system (PCC) with an open art solvent (35%wt. Monoethanolamine) from the current best available technology level of 95% to a capture fraction resulting in 100% fossil CO_2 capture (99.16% gross CO_2 capture). This involves two main design implications: adding 4 m of structured packing in the absorber, increasing height from 20 m to 24 m, and reducing lean solvent loadings down to 0.10 mol CO_2/mol MEA. Together, these design changes ensure sufficient driving force in the absorber column to reach the required CO_2 capture fraction while providing a sufficiently high rich loading at the bottom of the absorber to limit additional energy requirements. The relative simplicity of these proposed modifications indicates that the technology required to develop a CO_2 emission-free CCGT is available and close to, if not already, commercially ready. A novel conclusion of this research is that deep decarbonisation of fossil-based power generation to zero stack (or Scope 1) emissions can be done without a step change in the efficacy of current solutions.

A lean solvent loading of 0.10 mol CO_2/mol MEA in the CO_2 capture process limits the increase in specific reboiler duty to 4.2% (3.67 vs 3.52 GJ/tCO_2), minimises the reduction in thermal efficiency to 0.53% point (LHV), and results in a net increase in electricity output penalty of 8.2% (from 70.2 to 76.0 MW) and 4% increase in CAPEX. For 2023 UK capital costs and a natural gas price of 28 £/MWh, the Levelised Cost of Electricity (LCOE) and the Cost of CO_2 Avoided (CCA) of a CCGT fitted with PCC operating with 100% fossil CO_2 capture is 104 £/MWh_e and 128 £/tCO_2, respectively. Compared to 102 £/MWh_e and 125 £/tCO_2 for a CCGT operating with 96% fossil CO_2 capture, i.e. a 95% CO_2 capture fraction, the marginal CCA of reducing stack emissions from 5% to zero is 184 £/tCO_2. Under the assumptions detailed here, any CO_2 reduction incentive or penalty of 184 £/tCO_2 or over will push the market towards 100% fossil CO_2 capture.

Although a limited number of previous studies have investigated increasing CO_2 capture fractions above 95%. Most fail to thermodynamically optimise the absorption and desorption process through the use of lean loadings sufficient to ensure a high driving force at the top of the absorber, even at atmospheric CO_2 concentrations, and/or desorption conditions adequate to avoid an unnecessary increase in specific reboiler duty. This is particularly troublesome in CCGT applications where the high sensitivity to lean loading described in this manuscript is present. For example, Feron et al (Feron et al., 2019). calculate that designing a CCS-enabled CCGT to operate at a 100% vs a 96% fossil CO_2 capture fraction imparts an additional 1.4 – 1.8% point decrease in CCGT thermal efficiency, which is circa three times that presented in this work. Our analysis shows that this would result in a 1.6–2.4 £/MWh_e increase in the LCOE of zero residual CO_2 emission power from CCGT over the optimised process presented here. This increase is not dissimilar to the 2.8 £/MWhe increase in LCOE required to increase fossil CO_2 capture fractions from 96% to 100%, representing a significant saving.

Where the CO_2 capture process has been operated at conditions suitable for ultra-high CO_2 capture levels, no further investigation into the thermodynamic or financial implications for the associated CCGT has been completed. To the authors' knowledge, this is the first study to comprehensively assess the technical and economic implication of operating a commercially available CCGT at a CO_2 capture fraction compliant with that required to operate in a Net-Zero future. This is critical as it provides the "hard numbers" required to inform the

economic policy needed to increase the current best available technology CO_2 capture fraction of 95% up to that of a Net Zero commitment compatible CCGT (i.e. 99.2%).

The design insights provided in this manuscript are not only critical for the deployment of future CCGTs but also timely for the current wave of CCS projects. At the time of writing (2023), no CCS-enabled CCGTs are in operation globally. In the UK, the guidance for permitting new CCS-enabled power projects is to design to achieve a net CO_2 capture fraction of 95% annually. Considering the operational lifespan of a CCGT to be 25 years and the fact that constructing a CCGT usually takes a minimum of 3 years, it seems sensible to infer that, in the UK at least, no CCGTs built according to the current guidelines on CO_2 capture fractions can align with the Net Zero by 2050 commitments. Let alone the more ambitious targets of 2040 or 2045 set by some. Therefore, provision must be built into current designs to allow for an economically acceptable increase in the CO_2 capture fraction to ensure that assets are not stranded, or environmental targets are breached.

That being said, the market mechanisms are already in place within the UK to incentivise 100% fossil CO_2 capture. The power CCS business model within the UK at the time of writing exclusively pays power generators for decarbonised megawatts. This is done by multiplying the CO_2 capture fraction by net output for both variable payments (over a given time period) and as a capacity payment, with the remaining MW effectively representing a waste product for the producer. This work shows, for the first time, that despite the increase in both the specific and absolute energy penalty described above and for the cases analysed, increasing CO_2 always results in an increase in decarbonised power capacity and, as such, maximises revenue for the power producer. When calculating the levelised cost of electricity for this "decarbonised" power, i.e. the levelised cost of decarbonised electricity (LCODE). The additional CAPEX, required to achieve increased CO_2 capture fractions is offset by the increased net decarbonised power output owing to the increase CO_2 capture. For 20 m of absorber packing this appears to present a minimum at approximately 97–98% CO_2 gross capture. However, with 24 m of packing, this minimum is shifted to 98–99.16% gross CO_2 capture i.e. up to 100% fossil CO_2 capture. We find that on a LCODE basis there is a 2% decrease in the cost of producing decarbonised electricity when transitioning from 96% to 100% fossil CO_2 capture.

As with all GHG reduction pathways, a product's total life-cycle emissions must be accounted for, reduced in the first instance, and any unavoidable emissions recaptured. For a decarbonised CCGT, the three dominant sources of life-cycle emissions are considered in this study: embodied CO_2e emissions from the construction and decommissioning of the plant, CO_2e emissions from the CO_2 transport and storage network (T&S) and natural gas supply chain related GHG emissions. Under the assumption of a net zero future, any residual emissions must be recaptured using some form of negative emissions. For this study, a range of costs for direct air capture with permanent geological storage (DACCS) is used.

The CO_2e emission intensity of natural gas supply due to leakage ranges from 0.3 to 4.6 gCO_2e per MJ (HHV) for a supply chain emission rate range of 0.2–3% when calculated using GWP* over a 25-year operational life. Bauer et al. attributes a further 9–10 gCO_2e per MJ (HHV) to non-methane leakage related GHG emissions such as energy demand, transport and storage infrastructure and flaring. Therefore, this cradle-to-gate assessment leads to total natural gas supply chain carbon intensity of 9.3 – 14.6 gCO_2e per MJ (HHV). Furthermore, a detailed life cycle assessment completed by Herraiz et al. has estimated that the embodied GHG equivalent for the construction and decommissioning of a CO_2 capture plant at 0.85 kgCO_2e/tCO_2, with a further 19.2 kgCO_2e/tCO_2 captured attributed to operational emissions from the transport and storage network. Finally, values for the embodied GHG equivalent emissions associated with the construction and decommissioning of a CCGT plant are estimated from an LCA completed by the National Renewable Energy Laboratory (NREL) and set at 2 kgCO_2e/MWh produced. Combining these emission sources results in an equivalent CO_2 recapture burden of between 8.6 and 11.8 MtCO_2 over the plant's lifetime.

For a cost of DACCS consistent with the current literature of 100–1000 £/tCO_2, recapture of the life-cycle emissions of a decarbonised CCGT will add 10–114 £/MWh$_e$ to the LCOE (i.e., total LCOE of 114–218 £/MWh$_e$). For the UK case, with a natural gas supply chain fugitive emissions rate of 1.04% and a median DACCS price of 300 £/tCO_2, the LCOE and CCA are 133 £/MWh$_e$ and 175 £/tCO_2 respectively. While for the global median case of 1.5% natural gas supply chain fugitive emissions, the LCOE and CCA are 135 £/MWh$_e$ and 178 £/tCO_2. This translates to an increase in LCOE over an unabated CCGT of 71.5 £/MWh$_e$. The direct capture of stack CO_2 emissions and the recapture of CCS T&S operational emissions (Scope 1) accounts for 43.2 £/MW$_e$, Natural gas supply chain emissions (Scope 2) account for a further 26.3 £/MWh$_e$, and the recapture of construction emissions (Scope 3) make up the remaining 2.0 £/MWh$_e$.

The wide range presented here highlights the importance of prioritising the reduction of supply chain emissions as far as reasonably practical over recapture, as any intervention with a CCA less than the current cost of negative emissions will result in a reduced LCOE of the net zero electricity. Ultimately resulting in a more equitable and rapid transition to a sustainable energy future.

CRediT authorship contribution statement

Mathieu Lucquiaud: Writing – review & editing, Supervision, Project administration, Funding acquisition, Data curation, Conceptualization. **Daniel Mullen:** Writing – review & editing, Writing – original draft, Visualization, Validation, Methodology, Investigation, Formal analysis, Data curation.

Declaration of Generative AI and AI-assisted technologies in the writing process

During the preparation of this work the author(s) used Grammarly in order to assist with grammar and punctuation. After using this tool/service, the author(s) reviewed and edited the content as needed and take(s) full responsibility for the content of the publication

Declaration of Competing Interest

The authors declare the following financial interests/personal relationships which may be considered as potential competing interests: Daniel Mullen reports a relationship with SSE Thermal that includes: employment. If there are other authors, they declare that they have no known competing financial interests or personal relationships that could have appeared to influence the work reported in this paper.

Data availability

I have included the CAPEX model developed as part of this work in the supplementary information

Acknowledgement

Daniel Mullen would like to acknowledge the School of Engineering at the University of Edinburgh for providing financial support for this work. For the purpose of open access, the authors have applied a Creative Commons Attribution (CC BY) license to any Author Accepted Manuscript version arising.

Appendix A. Process parameters for a 100% fossil CO_2 capture CCGT

Parameter	Unit	Value
GT Thermal efficiency	*%*	43.1
Compressor pressure ratio	-	1:23.5
Air flow rate	*kg/s*	808
Air/Fuel ratio	-	35.3
Fine filter ΔP	*Pa*	1000
Fuel inlet temperature	^oC	120
Turbine inlet temperature (TIT)	^oC	1440
Turbine isentropic efficiency	*%*	90
Compressor isentropic efficiency	*%*	90
Mechanical Efficiency	*%*	99.9
Combustor ΔP	*%*	5
First stage Nozzle ΔT	^oC	44
Second stage Nozzle ΔT	^oC	13
Third stage Nozzle ΔT	^oC	6
GT Exhaust pressure	*Bar*	1.033
GT Exhaust temperature	^oC	629
HP Steam temperature	^oC	600
HP Turbine Inlet Pressure	*Bar*	186
Reheat Steam temperature	^oC	585
IP Turbine Inlet Pressure	*Bar*	41
LP Steam temperature	^oC	286
LP Turbine Inlet Pressure	*Bar*	4.1
Condenser pressure	*Bar*	0.045
CW water supply temperature	^oC	8
CW return temperature	^oC	25
Steam Turbine isentropic efficiency	*%*	85
Pump isentropic efficiency	*%*	70
Generator efficiency	*%*	99
Condenser thermal efficiency	*%*	80
HRSG thermal efficiency	*%*	99.7
Economiser steam side ΔP	*%*	2
Superheat steam side ΔP	*%*	1
HRSG gas side ΔP (per tube bank)	*%*	0.11
Mechanical efficiency (Turbine)	*%*	99.7
Mechanical efficiency (Else)	*%*	95
Minimum Pinch Temp	^oC	10
Booster fan Isentropic efficiency	*%*	85
Solvent (MEA composition)	*% wt*	35
Packing ΔP	*mbar/m*	2
Absorber/Desorber Flooding point	*%*	80
Desorber operating pressure	*KPa*	275
Desorber packing	MELLAPAK 252Y	
Absorber packing	MELLAPAK252Y	
Gas Mixture Model	Peng-Robinson	
Steam/Water Model	IAPWS-95	

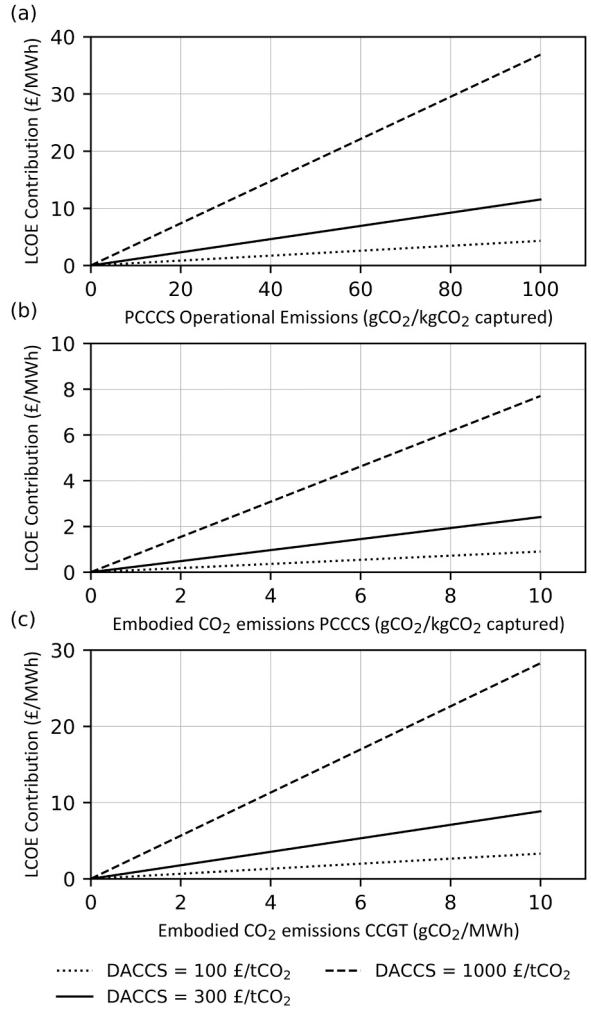


Fig. A11. Embodied and operational CO_2e emission sensitivity study.

Appendix B

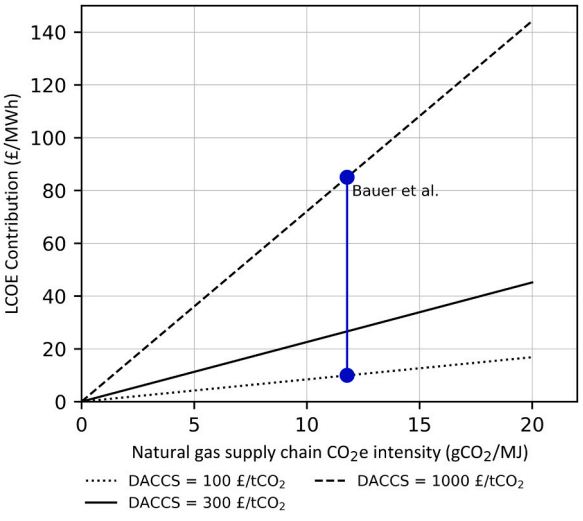


Fig. A12. LCOE vs Natural gas supply chain CO_2e intensity.

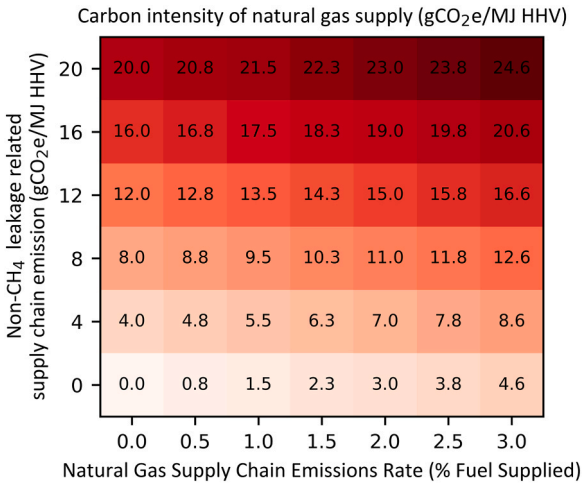


Fig. A13. Natural gas supply chain CO_2e intensity sensitivity study.

Appendix C. Supporting information

Supplementary data associated with this article can be found in the online version at doi:10.1016/j.egyr.2024.04.067.

References

Arcadis. International Construction Costs 2020. ⟨https://connect.arcadis.com/⟩: The Organisation; 2020.

Aronu, U.E., Mejdell, T., Hjarbo, K., Chikukwa, A., Grimstvedt, A., Lund, A., 2019. Baseline test of capture from bio flue gas with MEA at Tiller plant. Sintef. Report No.: 2021:00192.

Assessing the Cost Reduction Potential and Competitiveness of Novel (Next Generation) UK Carbon Capture Technology. ⟨https://www.gov.uk/⟩: Amec Foster Wheeler Group; 2018. Report No.: 13333-8820-RP-001.

Bauer, C., Treyer, K., Antonini, C., Bergerson, J., Gazzani, M., Gencer, E., et al., 2022. On the climate impacts of blue hydrogen produciton. Sustain. Energy Fuels 6. https://doi.org/10.1039/D1SE01508G.

Bechtel. Retrofitting an Australian Brown Coal Power Station With Post-Combustion Capture - A Conceptual Study. Bechtel Infrastructure and Power Corporation; 2018 October 2018.

Bechtel. CO_2 Capture Facility at Kårstø, Norway: Front-End Engineering and Design (FEED) Study Report. Feed Study. GASSNOVA; 2019 3 Aprial 2019. Report No.: 25474-000-30R-G04G-00001.

Benquet, C., Knarvik, A., Gjernes, E., Hvidsten Arne, O., Kleppe Romslo, K..Akhter, S., editors. First Process Results and Operational Experience with CESAR1 Solvent at TCM with High Capture Rates (ALIGN-CCUS Project) 15th International Conference on Greenhouse Gas Control Technologies; 2021 15-18th March: IEAGHG.

Braakhuis, L., Høisæter, K.K., Knuutila, H.K., 2022. Modeling the formation of degradation compounds during thermal degradation of MEA. Ind. Eng. Chem. Res. 61 (7), 2867–2881. https://doi.org/10.1021/acs.iecr.1c04496.

Braakhuis, L., Knuutila, H.K., 2023. Predicting solvent degradation in absorption–based CO2 capture from industrial flue gases. Chem. Eng. Sci. 279, 118940 https://doi.org/10.1016/j.ces.2023.118940.

Brandl, P., Bui, M., Hallett, J.P., Mac, D.N., 2021. Beyond 90% capture: possible, but at what cost? Int. J. Greenh. Gas. Control 105. https://doi.org/10.1016/j.ijggc.2020.103239.

Cain, M., Lynch, J., R. Allen, M., S. Fuglestvedt, J., J. Frame, D.H.Macey, 2019. A. Improved calculation of warming-equivalent emissions for short-lived climate pollutants. Clim. Atmos. Sci. 2 https://doi.org/10.1038/s41612-019-0086-4.

Christensen, P.D., Larry. COST ESTIMATE CLASSIFICATION SYSTEM – AS APPLIED IN ENGINEERING, PROCUREMENT, AND CONSTRUCTION FOR THE PROCESS INDUSTRIES AACE; 2005. Report No.: 18R-97.

Collodi, G., Azzaro, G., Ferrari, N., 2017. Techno-Economic Evaluation of SMR Based Standalone (Merchant) Hydrogen Plant with CCS. International Energy Agency of Greenhouse Gas. February 2017.

Cop26, P. WORLD LEADERS KICK START ACCELERATED CLIMATE ACTION AT COP26 ukcop26.org: COP26 Press; 2021 [Available from: ⟨https://ukcop26.org/world-leaders-kick-start-accelerated-climate-action-at-cop26/⟩.

Cownden, R., Mullen, D., Lucquiaud, M., 2023. Towards net-zero compatible hydrogen from steam reformation – Techno-economic analysis of process design options. Int. J. Hydrog. Energy 48 (39). https://doi.org/10.1016/j.ijhydene.2022.12.349.

Danaci, D., Bui, M., Petit, C., Dowell Mac, N., 2021. En Route to zero emissions for power and industry with amine-based post-combustion capture. Environ. Sci. Technol. 55 (15) https://doi.org/10.1021/acs.est.0c07261.

Davis, J..Rochelle, G., editors. Thermal degradation of monoethanolamine at stripper conditions. GHGT - 9; 2009; massachusetts: Energy Procedia.

Direct Air Capture. Paris: International Energy Agency; 2022.

Dispatchable Power Agreement business model summary. In: Department for Business, E. a. I. S., editor. ⟨www.gov.uk⟩: OGL; 2022.

Donald, R.W., 2007. Rules of Thumb in Engineering Practice. Wiley VCH.

Elliott, W.R. Front-End Engineering Design (FEED) Study for a Carbon Capture Plant Retrofit to a Natural Gas-Fired Gas Turbine Combined Cycle Power Plant (2×2x1 Duct-Fired 758-MWe Facility With F Class Turbines). ⟨https://www.energy.gov/⟩: Bechtel; 2022 March 2022.

Evaluating the Costs of Retrofitting CO_2 Captured in an Integrated Oil Refinery: Technical Design Basis and Economic Assumptions. IEA Greenhouse Gas R&D Programme; 2017 April 2017. Report No.: 2017-TR5.

Faramarzia, L., Thimsen, D., Hum, S., Maxon, A., Watson, G., Sa, P., et al., editors. Results from MEA Testing at the CO2 Technology Centre Mongstad: Verification of Baseline Results in 2015. 13th International Conference on Greenhouse Gas Control Technologies; 2016; Lausanne.

Feron, P.H.M., Cousins, A., Gao, S., Liu, L., Wang, J., Wang, S., et al., 2016. Experimental performance assessment of a mono-ethanolamine-based post-combustion CO2-capture at a coal-fired power station in China. Greenh. Gases: Sci. Technol. 7 (3) https://doi.org/10.1002/ghg.1654.

Feron, P., Cousins, A., Jiang, K., Zhai, R., Hla, S.S., Thiruvenkatachari, R., Burnard, K., 2019. Towards zero emissions from fossil fuel power stations. Int. J. Greenh. Gas. Control 87, 188–202. https://doi.org/10.1016/j.ijggc.2019.05.018.

Fuss, S., F Lamb, W., Callaghan, M.W., Hilaire, J., Creutzig, F., Amann, T., et al., 2018. Negative emissions - Part 2: costs, potentials and side effects. Environ. Res. Lett. 13 (6) https://doi.org/10.1088/1748-9326/aabf9f.

Gao, T., Selinger, J.L., Rochelle, G.T., 2019. Demonstration of 99% CO_2 removal from coal flue gas by amine scrubbing. Int. J. Greenh. Gas. Control 83, 236–244. https://doi.org/10.1016/j.ijggc.2019.02.013.

Ge-Power. 9HA Power Plants - GEA32927. 2017.

Ge-Power. 9HA.01 Sets Efficiency World Record. 2016. Report No.: GEA32885.

Goff, G.S., Rochelle, G.T., 2004. Monoethanolamine Degradation: O2 Mass Transfer Effects under CO2 Capture Conditions, 43. I&EC Research, pp. 6400–6408. https://doi.org/10.1021/ie0400245.

gPROMS products: gPROMS PROCESSBUILDER [Internet] 2021 [Available from: ⟨https://psenterprise.com/products/gproms/processbuilder⟩.

Herraiz Palomino, L., Su, D., Muslemani, H., Struthers, I., Thomson, C., Chalmers, H., Lucquiaud, M., 2023. Life cycle assessment of four waste incineration plant configurations including carbon capture and storage. Waste Manag. Res.: J. a Sustain. Circ. Econ.

Hirata, T., Tsujiuchi, T., Kamijo, T., Kishimoto, S., Inui, M., Kawasaki, S., et al., 2019. Near-zero emission thermal power plant using advanced KM CDR process™. Int. J. Greenh. Gas. Control 92, 102847.

Hume, S.A., Shah, M.I., Lombardo, G..Kleppe, E.R., editors. RESULTS FROM CESAR-1 TESTING WITH COMBINED HEAT AND POWER (CHP) FLUE GAS AT THE CO2 TECHNOLOGY CENTRE MONGSTAD. TCCS-11 - Trondheim Conference on CO2 Capture, Transport and Storage; 2021 June 21–23; Trondheim.

Knudsen, J.N., Jensen, J.N., Vilhelmsen, P.-J..Biedec, O., editors. First year operation experience with a 1 t/h CO2 absorption pilot plant at Esbjerg coal-fired power plant

Proceedings of European Congress of Chemical Engineering (ECCE-6); 2007; Copenhagen.
Martin, S., Lepaumier, H., Picq, D., Kittel, J., Bruin, T.D., Faraj, A., Carrette, P.-L., 2012. New amines for CO2 capture. IV. degradation, corrosion, and quantitative structure property relationship model. IEC Res. 51 (18), 6283–6289. https://doi.org/10.1021/ie2029877.
Masson-Delmotte, V., Pirani, A., Chen, Y., Matthews, J.B.R., Yelekçi, O., Lonnoy, E., et al., 2021. Climate Change 2021: The Physical Science Basis. Cambridge University Press: IPCC.
Matta, R.K., Mercer, G.D..Tuthill, R.S. Power Systems for the 21st Century - "H" Gas Turbine Combined-Cycles, GER-3935B. GE Power Systems; 2000. Report No.: GER-3935B.
Mcqueen, N., Vaz Gomes, K., Mccormick, C., Blumanthal, K., Pisciotta, M., Wilcox, J., 2021. A review of direct air capture (DAC): scaling up commercial technologies and innovating for the future. Prog. Energy 3 (3). https://doi.org/10.1088/2516-1083/abf1ce.
Michailos, S., Gibbins, J., 2022. A modelling study of post-combustion capture plant process conditions to facilitate 95–99% CO_2. Capture Lev. Gas. Turbine Flue Gases Front. Energy Res. 10.10.3389/fenrg.2022.866838.
Morgan, J.C., Chinen, A.C., Anderson-Cook, C., Tong, C., Carroll, J., Saha, C., et al., 2020. Development of a framework for sequential Bayesian design of experiments: application to a pilot-scale solvent-based CO2 capture process. Appl. Energy 262. https://doi.org/10.1016/j.apenergy.2020.114533.
Moser, P., Schmidt, S., Sieder, G., Garcia, H., Stoffregen, T., 2011. Performance of MEA in a long-term test at the post-combustion capture pilot plant in Niederaussem. Int. J. Greenh. Gas. Control 5 (4), 620–627. https://doi.org/10.1016/j.ijggc.2011.05.011.
Moser, P., Wiechers, G., Schmidt, S., Monteiro, J.G.M.S., Goetheer, E., Charalambous, C., et al., 2021. ALIGN-CCUS: Results of the 18-month test with aqueous AMP/PZ solvent at the pilot plant at Niederaussem – solvent management, emissions and dynamic behavior. Int. J. Greenh. Gas. Control 109. https://doi.org/10.1016/j.ijggc.2021.103381.
Mullen, D., Herraiz Palomino, L., Gibbins, J., Lucquiaud, M., 2023. On the cost of zero carbon hydrogen: a techno-economic analysis of steam methane reforming with carbon capture and storage. Int. J. Greenh. Gas. Control 126, 103904. https://doi.org/10.1016/j.ijggc.2023.103904.
National Carbon Capture Center [Internet] 2021 [Available from: ⟨https://www.nationalcarboncapturecenter.com/⟩.
Pre-Feasibility Study for Establishing a Carbon Capture Pilot Plant in Mexico. ⟨https://www.gob.mx/⟩: Nexant; 2016 18/05/2016.
Rates, E. US Dollar to British Pound Spot Exchange Rates for 2020 [Internet]: Exchange Rates; [Available from: ⟨https://www.exchangerates.org.uk/USD-GBP-spot-exchange-rates-history-2020.html⟩.
Review of next generation carbon capture technology for industrial, waste and power sectors. ⟨www.GOV.UK⟩: Department for Business, Energy & Industrial Strategy; 2022.
Rubin, E.S., 2012. Understanding the pitfalls of CCS cost estimates. Int. J. Greenh. Gas. Control 10, 181–190. https://doi.org/10.1016/j.ijggc.2012.06.004.
Shah, M.I., Silva, E., Gjernes, E..Åsen Ingvar, K. Cost Reduction Study for MEA based CCGT Post-Combustion CO2 Capture at Technology Center Mongstad. 15th Greenhouse Gas Control Technologies Conference; 15-18 March 2021; Abu dhabi: SSRN; 2021.
Sinnott, R., Towler, G., 2020. Chemical Engineering Design, Sixth ed. Elsevier.
Smith, M.A., Cain, M., Allen, M.R., 2021. Further improvement of warming-equivalent emissions calculation. Clim. Atmos. Sci. 4 https://doi.org/10.1038/s41612-021-00169-8.
Smith, R.W., Polukrt, P., Maslak, C.E., Jones, C.M..Gardiner, B.D. Advanced Technology Combined Cycles, GER-3936A. 2000,
Spath, P.L., Mann, M.K., 2000. Life cycle assessment of a natural gas combined-cycle power generation system. Natl. Renew. Energy Lab. Report No.: NREL/TP-570-27715 TRN: AH200115%%465.
Stark, C., Mike, T., Joffe, D., 2020. The sixth carbon budget: the UK's Path to Net Zero. Comm. Clim. Change, 9 December 2020.
Steyn, M.O., Jessica Turan, Guloren Zapantis, Alex Gebremedhin, Ruth. GLOBAL STATUS OF CCS 2022. ⟨www.globalccsinstitute.com⟩: Global CCS Institute; 2022.
Su, D., Herraiz, L., Lucquiaud, M., Thomson, C., Chalmers, H., 2023. Thermal integration of waste to energy plants with Post-combustion CO2 capture. Fuel 332. https://doi.org/10.1016/j.fuel.2022.126004.
THE CHEMICAL ENGINEERING PLANT COST INDEX [Internet] chemengonline.com: Chemical Engineering; 2022 [Available from: ⟨https://www.chemengonline.com/pci-home⟩.
UK Low Carbon Hydrogen Standard. ⟨www.gov.uk⟩: Crown copyright; 2022.
Weir, H., Sanchez-Fernandez, E., Charalambous, C., Ros, J., Moretz-Sohn Monteiro, J.G., Skylogianni, E., et al., 2023. Impact of high capture rates and solvent and emission management strategies on the costs of full-scale post-combustion CO2 capture plants using long-term pilot plant data. Int. J. Greenh. Gas. Control 126. https://doi.org/10.1016/j.ijggc.2023.103914.

4.1 Conclusion

This article presents a first assessment of the cost of zero life-cycle GHG electricity from a zero stack CO_2 emission CCGT with NETs used to recapture residual life-cycle emissions. The process modifications proposed, namely a 4m increase in absorber packing (20 to 24m) and a reduction in lean loading to 0.1 mol/mol from circa 0.2 - 0.25 mol/mol are moderate in nature and are expected to be achievable with commercially available technology.

When implemented these process modifications are predicted to limit the increase in specific reboiler duty (SRD) to 4.2% (3.67 vs 3.52 GJ/tCO_2) minimising the reduction in thermal efficiency to 0.53% point (LHV), and results in a net increase in electricity output penalty of 8.2% (from 70.2 to 76.0 MW), while the increase in plant capital expenditure (CAPEX) is limited to 4% and any increase solvent thermal degradation is predicted to have a negligible effect on plant economics.

A technoeconomic analysis reveals that for 2023 UK capital costs and a natural gas price of 28 £/MWh, the Levelised Cost of Electricity (LCOE) and the Cost of CO_2 Avoided (CCA) is 104 £/MWhe and 128 £/tCO_2 respectively for a 100% fossil CO_2 capture fraction, comparing favourably to the 102 £/MWh_e and 125 £/tCO_2 for a gross 95% CO_2 capture fraction. This leads to the novel conclusion that any CO_2 reduction incentive or penalty (i.e. CO_2 tax) above 184 £/tCO_2 will push the market towards 100% fossil CO_2 capture. Indeed, at the time of writing this is already the case in the UK, an analysis of the power CCS business model i.e. the DPA, shows that for the conditions described in this manuscript, a CCGT operating at a 100% fossil CO_2 capture fraction will return a higher revenue than one operating at a gross 95% CO_2 capture fraction.

The predicted recapture burden stemming from upstream and downstream emissions in the supply chain is estimated to be between 8.6 and 11.8 MtCO_2 over the plant's lifetime. For a cost of direct air capture and storage (DACCS) consistent with the current literature of 100–1000 £/tCO_2 this is predicted to add 10–114 £/MWh_e to the LCOE. For the global median case of 1.5% natural gas supply chain fugitive emissions and 300 £/CO_2 for DACCS, the LCOE and CCA are 135 £/MWh_e and 178 £/tCO_2 (an increase of 71.5 £/MWh_e over an unabated CCGT).

The design insights provided in this manuscript may prove critical for project developers considering implementing CCS to CCGTs, demonstrating for the first time that with minor process modifications the capture of 100% of the CO_2 generated in a CCGT is not only technically feasible, but also, in the UK at least, economical.

4.2 Highlights

- The CCA & LCOE for 100% fossil CO_2 capture is estimated at 128 £/tCO_2 & 104 £/MWh_e
- Permanent scope 2 and 3 emission recapture adds 10–114 £/MWh_{th} to electricity costs.
- The recapture of 8.6–11.8 MtCO_2 of CO_2 over the plant lifetime is required.
- Electricity output penalty, capital and operational costs increase by 8, 4 and 2.3%.
- CCS business models in the UK support 100% fossil CO_2 capture.

4.3 Limitations and Future Work

The following limitations were identified for the work described in this chapter; any future work should endeavour to resolve these limitations:

- This lifecycle study is limited to the GHG effect of the atmospheric methane and CO_2 equivalent emissions; additional GHGs such as NO_2 and SF_6 are not included. Likewise, non-GHG-related environmental considerations are out of scope.
- Although the increase in thermal degradation of MEA as a result of increased regeneration was investigated in this manuscript a more holistic and plant wide analysis is required to fully quantity the effect of operating at ultra-high CO_2 capture fractions. The reader is referred to Chapter 6 of this thesis for a detailed analysis.
- For decarbonised CCGTs to operate as a support to intermitted renewables in a decarbonised electricity grid they will be required to operate in a flexible manner, with frequent load changes and start-up/shut-down events. It is critical to the climate impact of these plants that CO_2 capture rates are maintained at high levels during these operational modes. The scope of this study was limited to steady state operations however the reader is referred to Chapter 7 of this thesis where efforts to close this knowledge gap is presented.

5. Thermodynamic Integration in Combined Fuel and Power (CFP) Plants Producing Low Carbon Hydrogen & Power with CCUS[5]

5.1 Abstract

Demand for low-carbon sources of hydrogen and power is expected to rise dramatically in the coming years. Individually, steam methane reformers (SMRs) and combined cycle gas power plants (CCGTs), when combined with carbon capture utilisation and storage (CCUS), can produce large quantities of on-demand decarbonised hydrogen and power respectively. The ongoing trend towards the development of CCUS clusters means that both processes may operate in close proximity, taking advantage of a common infrastructure for natural gas supply, electricity grid connection and the CO_2 transport and storage network.

This work expands on a novel integration method, first proposed by Herraiz et al., which utilizes flue gas sequential combustion to incorporate the SMR process into the CCGT cycle in a single "combined fuel and power" (CFP) plant. The merged steam cycles and redesigned the heat recovery system proposed in this work increase the 2nd law thermal efficiency by 2.6% points over un-integrated processes and 1.9% points the previous integration design.

Using a conventional 35% wt. monoethanolamine (MEA) CO_2 capture process designed to achieve two distinct and previously unexplored CO_2 capture fractions; 95% gross and, 100% fossil (CO_2 generated is equal to the quantity of CO_2 captured). The CFP configuration reduces the overall quantity of flue gas to be processed by 36-37% and increases the average CO_2 concentration of the flue gas to be treated from 9.9% to 14.4% (wet). This decreases the absorber packing volume requirements by 41 - 56% and decreases the specific reboiler duty by 5.5% from 3.46 - 3.67 GJ/tCO_2 to 3.27 – 3.46 GJ/tCO_2, further increasing the 2nd law thermal efficiency gains to 3.8 – 4.4% points over the un-integrated case.

A first of a kind techno economic analysis concludes that the improvements present in a CO_2 abated CFP plant results in a 15.1 – 17.3% and 7.6 – 8.0% decrease in capital and operational expenditure respectively for the CO_2 capture cases. This translates to an increase in the

[5] The work was accepted for publication to Frontiers in Energy Research as of December 2024 DOI: 10.3389/fenrg.2024.1511996

internal rate of return over the base hurdle rate of 7.5 - 7.8%, highlighting the potential for substantial cost reductions presented by the CFP configuration.

5.2 Introduction

Electricity produced via fossil fuel combustion is expected to continue to play an essential role in future energy grids by proving a large portion of the dispatchable power capacity needed to operate electricity grids with high penetration of intermittent renewable generation (Stark *et al.*, 2020). Likewise, hydrogen may play a role as an energy storage vector when produced via electrolysis at periods of excess renewable generation (green hydrogen). But if required in volumes predicted by 2050 (250 - 460TWth/pa in the UK) (Stark *et al.*, 2020) this is unlikely to be met exclusively with electrolytic hydrogen due the large build out of renewable capacity and storage systems that would be required to ensure security of supply. As a result, some dispatchable source of hydrogen production will likely be required, with the reforming of methane into hydrogen and CO_2 being the most likely candidate (Joffe *et al.*, 2018; UK Gov, 2021b). In both cases, i.e., fossil-based power and hydrogen, these production methods will need to be fully decarbonised in order to be compatible with a net zero energy system.

Post combustion capture (PCC) is the most technologically mature option for decarbonising natural gas-fired Combined Cycle Gas Turbines (CCGT). Both pre-combustion and post-combustion CCS schemes have been proposed for Steam Methane Reformers (SMR) (Collodi *et al.*, 2017) however, due to the need to supply heat to the reformation cycle, pre-combustion CO_2 capture from the high pressure syngas typically only captures ~60% of the CO_2 produced in the facility, with further decarbonisation typically reliant on post combustion, either solely, or as a combination of pre and post combustion, or the use of the autothermal reactor (ATR) process over the SMR process.

Although technically mature, PCC is a Capital Expenditure (CAPEX) intensive process. A proposed pathway for decreasing CAPEX is by increasing the CO_2 concentration of the flue gas to be treated. This reduces the diameter of the absorber column required to process the same amount of CO_2, a major component of total plant CAPEX. As an additional benefit, the increased CO_2 concentration can reduce the required height of absorber packing sections, further reducing CAPEX, and/or increase the rich loading of the solvent leaving the absorber column, reducing the specific reboiler duty (SRD). Models of a CCGT plant fitted with exhaust gas recirculation (EGR) show that a 36% decrease in flue gas flow rate translates to an 40% decrease in the required absorber packing volume and 2.9% reduction in SRD (Herraiz *et al.*, 2018). Separate models indicated that flue gas sequential firing (FGSF) in a CCGT with PCC

reduces total plant CAPEX by 15.3% vs an unfired CCGT for the same power output and CO_2 capture rate (González Díaz *et al.*, 2016).

In the case of FGSF, the reduction in CAPEX comes with a reduction in plant thermal efficiency from 51.3% in the unfired case to 43.1% when supplementary firing is implemented. As such, the reduction in plant CAPEX will be offset to some degree by an increase in plant operational expenditure (OPEX). For power generation plants, thermal efficiency is a key driver of economic viability, especially for CCGTs that operate primarily as the marginal power generation source in energy markets. It is then likely that using FGSF in CCGTs producing exclusively electricity will only be economically viable for applications where CO_2 demand is very high, such as enhanced oil recovery (EOR).

An alternative approach is to use the additional heat input from the supplementary fuel to drive an endothermic chemical reaction, therefore maintaining the 2nd law efficiency of the power generation and the rated electrical efficiency of the CCGT plant while producing an additional product. The thermal reformation of natural gas and steam into hydrogen can serve this purpose, maintaining power production thermal efficiency, reducing the CAPEX burden of the PCC plant and producing an additional decarbonised energy vector expected to be critical to the decarbonisation of global energy systems (Joffe *et al.*, 2018).

The production of power and hydrogen in a single plant, termed “Combined Fuel and Power” (CFP), could be achieved by installing the endothermic equipment of an SMR process, namely the reformer and steam production modules, downstream of a commercial gas turbine. The sequential combustion of the O_2 rich flue gas from the gas turbine would increase temperatures sufficiently to reform CH_4 and H_2O into a syngas (primarily H_2, CO and CO_2) with subsequent heat recovery producing steam for power generation, the reformation process and solvent regeneration in the CCS plant. This novel cycle would, in addition to any CAPEX and OPEX reductions, also take advantage of the multitude of shared infrastructure requirements between decarbonised CCGT and SMR plants (natural gas supply, electricity grid connection, CO_2 transport and storage networks, cooling water etc.).

This concept of co-generation of hydrogen and power has been previously suggested by Herraiz et al (Herraiz *et al.*, 2020). Herraiz et al. demonstrate that the integration of the reforming and power generation cycles can reduce flue gas flow rates to the PCC plant by circa 34%. Simultaneously increasing the average flue gas CO_2 concentration is increased from 10.5 vol % to 16.1 vol % (wet) when compared to the independent production of each energy vector. This results in a 17.5% reduction in absorber packing volume, a 4.3% reduction in SRD for solvent regeneration and a 5.6% increase in power output, intensifying the CO_2 capture process and reducing capital costs.

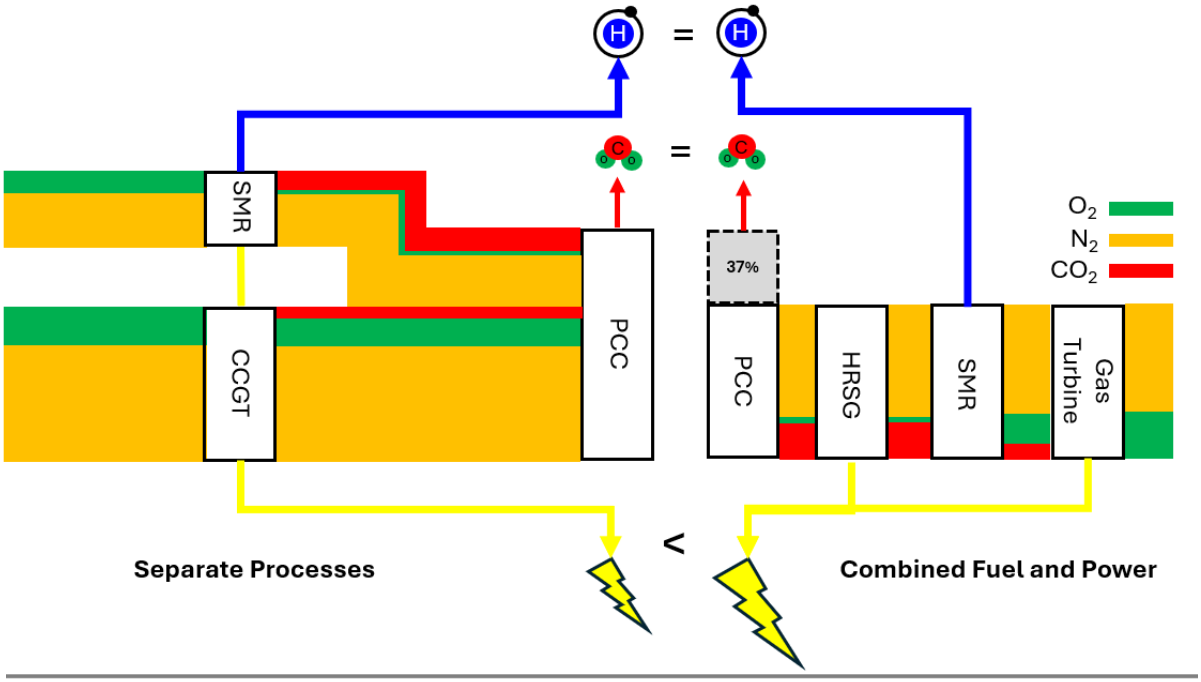


Figure 8: Thermodynamic Integration in Combined Fuel and Power (CFP) Plants Producing Low Carbon Hydrogen & Power with CCUS

However, the degree of integration between the CCGT and SMR process was minimal, with no optimisation or rationalisation of equipment, effectively maintaining both processes separated. Although this simplified the design and integration, while achieving large reductions in flue gas flow rates, this segregated approach resulted in large pinch temperatures within the flue gas and syngas heat recovery systems, ultimately negatively effecting the production efficiency of electricity and hydrogen from the process.

In this work, the authors propose a redesigned flue gas and syngas heat recovery system that minimizes exergy destruction in the system by optimizing pinch temperatures and prioritizing HP steam production, fully merging both the CCGT and SMR processes. This redesigned process is predicted to increase the thermal efficiency and reduce the cost of production

relative to the independence generation power and hydrogen and the configuration proposed by Herraiz et al.

5.3 SMR and CCGT integration

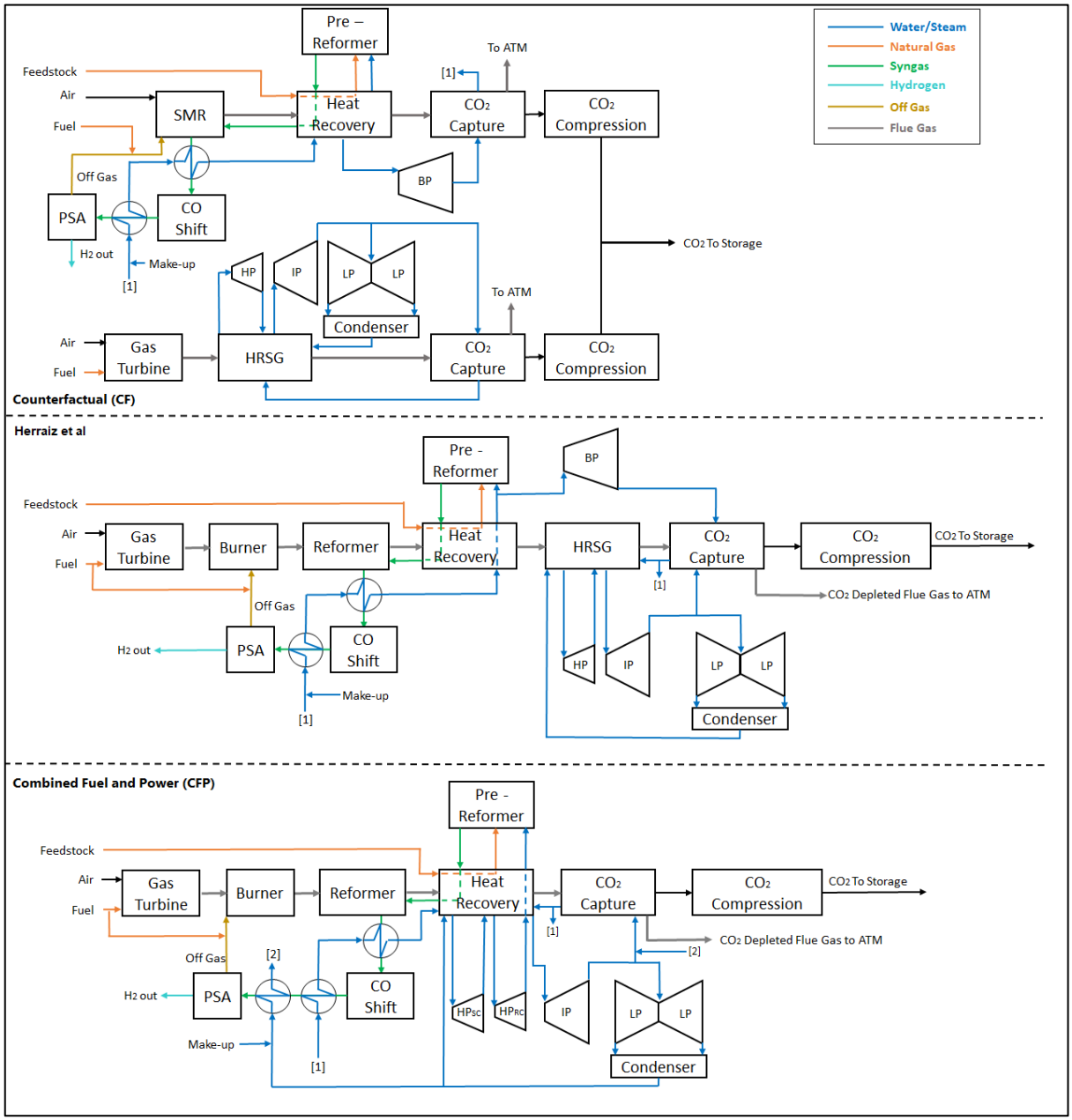


Figure 9 – Counterfactual (CF), Herraiz et al. and Combined Fuel and Power Plant

The counterfactual in Figure 9 is considered the baseline against which plant performance improvements are measured. In this case both SMR and CCGT processes are maintained separate with dedicated PCC plants feeding into a shared CO_2 T&S network in a CCUS "cluster" arrangement, these processes have been described in detail in previous work by the authors (Mullen *et al.*, 2023; Mullen and Lucquiaud, 2024) but do not notably deviate from standard configurations.

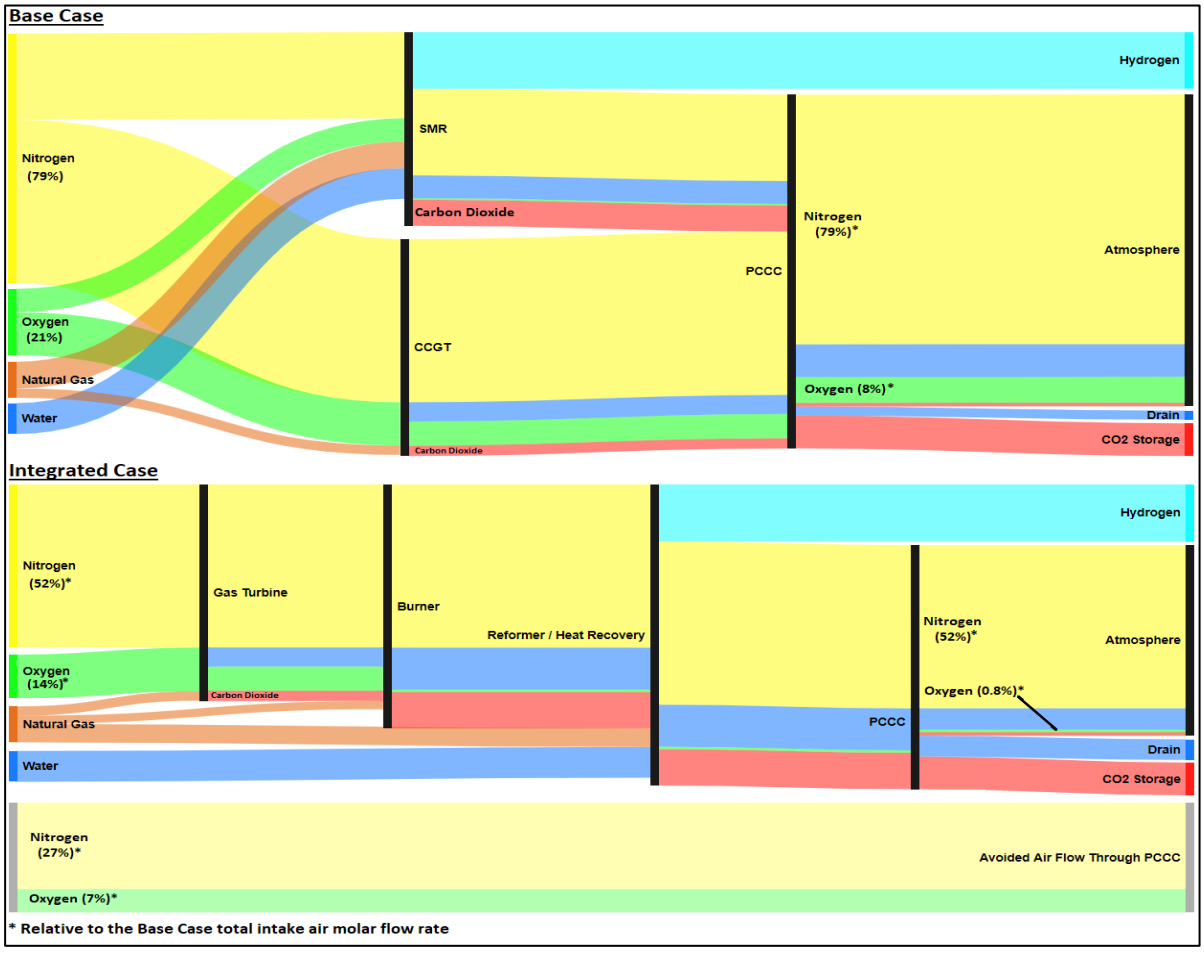


Figure 10 - Representation of fluid species flow rates though both the counterfactual and CFP cases. Power output not shown.

Herraiz et al. proposed the installation of an SMR downstream of a GT however the integration of both processes was limited to the sharing of a flue gas path and CO_2 capture plant (Figure 9). As commercial GTs operate with a large amount of excess air, O_2 is present in the flue gas at a concentration of 10 – 14 vol %. This is used for the combustion of a mixture of SMR off gases from the hydrogen purification system and supplementary natural gas, providing the additional heat required to drive the exothermic SMR reaction. O_2 concentration is reduced to

ca. 1 vol% and CO_2 concentration increased to ca. 16.5 vol% (saturated at 35°C), resulting in a 36-37% reduction in flue gas volume relative to the counterfactual (Figure 9). Despite the reduction in flue gas volume and increase in CO_2 concentration achieved by the Herraiz configuration, the degree of integration between the two processes is minimal, leading to inefficiencies.

The Combined Fuel and Power (CFP) configuration detailed in this work demonstrates a higher degree of thermal integration with a redesigned heat recovery system for the flue gas and syngas stream. High Pressure (HP) steam production is maximised and a new pre-heating module for the sequential burner fuel is included, both are strategically located to optimise heat recovery and minimise irreversibility's in the system (see Figure 11). This is in contrast to Herraiz et al. where HP steam is exclusively produced in the HRSG with the SMR producing steam at reformer pressure (25-35 bar), resulting in larger irreversibility due to the high pinch temperatures.

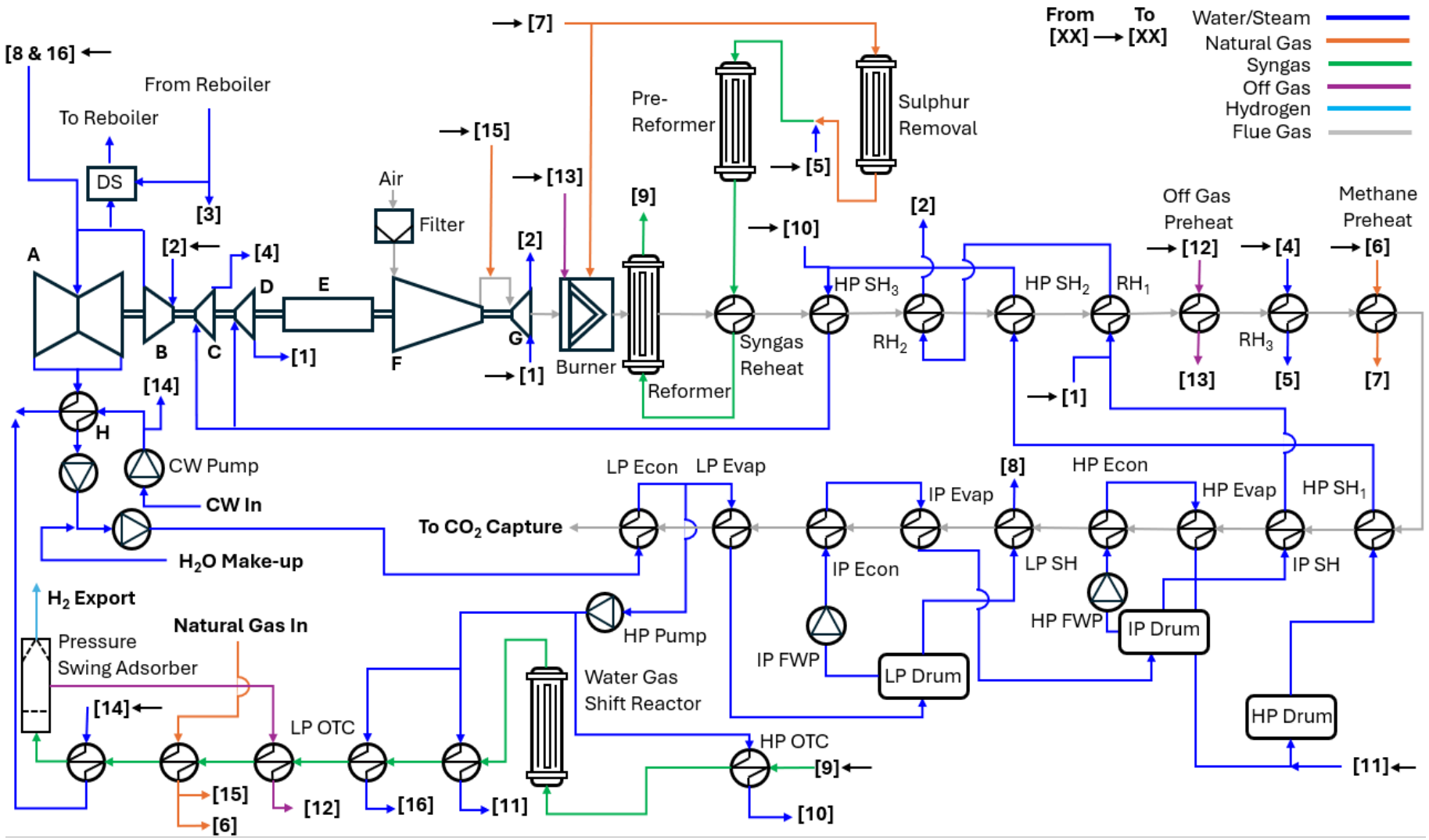


Figure 11 - Process flow diagram of the Combined Fuel & Power Plant. A - Low Pressure (LP) turbine, B – Intermediate Pressure (IP) turbine, C - High Pressure (HP) turbine exhausting at reformer pressure, D - High Pressure turbine exhausting at IP, E – Generator, F – Compressor, G – Gas Turbine. Feedwater Pump (FWP), Cooling Water (CW), Once Through Cooler (OTC), Superheat (SH), Economiser (Econ), Evaporator (Evap).

The CFP scheme proposes the use of two HP turbine cylinders in parallel. One exhausting the steam at intermediate pressure (IP) for use in further power generation (as in a conventional CCGT), whilst the other exhausts the steam at the reformer pressure (RP) for use in the reforming process. This configuration maintains the reduction in flue gas flow rates observed by Herraiz et al. while also increasing the thermal efficiency of the plant.

5.4 *Modelling Methodology*

An integrated CFP Plant model has been developed in gPROMS Process Builder (gPROMS, 2021), a process modelling platform that allows the creation of bespoke unit models for each specific plant operation using Peng-Robinson equation of state for gas mixtures and the Scientific Formulation IAPWS-95 for water and steam. The process modelling of the CO_2 capture plant is conducted using an open-source MEA model funded by the US Department of Energy and developed by the Carbon Capture Simulation for Industry Impact (CCSI) in ASPEN PLUS (ASPENtech, 2022). This model is validated against pilot-scale data from the US National Carbon Capture Centre (NCCC) (Morgan *et al.*, 2020). The reader is referred to Mullen et al. (Mullen *et al.*, 2023; Mullen and Lucquiaud, 2024) for a detailed description of the process modelling. However, the process does not notably differ from that of a traditional amine CO_2 capture plant and is illustrated in Figure 12.

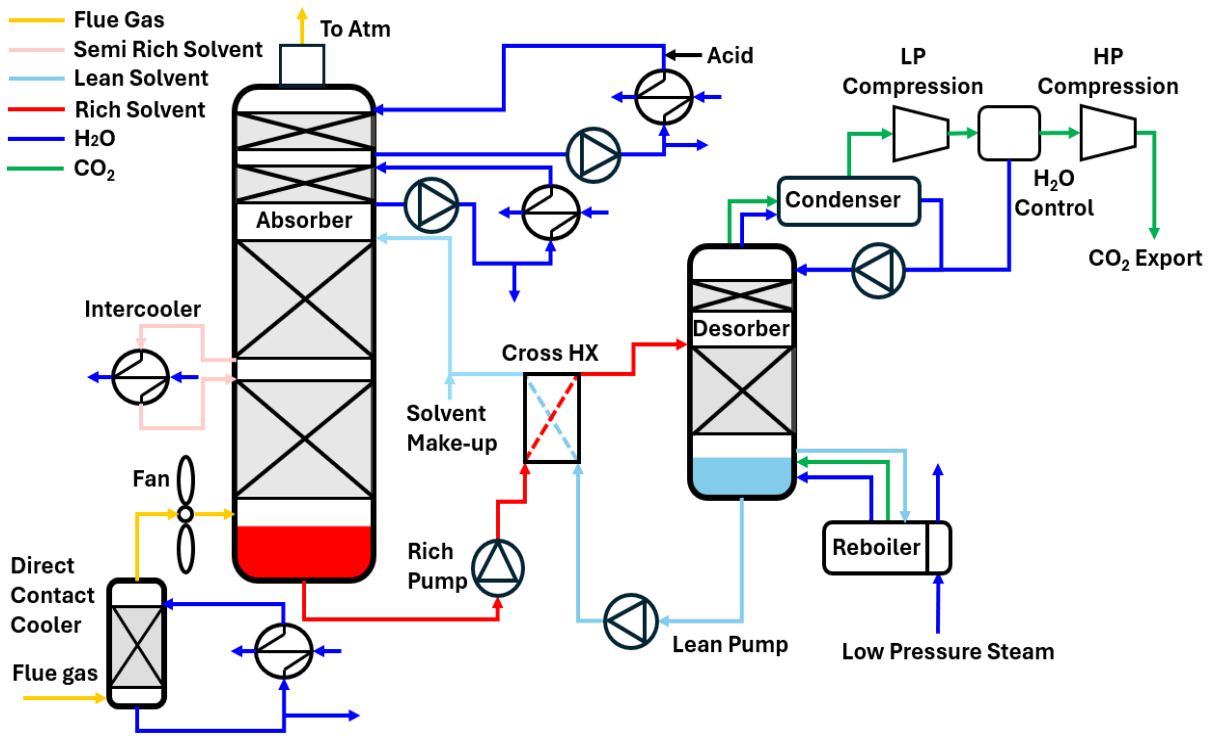


Figure 12: Illustration of the Post Combustion CO_2 capture process

5.4.1 Gas turbine

A GE H-Class 1 X 1 combined cycle gas turbine (GE 9HA.01) with a rated thermal efficiency of 63.5% (LHV) is chosen for the basis of design due to the availability of operational parameters in the public domain (Matta, Mercer and Tuthill, 2000; Smith *et al.*, 2000; General Electric, 2016, 2017). It should be noted that this technology is not limited to this Gas Turbine (GT) engine and could be applicable to any commercial CCGT plant.

The GE 9HA.01 operates at a pressure ratio of 23.5 and a turbine inlet temperature (TIT) of greater than 1430°C. At ISO ambient conditions, with a natural gas fuel source and 100% load, the GT has a power output of 446MW with a thermal efficiency of 43.1% (LHV). The flue gas exits the GT with a flow rate of 805 kg/s, a temperature of 629°C and ca. 11 vol % O_2 concentration. A detailed breakdown of all the design and performance parameters used in the model is presented in Appendix A. Hot gas path cooling is achieved by a hybrid system, with closed-loop steam cooling for the 1st & 2nd stage nozzles and compressed air extracted from the GT compressor supplying cooling air for the 3rd stage nozzles. No cooling is required for the 4th stage. Cooling steam is extracted from the HP turbine exhaust and IP superheater as required. The cooling steam passes through the stationary nozzles and is heated to approximately re-heat temperature, where it is then reintroduced to the steam cycle by mixing it with the hot re-heat steam from the HRSG prior to entering the IP turbine.

5.4.2 Reformer furnace & Flue gas heat recovery

Flue gas exiting the GT is sequentially fired using preheated mixture of the off-gas from the hydrogen purification system (containing unreacted natural gas and a small amount of H_2) and a controlled amount of supplementary natural gas. This mixture is ignited in the sequential burners, reaching a temperature of 1550°C and an O_2 concentration ca. 1 vol %. It is worth noting that this is the highest temperature seen in the heat recovery section of this plant but is lower than the typical maximum temperatures of 1800°C for conventional SMRs. Due to the lower adiabatic flame temperature and the larger flue gas flow rate in the CFP configuration, a redesign of the reformer is required to account for a reduction in radiative heat transfer and an increase in convective heat transfer compared to conventional SMR. Nonetheless this is not envisioned to be a substantial technical barrier as convective reformers are commercially available (Haldor Topsøe, 2007).

The flue gas passes through the reformer module reducing its temperature to 1150 - 1050ºC prior entering the heat recovery section where heat is recovered for the purposes of generating steam, natural gas pre-heating, off gas pre-heating and syngas re-heating. The 6 out of 17 tube banks will likely have to be manufactured from high grade alloys to withstand the higher than standard temperatures. This is already the case for conventional SMRs and is not likely to contribute to a marked CAPEX increase when compared to the counterfactual. The flue gas leaves the heat recovery section at approximately 80ºC, which is in line with typical CCGT designs but lower than the 130-140ºC typical in SMRs (Collodi *et al.*, 2017).

5.4.3 Steam cycle

The steam cycle used in this work is a subcritical triple pressure (186/41/3.7 bar) HRSG with re-heat. HP and IP steam temperatures are set at 600ºC and 585ºC respectively (General Electric, 2017). Feedwater to the steam generators comprises of condensate from the reboiler return and steam cycle condenser with the remainder made up from make-up water. There will be a higher requirement for make-up water in a CFP plant when compared to conventional CCGTs, as a portion of the water is consumed in the reforming and shift reactions. However, the quantity of make-up water is a function of the reforming process and constant across all cases.

Steam for the CO_2 capture process is extracted from the IP/Low Pressure (LP) crossover, with additional LP steam supplied via a once through cooler (OTC) fitted to the syngas cooling system. Supplementary HP steam is generated via heat recovery from the reformer syngas stream in a HP OTC. Two HP turbine cylinders are considered in this plant arrangement. The first one, denoted C in Figure 11, acts as the conventional CCGT HP turbine and exhausts steam at IP pressure to the re-heaters. The second one, shown in blue, exhausts steam at the required reformer operating pressure, in this case 34 bar. This is then re-heated in the HRSG up to 500ºC for use in the reforming cycle. GT fuel pre-heating is completed in the syngas heat recovery section, removing the need for extraction of IP water from the IP economiser. LP steam for use in various plant applications including de-aeration is generated in the HRSG at 277ºC and 3.7 bar. A minimum pinch and approach temperature of 10ºC and 15 ºC respectively was chosen for the steam cycle

5.4.4 Reforming Process

The reforming cycle used in this model is based on the technical and operational parameters of a conventional SMR with PCC as described in a report commissioned by the IEAGHG in 2017 (Collodi *et al.*, 2017). Modifications were made to the heat recovery process for the purpose of integration into the CFP plant. Steam at 34 bar is extracted from the exhaust of one of the two HP turbine cylinders in parallel (as described in section 5.4.3) and used as process steam for methane reforming. This steam is re-heated up to 500°C and mixed with a pre-heated and pre-treated stream of natural gas feedstock at the same temperature and pressure. The ratio of steam to natural gas feedstock entering the pre-reformer is set to give a steam-to-carbon ratio of 2.5 in the reformer. This mixture then enters pre-reformer, which is an adiabatic reactor that converts 100% of the C2+ hydrocarbons and olefins present in the feedstock into CO and H_2. After pre-reforming the syngas is re-heated to 600°C prior to entry to the catalyst-filled reformer tubes where steam reacts with methane at ca. 913°C to form a syngas consisting of equilibrium amounts of CH_4, H_20, H_2, CO_2 and CO.

Condensate returning from the reboiler of the PCC plant at ~130°C is pumped to HP turbine inlet pressure and fed through heat exchangers on both sides of the water-gas-shift reactor (WGSR). A HP OTC cools the inlet stream to 320°C while generating HP steam at 600 ^{o}C and a HP economiser cools the outlet stream to the dew-point temperature at approximately 150°C while heating HP water up to saturation temperature prior to being sent to the HRSG HP drum for evaporation and superheating. The WGSR converts ca. 72% of the CO and the equal number of moles of H_2O in the syngas stream to H_2 and CO_2. Heat recovery from the syngas stream is maximized via, an LP OTC generating LP steam for use in the PCC plant and two additional heat exchangers which preheat Natural Gas and the off gas from the Pressure Swing Absorber (PSA) hydrogen purification system. Final cooling of the syngas stream to 40°C is completed prior to entry into the PSA for H_2 separation.

5.4.5 2nd Law (Exergy) Analysis

The 2nd law of thermodynamics provides a framework for determining the maximum amount of useful work or “exergy” that can be extracted from a system assuming a perfectly efficient or reversable process. It is useful to compare the performance of a process relative to the idealised process, which is often termed the 2nd law (used throughout this manuscript) or exergy efficiency and is defined at the ratio of the useful work output of the system to the reversible or idealised work output.

A detailed 2nd law or exergy analysis is conducted for the proposed CFP plant, with the aim of identifying areas of high exergy generation and areas for process improvements.

The exergy analysis was completed by defining each distinct component in the plant, operating at steady state, as a control volume with adiabatic boundaries. An exergy balance was then completed on each control volume as defined by Equation 3 to determine the degree of irreversibility for that component. Exergy at the inlet to the compressor fine filter was assumed to be zero.

$$\dot{\phi}_{cv} = \sum_j \left(1 - \frac{T_O}{T_j}\right) \dot{Q}_j - \dot{W}_{cv} + P_o \dot{V} + \sum_i \dot{m}_i \varphi_i - \sum_i \dot{m}_e \varphi_e - \dot{\phi}_{destruction} \qquad (3)$$

Where:

$$\varphi = (h - h_o) - T_o(S - S_o) + (\delta - \delta_o)$$

Subscripts i and e describe the conditions at the inlets and outlets of a control volume respectively, j the conditions at a heat source and o the reference state. $\dot{\phi}$ denotes flow of exergy, $\dot{Q}$ heat flow, $\dot{V}$ volumetric change, $\dot{m}$ mass flow, $\dot{W}$ work flow, *h* enthalpy, *S* entropy, *T* temperature and δ chemical exergy.

The exergy efficiency of the plant ($\eta_{2nd\ law}$) was then calculated in accordance with Equation 4

$$\text{Exergy Efficieny } (\eta_{2nd\ law}) = \frac{\sum \dot{\phi}_{out\ (used)}}{\sum \dot{\phi}_{in}} = 1 - \frac{\sum \dot{\phi}_{irriversable} + \sum \dot{\phi}_{out\ (unused)}}{\sum \dot{\phi}_{in}} \qquad (4)$$

Where:

$$\dot{\phi}_{in} = \dot{\phi}_{Natural\ Gas} + \dot{\phi}_{H20}\ ;\ \dot{\phi}_{out\ (used)} = \dot{W}_{out} + \dot{\phi}_{H2}\ ;$$

$$\dot{\phi}_{out\ (unused)} = \dot{\phi}_{Stack} + \dot{\phi}_{CO2} + \dot{\phi}_{CW}$$

5.4.6 Technoeconomic Assessment

A multi-level factorial cost model previously developed and published by the author is used to calculate PCC plant Engineering, Procurement and Construction (EPC) cost with an estimated accuracy of +35%/-15% (AACE Class 4) (Christensen Larry, 2005).

Equipment costs for the CCGT & SMR components of the CFP plant were reverse calculated using Equation 5 from published EPC costs (J. Murphy and S. Ferguson, 2018; UK Gov, 2021a) and a suite of economic parameters (Appendix A), SMR components were scaled to the appropriate size using Equation 6 and a scaling factor of 0.79 (Sinnott and Towler, 2020). A conservative assumption that all SMR equipment in a standard SMR will be utilised in the CFP was applied. The equipment costs factor in Equation 5 was taken as the summation of the CCGT and Scaled SMR equipment. In practice it is likely that equipment costs will be somewhat reduced as equipment is shared between processes. Equation 5 was then used to calculate the total CFP EPC cost and Equation 7 used to estimate a total plant CAPEX.

$$EPC = \left(f_{contractor\ fee} + f_{contingency}\right) * \left\{ \begin{matrix} f_{project\ management} * \\ \left(f_{civil} + f_{utility} + f_{electrical}\right) * \\ \sum \left(I + \left(f_{installation} + f_{\frac{tax}{freight}} \right) \right) \\ * Equipment\ Cost \end{matrix} \right\} \quad (5)$$

$$SC = RC * \left(\frac{SP}{RP}\right)^{Exp} \quad (6)$$

$$CAPEX = (EPC_{CFP} + EPC_{PCC}) * \left(\begin{matrix} 1 + f_{owners} + f_{regulatory} + f_{spares\ \&\ start-up} + \\ f_{connections} + f_{consultancy} \end{matrix} \right) + Interest\ during\ construction \quad (7)$$

Where Exp is the Scaling Exponent, RC is the reference plant cost, *RP* is the reference plant parameter, *SC* is the scaled plant cost, *SP* is the scaled plant parameter, f_i represents a factorial cost, and *I* is the equipment instrumentation cost. Reference Appendix A for the economic parameters used in this work.

Net Present Value (NPV) and Internal Rate of Return (IRR)

The net present value (NPV) of an asset is the present value of all the future cash flows (positive and negative) that asset will generate (Equation 8), all future cashflows are discounted using a defined discount rate.

$$NPV = \sum_{t=0}^{n} \frac{(Cash\ in - Cash\ Out)_t}{(1 + Discount\ Rate)^t} \quad (8)$$

$$(n = Number\ of\ periods)$$

A positive NPV indicates that an asset is predicted to return greater profitability than an alternative investment at the applied discount rate. The Internal Rate of Return (IRR) is the discount rate that makes the NPV of a project zero. i.e., it is the expected compound annual rate of return that will be earned on a project or investment. Business will typically apply a "hurdle rate" to a project which defines the minimum acceptable IRR from an investment and is highly dependent on the perceived risk, i.e., a low-risk investment would be expected to have a lower hurdle rate than a high-risk investment.

The levelised cost of a product i.e., electricity (LCOE) or hydrogen (LCOH) is the average net present cost of a unit of a product over the lifetime of the asset for a given IRR. Or in other words, the present value average minimum price of a product that will provide the required return on investment. An estimate LCOE and LCOH for an IRR of 7.8% (David Menmuir *et al.*, 2022) is available in Mullen et al. (Mullen *et al.*, 2023; Mullen and Lucquiaud, 2024) for CCGTs and SMRs at a range of CO_2 capture rates and is summarised in Table 2.

Table 2: Levelised Cost of Electricity and Hydrogen (Mullen et al.) for a three CO_2 capture fractions

	Unit	100% $_{Fossil}$	95% $_{Gross}$	0%
Levelised Cost of Electricity	*(£/MWhe)*	104	102	63
Levelised Cost of Hydrogen	*(£/MWh HHV)*	69	66	44

The values provided in Table 2 are used to assess the profitability of a CFP plant compared to hydrogen and electricity production in dedicated SMRs and CCGTs (i.e., the counterfactual in this study) by assuming that they operate in the same market. Therefore, the LCOE and

LOCH serves as an estimate for the average minimum sale price for each product from the CFP. The resultant NPV of the CFP plant and associated change in IRR is reported.

5.5 Results and Discussion

5.5.1 Thermal performance of the CFP plant

The thermal performance of the CFP plant and counterfactual i.e., segregated operation of a CCGT and SMR, is presented in Table 3, in this instance without CO_2 capture to demonstrate the increase in thermal efficiency occurring as a result of the thermal integration.

Marginally higher quantities of natural gas fuel are required in the CFP plant compared to the counterfactual to reduce levels of excess O_2 in the flue gas down to 1% vol. Nevertheless, the higher level of thermal integration and optimised heat recovery system from both the flue and syngas streams results in an increase in electrical output of 128MW, leading to an increase in 2nd law thermal efficiency of 2.6% points over the counterfactual and 1.9%-point increase over the previous integration design by Herraiz et al. Further comparisons to Herraiz et al. are not feasible for the remainder of this manuscript as the CO_2 capture plant modelling techniques diverge and would not represent a valid comparative basis.

Table 3: Thermal performance of Combined Fuel & Power plant

Parameter	*Unit*	*SMR*	*CCGT*	Counterfactual[6]	Combined Fuel & Power Plant (Herraiz et al.)	Combined Fuel & Power Plant (this work)
Fuel $_{(HHV)}$	*MW_{th}*	*2722*	*1147*	3869	4333	3916
Output Power	*MW_e*	*146*	*664*	810	9037	938
Output H_2 $_{(HHV)}$	*MW_{th}*	*2000*	-	2000	2281	2000
$\eta_{(2nd\ law)}$	*%*	*61.1*	*71.6*	68.5	69.3	71.1
CO_2 Emissions	*Kg/s*	*59*	*140*	199	244	202

6 Output of the counterfactual is the summation of the CCGT and SMR models
7 Coefficient of Power (thermal energy vs the electrical energy that could be extracted) of steam for solvent regeneration is not provided in Herraiz et al, in lieu of this a COP of is assumed and net power output calculated.

5.5.2 Performance with CO_2 Capture Integration

The performance of the counterfactual and CFP cases with CO_2 capture at two distinct CO_2 capture fractions, 95% gross CO_2 capture and 100% fossil CO_2 capture, is presented in Table 4.

The CFP plant is shown to have a 36 – 37% reduction in saturated flue gas flow rate to the absorber depending on the CO_2 capture fraction considered. This results in a 56 – 41% reduction in the volume of absorber packing required. The increase in net CO_2 concentration of the flue gas into the absorber results in a 5.5% decrease in specific reboiler duty (SRD). This, along with the increased thermal efficiency of the CFP process results in an increase in the 2nd law thermal efficiency of 3.8 – 4.4% points over the counterfactual. A detailed breakdown of the outputs of the CO_2 capture plant modelling is available in Appendix A.

Table 4: Comparison of the Combined Fuel & Power Plant (CFP) performance with CO_2 capture with the Counterfactual (CF) shown in Figure 9.

		95% (Gross)		**100% (Fossil)**	
Parameter	*Unit*	CF	CFP	CF	CFP
Fuel (HHV)	MW_{th}	4057	3916	4139	3916
Output Power	MW_e	653	711	654	691
Output H_2 (HHV)	MW_{th}	2000	2000	2000	2000
η (2nd Law)	%	61.2	65.0	60.1	64.5
CO_2 Emissions	Kg/s	10.0	9.7	0.0	0.0
CO_2 Captured	Kg/s	207	192	213	202
Flue Gas mass flow rate	Kg/s	1316	848	1343	848
Specific Reboiler Duty	GJ/tCO2	3.46	3.27	3.67	3.47
Reboiler Duty	MJ	715	628	782	700
Absorber Packing Volume	m^3	5183	3079	6989	3079

Figure 13 details the heat recovery from the sequentially fired GT flue gases and the syngas stream for the CFP plant at a 100% fossil CO_2 capture fraction. It is evident that the temperatures directly downstream of the sequential burners are higher than those typically seen in CCGTs. They are, however, marginally lower than those seen in conventional SMRs, suggesting that this would not cause a marked change in capital costs when compared to the counterfactual. Downstream from the off-gas pre-heater, the flue gas temperatures are more typical of those seen in CCGT's (González Díaz *et al.*, 2016) and as such standard construction materials and manufacturing techniques can be used.

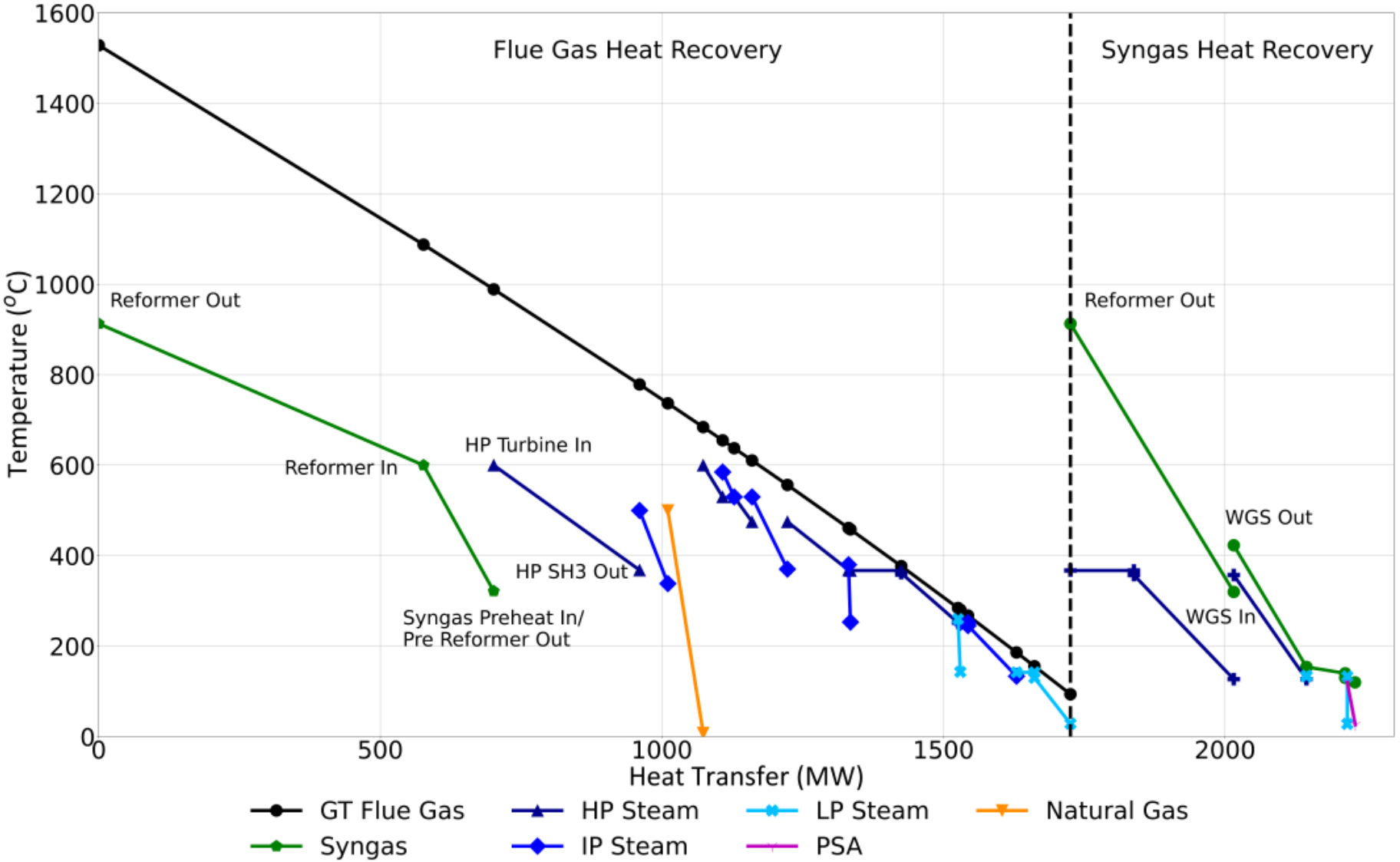


Figure 13: Combined Fuel & Power plant at 100% fossil CO_2 capture. Heat transfer diagram demonstrating heat recovery from the sequentially combusted GT flue gases and hot syngas leaving the reformer.

5.5.3 Exergy analysis

A detailed exergetic analysis is completed for the counterfactual and CFP plants to identify areas of high exergy destruction and aid in the design of the CFP process. Figure 14 demonstrates the quantity and location of the exergetic efficiency gains realised.

The primary location of improvement is in the combustion system downstream of the GT, which serves as the SMR burners. Due to the high flue gas flow rate these burners operate at a lower adiabatic flame temperature than traditional SMRs resulting in less exergy destruction. The lower flame temperature also facilitates a reduction in pinch temperatures between the reformer model and the flue gas, allowing a modest reduction in exergy destruction. Further improvements were realised through the optimised heat recovery system in the flue gas and syngas streams, minimising pinch temperatures and prioritising HP steam generation where possible. Lower flue gas temperatures leaving the heat recovery system aided efficiency gains while the reduced energy requirement of the CO_2 capture plant was the final process improvement realised.

Any increased rates of exergy destruction were seen primarily as a result of the higher demand on the turbo machinery (i.e., steam turbines) and increased absolute auxiliary loads.

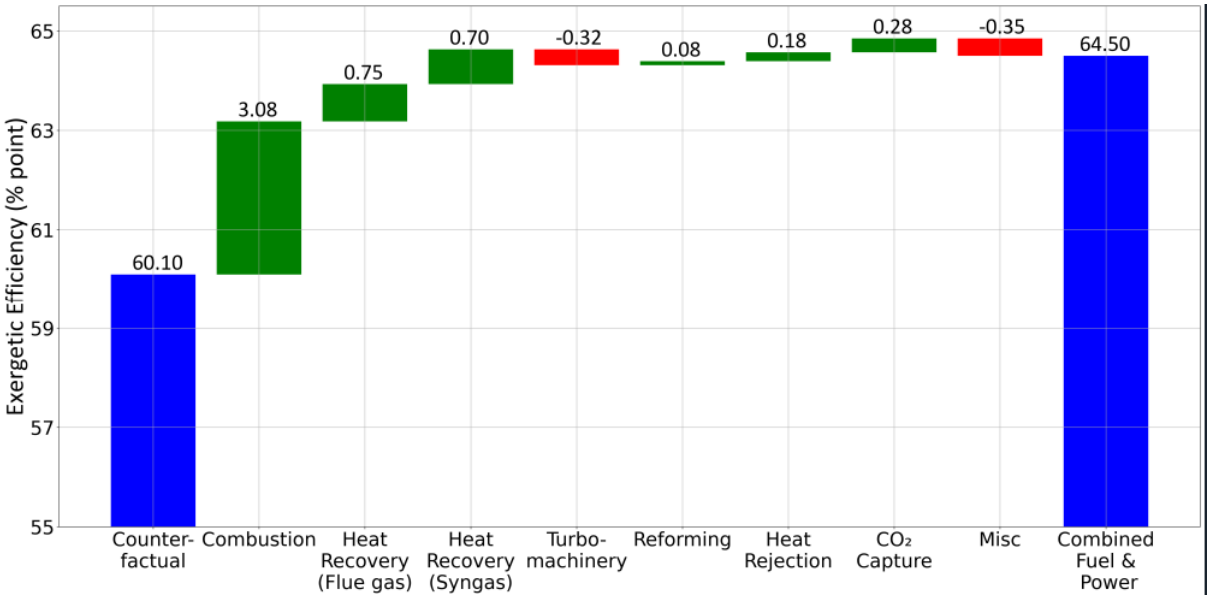


Figure 14: Exergetic efficiency gains in Combined Fuel & Power process compared to the Counterfactual

5.5.4 Technoeconomic analysis

A detailed technoeconomic analysis as described in Section 5.4.6 has been completed and presented in Table 5.

A 15.1 - 17.3% decrease in total plant CAPEX is predicted as a result of the reduced flue gas flow rate while increases in efficiency leads to a net reduction in plant OPEX of 7.6 – 8.0%. By assuming that the CFP operates in the same energy market as CCGTs and SRMs and therefore has an average product sale price equivalent to the LCOE and LOCH electricity and hydrogen respectively. The residual NPV of the CFP plant is M£1,621 and 1,763 for the 95% gross CO_2 capture and 100% fossil CO_2 capture cases respectively at the assumed hurdle rate for similar energy projects (David Menmuir *et al.*, 2022). When this NPV is incorporated into the technoeconomic analysis (i.e. is set to zero) it results in a predicted IRR of 12.9 and 13.2% for the CFP plant, a 5.1 and 5.4% increase over the counterfactual (7.8%).

Table 5: Technoeconomic analysis. Levelised Cost of Hydrogen and Power from Mullen et. al. Net present value of the combined fuel and power plant set to zero and resultant increase in internal rate of return reported.

CO_2 capture case		**100% (Fossil)**			**95% (Gross)**		
Parameter	*Unit*	Base	CFP	Δ	Base	CFP	Δ
CAPEX	M£	4002	3309	-17.3%	3785	3211	-15.1%
OPEX	M£/pa	353	325	-8.0%	342	316	-7.6%
IRR	%	7.8	13.2	+5.4 % point	7.8	12.9	+5.1% point

5.6 Conclusion

A novel thermal integration configuration for the co-generation of low to zero-carbon hydrogen and power in a single combined fuel and power (CFP) plant with post combustion capture (PCC) operating at two distinct CO_2 capture fractions is investigated:

- 95% gross, considered the minimum permittable in the UK
- 100% fossil, wherein the CO_2 generated in the plant is equal to the quantity of CO_2 captured

The concept of co-generation of hydrogen and power has been previously suggested by Herraiz et al. (Herraiz *et al.*, 2020), placing the traditional hydrogen reforming process directly into the flue gas path downstream of sequential burners that re-fire the O_2 rich flue gas exiting the gas turbine exhaust. However, the degree of integration between the two processes was minimal, leading to inefficiencies. In this work, the authors propose a redesigned heat flue gas and syngas recovery system that minimizes exergy destruction in the system by optimizing pinch temperatures and prioritizing HP steam production, fully merging both the CCGT and SMR processes. This redesigned process is predicted to increase the thermal efficiency of the plant relative to the counterfactual i.e., an independent CCGT and SMR, by 2.6% points and an estimated 1.9% points when compared to Herraiz et al.

When PCC is employed, flue gas volumes to the CO_2 capture plant are reduced in the CFP by 36 - 37%, relative to the counterfactual. This is the result of all viable O_2 in the incoming combustion air being consumed in the combustion process, thereby avoiding the treatment of excess N_2 as is typical for CCGTs. Concurrent to the reduction flue gas flow rate, the increase in net CO_2 concentration to be treated in the CO_2 capture plant (9.9 to 14.4 % vol (wet)) is estimated to reduce the specific reboiler duty by 5.5% This, along with the increased thermal efficiency of the CFP process increases the 2nd law thermal efficiency by 3.8 - 4.4% points over the counterfactual.

In addition to the novel integration design, this manuscript quantifies, for the first time, the cost reduction potential of the CFP configuration through a rigorous technoeconomic analysis, an essential advancement over the previous work but Herraiz et al. The reduction in flue gas flow rate and increase in thermal efficiency is predicted to result in a 15 - 17% decrease in total plant CAPEX and 7.6 - 8.0% reduction in plant OPEX for a 95% gross and 100% fossil CO_2 capture fraction respectively. By assuming that the CFP plant operates in the same energy market as CCGTs and SMRs these CAPEX and OPEX reductions are predicted to translate

to a 5.1 and 5.4% increase in the predicted internal rate of return over the counterfactual, representing a substantial increase in profitability.

Implicit in this assumption is that the CFP configuration can respond to the same market dynamics as independently operating CCGT and SMR processes. Although this has not been investigated in detail as part of this work there is no identified technical barriers to operating within the typical turndown ratios of a CCGT (~40%). However, process and permissible ramp rates on the SMR equipment may limit the rate at which this can occur. Likewise, conflicting market demands may negatively impact the profitability of this process, for example should the demand for hydrogen be high at times of low power prices. Further work should seek to investigate what impact a dynamic market and process limitations has on the profitability of the proposed CFP configuration.

Nevertheless, from the presented work it is clear that the described CFP process can present a large opportunity for cost reductions in the production of low to zero carbon power and hydrogen by utilising opportunistic synergies arising from the deployment of CCS in large industrial clusters.

5.7 Limitations and Future Work

The following limitations were identified for the work described in this chapter; any future work should endeavour to resolve these limitations:

- Although all of the components required to construct a CFP plant as described in this manuscript are expected to be commercially available, detailed engineering is required to confirm the viability and cost of the design presented.
- A redesign of the reformer modules and refractory is likely to be required to account for the reduced operational temperatures and increase flue gas flow present in the CFP scheme.
- The scope of this study is limited to base load operations. However, dispatchable power generation is likely to require frequent and daily load changes while hydrogen production is expected to vary considerably on a seasonal basis. Further studies should investigate dynamic operations of the CFP configuration to establish the capacity to vary the production rate of each energy vector to match market demands.

6. Monoethanolamine (MEA) degradation rates in post-combustion capture plants with 100% fossil CO_2 capture

Chapters 3, 4 and 5 of this thesis investigate the process modifications required to efficiently capture 100% of the CO_2 generated in power production via combined cycle gas turbines (CCGT) and hydrogen production via steam methane reformers (SMR). It is consistently demonstrated that three distinct but moderate design modifications are required to efficiently achieve this:

- **A minimum of 16 – 20m of absorber packing and up to 24m:** Exact value is dependent on the CO_2 concentration in the flue gas and lean loading utilised however this represents an increase of typically circa 4m over "standard designs". This increases the residence time of the solvent with the flue gas to be treated, ensuring sufficient absorption of CO_2 even at very low partial pressures.
- **Reduced lean solvent loadings:** Reducing lean loadings from 0.20 – 0.25 mol/mol to circa 0.10 – 0.16 mol/mol, in conjunction with any increased packing height, further ensures that driving force of absorption in the upper portions of the absorber is maintained.
- **Increase Regeneration Pressures:** To efficiently achieve the required decrease in lean loading an increase in the operating pressure of the desorber will be required (210 – 275KPa vs 170 – 190KPa), with an associated and unavoidable increase in reboiler temperatures (125 - 135°C vs 115 – 125°C).

The above process modifications are shown to effectively limit the increase in energy penalty required to achieve very high rates of CO_2 removal (+99%) and, although moderate in nature, represent unexplored process conditions that may result in a change in the observed solvent degradation rate. This is because monoethanolamine (MEA) will degrade when exposed to oxygen-rich atmospheres (oxidative degradation), therefore increased exposure time in the absorber is thought to increase this, and at high temperatures (thermal degradation) as the carbamate in the solvent polymerises, however the decreased carbamate concentration in lean solvent solutions may limit the effect somewhat despite the increase in regeneration temperature.

This work takes three energy conversion processes, a CCGT, SMR ((Mullen *et al.*, 2023; Mullen and Lucquiaud, 2024) and an energy from waste facility (EfW) (Su *et al.*, 2023) operating at 95% CO_2 capture as the counterfactual and the CO_2 capture fraction required to

achieve 100% fossil CO_2 capture (99.2, 99.8 & 99.7% respectively). A new MEA degradation framework developed by the co-authors (Braakhuis, Høisæter and Knuutila, 2022; Braakhuis and Knuutila, 2023) is applied to quantify the effect increasing CO_2 capture fractions is predicted to have on specific MEA degradation rates.

I&EC research
Industrial & Engineering Chemistry Research

Open Access
This article is licensed under CC-BY 4.0

pubs.acs.org/IECR
Article

Monoethanolamine Degradation Rates in Post-combustion CO_2 Capture Plants with the Capture of 100% of the Added CO_2

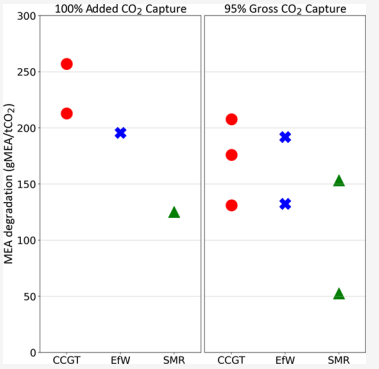
Daniel Mullen,* Lucas Braakhuis, Hanna Katariina Knuutila, Jon Gibbins, and Mathieu Lucquiaud

Cite This: *Ind. Eng. Chem. Res.* 2024, 63, 13677−13691

Read Online

ACCESS | Metrics & More | Article Recommendations | Supporting Information

ABSTRACT: Residual emissions from post-combustion CO_2 capture plants must be reduced to zero or recaptured from the atmosphere to be compatible with long-term climate change goals. For amine-based CO_2 capture, increasing CO_2 capture fractions requires maintaining sufficient driving force of absorption at the top of the absorber column by reducing lean solvent loadings. To produce low lean loadings without excessively increasing the specific thermal energy input, increased operational pressures are required in the CO_2 stripper, inevitably leading to higher temperatures, which may increase the specific thermal degradation rate of the solvent. Concurrently, for solvents that react rapidly with dissolved O_2, increased residence time in the absorber due to the increased packing heights also associated with high capture fractions may increase the specific oxidative degradation rate as the direct contact with O_2 in the flue gas is extended. Through process modeling and the application of a newly developed monoethanolamine (MEA) degradation framework, we investigate the effect on solvent degradation rates of increasing CO_2 capture rates up to those that result in no net CO_2 addition to the atmosphere. We do this for three key energy-producing processes: a combined cycle gas turbine, an energy from waste facility, and a steam methane reformer. In a first-of-a-kind study, we demonstrate that for a 35 wt % MEA-based solvent under steady-state conditions, solvent degradation is predicted to increase by 24−138% as a result of decreasing lean loadings and increased absorber residence time (process modifications that are thought to be beneficial when increasing CO_2 capture fractions) from 53 to 208 gMEA/tCO_2 when a 95% CO_2 gross capture fraction is achieved to 125−257 gMEA/tCO_2 when 99.2−99.8% is achieved (i.e., when 100% of the added CO_2 is captured). Further analysis provides evidence that process modifications, such as intercooling of the absorber column and reduced stripper sump residence times, may be useful in reducing the rates of solvent degradation, providing critical insights to future test campaigns and project developments. However, limitations of this study remain; the degradation framework provides the instantaneous predicted MEA consumption rate of the system at a point in time and does not consider the catalytic effects that many impurities present in an operation plant will have on the reactions, potentially impacting degradation rates. Nonetheless, this serves as the first step toward understanding the effect of increasing CO_2 capture fractions in post-combustion CO_2 capture plants. Long-term tests with appropriate solvent management practices are required to fully quantify solvent degradation rates when operating at 100% added CO_2 capture fractions.



Downloaded via 136.228.225.169 on August 7, 2024 at 09:48:02 (UTC).
See https://pubs.acs.org/sharingguidelines for options on how to legitimately share published articles.

1. INTRODUCTION

Global anthropogenic CO_2 equivalent (CO_2e) emissions continue to rise year on year, resulting in a predicted global surface temperature rise of 3.2 °C (2.2−3.5 °C) by 2100 if all implemented climate policy targets are reached,[1] the Sixth Assessment Report by the International Panel on Climate Change (IPCC) states that "All global modeled pathways that limit warming to 1.5°C (>50%) with no or limited overshoot, and those that limit warming to 2°C (>67%), involve rapid and deep and, in most cases, immediate greenhouse gas emissions reductions in all sectors this decade". Within the global emissions scenarios considered within the sixth assessment report, those that have a greater than 67% chance of limiting global temperature rise to less than 2 °C include between 196−280 Gt of sequestered CO_2 from fossil CO_2 alone by 2100,[2] not including atmospheric CO_2 removal via bioenergy with CCS (BECCS) or direct air CO_2 capture and storage (DACCS). The International Energy Agency's (IEA) Sustainable Development Scenario, in which global emissions from the energy sector reach net zero by 2070, includes 240 Gt CO_2 sequestered by 2070, accounting for 15% of emission reductions.[3] As of 2023, around 40 carbon capture and storage (CCS) facilities are in operation globally, capturing approximately 0.045 $GtCO_2$/pa, with an additional 50 planned to come online by 2030, capturing an additional 0.125 $GtCO_2$/pa.[4] Although ambitious, this is an order of magnitude short of the approximate 1.2 $GtCO_2$/pa capacity needed in the Sustainable Development Scenario, highlighting the wide gap

Received: April 24, 2024
Revised: July 23, 2024
Accepted: July 23, 2024
Published: July 29, 2024



ACS Publications
© 2024 The Authors. Published by American Chemical Society

https://doi.org/10.1021/acs.iecr.4c01525
Ind. Eng. Chem. Res. 2024, 63, 13677−13691

between aspirations and actions. It is clear that if CCS is to contribute significantly to global climate change mitigation efforts, a rapid increase in the deployment of CCS facilities is required.

Post-combustion capture (PCC) encompasses any technology that separates CO_2 from a gas mixture downstream of an industrial process. Typically, this is a high-volume flow rate of combustion products and possibly additional CO_2 released from process materials, e.g. limestone, at atmospheric pressure, containing mainly nitrogen, water, and oxygen, with varying quantities of CO_2 (2−25 vol %). Depending on the process, the flue gas to be treated may contain trace impurities to varying degrees, including CO, NO_x, SO_x, volatile organic compounds (VOCs) and ammonia (NH_3), to name a few. Potential applications for PCC deployment cover all facets of the industrial decarbonization landscape, from the energy sector by decarbonizing critical dispatchable power infrastructure such as combined cycle gas turbines (CCGT) and coal-fired power plants and decarbonizing home heating and transport with blue hydrogen production to raw material production such as cement, glass and metal. Additional cross-industry applications lie in waste and biogenic fuel combustion, contributing to energy production, waste management, raw material recovery and negative emissions. Numerous technologies are under consideration for large-scale post-combustion capture, including solid adsorption, CO_2 selective membranes, and cryogenic separation; however, the most technologically and commercially mature and the focus of this article is amine-based CO_2 capture.

Amine-based post-combustion CO_2 capture functions on the principle that amine groups will bond with acid gases, such as CO_2, to form a carbamate or bicarbamate compound in a temperature-reversible reaction and, as such, can be used to separate acid gases from a dilute gas stream in a two-step absorption and desorption thermal swing process. Absorption typically occurs in a packed bed absorber column at close to atmospheric conditions. Within this column, the flue gas contacts in a counter-current fashion with descending CO_2 lean liquid solvent, transferring CO_2 in the gas phase to the amine solution as it travels up through the column. For a given liquid-to-gas ratio, the residence time of the liquid solvent in the packed bed absorber column, and so also the duration of exposure of the liquid solvent to the gases, in particular CO_2, O_2, NO_x and combustion impurities, contained in the flue gas, is proportional to the packing height.

CO_2 lean flue gas leaves the top of the absorber column after emission control techniques to minimize unwanted carryover of amine and amine-derived products, while CO_2-rich liquid solvent leaves the bottom of the column for regeneration. Regeneration occurs in a separate pressurized stripper packed bed column; CO_2-rich solvent descends through the stripper and condenses steam, which has been generated at the bottom of the column. As the steam condenses, it heats the rich solvent and reverses the carbamate/bicarbamate forming reaction, liberating CO_2. Mostly, CO_2 lean solvent exits the stripper packing and passes through a reboiler, where a thermal energy source heats the solvent, further liberating CO_2 and generating the stripping steam. The highest temperature in the post-combustion capture process occurs in the reboiler. CO_2/H_2O vapor leaves the top of the stripper column for drying, conditioning and compression for export while the now CO_2 lean solvent is returned to the absorber. At all stages the steam also provides a stripping function, by reducing the partial pressure of the CO_2; the ratio of CO_2 to H_2O vapor at equilibrium with the solvent depends on total pressure, solvent loading and temperature.

Amine CO_2 capture solvents are ammonia (NH_3) derivatives where a substituent, such as an alkyl or aryl group, has replaced one or more hydrogen atoms. They can be broadly characterized into primary (with monoethanolamine (MEA) being the most widely known example for CCS applications), secondary and tertiary amines, representing how many hydrogen atoms have been substituted for alkyl or aryl groups. Due to its reactivity, low cost and ease of reclamation, MEA continues to serve as a viable solution for CO_2 capture from low-concentration CO_2 flue gases. Stainless steel construction or corrosion inhibitors for carbon steel constructions can mitigate the corrosion concerns present for higher concentration solutions, while advanced configurations and control processes continually improve thermodynamic efficiency, particularly at high CO_2 capture fractions.

Historically, CO_2 capture fractions, defined as the mass of CO_2 exported divided by the mass of CO_2 entering the absorber, of 90% were targeted. However, in recent years, net-zero commitments have challenged this assumption's viability, as 10% residual emissions from PCC is clearly incompatible with these goals unless some form of permanent negative CO_2 emission technology is concurrently employed to recapture the residual emissions. The economically optimal CO_2 capture fraction will be the point at which the marginal cost of increasing the CO_2 capture fraction is more than the lowest cost permanent negative CO_2 emission technology that is available to recapture and permanently store the emitted CO_2 (a point that will change as both technologies are deployed at scale). In the absence of a definitive economic optimum, the CO_2 capture fraction that results in no net addition of CO_2 to the atmosphere is considered for this work. This CO_2 capture fraction is dependent on the ratio of atmospheric CO_2 entering the boundary of the facility with atmospheric air (typically used for combustion) and the added CO_2 generated by that combustion or other processes within the facility, and, as such, varies from application to application (see eq 1). However, it typically falls between 99.2% for a CCGT up to 99.8% for a steam methane reformer (SMR). Mullen et al.[5,6] term this CO_2 capture fraction as 100% fossil CO_2 capture; however, 100% added CO_2 will be used in this article to account for biogenic CO_2. This terminology will be adopted throughout this article, while capture fractions below this will be reported as gross CO_2 capture fractions, as is typical for the industry.

$$\text{Fossil } CO_2 \text{ capture fraction} = \frac{m_{CO_2,T\&S}}{m_{CO_2,produced} - m_{CO_2,atmospheric}} (\%) \quad (1)$$

where $m_{CO_2,T\&S}$ is the mass of CO_2 exported to transport and storage, $m_{CO_2,produced}$ is the mass of CO_2 produced during the process, and $m_{CO_2,atmospheric}$ is the mass of atmospheric CO_2 entering the process.

Increasingly, CO_2 capture fractions above 95% up to, or slightly above, 100% added CO_2 capture is the focus of emerging research. Mullen and Lucquiaud[5] provide a detailed analysis of the currently available literature, critically assessing seven modeling studies[6−12] and six pilot plant facilities[13−18] where CO_2 capture fractions over 95% were achieved. The authors identify lean loading as the critical factor to ensure thermodynamically efficient operation at increased CO_2

https://doi.org/10.1021/acs.iecr.4c01525
Ind. Eng. Chem. Res. 2024, 63, 13677−13691

capture fractions. Lean loading must be sufficiently low to provide a strong driving force of absorption at the top of the absorber despite decreased CO_2 concentrations, a consideration typically absent or insufficiently considered in the current literature. As well as increasing the absorption rate throughout the absorber, low lean loadings facilitate increased cyclic capacity of the solvent (CO_2 absorbed per unit of solvent), minimizing the quantity of water to be moved through the system and maximizing rich loading. These factors will contribute to a decreased energy requirement for solvent regeneration. Where the importance of low lean loadings was recognized, solvent regeneration to the loadings required is typically mismanaged. Michailos and Gibbins[12] describe what has been termed the stripper "inflection point". They present a modeling study using a 35 wt %. MEA solution on a flue gas representative of a commercial CCGT and study 95 and 99% gross CO_2 capture fractions over a range of lean loadings and absorber packing heights. They show that as lean loadings decrease under constant stripper pressure and incoming rich loading conditions, the energy requirement for regeneration per unit of CO_2 captured, known as the specific reboiler duty (SRD), increases exponentially below a low loading value that depend on the specific conditions. This phenomena has historically led to the conclusion reducing lean loadings and, by extension, increasing CO_2 capture fractions will result in exponential increases in SRDs.

However, Michailos and Gibbins showed that the inflection point can be shifted to lower lean loadings by increasing the stripper pressure, noting, though, that reboiler temperatures will increase proportionately as a result. This change in inflection point loading arises because the rapid increase in SRD corresponds to the point where the water vapor to CO_2 ratio in the reboiler rises to a level at which it cannot be condensed to near-equilibrium partial pressure and temperature with the incoming rich solvent at the top of the stripper column. This leads to increasing levels of water vapor in the CO_2 at the top of the column, representing a significant heat loss. An increase in stripper pressure shifts the vapor liquid equilibrium (VLE) in the reboiler toward lower water vapor/CO_2 ratios for a given lean loading, at the expense of higher reboiler temperatures.

Mullen et al.[5,6] build upon the work of Michailos and Gibbins by completing an in-depth techno-economic assessment on 100% added CO_2 capture for both an SMR and a CCGT using a 35 wt %. MEA solution. They find that, although the thermal efficiency of the process decreases and the cost of the product increases relative to achieving 95% CO_2 capture fractions, the effect is modest and is primarily due to the increase in the absolute quantity of CO_2 captured rather than any nonlinearity in the specific cost to capture CO_2 as the CO_2 capture fraction increases.

The authors further conclude that, for the assumed conditions of this study, unless the cost of negative emission technologies with permanent CO_2 storage falls below 184 £/tCO_2, increasing CO_2 capture fractions to 100% of the added CO_2 is the most economical method of fully decarbonizing a CCGT. Mullen et al. also show that the CO_2 intensity of the counterfactual to hydrogen combustion, i.e. natural gas combustion, means that the cost of CO_2 avoided falls as the CO_2 capture fraction increases for the SMR process considered, despite the increase in product cost. Mullen et al. suggest two design changes to achieve 100% added CO_2 capture: increased reboiler operating pressures and, by extension, temperatures, which facilitate efficient solvent regeneration for low lean loadings, and, in the CCGT case, a moderately increased absorber packing height, from 20 to 24 m, to increase the mass transfer area. Although moderate from a process and technological perspective, these two design changes will expose the solvent to previously largely unexplored process conditions, with higher regeneration temperatures, lower lean loadings and increased duration of exposure to the oxygen content of the flue gas. Each of these process modifications may lead to an increase in specific solvent degradation rates. Mullen et al. note that this is a knowledge gap and assumes an MEA replacement rate of 2 kg/tCO_2, quoting experience from MEA-based pilot plant studies, which report a range of 0.17−1.5 kg/tCO_2.[14,19−23] This article uses emerging models[24,25] developed by Braakhuis and Knuutila, two coauthors, to shed light on the effect on MEA degradation rates of the process conditions thought to be thermodynamically beneficial when operating at 100% added CO_2 capture.

MEA will degrade when exposed to oxygen-rich atmospheres (oxidative degradation)[26] or high temperatures (thermal degradation).[27] Unless effectively controlled, solvent degradation products in the circulating solvent can reduce CO_2 capture performance, increase atmospheric emissions and operational costs and accelerate equipment corrosion.[28] Degradation causes a loss of solvent directly while further solvent losses may occur as part of solvent reclaiming, which is required for sustained operation to remove all degradation products at the rate they are formed and maintain constant solvent health.

One of the main degradation mechanisms for MEA is carbamate polymerization, often referred to as thermal degradation. This mostly occurs at elevated temperatures within the CO_2 capture process, most notably within the stripper sump and reboiler, where temperatures often exceed 120 °C for extended periods. It also occurs when the solvent is descending through the stripper packing and during preheating of the solvent, albeit for relatively short periods and at lower temperatures than the reboiler. When the carbamate, formed when CO_2 reacts with MEA, is subjected to increased temperatures ring closure and dehydration occur to form 2-oxazolidinone (OZD). OZD is sensitive to nucleophilic attacks and reacts with MEA, forming dimers, oligomers, imidazolidinones, and other cyclic compounds. The cyclization of the carbamate leading to the formation of OZD is the rate-limiting reaction. This rate was found to be dependent on both temperature and CO_2 loading. Higher CO_2 loadings have been shown to increase degradation rates, possibly by forming more of the carbamate or increasing the availability of proton donors, which can catalyze dehydration. A detailed review of thermal degradation methods is available in Braakhuis et al.[24]

Oxidative degradation of an amine is a two-step process involving the dissolution of O_2 from the flue gas into the solvent, followed by a liquid phase reaction between the dissolved O_2 and the amine. The observed amine degradation rate is thus a function of O_2 solubility, mass transfer resistances, and kinetic reaction parameters. Process parameters, such as temperature, O_2 partial pressure, amine concentration, and CO_2 loading, influence each of these mechanisms. A detailed review of oxidative degradation methods is available in Braakhuis and Knuutila.[25] Braakhuis et al. define two categories of oxidative degradation: direct and indirect. Direct oxidative degradation occurs within the absorber where the solvent is in direct contact with the flue

https://doi.org/10.1021/acs.iecr.4c01525
Ind. Eng. Chem. Res. 2024, 63, 13677−13691

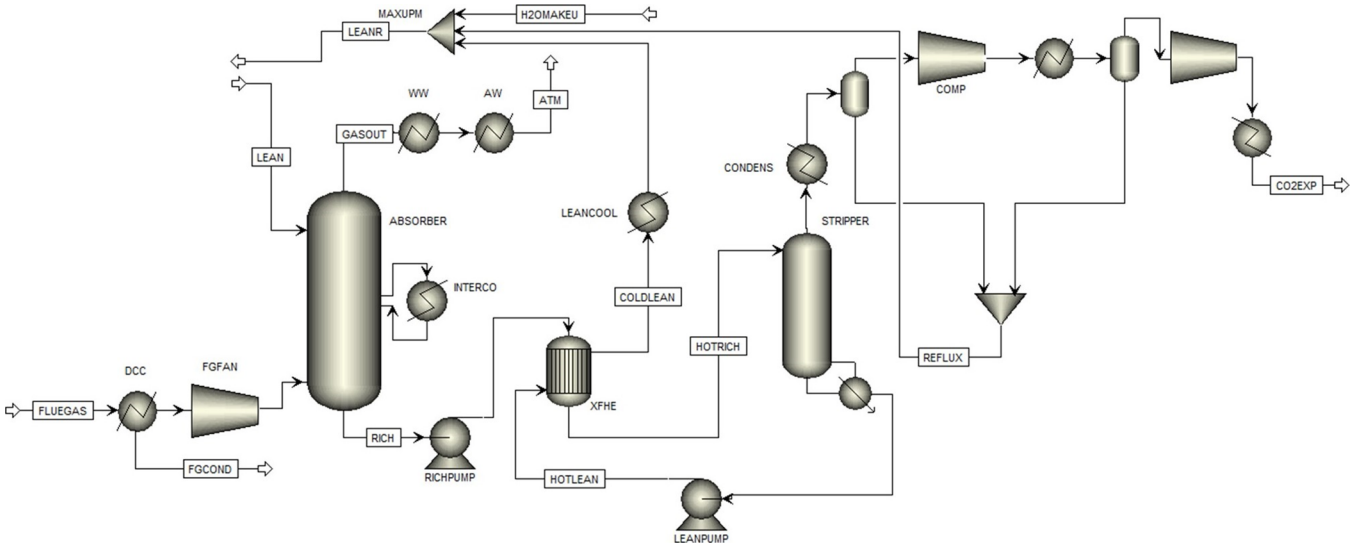


Figure 1. ASPEN PLUS process model.

gas, and the quantity of dissolved oxygen is replaced while consumed. The magnitude of this effect is a function of the rate of mass transfer of O_2 from the gas phase to the liquid phase and is expected to vary depending on the location within the absorber as the bulk temperature and the solvent loading change. Indirect degradation happens downstream of the absorber, where no further contact with an oxygen-rich flue gas occurs; in this case, the degree of oxidative degradation is limited to the quantity of dissolved oxygen in the solvent when no longer in contact with the flue gas. This can be mitigated with process modifications that reduce the quantity of dissolved O_2 that is carried over to the absorber sump, for example, flashing or N_2 sparging of rich solvent.

The process considerations proposed by Mullen et al. for 100% added CO_2 capture might be expected to adversely affect the degree of MEA degradation within post-combustion CO_2 capture plants. Higher reboiler temperatures will obviously increase the degree of thermal degradation, all other things being equal. However, the associated reduced loading (i.e., carbamate concentration) in the reboiler may somewhat mitigate this. Concurrently, a reduced average loading in the absorber may increase the solubility of O_2 overall and lead to increased oxidative degradation. Additional packing, the inclusion or absence of intercooling, and liquid-to-gas ratios will also all contribute to the uncertainty surrounding MEA degradation rates at 100% added CO_2 capture fractions.

This work applies the oxidative (Braakhuis and Knuutila[25]) and thermal degradation (Braakhuis et al.[24]) models for an MEA solvent with process modeling completed by Mullen et al.[5,6] to compare the specific quantity of MEA degradation for three industrial flue gas sources (CCGT, EfW and SMR processes) at two distinct CO_2 capture fractions (95% gross CO_2 capture and 100% added CO_2 capture), with the inclusion or not of intercooling serving as a third variable. For the first time, we quantify the expected additional solvent degradation rate when operating at a 100% added CO_2 capture fraction, facilitating an assessment of the resulting impact on process economics. It is important to note that the operational conditions proposed for 100% added CO_2 capture operation would also provide a reduced energy penalty for lower CO_2 capture fraction operation should the resulting solvent degradation rates be deemed economically acceptable. Likewise, if solvent degradation is more critical to a project than thermal efficiency, lean loadings sufficient to achieve high CO_2 capture fractions can be achieved at lower temperature regeneration conditions. Advance process configurations such as "pump-around" intercooling in the absorber, as opposed to the "in-and-out" scheme used in this study, may aid in increasing CO_2 capture rates while using higher lean loading than those considered in this study. This has been proposed in a modeling study by Gao,[29] where 99% CO_2 capture was achieved using a 30 wt % MEA solution at a lean loading of 0.2 mol/mol and two pump-around intercooling loops.

The goal of the inclusion of intercooling in this study was to investigate the effect of reduced absorber temperatures on oxidative degradation, which can be achieved with in-and-out intercooling. Therefore, this configuration has not been included in this work to limit the number of cases presented; however, it would be expected to result in a reduction in thermal degradation proportionate to the reduction in regeneration temperatures. This should be considered in conjunction with any change in CAPEX or SRD due to increased absorber heights, additional intercooling loops or changes in solvent properties.

This work aims to compare the solvent degradation rates at proposed design points for the considered CO_2 capture fractions that the authors consider to be valid and viable, acknowledging that such design points are project-specific and do not represent an absolute economic optimum, as no such point can exist except for specific project conditions.

1.1. Limitations of the Study. This study serves as a first step toward quantifying the effect of achieving 100% added CO_2 capture in post-combustion CO_2 capture plants using an MEA solvent solution. However, limitations of this study remain; the degradation framework provides only the instantaneous predicted MEA consumption rate of the system at a point in time. As such, it does not consider the effect of cumulative production of degradation compounds within the solvent as the operation continues over an extended period and their concentrations balance with removals by reclaiming; degradation compounds within the solvent may catalyze MEA degradation and thus accelerate the reaction. Additionally, although thermal and oxidative degradation mechanisms are considered in the framework, they are considered independent,

https://doi.org/10.1021/acs.iecr.4c01525
Ind. Eng. Chem. Res. 2024, 63, 13677−13691

Table 1. CO_2 Capture Case

process	CO_2[a] (vol %)	O_2[a] (vol %)	flow[a] rate (kg/s)	case	lean loading (mol/mol)	CO_2 capture (%[b])	intercooler (#)	absorber packing (m)	stripper packing (m)	stripper pressure (KPa)
CCGT	4.7	11.0	792	0.1 CCGT	0.1	99.2	0	24	20	275
				0.1 CCGT IC	0.1	99.2	1	24	20	275
				0.2 CCGT	0.2	95	0	20	20	149
				0.2 CCGT IC	0.2	95	1	20	20	149
				0.1 CCGT 95	0.1	95	0	24	20	275
EfW	11.1	6.7	31	0.1 EfW IC	0.1	99.7	1	20	20	275
				0.2 EfW	0.2	95	0	20	20	149
				0.2 EfW IC	0.2	95	1	20	20	149
SMR	19.5	1.2	275	0.1 SMR IC	0.1	99.8	2	20	20	275
				0.2 SMR	0.2	95	0	20	20	149
				0.2 SMR IC	0.2	95	2	20	20	149

[a]Saturated at 40 °C. [b]Gross CO_2 capture fraction.

and no interactions between the respective degradation compounds are accounted for. Finally, this study does not consider the catalytic effect of corrosion compounds on solvent degradation due to the complexity of the reaction mechanisms and the limited experimental data; these will also rise until balanced by removals in reclaiming. Considering the limitations highlighted above, the results presented in this article should be considered predictive only for a perfectly clean solvent. Over an extended period of operation, actual MEA degradation rates are expected to diverge from those predicted by the framework, likely trending toward increasing degradation, unless contaminants within the solvent are maintained at a very low level through a high rate of solvent reclaiming.

Additionally, the cases presented here are not intended to represent an optimum for CO_2 capture fraction, thermodynamic performance or solvent degradation but merely to demonstrate the effect process parameters can have on each of the above. Case-by-case optimization will be required on a project basis. However, the results presented in this work can serve to advise designers on methods of reducing or controlling solvent degradation rates.

2. METHODOLOGY

2.1. Process Modeling for CO_2 Capture. The process modeling of the CO_2 capture plant (Figure 1) is conducted using an open-source MEA model funded by the US Department of Energy and developed by the Carbon Capture Simulation for Industry Impact (CCSI) in ASPEN PLUS.[30] This model is validated against pilot-scale data from the US National Carbon Capture Centre (NCCC).[31] The reader is referred to Mullen et al.[5,6] for a detailed description of the process modeling. However, the process does not notably differ from that of a traditional amine CO_2 capture plant.

Three distinct CO_2 capture applications covering a range of CO_2 flue gas concentrations have been considered for this work. A GE H-Class 1 × 1 combined cycle gas turbine (GE 9HA.01) with a rated thermal efficiency of 63.5% (LHV) serving a CCGT application, A 500 t/day of municipal solid waste (MSW) moving grate plant serving as the energy from waste (EfW) application and a 1000 MWh_{th} (HHV) steam methane reformer (SMR) for hydrogen production as the final case. Two CO_2 capture fractions were considered for each case, 95% (gross) and 100% (added), and two lean loadings of 0.1 and 0.2 mol/mol, while the inclusion or not of intercooling served as an additional variable. An additional CCGT case was considered where 95% CO_2 capture was achieved at low lean loading and increased absorber packing to illustrate the energy-saving potential of these design modifications irrespective of CO_2 capture fractions. This leads to a total of 11 cases assessed in this work (see Table 1). A 35 wt %. MEA solution was used in all cases. Flue gas compositions and flow rates were extracted from previously completed works by Mullen et al.[5,6] and Su et al.[11]

For each of the cases described in Table 1, the stripper pressure is modified to ensure that the inflection point described in Michailos and Gibbins[12] is not passed. This leads to variable stripper operational pressures and, by extension, solvent regeneration temperature. Stripper packing was maintained at 20 m for all cases as per Eliot,[34] however reduced packing beds, if thermodynamically acceptable, would reduce residence times and therefore thermal degradation. This is a project by project consideration.

Plated heat exchangers were assumed for all heat exchangers within the system, with holdup volume and residence time calculated using eq 2.

$$\text{Residence Time} = \frac{\text{Holdup Volume}}{\dot{V}} = \frac{Q \times \text{Surface compactness} \times \dot{V}}{k \times \text{LMTD}} \quad (2)$$

where $\dot{V}$ is the lean solvent volumetric flow rate, LMTD is the log mean temperature difference, and k is the thermal conductivity. Surface compactness is assumed to be 150 m^2/m^3 as per Zohuri,[32] while thermal conductivity values of 3894 w/m^2 K for the reboiler and 1932 w/m^2 K for the cross heat exchanger were taken from Woods.[33] The LMTD was maintained at 6 °C for the reboiler and a minimum approach temperature of 5 °C was applied for the cross HX, leading to an LMTD of ca. 7−8.5 °C in all cases. Should high residence times in these pieces of equipment be found to increase

https://doi.org/10.1021/acs.iecr.4c01525
Ind. Eng. Chem. Res. 2024, 63, 13677−13691

Table 2. Reactions and Kinetic Parameters for the Thermal Degradation Model as per Braakhuiset and Knuutila[25a]

	reaction	reaction rate [mol·m^{-3}·s^{-1}]	k_{ref} [m^3·mol^{-1}·s^{-1}]	activation energy [J/mol]
1	MEA → HEEDA + H_2O	$R_1 = k_{r,1}[MEA][CO_2]$	1.599×10^{-11}	1.511×10^5
2	MEA + HEEDA → TRIMEA	$R_2 = k_{r,2}[HEEDA][CO_2]$	1.117×10^{-10}	1.215×10^5
3	HEEDA + CO_2 → HEIA	$R_3 = k_{r,3}[HEEDA][CO_2]$	3.054×10^{-10}	1.426×10^5
4	TRIMEA + CO_2 → AEHEIA	$R_4 = k_{r,4}[TRIMEA][CO_2]$	2.839×10^{-10}	1.362×10^5
5	2 MEA → BHEU + H_2O	$R_4 = k_{r,5}[MEA][CO_2]$	5.170×10^{-13}	1.511×10^{5b}

[a]Reference temperature (T_{ref}) is 400 K). [b]Could not be determined in the original work and was assumed to be equivalent to reaction no. 1.

Table 3. Degradation Reactions, Reaction Rate Equations, and Parameters for the Oxidative Degradation Model[24a]

	reaction	reaction rate [mol·m^{-3}·s^{-1}]	k_{ref} [m^3·mol^{-1}·s^{-1}]	activation energy [J/mol]
5	MEA + $1.3O_2$ → 0.1 HSS	$R = k[MEA][O_2]^{0.469}$	6.790×10^{-7}	7.908×10^4

[a]Reference temperature for the oxidative rate coefficients is 338.15 K.

degradation excessively, this can be mitigated by increasing the LMTD at the cost of increased irreversibility in the system, however this may result in adverse effects due to higher metal skin temperatures as only bulk liquid temperatures were considered in this analysis.

Absorber and stripper sump levels were taken at 1.1 and 5 m, respectively, as per Elliot.[34] This maintains the hydraulic head to critical components similar to that of published FEED studies. This contributes to the varying residence times between cases. Should extended residence times in absorber and stripper sumps be required for operational reasons, an increase in sump level may be required. A flooding limit of 80% of the flooding value was imposed on all columns, leading to varying column diameters (see Mullen et al.[5,6] and Su et al.[11] for design parameters), and the total solvent inventory was assumed to be 150% of the summation of all equipment volumes and packing holdup. A complete list of model assumptions and equipment residence times is available in Table S1 of the Supporting Information.

2.2. Degradation Model. The kinetic degradation models for MEA used in this work have been adapted from previously developed oxidative and thermal degradation models described in Braakhuis and Knuutila[25] and Braakhuis et al.[24] The kinetic rate constants in both models are defined using the adjusted form of the Arrhenius equation shown in eq 3. The equations use a reference temperature and reaction rate coefficient at this temperature, simplifying the parameter fitting and optimization.

$$k = k_{ref} \cdot \exp\left[-\frac{E_A}{R_{id}}\left(\frac{1}{T} - \frac{1}{T_{ref}}\right)\right] \quad (3)$$

2.2.1. Thermal Degradation. The thermal degradation model for MEA describes the consumption of the solvent and the formation of intermediates and degradation products. The model is developed for 30 wt % MEA and is valid at loadings between 0.1−0.5 mol CO_2/mol MEA and temperatures up to 160 °C. This model has been extrapolated to apply to a 35 wt % solution, as similar degradation rates are expected, as reported by Høisæter et al.[35] Although no experimental data was available below 100 °C, the predicted reaction rates are insignificant at these temperatures, and the model can be extrapolated.[24] The modeled degradation reactions, reaction rate equations, and fitted parameters are given in Table 2. Braakhuis et al. note that the direct measurement of intermediate reactant in the polymerization of carbamate, 2-oxazolidinone (OZD), is challenging, with limited reliable data available. However, at loadings below 0.5 mol/mol, as is the case for the processes considered in this study, Braakhuis et al. assumed that the vast majority of CO_2 in the solution is present in the form of carbamate, and as such, the free concentration of CO_2 in the solvent could then be used as a surrogate for the concentration of OZD.

There was insufficient experimental data to effectively assess the formation of 1,3-bis(2-hydroxyethyl)urea (BHEU) at various temperatures, and it was impossible to determine this reaction's activation energy accurately. The reaction mechanisms for forming BHEU are expected to resemble those of HEEDA (reaction no. 1) closely. Therefore, Braakhuis et al. consider it reasonable to assume that the activation energies for both reactions are similar. As such, the same activation energy is applied to model the formation of BHEU.

2.2.2. Oxidative Degradation. The kinetic model for oxidative degradation of MEA has been adapted from the work by Braakhuis and Knuutila.[25] The model is developed using experimental data produced by Vevelstad et al.,[36] who used an agitated bubble reactor at temperatures between 55 and 75 °C and gas phase oxygen concentrations between 6 and 98 vol %. Liquid phase mass transfer resistances for O_2 were expected to be present in the agitated bubble reactor, especially at higher temperatures. This would reduce the availability of dissolved O_2 and limit the overall degradation rate. Therefore, mass transfer resistances have been approximated and accounted for during the development of the degradation mode.[25]

The oxygen solubility model by Buvik et al.[37] is used in this work. This novel solubility model considers the effects of temperature and concentration of ionic species in the solvent and thus accounts for reduced solubilities in CO_2-loaded solvents. Dissolved metals, such as iron and copper, have been shown to catalyze the degradation reaction significantly.[38,39] However, dissolved metals were not present during the degradation experiments used in the model development.[35] Therefore, the degradation model does not consider the catalytic effect of dissolved metals. Additionally, the experimental data set[36] utilized by Braakhuis and Knuutila is limited to experiments completed at 55−75 °C with the model extrapolated to lower temperatures, therefore increased uncertainty at lower temperatures can be expected.

The reaction rate and rate coefficients for the oxidative degradation model for MEA are shown in Table 3. The oxygen stoichiometry in the overall oxidative degradation reaction is estimated to be around 1.30 to 1.44 mol O_2/mol MEA.[40] The degradation model assumes a stoichiometry of 1.30, which

https://doi.org/10.1021/acs.iecr.4c01525
Ind. Eng. Chem. Res. 2024, 63, 13677−13691

Table 4. Process Modeling Results for the EfW and SMR Cases, 100% Added CO_2 Capture Is Unachievable without Intercooling

process	CO_2[a] (vol %)	O_2[a] (vol %)	case	lean loading (mol/mol)	CO_2 capture (%[b])	intercooler (#)	L/G (kg/kg)	SRD (GJ/tCO_2)	rich loading (mol/mol)	cycle (min)	reboiler temperature (°C)
CCGT	4.7	11.0	0.1 CCGT	0.1	99.2	0	0.89	3.67	0.441	36.7	135.6
			0.1 CCGT IC	0.1	99.2	1	0.90	3.74	0.436	36.4	135.2
			0.2 CCGT	0.2	95	0	1.24	4.04	0.440	31.1	114.9
			0.2 CCGT IC	0.2	95	1	1.25	4.09	0.438	31.0	114.7
			0.1 CCGT 95	0.1	95	0	0.78	3.42	0.473	40.0	135.7
EfW	11.1	6.7	0.1 EfW IC	0.1	99.7	1	1.72	3.63	0.451	30.8	135.5
			0.2 EfW	0.2	95	0	2.49	3.65	0.471	27.0	114.8
			0.2 EfW IC	0.2	95	1	2.49	3.67	0.471	26.1	114.6
SMR	19.5	1.2	0.1 SMR IC	0.1	99.8	2	3.31	3.64	0.454	27.6	135.2
			0.2 SMR	0.2	95	0	4.16	3.61	0.475	24.7	114.9
			0.2 SMR IC	0.2	95	2	4.44	3.85	0.457	25.6	114.7

[a]Saturated at 40 °C. [b]Gross CO_2 capture fraction.

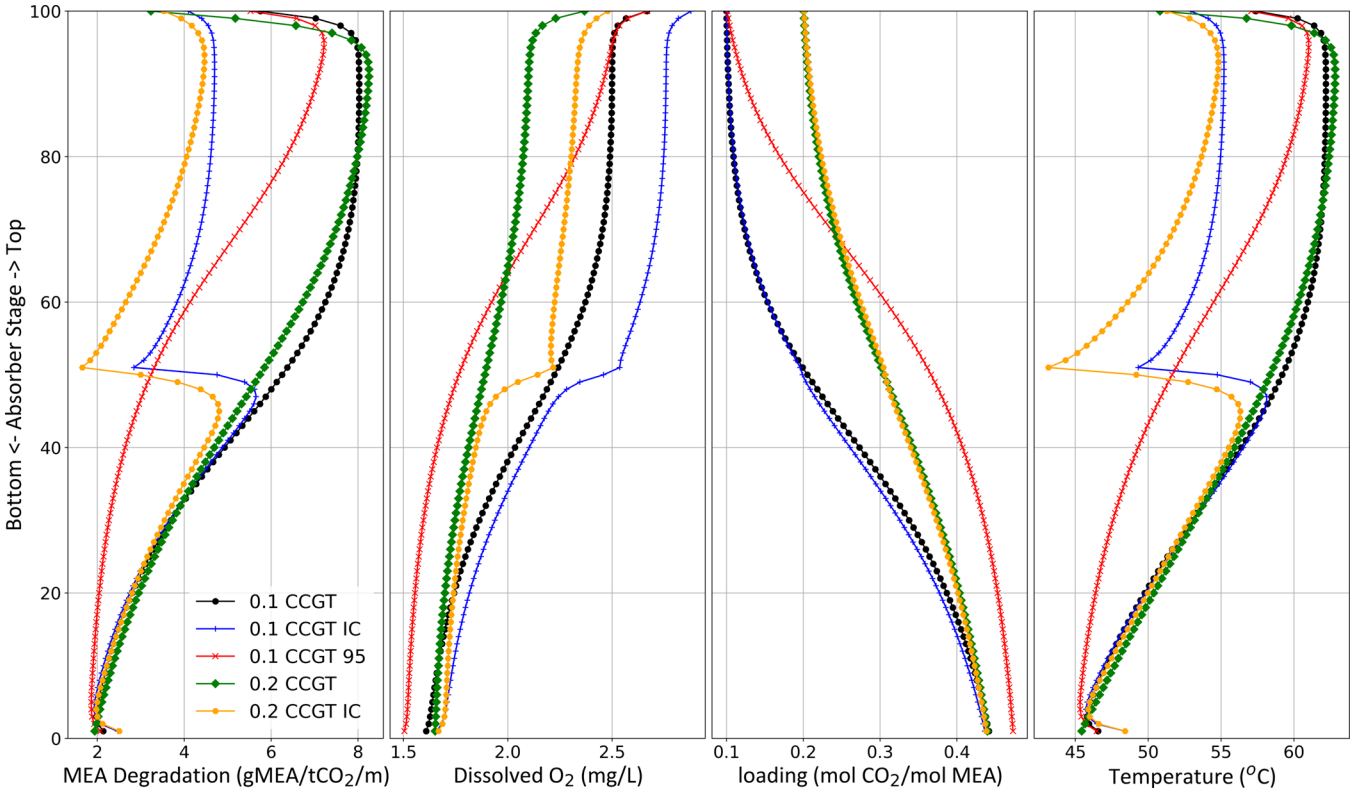


Figure 2. CCGT absorber profiles for MEA degradation rates, dissolved O_2 content in the liquid phase, and CO_2 loading of the solvent and bulk temperature.

serves as a worst-case assumption.[25] Braakhuis et al. account for the depletion of MEA and dissolved O_2 but do not predict the rates of degradation compound formation as the complex nature of oxidative degradation mechanisms makes such predictions challenging.

3. RESULTS AND DISCUSSION

3.1. Process Modeling. The outputs of the process modeling are described in Section 3.1 are detailed in Table 4. As previously described by Mullen et al.[5,6] and Su et al.,[11] when lean loading is reduced accordingly as CO_2 capture fraction increases and regeneration conditions are optimized, minimal differences in the specific energy requirements are observed, and in some cases, a reduction is seen. This is most pronounced in the CCGT case as the driving force of absorption at the top of the absorber is still moderately low, even for a 95% CO_2 capture rate at a lean loading of 0.2 mol/mol. A reduced SRD is predicted in all 95% CO_2 capture cases if lean loading is reduced below 0.2 mol/mol, as per Mullen et al. and Su et al. However, this research aims not to optimize thermal efficiency but to compare solvent degradation rates at typical operational conditions with those considered beneficial when achieving 100% added CO_2 capture. Nonetheless, an additional case was included where a 95% CO_2 capture rate was achieved for a CCGT flue gas at 0.1 mol/mol lean loading and 24 m of absorber packing. A 15.3% reduction in SRD was observed, representing a substantial energy saving at the expense of a 23.7% increase in solvent degradation rates, which

https://doi.org/10.1021/acs.iecr.4c01525
Ind. Eng. Chem. Res. 2024, 63, 13677−13691

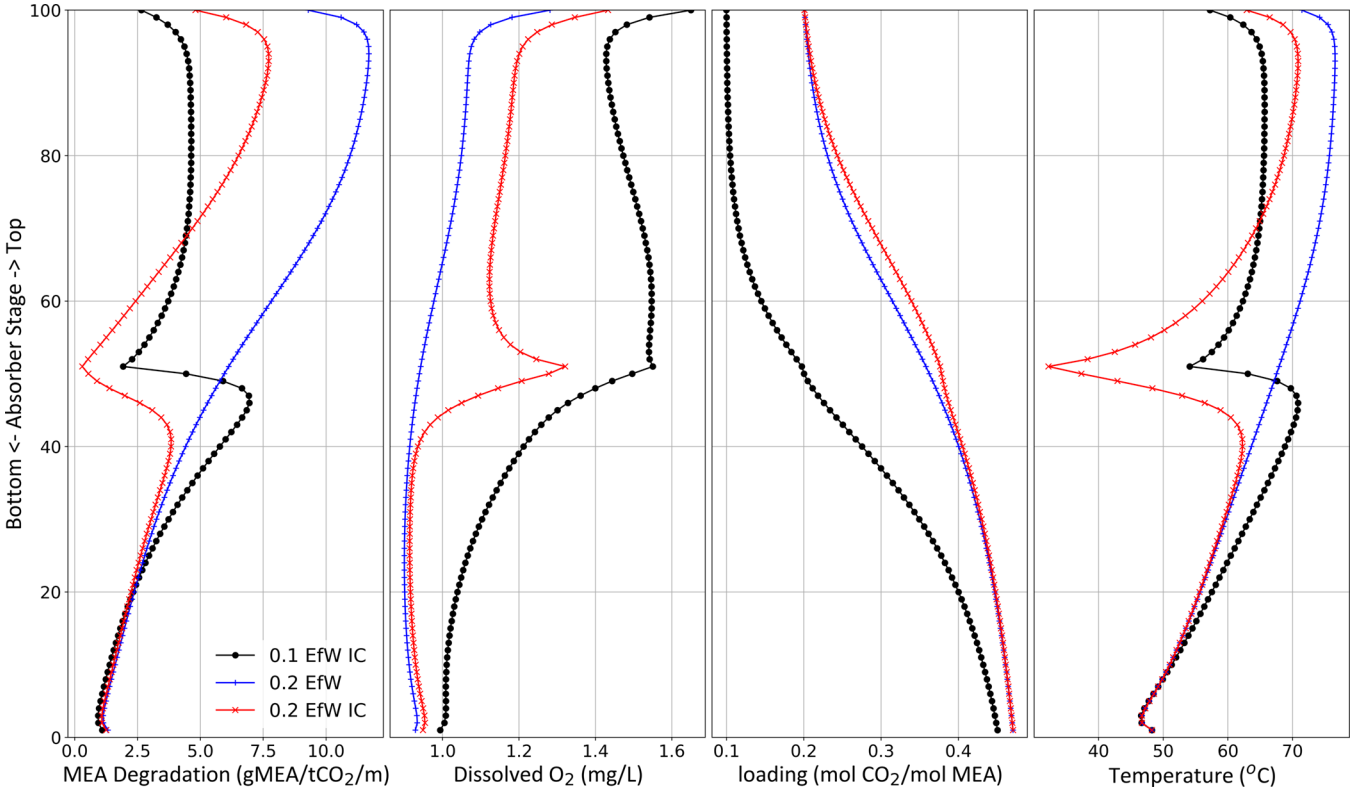


Figure 3. EfW absorber profiles for MEA degradation rates, dissolved O_2 content in the liquid phase, and CO_2 loading of the solvent and bulk temperature.

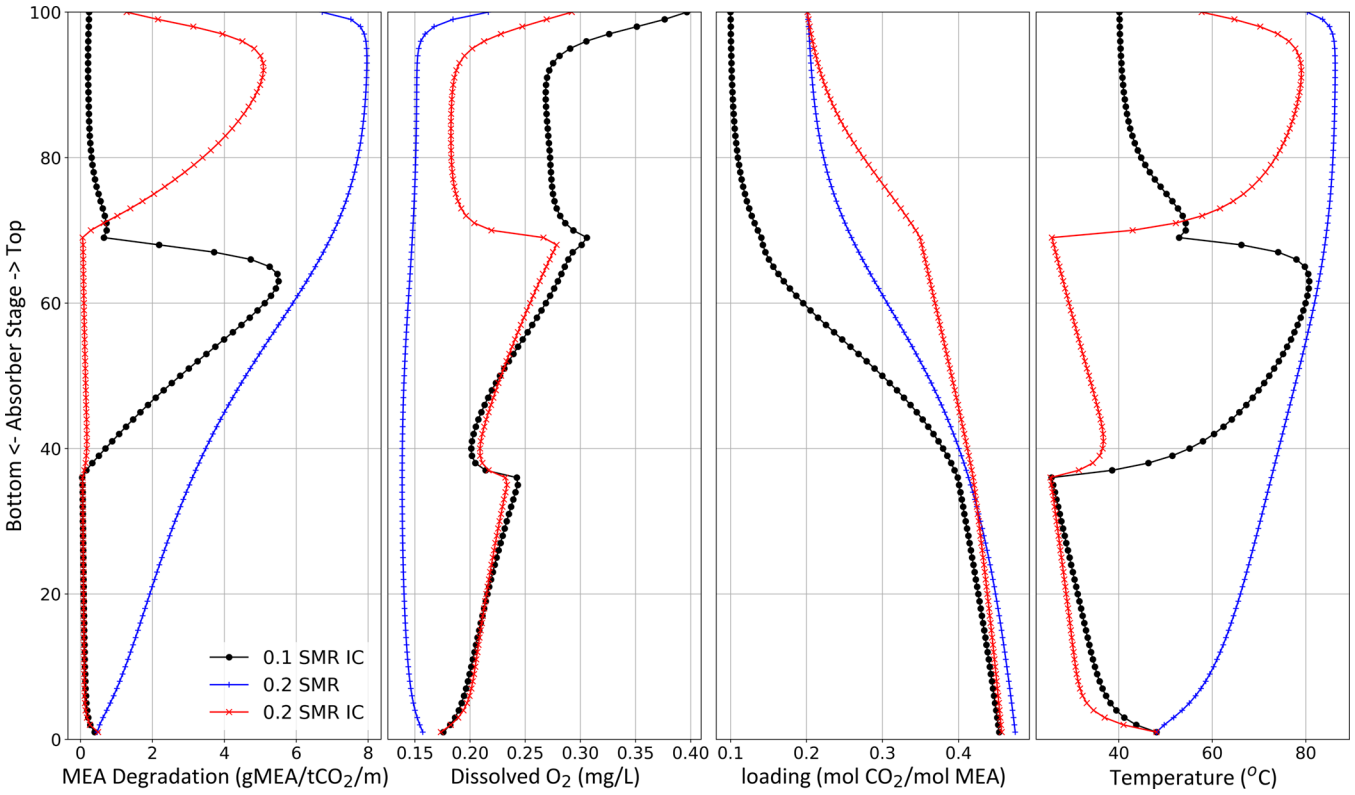


Figure 4. SMR absorber profiles for MEA degradation rates, dissolved O_2 content in the liquid phase, and CO_2 loading of the solvent and bulk temperature.

is discussed in Section 3.2, and an undetermined effect on plant CAPEX and CO_2 compressor power. This demonstrates that the energy benefits of low lean loading operation are not specific to high CO_2 capture fractions and must be a project by

https://doi.org/10.1021/acs.iecr.4c01525
Ind. Eng. Chem. Res. 2024, 63, 13677−13691

project cost optimization decision. Indeed, if solvent degradation is more critical to a project than thermal efficiency, lean loadings sufficient to achieve high CO_2 capture fractions can be achieved at lower pressure/temperature regeneration conditions.

The inclusion or otherwise of an intercooler had minimal effect on CO_2 capture in the CCGT cases. Due to the low concentration of CO_2 in the flue gas, the quantity of heat released in the exothermic reaction is not sufficient to increase the bulk gas temperature to the degree that the driving force of absorption is reduced sufficiently to necessitate intercooling. This is not the case for the EfW and SMR 100% added CO_2 capture cases. The reduced solvent flow rate (due to the reduced lean loading) coupled with the increase in CO_2 concentration in the flue gases leads to absorber pinching, where low/no mass transfer occurs. As a result, 100% added CO_2 capture is not achievable for these specific design cases without intercooling. Intercooling appears to have a minimal or negative effect on thermal efficiency for the 95% CO_2 capture cases as the driving force limiting higher temperatures is pushed to the top of the absorber; further optimization of return temperatures, intercooler location or additional packing beds may mitigate this. However, this is beyond the scope of this work. It should also be noted that, for simplicity, in the CCGT cases with 24 m meters of packing, the intercooler location was maintained at the center of the absorber. In reality, this is unlikely as it does not relate to an interbed location where the installation of intercooling would be most simple; as this case represents a 3 bed × 8 m packing absorber, an intercooler would be situated between one or both of the liquid collection/redistribution sections between each bed. Additionally, in situ absorber intercooling was assumed within the degradation framework with no residence time or hold-up volume ascribed to the intercoolers; this may result in an underestimation of the oxidative degradation rates in the intercooler cases. However, this effect is expected to be minor if residence times and intercooler return temperatures are low.

3.2. Solvent Degradation. Figures 2, 3, and 4 show the profiles of O_2 concentration and CO_2 loading of the solvent along the absorber length for each case, along with bulk temperature and the predicted oxidative MEA degradation rate. The results presented are intersection averages of each modeled absorber section (1−100). The high O_2 concentration seen at the top of the absorber occurs due to the rapid dissolution of O_2 into the liquid phase over the final section of the absorber. A lower lean loading in itself does not appear to largely affect oxidative degradation rates. This is due to the order of the degradation reaction with respect to O_2 being low at 0.47, so an increase in the concentration of dissolved O_2 will have a progressively smaller impact on the degradation rate and the subtle effect of increased solubility and unloaded MEA concentration at lower lean loadings appears eclipsed by the much more dominant effect temperature has on the reaction rate.

More critically, and an entirely novel observation, is that, by the same virtue, total MEA degradation rates within the absorber are approximately comparable over the range of flue gas O_2 concentration studied. While increasing O_2 concentration will increase the concentration of O_2 in the solvent, the resulting increase in MEA degradation is muted by the low reaction order. However, O_2 leaner flue gases have increased concentrations of CO_2 in post-combustion applications; in the absence of intercooling, the high CO_2 concentration will tend to lead to higher temperatures in the absorber as more energy is released by the exothermic reaction between MEA and CO_2 per unit of flue gas processed. As the oxidative degradation reaction is strongly influenced by temperature, the increase in bulk temperature throughout the absorber present in low O_2/high CO_2 concentration flue gases appears to, at least partially, offset the effect of decreased dissolved O_2 concentrations; this is clearly illustrated in Figure 5.

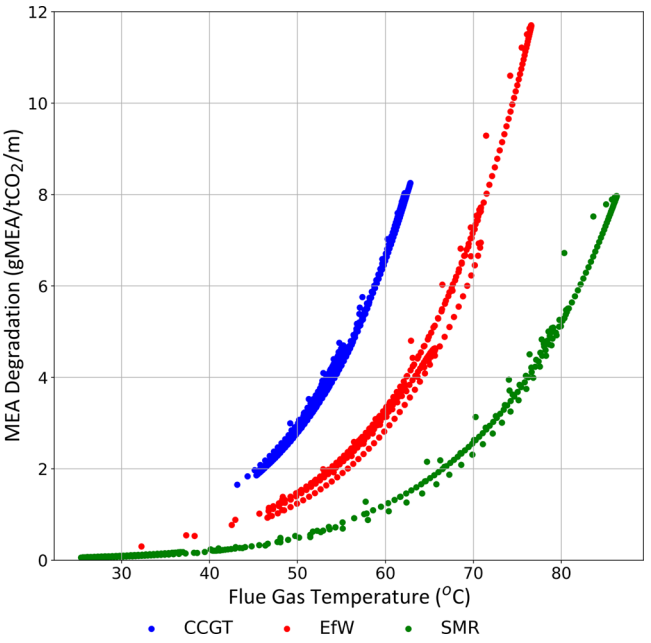


Figure 5. MEA degradation in the absorber packing vs flue gas temperature at different locations in the absorber.

This is most prominently observed in the cases with intercooling included, with a 30−80% decrease in oxidative degradation predicted. This indicates that regardless of the CO_2 capture rate or loading, intercooling can be an effective measure for reducing solvent degradation rates. This must, however, be considered in conjunction with the increased CAPEX and operational requirements that result from including intercooling. Notably, a 43% increase in oxidative degradation in the absorber packing is seen when comparing the 100% added capture and 95% gross capture CCGT cases at 0.1 mol/mol lean loading without intercooling in both cases. This is the result of increased temperatures in the absorber at the higher CO_2 capture fractions. Comparable degradation rates can be seen between the same 95% case and the 100% added capture case (with intercooling), a novel conclusion which indicates that intercooling may be a particularly potent mechanism for reducing solvent degradation in CCGTs at high CO_2 capture fractions despite giving a minor increase in SRD in the cases presented in Table 4 (likely due to decreased reaction rates at lower solvent temperatures). Likewise, the intercooler arrangement presented here does not represent an optimum; further benefits may be observed by revising return temperatures or the inclusion of an additional intercooler, which may have benefits outwit reducing oxidative degradation as this optimization may allow a marginally higher lean loading to be utilized while maintaining the same CO_2 capture performance, reducing thermal degradation.

https://doi.org/10.1021/acs.iecr.4c01525
Ind. Eng. Chem. Res. 2024, 63, 13677−13691

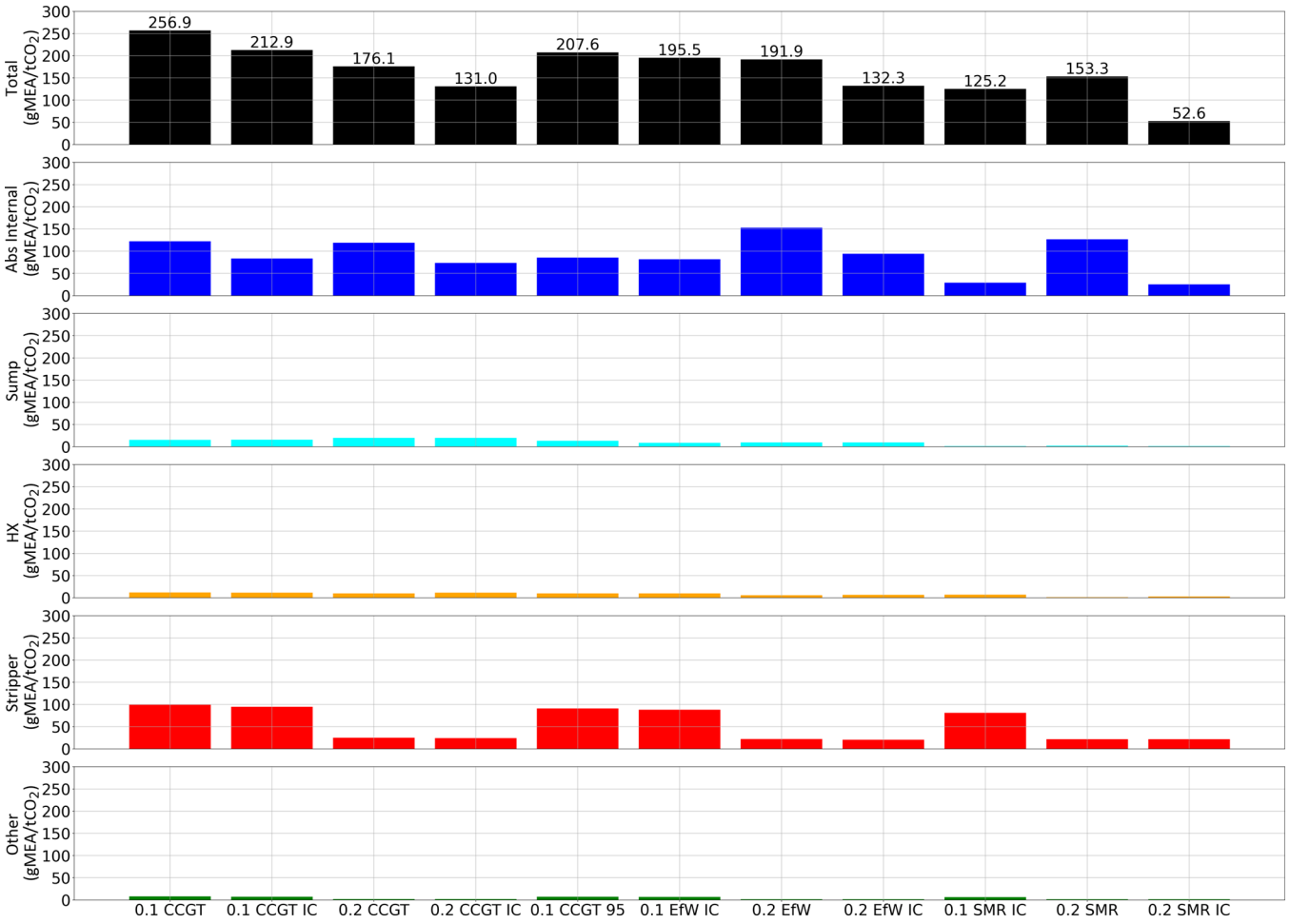


Figure 6. Total and location-specific MEA degradation rates.

Figure 6 and Table 5 detail the predicted total and location-specific MEA degradation rates in the CO_2 capture process. As

Table 5. MEA Degradation Rates

case	total	Abs internal	Abs sump	cross HX	stripper (including reboiler)	other
0.1 CCGT	256.9	122.2	15.6	12.0	99.2	7.9
0.1 CCGT IC	212.9	83.4	15.7	11.8	94.8	7.3
0.2 CCGT	176.0	119.1	19.9	9.9	25.3	1.8
0.2 CCGT IC	131.0	73.7	19.9	11.5	24.2	1.8
0.1 CCGT (95)	207.6	85.7	13.5	9.8	91.2	7.4
0.1 EfW IC	195.6	81.8	8.7	10.0	88.2	6.9
0.2 EfW	191.9	152.9	9.7	5.7	22.0	1.5
0.2 EfW IC	132.3	94.2	9.5	6.7	20.4	1.6
0.1 SMR IC	125.2	29.0	1.5	6.9	81.3	6.4
0.2 SMR	153.3	126.9	2.2	1.2	21.6	1.4
0.2 SMR IC	52.6	25.4	1.5	2.7	21.6	1.3

MEA reacts rapidly with oxygen, the majority of the oxidative degradation occurs within the absorber internals, with the absorber sump and downstream equipment contributing minimally as the remaining dissolved O_2 in the solvent is consumed. The effect is more prominent in O_2-rich flue gases as a higher concentration of dissolved O_2 is carried over into the absorber sump.

For the 100% added CO_2 capture cases, i.e. lean loadings of 0.1 mol/mol, thermal degradation increases by a factor of 3−4 due to the increased temperatures experienced by the solvent in the regeneration system. The increase in reaction rate due to increased temperatures outstrips the decrease from the reduced carbamate concentration in leaner solutions, resulting in the net increase in degradation seen, albeit dampened to some degree. This indicates that a designer should utilize the lowest regeneration pressure that will achieve the required trade-offs between solvent degradation, energy efficiency and CAPEX. This is clearly shown in Figure 7, which details the distribution of MEA thermal degradation at key plant locations. A grouping of degradation profiles by lean loading is immediately apparent, with minimal difference seen between the three processes analyzed. The assumed residence times for each piece of equipment are available in Table S2 of the Supporting Information.

Figure 8 illustrates the consumption of O_2 dissolved within the solvent once direct contact with the flue gas ceases. The degradation framework assumes that once the solvent exits the absorber packing and enters the sump (modeled as a continuously stirred tank reactor), it is no longer in contact with O_2 from the flue gas. From this point onward, degradation occurs indirectly through previously dissolved O_2. For clarity, only the CCGT cases are shown; however, the EfW and SMR cases follow similar trends and can be seen in Figures S1 and S2 of the Supporting Information.

https://doi.org/10.1021/acs.iecr.4c01525
Ind. Eng. Chem. Res. 2024, 63, 13677−13691

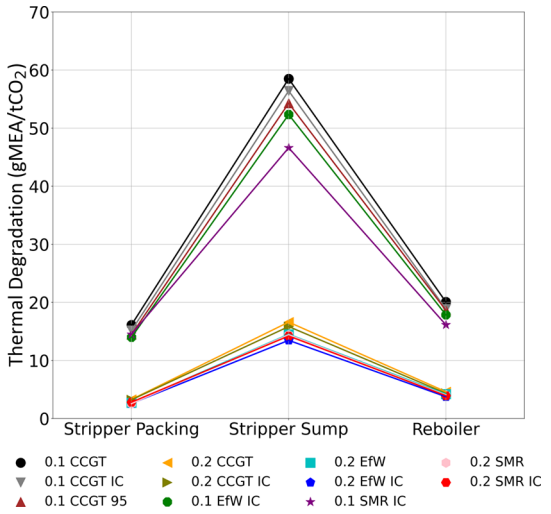


Figure 7. MEA degradation due to thermal degradation at key plant locations.

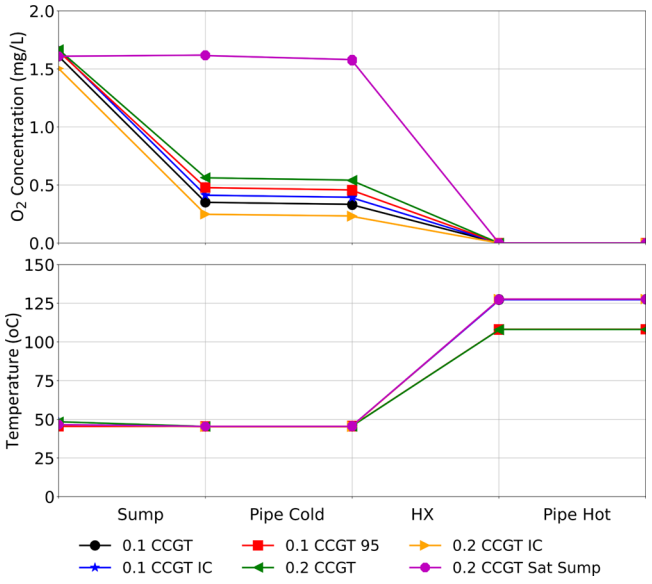


Figure 8. O_2 concentration within solvent at key plant locations (CCGT).

In reality, it is anticipated that the solvent in the absorber sump will still have some exposure to the flue gas, either through contact at the interface or due to the introduction of entrained bubbles resulting from the downcoming solvent. To assess the impact of this kind of exposure on the degradation rate, we predicted the degradation rates under a worst-case scenario by assuming that the solvent in the sump is fully saturated with O_2 throughout the residence time, see Figure 8. Therefore, the solvent leaving the sump is also fully saturated with O_2. In this case, the total MEA degradation rate is increased from the baseline 256.9 to 291.3 g/tCO_2, a 13.4% increase. However, it is unlikely that the solvent will be entirely saturated with O_2 in the absorber sump, as previous oxidative degradation experiments conducted in agitated bubble reactors found that mass transfer limitations for O_2 are present.[25] Nevertheless, it is essential to consider this effect, especially when operating with long sump residence times or flue gases rich in O_2, resulting in high dissolved O_2 concentrations. Process modifications that mitigate prolonged contact between the solvent and the flue gas may be beneficial, as also discussed in.[25] Likewise, process modifications that remove dissolved O_2 from the solvent solution, either prior to or post sump, i.e. flashing or sparging, should reduce indirect oxidative degradation proportional to its removal efficiency.

Minimal MEA consumption occurs in the cold-rich solvent pipeline to the heat exchanger (both pipework and heat exchangers are modeled as plug flow reactors) due to the low residence time and temperature. Within the heat exchanger, dissolved O_2 consumption increases rapidly due to the increased reaction rate stemming from the increased temperatures. By the time the solvent reaches the stripper column, O_2 is predicted to have been entirely consumed in all cases, as also seen in previous work.[25] Minimal O_2 in the export CO_2 stream is a crucial CO_2 pipeline specification due to downstream pipeline integrity concerns. As a result, deoxygenation systems are often included in the design downstream of the stripper at considerable capital expenditure. That being the case, confirmation of total O_2 consumption in the solvent prior to the stripper through pilot or operational studies may allow the omission or reduction in the capacity of the deoxygenation system, leading to a reduction in capital and operational expenditure for systems using aqueous MEA as solvent. This may not be the case for alternative solvents with greater resistance to oxidative degradation.

A design variable available to designers is the hold-up volume of solvent in column sumps. Having a high volume of hold-ups can buffer against operational upsets but comes with the cost of increased solvent exposure to degradation conditions as residence times increase. To investigate the magnitude of this effect, a sensitivity study was conducted wherein the residence time in both the absorber and stripper sumps was varied independently; the results are presented in Figure 9.

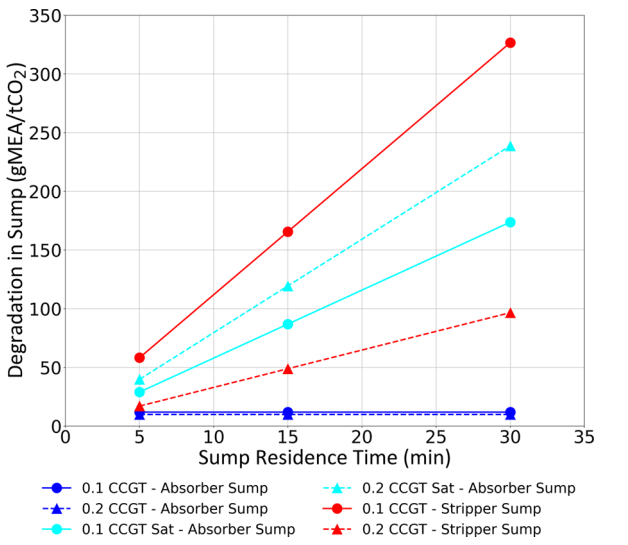


Figure 9. Sump residence time sensitivity study.

When considering the absorber sump, the sensitivity of the stored rich solvent is highly dependent on the assumptions made regarding the degree of O_2 mass transfer into the rich solvent. Where no mass transfer of O_2 occurs, analogous to an independent storage system with minimal contact with atmospheric air or gas capping, no increase in oxidative degradation occurs as the degradation reaction quickly reaches

https://doi.org/10.1021/acs.iecr.4c01525
Ind. Eng. Chem. Res. 2024, 63, 13677−13691

Table 6. Predicted MEA Consumption Rates (gMEA/tCO$_2$)

95% gross CO$_2$ capture	MEA degradation (g/tCO$_2$)	100% added CO$_2$ capture	MEA degradation (g/tCO$_2$)	change in MEA consumption (g/tCO$_2$)	relative change in MEA consumption (%)
0.1 CCGT	207.6	0.1 CCGT	256.9	+49.3	+23.7
0.2 CCGT	176.0	0.1 CCGT	256.9	+80.8	+45.9
0.2 CCGT IC	131.0	0.1 CCGT IC	212.9	+81.9	+62.5
0.2 EfW IC	132.3	0.1 EfW IC	195.6	+63.2	+47.8
0.2 SMR IC	52.6	0.1 SMR IC	125.2	+72.6	+138.2

equilibrium as the dissolved O_2 in the solvent is consumed. However, if the stored solvent remains saturated with O_2, the increase in degradation is linear with residence time. As previously mentioned, the likely effect is somewhere between these two extremes as O_2 is carried into the solvent via mass transfer at the boundary or flue gas entrainment driven by the downcoming solvent. The risk of flue gas entrainment may be mitigated by the inclusion of a liquid collector at the bottom of the absorber packing; however, this should be considered in conjunction with the resultant increase in absorber height and pressure drop, which would result from its inclusion. The reduction of absorber sump residence times with independent rich solvent storage systems may provide a benefit if longer-term storage is required. As these results are presented on a specific basis, i.e. per tCO$_2$ captured, a divergence is observed in the reported MEA degradation occurring in the absorber sump between the 0.1 and 0.2 CCGT saturated sump cases, despite similar dissolved O_2 concentrations and temperatures, as the 0.2 CCGT case is exposed to more cycles of absorption/desorption per article of CO_2 captured than the 0.1 CCGT case.

For the stripper sump, the degree of expected thermal degradation experienced by the solvent per cycle increases linearly with residence time. This is particularly critical at higher temperatures as the slope of the additional degradation is increased due to the less favorable conditions. A buffer store of lean and rich solvent can aid in operational flexibility by enabling the rapid response to changing absorber conditions without the delay of producing additional lean solvent. However, the results presented here indicate that utilising the stripper sump to provide this storage capacity will lead to excessive thermal degradation. Storage of any lean solvent in excess of the minimum level required by the regeneration system in a separate storage tank after the cross-heat exchanger (i.e., ambient storage) could mitigate this by minimizing the holdup time in the stripper sump.

Table 6 details the absolute and relative change in MEA degradation rates predicted to occur when transitioning from 95% gross CO_2 capture to 100% added CO_2 capture for the design points presented in this work. The increase ranges between 21 and 112%, primarily due to the increased rate of thermal degradation in the regeneration section. Solvent replacement OPEX is a function of solvent consumption rate and solvent cost and, therefore, Table 6 can indicate OPEX incurred as a result of replacing this degraded solvent. To provide economic context, using a representative cost for an MEA solvent of 0.5−5£/kg MEA results in an increased OPEX of between 0.02−0.38 £/tCO$_2$. However, the cost indication provided here does not include any additional costs associated with the increased intensity of emission mitigation or solvent management (i.e., increased rates of thermal reclaiming) that are likely if solvent degradation increases, or any increase in volatile solvent losses due to the lower lean loading or higher absorber exit temperatures—these considerations are beyond the scope of this work.

Finally, it is worth noting that the MEA degradation rates presented here i.e. 53−257 g/tCO$_2$ is lower than the MEA make up rates reported as part of test campaigns i.e. 0.17−1.5 kg/tCO$_2$.[13−18] This is partially due to the limitations of this study (Section 1), but also that the values reported in these campaigns include additional losses in the system such as the loss of amines through atmospheric emission or emission control systems, process upsets and spills or any losses in the solvent reclamation system, to mention a few.

4. CONCLUSIONS

This article presents, for the first time, an assessment of monoethanolamine (MEA) degradation rates when capturing 100% of the added CO_2 produced as part of three distinct energy production processes fitted with a postcombustion CO_2 capture (PCC) process utilizing a 35 wt %. MEA solvent. The three processes considered, a combined cycle gas turbine (CCGT), energy from the waste facility (EfW) and a steam methane reformer (SMR), cover the expected range of O_2 (1.2−11.0 vol %) and CO_2 concentrations (4.7−19.5 vol %) within industrial flue gases likely to be relevant in PCC applications. Thus, the MEA degradation rates presented can form a likely range for PCC systems using an MEA solvent within the bounds of the study limitations highlighted throughout.

Flue gas conditions are extracted from the previously published works of Mullen et al.[5,6] and Su et al.[11] and form the input to the process model of the CO_2 capture plant, which uses an open-source model developed by the Carbon Capture Simulation for Industry Impact (CCSI) in ASPEN PLUS.[30] For each process, two distinct CO_2 capture fractions are considered: 95% gross CO_2 capture, which forms the basis for comparison and a CO_2 capture fraction resulting in the capture of 100% of the added CO_2 produced by the process (99.2, 99.6, and 99.7% for the CCGT, EfW and SMR respectively). The process modifications used to achieve 100% added CO_2 capture have previously been described by Mullen et al. and involve the reduction of the solvent lean loading from the typical value of ca. 0.2 mol/mol to ca. 0.1 mol/mol and, in the case of the CCGT, 4 m of additional packing within the absorber column. Mullen et al. have shown that the additional specific thermodynamic penalty of operating at 100% added CO_2 capture is minimal if these process modifications are implemented and conclude that to operate efficiently at the reduced lean solvent loading, an increase in stripper operational pressure is required to suppress the production of surplus steam within the regeneration system and minimize energy losses. This increase in operating pressure necessitates an increase in regeneration temperature within the reboiler, a process modification that the authors suggest may increase the thermal degradation of the solvent. Concurrently, a reduced

https://doi.org/10.1021/acs.iecr.4c01525
Ind. Eng. Chem. Res. 2024, 63, 13677−13691

average loading in the absorber may increase the solubility of O_2 overall and, coupled with increased residence time due to the increased packing height, may lead to increased oxidative degradation.

This study applies thermal and oxidative degradation models developed by Braakhuis et al.[24,25] to investigate how these process modifications affect the predicted MEA degradation rates compared to operational conditions, which achieve a gross 95% CO_2 capture fraction. Additionally, we investigate the effect absorber intercooling, sump O_2 dissolution and residence times rates have on total degradation.

Initially, we show that for an MEA solvent, oxidative degradation primarily occurs within the absorber packing and that, while the solubility of O_2 into the solvent and the partial pressure of O_2 in the flue gas will affect total oxidative degradation rates, the effect is dampened by the low order of reaction relative to O_2 concentration. In the absence of intercooling, higher CO_2 concentrations in the flue gas will tend to lead to higher temperatures in the absorber, as more energy is released by the exothermic reaction between MEA and CO_2 per unit of flue gas processed. As the oxidative degradation reaction is strongly influenced by temperature, the increase in flue gas temperature present in low O_2/high CO_2 concentration flue gases appears to, at least partially, offset the effect of decreased dissolved O_2 concentrations. We find that, for the conditions analyzed in this work and for equivalent intercooling regimes, oxidative degradation rates within the absorber packing are approximately equal over the three processes analyzed, as decreased dissolved O_2 concentrations are offset by increased temperatures.

The inclusion of intercooling consistently reduces total oxidative degradation rates as the bulk temperature within the absorber is reduced, and the reaction rate is proportionately reduced. This effect is predicted to result in a 30−70% reduction in oxidative degradation within the absorber packing. This indicates that, regardless of CO_2 capture fraction or loading, intercooling can be an effective measure for reducing solvent degradation rates. This must, however, be considered in conjunction with the increased CAPEX and operational complexity of including intercooling plus possibly a slight reduction in rich loading. Notably, a 43% increase in oxidative degradation in the absorber packing is seen when comparing the 100% added capture and 95% gross capture CCGT cases at 0.1 mol/mol lean loading (both without intercooling). This is the result of a compounded effect of increased temperatures in the absorber at the higher CO_2 capture fraction and the 20−24 m increase in absorber packing height, increasing residence times. But comparable degradation rates can be seen between the same 95% case and the 100% added capture case when intercooling is included. This novel conclusion indicates that intercooling may be a particularly potent mechanism for reducing solvent degradation in CCGTs at high CO_2 capture fractions.

The degradation framework assumes that once the solvent exits the absorber packing and enters the sump it is no longer in contact with O_2 from the flue gas. The authors consider this assumption optimistic as, in reality, the solvent in the absorber sump will still have some exposure to the flue gas or downcoming solvent, replacing the consumed O_2 to some degree. To investigate the magnitude of this effect, a sensitivity analysis shows that when a continually O_2-saturated sump is assumed, the magnitude of total MEA degradation within the system for the CCGT case with 100% added CO_2 capture increases by 13.4%, placing an upper bound on the magnitude of this effect as it expected that dissolved O_2 in the sump is unlikely to be entirely replaced by the stated mechanisms. Likewise, process modifications that remove dissolved O_2 from the solvent solution, either prior to or post sump, i.e. flashing or sparging, should reduce indirect oxidative degradation proportional to its removal efficiency. Due to the increased temperatures seen in the cross-heat exchanger, by the time the solvent reaches the stripper column, the dissolved O_2 is predicted to have been entirely consumed in all cases. Reduced O_2 concentration in the export CO_2 stream is a crucial CO_2 pipeline specification due to downstream pipeline integrity concerns. As a result, deoxygenation systems are often included in the design downstream of the stripper at considerable capital expenditure. That being the case, should this be confirmed through pilot or operational studies, it may allow the omission or reduction in the capacity of the deoxygenation system, leading to a reduction in capital and operational expenditure. This may not be the case for alternative, less reactive, solvents.

When considering thermal degradation, a pronounced effect is evident. Despite the decreased carbamate concentration in the leaner solvent reducing the rate of thermal degradation at a given temperature, the increased regeneration temperature required to achieve a lower lean loading outstrips this limiting effect, resulting in a 3−4-fold increase in thermal degradation when regeneration pressure (and temperature as a result) is increased to efficiently produce a solvent with a lean loading of 0.1 mol/mol vs 0.2 mol/mol. This appears to be an unavoidable consequence of operating at higher regeneration pressures and indicates that a designer should utilize the lowest regeneration pressure, and hence temperature, that will achieve the required trade-offs between solvent degradation, energy efficiency and CAPEX while being aware of the increased degradation rate and adjusting the solvent management regime accordingly. Additionally, advanced process configurations and/or optimized intercooling regimes may allow high CO_2 capture fractions to be achieved at a higher lean loading than those considered in this work; if so, an associated reduction in the expected degree of thermal degradation could be expected.

This work highlights stripper sump residence time as a key design variable for minimizing thermal degradation. A buffer store of lean solvent can aid in operational flexibility by enabling the rapid response to changing absorber conditions without the delay of producing additional lean solvent. However, utilizing the stripper sump to provide this storage capacity will lead to excessive thermal degradation. Storage of cold lean solvent after the cross-heat exchanger could mitigate this.

Some key limitations apply to this study. The degradation framework used in this work does not consider the effect of long-term degradation compound accumulation and removal within the circulating solvent, interactions between the thermal and oxidative degradation compounds or the catalytic effect of corrosion compounds on solvent degradation. As such, the results presented in this article should be considered predictive only for a perfectly clean solvent. Over an extended period of operation, actual MEA consumption rates are expected to diverge from those predicted by the framework, particularly as dissolved metals catalyze oxidative degradation, likely trending toward increasing consumption unless contaminants within the solvent are maintained at a low level via an effective solvent reclamation system. Also, we do not consider the effect any additional solvent degradation will have on atmospheric

https://doi.org/10.1021/acs.iecr.4c01525
Ind. Eng. Chem. Res. 2024, 63, 13677−13691

emissions or the associated control techniques, solvent management regimes or waste production. Additionally, the operational conditions proposed for 100% added CO_2 capture operation would also provide a reduced energy penalty for lower CO_2 capture fraction operation should the resulting solvent degradation rates be deemed economically acceptable. Likewise, if solvent degradation is more critical to a project than thermal efficiency, lean loadings sufficient to achieve high CO_2 capture fractions can be achieved at lower temperature regeneration conditions. Finally, the intercooler arrangements presented here are not considered optimum, and it is likely that further benefits, both thermodynamic and degradation-related, could be achieved with a dedicated optimization effort. This work aims to compare the solvent degradation rates at proposed design points for the considered CO_2 capture fractions that the authors consider to be valid and viable, acknowledging that such design points are project-specific and do not represent an absolute economic optimum, as no such point can exist.

Even so, this study serves as a first step toward quantifying the effect increasing CO_2 capture fractions in post-combustion CO_2 capture plants will have on solvent degradation. We identify key areas for further study and validation in test facilities as well as design considerations that may help mitigate solvent degradation. The learnings presented here can serve to advise project designs and researchers alike when considering operating at 100% added CO_2 capture, a development the authors believe to be critical if post-combustion CO_2 capture is to be compatible with a Net Zero world.

■ ASSOCIATED CONTENT

Supporting Information

The Supporting Information is available free of charge at https://pubs.acs.org/doi/10.1021/acs.iecr.4c01525.

Additional model parameters sufficient for reproduction and supporting graphics (PDF)

■ AUTHOR INFORMATION

Corresponding Author

Daniel Mullen − *School of Engineering, University of Edinburgh, Edinburgh EH9 3DW, U.K.;* orcid.org/0009-0000-5316-2714; Email: d.t.mullen@sms.ed.ac.uk

Authors

Lucas Braakhuis − *Department of Chemical Engineering, Norwegian University of Science and Technology (NTNU), NO-7491 Trondheim, Norway*

Hanna Katariina Knuutila − *Department of Chemical Engineering, Norwegian University of Science and Technology (NTNU), NO-7491 Trondheim, Norway;* orcid.org/0000-0003-2057-1743

Jon Gibbins − *Department of Mechanical Engineering, University of Sheffield, Sheffield S3 7RD, U.K.;* orcid.org/0000-0003-0963-4555

Mathieu Lucquiaud − *Department of Mechanical Engineering, University of Sheffield, Sheffield S3 7RD, U.K.*

Complete contact information is available at: https://pubs.acs.org/10.1021/acs.iecr.4c01525

Notes

The authors declare the following competing financial interest(s): D.M. is an employee of SSE Thermal.

■ ACKNOWLEDGMENTS

The authors would like to acknowledge the School of Engineering at the University of Edinburgh and the Department of Chemical Engineering at the Norwegian University of Science and Technology for providing financial support for this work. Additionally, financial support has been provided by the NCCS Research Centre, which is performed under the Norwegian research programme Centre for Environment-friendly Energy Research (FME). The authors acknowledge the following partners for their financial contributions: Aker BP, Aker Carbon Capture, Allton, Ansaldo Energia, Baker Hughes, CoorsTek Membrane Sciences, Elkem, Eramet, Equinor, Gassco, Hafslund Oslo Celsio, KROHNE, Larvik Shipping, Norcem Heidelberg Cement, Offshore Norge, Quad Geometrics, Stratum Reservoir, TotalEnergies, Vår Energi, Wintershall DEA and the Research Council of Norway (257579/E20). For the purpose of open access, the authors have applied a Creative Commons Attribution (CC BY) license to any Author Accepted Manuscript version arising from this work.

■ NOMENCLATURE

CCS	Carbon Capture and Storage
CCGT	Combined Cycle Gas Turbine
EfW	Energy from Waste
SMR	Steam Methane Reformer
MSW	Municipal Solid Waste
PCC	Post Combustion Capture
NCCC	National Carbon Capture Centre
MEA	Monoethanolamine
CAPEX	Capital Expenditure
OPEX	Operational Expenditure
T&S	Transport and Storage
CCSI	Carbon Capture Simulation Initiative
GE	General Electric
L/G	Liquid over Gas ratio (kg/kg)
VLE	Vapor Liquid Equilibrium
SRD	Specific Reboiler Duty (GJ/tCO_2)
DACCS	Direct Air CO_2 Capture and Storage
BECCS	Bioenergy with CCS
IEA	International Energy Agency
VOCs	Volatile Organic Compounds
HHV	Higher Heating Value (kJ/kg)
LHV	Lower Heating Value (kJ/kg)
LMTD	Log Mean Temperature Difference (°C)
HX	Heat Exchanger

■ REFERENCES

(1) Calvin, K.; Dasgupta, D.; Krinner, G.; Mukherji, A.; Thorne, P. W.; Trisos, C. *IPCC, 2023*; IPCC, 2023.

(2) Arango, J.; Calvin, K.; Guivarch, C.; Hasegawa, T.; Jiang, K.; Kriegler, E.; Matthews, R.; Peters, G. P.; Rao, A.; Robertson, S.; Sebbit, A. M.; Steinberger, J.; Tavoni, M.; van Vuuren, D. P. Mitigation Pathways Compatible with Long-Term Goals. In *Climate Change 2022 - Mitigation of Climate Change*; Cambridge University Press, 2023; pp. 295−408.

(3) IEA. *CCUS in Clean Energy Transitions*; IEA: Paris, 2020. https://www.iea.org/reports/ccus-in-clean-energy-transitions (accessed 2024-02-20).

(4) IEA. *Capacity of Current and Planned Large-Scale CO_2 Capture Projects vs. the Net Zero Scenario, 2020−2030*; IEA: Paris, 2023. https://www.iea.org/data-and-statistics/charts/capacity-of-current-and-planned-large-scale-co2-capture-projects-vs-the-net-zero-scenario-2020-2030 (accessed 2024-02-20).

(5) Mullen, D.; Lucquiaud, M. On the Cost of Zero Carbon Electricity: A Techno-Economic Analysis of Combined Cycle Gas Turbines with Post-Combustion CO_2 Capture. *Energy Reports* **2024**, *11*, 5104−5124.
(6) Mullen, D.; Herraiz, L.; Gibbins, J.; Lucquiaud, M. On the Cost of Zero Carbon Hydrogen: A Techno-Economic Analysis of Steam Methane Reforming with Carbon Capture and Storage. *Int. J. Greenhouse Gas Control* **2023**, *126*, No. 103904.
(7) Danaci, D.; Bui, M.; Petit, C.; Mac Dowell, N. En Route to Zero Emissions for Power and Industry with Amine-Based Post-Combustion Capture. *Environ. Sci. Technol.* **2021**, *55* (15), 10619−10632.
(8) Feron, P.; Cousins, A.; Jiang, K.; Zhai, R.; Thiruvenkatachari, R.; Burnard, K. Towards Zero Emissions from Fossil Fuel Power Stations. *Int. J. Greenhouse Gas Control* **2019**, *87*, 188−202.
(9) Brandl, P.; Bui, M.; Hallett, J. P.; Mac Dowell, N. Beyond 90% Capture: Possible, but at What Cost? *International Journal of Greenhouse Gas Control* **2021**, *105*, No. 103239.
(10) Cownden, R.; Mullen, D.; Lucquiaud, M. Towards Net-Zero Compatible Hydrogen from Steam Reformation − Techno-Economic Analysis of Process Design Options. *Int. J. Hydrogen Energy* **2023**, *48* (39), 14591−14607.
(11) Su, D.; Herraiz, L.; Lucquiaud, M.; Thomson, C.; Chalmers, H. Thermal Integration of Waste to Energy Plants with Post-Combustion CO_2 Capture. *Fuel* **2023**, *332*, No. 126004.
(12) Michailos, S.; Gibbins, J. A Modelling Study of Post-Combustion Capture Plant Process Conditions to Facilitate 95−99% CO_2 Capture Levels From Gas Turbine Flue Gases. *Front Energy Res.* **2022**, *10*, No. 866838.
(13) Hume, S. A.; Shah, M. I.; Lombardo, G.; Kleppe, E. R. Results from Cesar-1 Testing with Combined Heat andPower (Chp) Flue Gas at the Co2 Technology Centre Mongstad. In *TCCS-11 - Trondheim Conference on CO_2 Capture, Transport and Storage*; Trondheim, 2021.
(14) Moser, P.; Wiechers, G.; Schmidt, S.; Monteiro, J. G. M.-S.; Goetheer, E.; Charalambous, C.; Saleh, A.; van der Spek, M.; Garcia, S. ALIGN-CCUS: Results of the 18-Month Test with Aqueous AMP/PZ Solvent at the Pilot Plant at Niederaussem − Solvent Management, Emissions and Dynamic Behaviour. *International Journal of Greenhouse Gas Control* **2021**, *109*, No. 103381.
(15) Hirata, T.; Tsujiuchi, T.; Kamijo, T.; Kishimoto, S.; Inui, M.; Kawasaki, S.; Lin, Y.-J.; Nakagami, Y.; Nojo, T. Near-Zero Emission Thermal Power Plant Using Advanced KM CDR Process™. *International Journal of Greenhouse Gas Control* **2020**, *92*, No. 102847.
(16) Shah, M. I.; Silva, E.; Gjernes, E.; Åsen, K. I. Cost Reduction Study for MEA Based CCGT Post-Combustion CO_2 Capture at Technology Center Mongstad. In *Proceedings of the 15th Greenhouse Gas Control Technologies Conference 15-18 March*, **2021**.
(17) Gao, T.; Selinger, J. L.; Rochelle, G. T. Demonstration of 99% CO_2 Removal from Coal Flue Gas by Amine Scrubbing. *International Journal of Greenhouse Gas Control* **2019**, *83*, 236−244.
(18) Benquet, C.; Knarvik, A.; Gjernes, E.; Hvidsten Arne, O.; Kleppe Romslo, K.; Akhter, S. First Process Results and Operational Experience with CESAR1 Solvent at TCM with High Capture Rates (ALIGN-CCUS Project). In *15th International Conference on Greenhouse Gas Control Technologies*; IEAGHG, 2021.
(19) Feron, P. H. M.; Cousins, A.; Gao, S.; Liu, L.; Wang, J.; Wang, S.; Niu, H.; Yu, H.; Li, K.; Cottrell, A. Experimental Performance Assessment of a Mono-ethanolamine-based Post-combustion CO_2 -capture at a Coal-fired Power Station in China. *Greenhouse Gases: Science and Technology* **2017**, *7* (3), 486−499.
(20) Faramarzi, L.; Thimsen, D.; Hume, S.; Maxon, A.; Watson, G.; Pedersen, S.; Gjernes, E.; Fostås, B. F.; Lombardo, G.; Cents, T.; Morken, A. K.; Shah, M. I.; de Cazenove, T.; Hamborg, E. S. Results from MEA Testing at the CO_2 Technology Centre Mongstad: Verification of Baseline Results in 2015. *Energy Procedia* **2017**, *114*, 1128−1145.
(21) Aronu, U. E.; Mejdell, T.; Hjarbo, K.; Chikukwa, A.; Grimstvedt, A.; Lund, A. *Baseline Test of Capture from Bio Flue Gas with MEA at Tiller Plant*; Sintef, 2019. https://sintef.brage.unit.no/sintef-xmlui/bitstream/handle/11250/3027279/CLIME+Report_Open+Access_Final_Signed.pdf?sequence=1.
(22) Moser, P.; Schmidt, S.; Sieder, G.; Garcia, H.; Stoffregen, T. Performance of MEA in a Long-Term Test at the Post-Combustion Capture Pilot Plant in Niederaussem. *International Journal of Greenhouse Gas Control* **2011**, *5* (4), 620−627.
(23) Knudsen, J. N.; Jensen, J. N.; Vilhelmsen, P.-J.; Biedec, O. First Year Operation Experience with a 1 t/h CO_2 Absorption Pilot Plant at Esbjerg Coal-Fired Power Plant. In *Proceedings of European Congress of Chemical Engineering (ECCE-6)*; Copenhagen, 2007.
(24) Braakhuis, L.; Høisæter, K. K.; Knuutila, H. K. Modeling the Formation of Degradation Compounds during Thermal Degradation of MEA. *Ind. Eng. Chem. Res.* **2022**, *61* (7), 2867−2881.
(25) Braakhuis, L.; Knuutila, H. K. Predicting Solvent Degradation in Absorption−Based CO_2 Capture from Industrial Flue Gases. *Chem. Eng. Sci.* **2023**, *279*, No. 118940.
(26) Goff, G. S.; Rochelle, G. T. Monoethanolamine Degradation: O $_2$ Mass Transfer Effects under CO $_2$ Capture Conditions. *Ind. Eng. Chem. Res.* **2004**, *43* (20), 6400−6408.
(27) Davis, J.; Rochelle, G. Thermal Degradation of Monoethanolamine at Stripper Conditions. *Energy Procedia* **2009**, *1* (1), 327−333.
(28) Martin, S.; Lepaumier, H.; Picq, D.; Kittel, J.; de Bruin, T.; Faraj, A.; Carrette, P.-L. New Amines for CO $_2$ Capture. IV. Degradation, Corrosion, and Quantitative Structure Property Relationship Model. *Ind. Eng. Chem. Res.* **2012**, *51* (18), 6283−6289.
(29) Gao, T. *Absorber Modelling and Design in Amine Scrubbing for Carbon Capture*, Ph.D. Dissertation, The University of Texas at Austin: Austin, 2021, https://hdl.handle.net/2152/892762021 (accessed 2024-05-30).
(30) Morgan, J. C.; Chinen, A. S.; Anderson-Cook, C.; Tong, C.; Carroll, J.; Saha, C.; Omell, B.; Bhattacharyya, D.; Matuszewski, M.; Bhat, K. S.; Miller, D. C. Development of a Framework for Sequential Bayesian Design of Experiments: Application to a Pilot-Scale Solvent-Based CO_2 Capture Process. *Appl. Energy* **2020**, *262*, No. 114533.
(31) *National Carbon Capture Center [Internet]*. https://www.nationalcarboncapturecenter.com/ (accessed 2024-05-30).
(32) Zohuri, B. Compact Heat Exchangers Design for the Process Industry. In *Compact Heat Exchangers*; Springer International Publishing: Cham, 2017; pp. 57−185.
(33) Donald, R. W. *Rules of Thumb in Engineering Practice*; Wiley VCH, 2007.
(34) Elliott, W. R.*Front-End Engineering Design (FEED) Study for a Carbon Capture Plant Retrofit to a Natural Gas-Fired Gas Turbine Combined Cycle Power Plant (2 × 2 × 1 Duct-Fired 758-MWe Facility With F Class Turbines)*; Bechtel National, Inc., https://www.energy.gov/, 2022. https://ukccsrc.ac.uk/wp-content/uploads/2022/05/Sherman_FEED_compressed.pdf (accessed 2024-05-24).
(35) Høisæter, K. K.; Vevelstad, S. J.; Braakhuis, L.; Knuutila, H. K. Impact of Solvent on the Thermal Stability of Amines. *Ind. Eng. Chem. Res.* **2022**, *61* (43), 16179−16192.
(36) Vevelstad, S. J.; Johansen, M. T.; Knuutila, H.; Svendsen, H. F. Extensive Dataset for Oxidative Degradation of Ethanolamine at 55−75°C and Oxygen Concentrations from 6 to 98%. *International Journal of Greenhouse Gas Control* **2016**, *50*, 158−178.
(37) Buvik, V.; Bernhardsen, I. M.; Figueiredo, R. V.; Vevelstad, S. J.; Goetheer, E.; van Os, P.; Knuutila, H. K. Measurement and Prediction of Oxygen Solubility in Post-Combustion CO_2 Capture Solvents. *Int. J. Greenh. Gas Control* **2021**, *104*, No. 103205.
(38) Chi, S.; Rochelle, G. T. Oxidative Degradation of Monoethanolamine. *Ind. Eng. Chem. Res.* **2002**, *41* (17), 4178−4186.
(39) Goff, G.; Rochelle, G. Oxidative Degradation of Aqueous Monoethanolamine in CO_2 Capture Systems Under Absorber Conditions. In *Greenhouse Gas Control Technologies - 6th International Conference*; Elsevier: Kyoto, Japan, 2003; pp. 115−120.
(40) Léonard, G.; Toye, D.; Heyen, G. Experimental Study and Kinetic Model of Monoethanolamine Oxidative and Thermal Degradation for Post-Combustion CO 2 Capture. *International Journal of Greenhouse Gas Control* **2014**, *30*, 171−178.

6.1 Conclusion

This article presents, for the first time, an assessment of MEA degradation rates expected when capturing 100% of the added CO_2 produced as part of three distinct energy conversion processes (CCGT, EfW and SMR) fitted with a PCC process and utilising a 35 wt %. MEA solvent. These processes cover the expected range of O_2 (1.2−11.0 vol %) and CO_2 concentrations (4.7−19.5 vol %) relevant in PCC applications.

It is predicted that, for an MEA solvent, the primary location for oxidative degradation is within the absorber packing itself due to the rapid rate of reaction of dissolved O_2 with MEA. As the CO_2 capture reaction is strongly exothermic, flue gases with high CO_2 concentrations (and as a result lower O_2 concentrations) experience higher temperatures in the absorber relative to lower CO_2 concentration flue gases. As the oxidative degradation rate is strongly sensitive to temperature while the O_2 concentration has a low order in the reaction kinetics this increased temperature appears to mostly offset any reduction in degradation that would be expected due to the reduced O_2 concentration. As such relative insensitivity is observed to O_2 concentration with similar rates of degradation observed across all 3 flue gases analysed, an entirely novel observation.

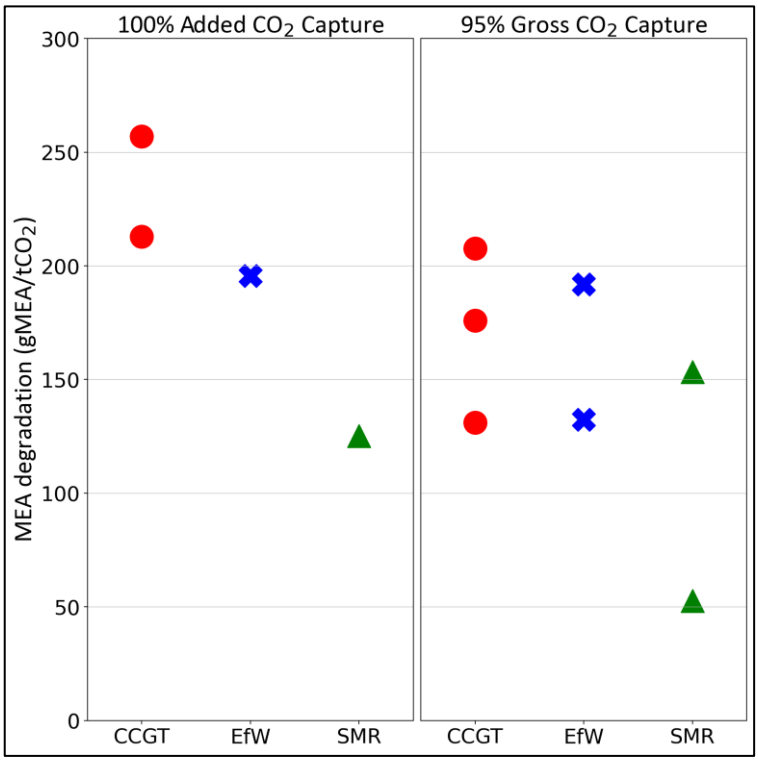


Figure 15: Monoethanolamine (MEA) degradation rates in post-combustion capture plants with 100% fossil CO_2 capture - Graphical Abstract

By the same virtue, intercooling of the solvent and thus reducing the average temperature of the flue gas in the absorber was found to have a strong dampening effect on the oxidative degradation reaction across all cases with reductions in specific degradation of the order of 30-70% observed. Without intercooling, increasing CO_2 capture fractions, for the same lean loading for a CCGT was found to increase oxidative degradation by 43% due to the compound effect of increased average temperatures and the additional residence time due to the increased packing hight. However, intercooling was again found to be an effective mitigation measure. Oxidative degradation rates in the absorber sump (or external storage tank) were found to be minimal, however strongly dependant on the degree of continued O_2 exposure, as the dissolved O_2 present in the solvent when leaving the absorber packing is rapidly consumed, reaching equilibrium levels. Reducing the exposure to O_2 in external storage tanks though limited head space or N_2 caping would likely serve to arrest continued degradation.

When considering thermal degradation, the reduction in lean loading (and associated increase in regeneration temperature) thought to be necessary to achieve 100% fossil CO_2 capture has a pronounced effect on specific thermal degradation rates, with a 3-to-4-fold increase observed despite the dampening effect of the reduced carbamate concentration. However, reducing the residence time of the solvent in the desorber sump was shown to be an effective mitigation measure. Nevertheless, it is likely that some degree of increase in thermal degradation rate can be expected when using lower lean loadings.

Over the three processes analysed, increasing CO_2 capture fractions from 95% gross to 100% fossil CO_2 capture increase specific degradation by between 21 and 112%, primarily due to the increased rate of thermal degradation in the regeneration section. However, as MEA is a low-cost solvent (circa 0.5 – 5£/kg) the effect on plant economics is predicted to be minimal with an estimated increase in OPEX due to additional solvent replacement of between $0.02{-}0.38$ £/tCO_2.

6.2 Highlights

- Capturing 100% of the CO_2 in flue gases is predicted to increase solvent degradation by 24−138% compared to 95% gross CO_2 capture.
- Oxidative degradation in low O_2/high CO_2 concentration flue gases is partially mitigated by lower average flue gas temperatures.
- Intercooling consistently reduces total oxidative degradation
- Extending durations of rich solvent storage is not expected to increase rates oxidative degradation if O_2 dissolution is impeded
- Increased regeneration temperatures result in a 3−4-fold increase in thermal degradation rates however reduced sump residence time is an effective mitigation measure

6.3 Limitations and Future Work

The following limitations were identified for the work described in this chapter; any future work should endeavour to resolve these limitations:

- The degradation framework provides only the instantaneous predicted MEA consumption rate of the system at a point in time. As such, it does not consider the effect of cumulative production of degradation compounds within the solvent. Degradation compounds within the solvent may catalyse MEA degradation and thus accelerate the reaction.
- Thermal and oxidative degradation mechanisms are considered independent in the framework and no interactions between the respective degradation compounds are accounted for.
- This study does not consider the catalytic effect of corrosion compounds on solvent degradation due to the complexity of the reaction mechanisms and the limited experimental data.
- The thermal degradation model for MEA is developed for 30 wt % MEA and is valid at loadings between 0.1−0.5 mol CO_2/mol MEA and temperatures up to 160 °C. This work assumes that it is valid to extrapolate this model to a 35% wt. as Høisæter et al. (Høisæter et al., 2022) demonstrate that thermal degradation rates appear insensitive to solvent concentration.

7. Abatement of CO_2 emissions during start-up and shutdown of post-combustion capture plants

Chapter 4 of this thesis identifies the flexible operation of a combined cycle gas turbines (CCGT) decarbonised with post combustion capture (PCC) while maintaining high rates of CO_2 capture as a key knowledge gap if CCGTs are to provide dispatchable support to intermitted renewables in a decarbonised electricity grid. This is illustrated by Calvert and MacKenzie (Calvert and MacKenzie, 2020), who provide indicative estimates for the number of starts and operating hours that could be expected for a CCGT operating under 3 distinct operational scenarios in the UK (Table 6).

Table 6: Typical UK CCGT load profiles (Calvert and MacKenzie, 2020)

Load Scenario	Annual Starts (Hot + Cold)	Annual Operating Hours
Baseload	30 (24 + 6)	8094
Two-shift	276 (221 + 55)	3854
Mid-merit	395 (355 + 40)	180

In contrast to this, historical applications of PCC were typically designed to operate under steady state conditions with minimal requirements to respond to load changes or start-up/shutdown (SUSD) events, the infrequent rate of occurrence of these events meant that there was minimal financial incentive to maintain CO_2 capture fractions at steady state values during transient operations, therefore dynamic operation of PCC plants represents a novel design case.

In order for a given CO_2 capture fraction to be achieved the CO_2 absorber must be supplied with the appropriate quantity of lean solvent at the appropriate loading. Under dynamic operations this can be challenging as increasing/decreasing and/or variable flue gas compositions require a rapid response in the production rate and quality of lean solvent. However, thermal inertia in the desorber column limits the ability of the regeneration system to meet these requirements. This is particularly stark during plant start-up as lean solvent is required as soon as combustion begins while production of lean solvent cannot occur until the regeneration system is at operational pressure and temperature.

This chapter describes the outputs of a project for which the author provided extensive technical input, with a particular focus on the procurement and analysis of operational data from a commercial CCGT to explore the use of “early” and “late” steam available during SUSD events. This is the primary novel contribution of the author although technical support was provided to all aspects of the project.

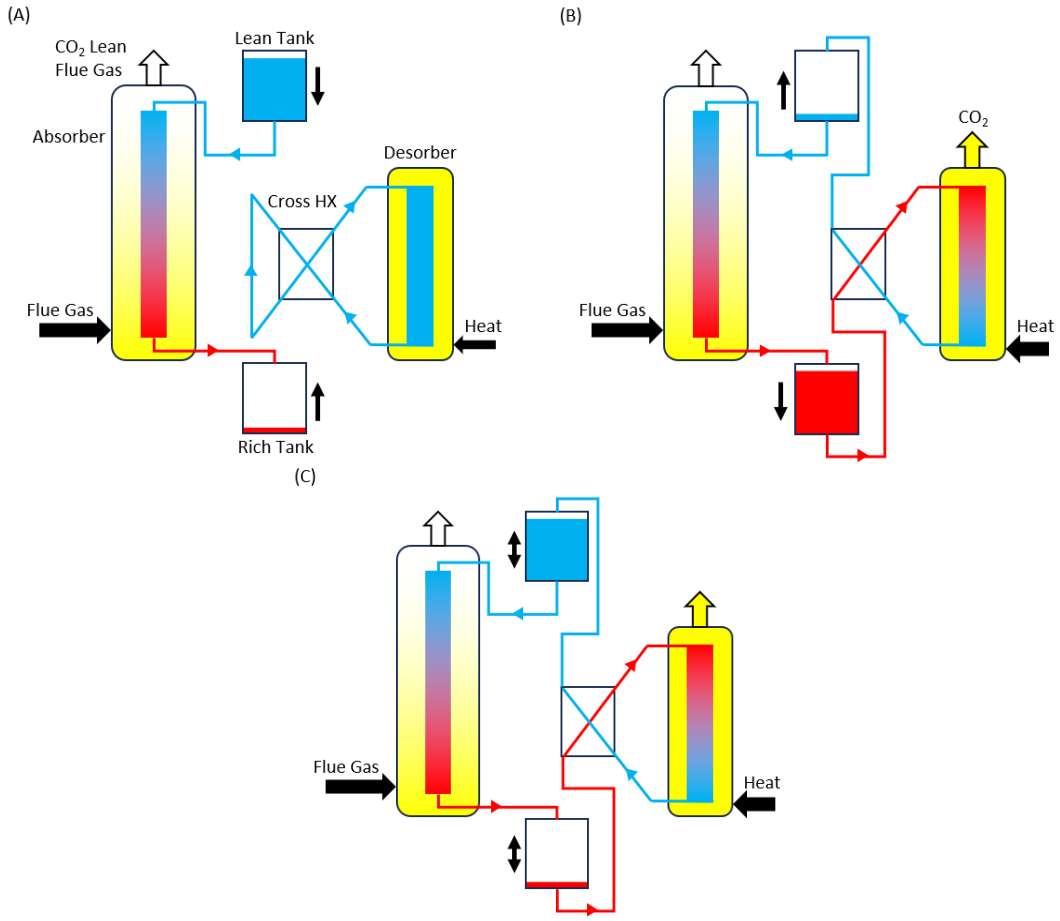


Figure 16: Illustrative diagram of Solvent Storage during start up. Lean & rich solvent in blue and red respectively while CO_2 is shown in yellow (1) CO_2 capture while desorber reaches operating conditions. (2) Rich solvent regeneration concurrently with CO_2 capture. (3) Normal operation.

The aim of this project is to demonstrate the viability of the solvent storage concept, that is the decoupling of the absorber and desorber systems via inline solvent storage (Calvert and MacKenzie, 2020), facilitating time shifted solvent regeneration and enabling CCGTs fitted with PCC to achieve CO_2 capture fractions comparable to steady state operations during all operational modes, including SUSD events.

17th International Conference on Greenhouse Gas Control Technologies, GHGT-17

20th -24th October 2024 Calgary, Canada

Flexibly Operated Capture Using Solvent Storage (FOCUSS) – Results

Daniel Mullen[1,2,*], Xiaomian Baxter[1], James Bowers[1], Harry Ellicott[1], Tom Ilett[3], Sam Atkinson[3], Mohamed Pourkashanian[4], Muhammad Akram[4], Abdulaziz Gheit[4], Mathieu Lucquiaud[4], Jonathan Gibbins[4]

[1]*SSE Thermal, One Forbury Place, 43 Forbury Road, Reading, RG1 3JH, UK*
[2] *School of Engineering, University of Edinburgh, School of Engineering, Sanderson Building, Edinburgh, EH9 3FB, UK*
[3]*AECOM, London, Aldgate Tower, 2 Leman Street, London, E1 8FA, UK*
[4] *School of Mechanical, Aerospace and Civil Engineering, University of Sheffield, Sir Frederick Mappin Building, Sheffield, S1 4DT, UK*

Abstract

This article describes the pilot scale plant upgrades, process modeling and test campaigns completed to date as part of the Flexibly Operated Capture Using Solvent Storage (FOCUSS) project. These campaigns successfully demonstrated that the use of solvent storage in a post-combustion capture process can maintain a net CO_2 capture fraction of greater than 95% during simulated startup and shutdown (SUSD) events using a 35% wt. MEA solution. Additionally, using normalized data from a commercial Combined Cycle Gas Turbine (CCGT) plant, we quantify the availability of "early and late" steam during SUSD events, that is steam produced that cannot be used in the steam turbines but is acceptable for use in the CO_2 capture plant. Since this steam would otherwise be dumped to the condenser and thus wasted, it offers the opportunity to avoid the use of additional fuel in ancillary gas boilers to achieve 95% CO_2 capture for SUSD.

It is estimated that the utilization of 'early steam' for equipment heating and solvent regeneration during startup reduces the required rich solvent tank capacity (and additional solvent inventory) to an additional circa 50% of the existing solvent inventory when capturing 95% of SUSD emissions, compared to circa 350% without early steam for SUSD abatement. Process modeling indicates that, if it takes less than 15 minutes to reach CO_2 export quality from the point of the desorber reaching operating conditions, all of the rich solvent generated during cold, warm and hot startups can be regenerated during the startup sequence, utilizing energy that is typically wasted. In the case of a hot start, any delay above 15 minutes is predicted to require some level of solvent regeneration during normal operation or shutdown. Similar to startup, substantial waste steam is available during the shutdown sequence, with the potential to regenerate over 50% of the base solvent inventory in preparation of the next start, further demonstrating the economic benefits available to flexible CCS plants using solvent storage.

Finally, drawing from the learnings from the pilot plant campaigns and process modeling completed as part of FOCUSS we propose an operational SUSD sequence ensuring that greater than 95% CO_2 capture fractions are maintained throughout a SUSD event while maximizing energy efficiency and minimizing capital expenditure.

Keywords: Post-combustion CO_2 capture; CCGT; Net Zero; Flexible power; CCUS

1. Introduction

In modern energy systems with a high penetration of intermittent renewable generation, frequent load changes of dispatchable power generation plants are required to match supply with demand and ensure an uninterrupted supply of power to consumers. Due to their high degree of flexibility, rapid response times, and high thermal efficiency, combined-cycle gas turbines (CCGT) are often used for this function. As energy systems progress towards complete decarbonisation, and assuming that consumers will continue to require uninterrupted access to power, the need to dispatch on-demand power to the grid will remain. However, it must now be decarbonised to reflect the ongoing energy transition and net zero commitments.

Carbon Capture and Storage (CCS) has the potential to aid in the decarbonisation of fossil-based power generation, notably, the highly flexible and efficient CCGTs that dominate many power grids, through the use of amine-based post-combustion capture (PCC) technology (1). For decarbonized and flexible power generation, the ability to maintain a high level of CO_2 capture during load changes and startup/shutdown (SUSD) events is crucial for compliance with long term climate mitigation targets. Otherwise, to maintain an average CO_2 capture rate equal to that of the design basis, steady state CO_2 capture fractions would have to increase to compensate for reduced capture performance during SUSD, reducing the net export capacity of the facility for that period or accept the additional CO_2 emissions and the associate emission fees or cost of high quality CO_2 offsets.

Historically, applications of CCS have primarily been implemented in industries, primarily in gas processing applications, where steady-state operations is the norm, experiencing minimal load changes and SUSD sequences. Therefore, operating under dynamic conditions while maintaining a high level of CO_2 capture poses a novel challenge to power plant designers. In a typical amine-based PCC capture plant, the availability of steam, thermal inertia, and holdup in columns can limit the plant's ability to respond rapidly to shifts in plant output. The use of ancillary natural gas boilers is often proposed as a method for increasing CO_2 capture fractions during SUSD as they facilitate the rapid generation of steam which is decoupled from the CCGT process. However, the additional supply chain and direct emissions (unless also captured) limit the net improvement in CO_2 capture fraction. Indeed, Bui et al. (2) demonstrate that this method may result in a curtailment on the annual permissible number of SUSD sequences for a CCGT to limit lifecycle emissions, likely impacting the profitability of the facility. This provides a strong incentive to deploy an alternative method that increases the net CO_2 capture fraction of a SUSD sequence up to steady state values, ensuring that CCGTs can provide unrestricted, flexible and low carbon power to a decarbonised electricity grid. This work investigates the use of stored lean and rich solvent to ensure that the CO_2 absorber is supplied with the correct solvent flow rate and loading across all operating modes, effectively eliminating the effect of short-term transients on the instantaneous CO_2 capture fraction within the bounds of the available storage.

1.1. Solvent Storage

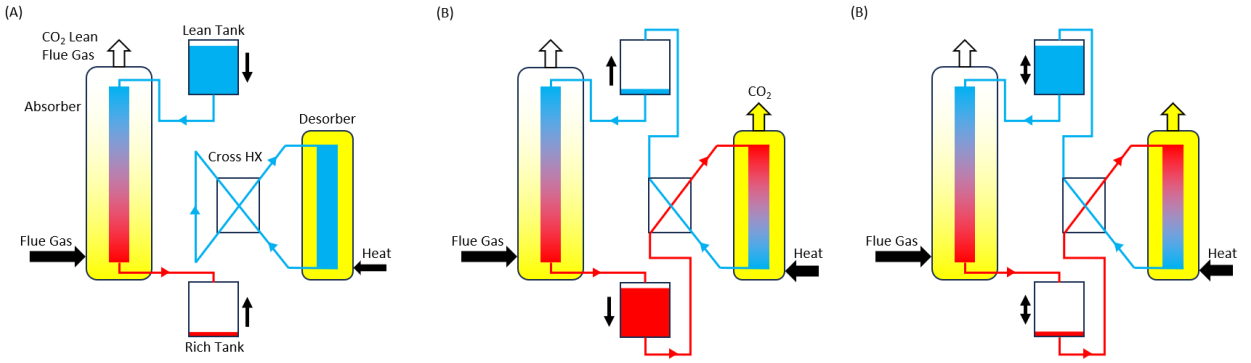


Figure 1: Illustrative diagram of Solvent Storage during start up. Lean & rich solvent in blue and red respectively while CO_2 is shown in yellow (1) CO_2 capture while desorber reaches operating conditions. (2) Rich solvent regeneration concurrently with CO_2 capture. (3) Normal operation

For the CO_2 capture fraction in the CO_2 absorber of an amine-based PCC plant to be met, lean solvent must be supplied to the absorber at a rate and loading that will provide the driving force and capacity to absorb the required amount of CO_2. It then follows that any method to capture CO_2 during transient operations must focus on supplying the required amount of adequately lean solvent to the absorber at all times. Prior to startup, a quantity of lean or semi lean solvent

will be present in various locations within the PCC plant, namely the lean pipework, heat exchangers and desorber sump. This solvent inventory will facilitate some degree of CO_2 capture during startup. It is, however, not expected to be available in sufficient quantities to achieve net CO_2 capture rates equivalent to steady state operation (3), resulting in a predicted net CO_2 capture fraction of 39% for a hot start (< 8hrs offline) and 30% for a cold start (> 64hrs offline). In order to bridge this gap, increasing the quantity of lean solvent in the system prior to a start-up and increasing the capacity to store rich solvent is proposed (Figure 1). This ensures that the absorber is always provided with enough lean solvent until the regeneration system is ready, while maximizing the loading of the stored rich solvent. Regeneration of this stored rich solvent begins once the desorber reaches operational conditions and is completed in advance of the next plant shutdown.

1.2. Flexibly Operated Capture Using Solvent Storage (FOCUSS)

The Flexible Operated Capture Using Solvent Storage (FOCUSS) project is funded by the UK Department for Energy Security and Net Zero (DESNZ) under the Carbon Capture, Usage and Storage (CCUS) Innovation 2.0 Programme. It is an industry-led project managed and delivered by a consortium consisting of SSE Thermal (project lead), the University of Sheffield and AECOM. Through pilot scale test campaigns and process modelling, FOCUSS aims to accelerate the time to market for solvent storage technology which will enable amine-based PCC plants to achieve 95-99% CO_2 capture fractions at all times, including during start-up, shut-down and other transients. The project duration is from May 2022 to March 2025. A high-level overview of the work packages associated with this work is provided in Figure 2.

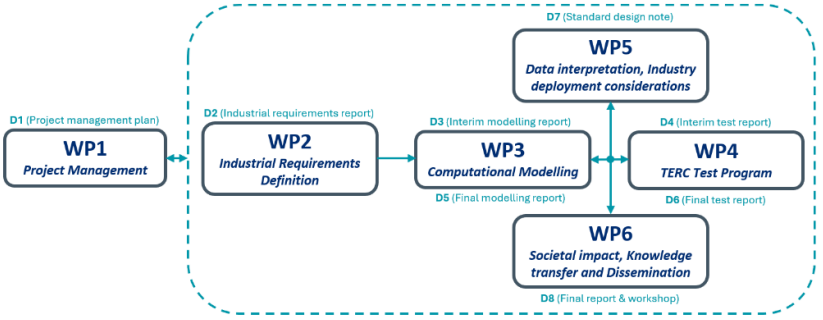


Figure 2: FOCUSS work packages and deliverables

2. Methodology

2.1. Amine Capture Plant (ACP) at the Translational Research Centre (TERC)

The pilot amine CO_2 capture plant (ACP) at TERC is designed to operate at 100 - 250 Nm^3/h gas flow and 300 – 1600 kg/h solvent, with a design capacity of 1tpd CO_2 captured (200Nm^3/h @ 15 vol % CO_2). The plant can be fed with a synthetic flue gas mixture of air plus CO_2 and N_2, from bulk storage or with actual flue gas from onsite combustion facilities. The plant is equipped with a full absorption and desorption cycle consisting of two absorber vessels (the second absorber can be connected in series to extend the effective packing height or can be bypassed), a desorber vessel with an integrated kettle reboiler fed from an electrically powered pressurised water heater (PWH), a cross-heat exchanger, carbon filter, trim cooler, flue gas fan, pumps, control system and a water wash section. A gas pre-treatment column for use as a Flue Gas Desulphurisation (FGD) unit or as a Direct Contact Cooler (DCC) is available but was bypassed for FOCUSS. The absorber columns are equipped with 2 beds of 3m Koch-Glitsch Flexipac 350X structured packing (with a maximum total height of 12 m), with liquid re-distribution above each bed. The desorber is packed with 7 m of Koch-Glitsch IMTP25 random packing. Each column has six temperature measurement points for temperature profiling. CO_2 product leaving the desorber is cooled in a condenser prior to analysis and venting. A blower is used to drive the gas through the plant, while Fourier-transform infrared spectroscopy (FTIR) is used for gas analysis. For this test campaign, synthetic flue gas consisting of atmospheric air with added CO_2 was used.

2.2. Background Tests – PCC CARER

A prior project funded by the UKCCSRC, SSE Thermal and Bechtel and delivered by the University of Sheffield, Post-Combustion Capture – Cost and Residual Emission Reduction (PCC - CARER) (4), undertook a suit of test runs (Figure 3 & Table 1) at the ACP with the aim of exploring the plant parameters and control philosophy required to obtain CO_2 capture levels above 95% while achieving high rich loadings (> 0.45 mol/mol) using an 35% wt. MEA

solvent with lower lean loadings than previously reported (< 0.15 mol/mol). This campaign provided a number of learnings which were incorporated into the design of the plant upgrades for FOCUSS, namely the very high sensitivity of CO_2 capture fraction to lean solvent flow rate and loading when achieving ultra-high capture fractions. This provides a strong operational incentive for solvent storage as it ensures an uninterrupted supply of solvent at the required, low lean loading independent of desorber operation.

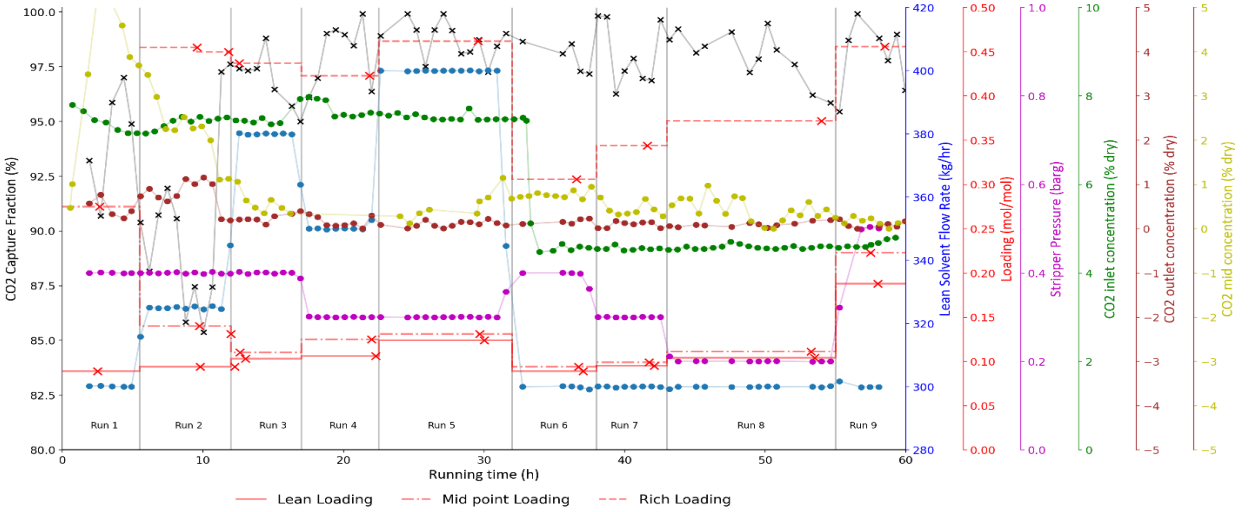


Figure 3: PCC - CARER Test Campaign, Mid-point loading and CO_2 mid concentration taken between absorber columns

Table 1: PCC - CARER Runs Summary

#	Lean flow (kg/hr)	Lean loading (mol /mol)	Rich loading (mol/mol)	Inlet CO_2 (dry %)	Outlet CO_2 (dry %)	Gas flow (Nm^3/hr)	Capture Rate
1	325.1	0.159	0.455	7.40	1.16	207.7	85.34%
2	325.6	0.108	0.450	7.42	0.20	208.5	97.49%
3	380.0	0.135	0.437	7.43	0.01	209.4	99.84%
4	350.1	0.093	0.423	7.53	0.08	208.5	98.98%
5	400.2	0.181	0.462	7.46	0.22	209.4	97.25%
6	300.0	0.081	0.306	4.52	0.14	209.8	97.03%
7	299.8	0.113	0.344	4.53	0.04	209.3	99.19%
8	300.1	0.139	0.372	4.58	-0.01	209.7	100.26%
9	300.0	0.229	0.456	4.90	0.35	207.1	93.27%

2.3. Amine Capture Plant Upgrades

Before undertaking FOCUSS testing, the TERC ACP was upgraded to include solvent storage. A detailed design process was undertaken with the aim of imposing minimal impact on the design of the ACP while allowing the completion of the test program. The upgrades were moderate and unobtrusive in nature and included the installation of intermediate bulk containers (IBC) for lean (providing an equivalent run time of circa 7.5 hours at minimum flow) and rich solvent storage, temporary pipework and a high temperature pressurized hot water (PHW) heater to facilitate higher temperature reboiler operation (Figure 4).

2.4. Operational Data – CCGT

During the start-up sequence of the heat recovery steam generator (HRSG) in a CCGT, steam is produced at various pressures that cannot be admitted to the steam turbine(s) (ST). This is typically depressurized and dumped into the main condenser until steam quality is reached and warming of the ST is completed. At this point power generation from the ST commences and the quantity of steam bypassed to the condenser gradually decreases as the ST reaches full load. For a given CCGT the timing, quantity and duration of this steam dumping process is dependent on the type of start being completed i.e. hot, warm or cold as defined by the time since the last operation. In a CCGT that uses PCC, this waste “early steam” could, with minor modifications to the plant, be expanded down to the operational

pressure range of the desorber reboiler, de-superheated and used to accelerate the start-up sequence of the PCC process through equipment preheating and solvent regeneration.

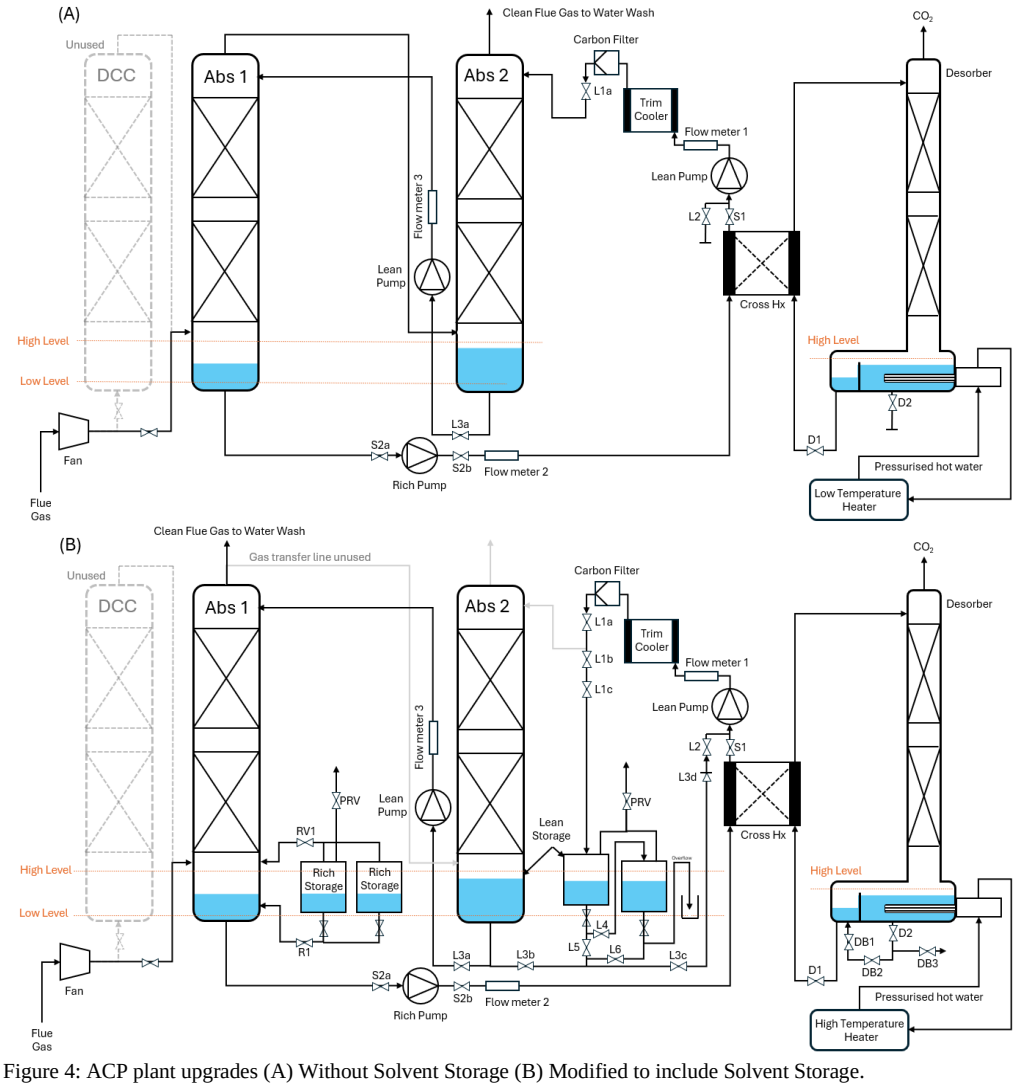


Figure 4: ACP plant upgrades (A) Without Solvent Storage (B) Modified to include Solvent Storage.
Note: As Absorber 2 was not use in this campaign the absorber sump was used to increase the quantity of lean solvent storage

Likewise, during a shutdown sequence, when steam quality in the HRSG drops to the point that it cannot be use in the ST (late steam), it could be used for further solvent regeneration rather than being dumped to the condenser. Without solvent storage, this early and late steam could be used to increase the average capture rate of a given SUSD sequence. There is, however, a mismatch between the timing of steam availability and the solvent regeneration requirements, with rich solvent storage capacity being the limiting factor. By combining the use of late/early steam with solvent storage, it can be fully utilised in an energy efficient manner and increase the average CO_2 capture rate of a SUSD event to levels comparable to baseload operation, without requiring the use of additional fuel for auxiliary steam generation, as suggested by others (2).

SSE Thermal procured 17 startup and 3 shutdown sequences from a commercial CCGT to investigate the potential for early and late steam to aid in the decarbonisation of the SUSD of a PCC. The plant data presented is normalized to 100% load, while time has been normalized to GT full load at 100%. The data was then translated into absolute figures for analysis utilizing steady state data from Elliot et al. (5), SUSD times and preheating calculation

methodology from MacKenzie et al. (3) and hold up volumes from Mullen et al. (6). Margins of 10% and 5% were assumed on the reboiler and CO_2 export capacity respectively.

3. Results

3.1. Phase 1 test program

Phase 1 of the planed test program took place in August 2023. As delivery of the stainless-steel IBCs planned for use as rich solvent storage were delayed, a bypass was installed into the weir of the desorber reboiler to facilitate complete draining of the reboiler. As a result, in this phase of the test program the desorber kettle reboiler served as a storage location for rich solvent, with an approximate capacity of 400 liters i.e. about 1hr of operation. Over 5 days of testing the following test goals were achieved, with the main limitation being the limited operating times from storage, and the need to send flue gas to the absorber before solvent. This is the reverse of what would be done in practice, and in subsequent tests in the project after dedicated rich solvent storage was available.

3.1.1. Mapping Absorber performance at constant lean loading

A novel mode of operation was demonstrated (Figure 5a) where, for a fixed flue gas flow rate and composition and a constant lean loading, the CO_2 capture fraction rises as the lean solvent flow rate increases. This occurs at a deceasing rate as the remaining concentration of CO_2 in the flue gas approaches equilibrium with the solvent. At the same time, the rich solvent loading leaving the absorber falls (Figure 5b), leading to a progressive increase in specific reboiler duty (SRD). If a higher CO_2 capture fraction is required, it is more advantageous to operate at a lower lean loading rather than at an increased solvent flow rate. Likewise, operation at low solvent flowrates is non optimal because the solvent has unused capacity to capture CO_2 at a higher fraction without a marked decrease in rich loading, and hence an increase in SRD.

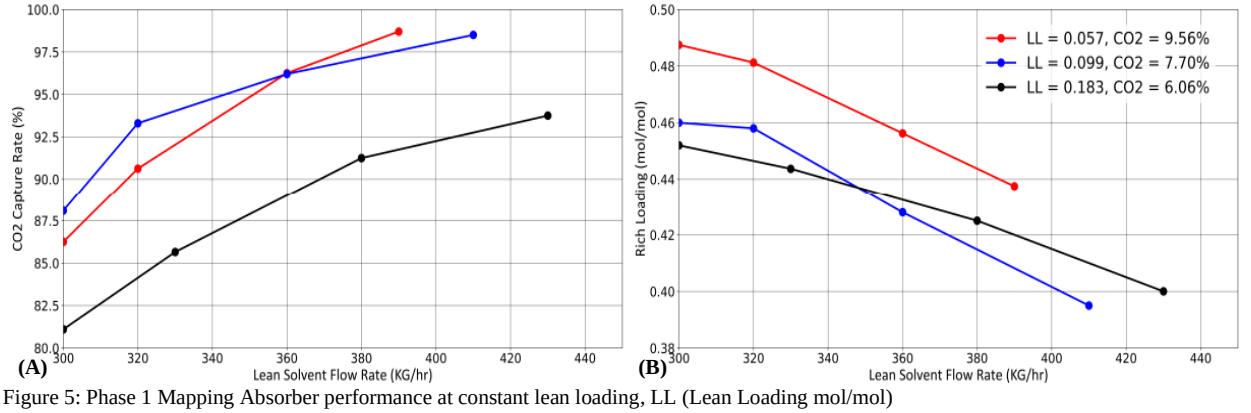


Figure 5: Phase 1 Mapping Absorber performance at constant lean loading, LL (Lean Loading mol/mol)

It is envisioned that operationally, a 'map' of absorber performance would be produced for a range of flue gas conditions, lean loadings and CO_2 capture fractions to facilitate rapid response to varying conditions. Phase 1 facilitated a first pass at completing these absorber maps, although the limited solvent storage constrained the extent to which the asymptotic approach to the lean equilibrium capture limit at higher flow rates can be explored. Further testing will expand on this.

This optimisation concept, in particular the asymptotic approach to equilibrium, has not been demonstrated in previous pilot plant studies since a flow of solvent at a constant lean loading is required. This cannot be achieved dynamically without solvent storage due to the feedback between absorber and desorber operation. Typically, an increase in solvent flowrate will result in an increase in lean solvent loading for a constant desorber heat input and pressure, if not mitigated by an appropriate change to desorber conditions, and this will eventually lead to a reduction in CO_2 capture performance. Likewise, a reduced solvent flow rate for a constant desorber heat input and pressure will result in a decreasing lean loading. This will typically result in a more gradual decrease in CO_2 capture performance than seen in Figure 5a. It should be noted, however, that there is a limit on how low the lean loading can be for a given desorber pressure; attempting to achieve lean loadings below the desorber 'inflection point' (7) leads to an exponential, and unnecessary, increase in specific reboiler duty (SRD).

3.1.2. Start-up sequence with high capture rates

An absorber start-up sequence with high net CO_2 capture rates was demonstrated. As noted in section 3.1, limited storage meant that flue gas flow was, unrealistically, started before solvent flow. Initially, lean solvent from the storage tanks was pumped to the absorber to react with the already flowing flue gas. Due to limited rich storage capacity, rich solvent was then sent to the desorber sump, with the desorber already at operational conditions. After this first phase, the flow of lean solvent from storage was stopped and lean solvent from the desorber was sent directly to the absorber, representing normal operation for a further ~ 20min. The flow from the desorber was then increased while the flow to the absorber was maintained constant, with the excess flow diverted to refill the lean tank. Post tank refill, the solvent flow from the desorber was returned to normal operational levels and the test was completed.

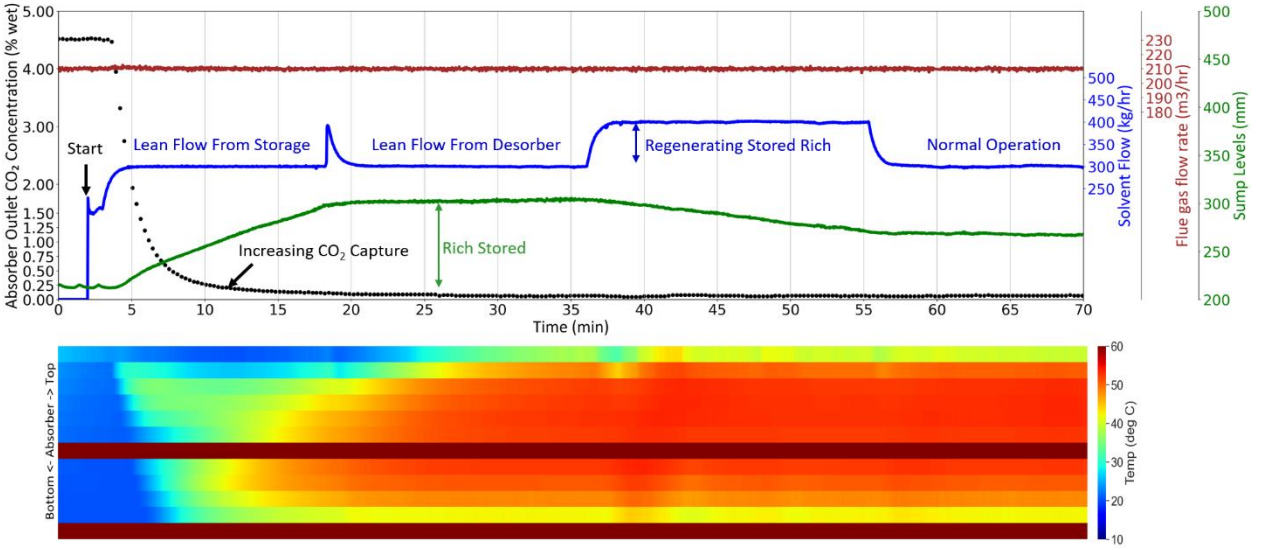


Figure 6: Phase 1 Startup Sequence

For this test a full cold startup sequence, including flue gas capture from the onset, was not possible due to limited storage capacity. All the main independent control sequences of a cold start were, however, demonstrated with high levels of CO_2 capture achieved. One lesson learned throughout the test campaign is that an in-series arrangement, rather than an in-parallel arrangement, of the tanks would provide better control as it decouples the absorption and desorption steps more effectively. It was also confirmed that the solvent flow should begin before flue gas flow to ensure prior wetting of the packing. The length of time (~15min in Figure 6) that the CO_2 capture fraction took to reach the high levels seen later in the test precludes starting the flue gas flow and lean solvent flow at the same time in practical applications.

3.1.3. Desorber start-up

A desorber start-up sequence, initially without solvent circulation (no flow of solvent in or out) and then, once operational conditions were met, switching to circulating/normal operation was completed and proved straightforward. However, the pressure control valve settings for the desorber resulted in cyclical instability, so an assessment of lean loading, and hence potentially its control via the reboiler solvent temperature, proved imprecise. Improved desorber pressure control within the limits of the existing equipment, which had not originally been an area for attention, was addressed in future tests.

3.2. Early & Late steam

A series of SUSD sequences from a commercial CCGT were provided by SSE Thermal, these were categorized into hot (< 8hrs offload), warm (8 – 64hrs offload) and cold (> 64hrs offload). Along with Gas Turbine (GT) & Steam Turbine (ST) loads, the flue gas flow rate/composition and steam flows were analysed. From this, the quantity and condition of steam that, in the early stages of startup and late stages of shutdown, is dumped to the condenser while

steam turbines are warmed, was established. Adiabatic expansion and mixing of the disparate steam sources, mainly intermediate pressure (IP) steam, was assumed and the available quantity of steam that could be utilized in the CO_2 capture plant was estimated (Figure 7).

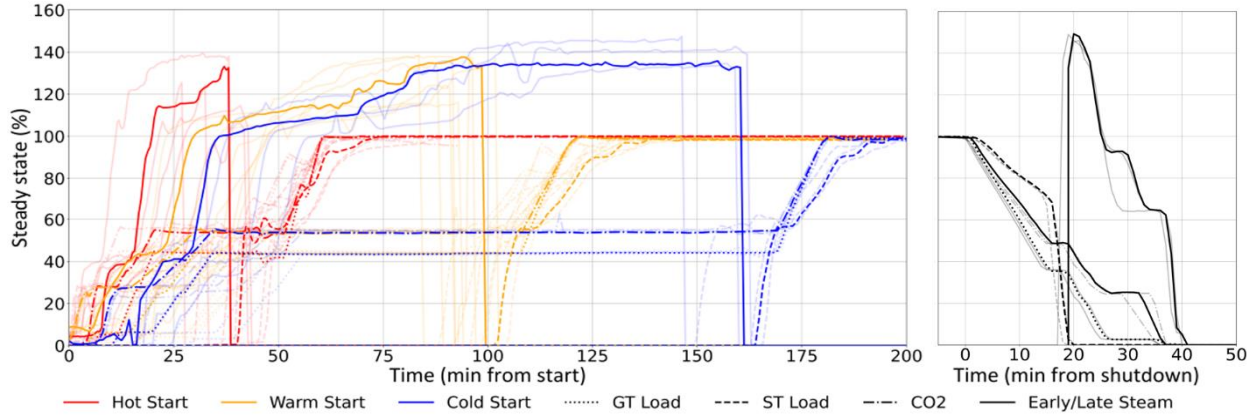


Figure 7: CCGT Startup and Shutdown Sequences

The proposed SUSD sequence described in Table 3 was modelled in Python 3.9. The outputs are presented in Figure 9 (Startup) and Figure 8 (Shutdown). Early steam is available at high levels from very early in the startup sequence (after 10-20 minutes) while late steam is available for circa 20 minutes after the ST shutdown. In both cases the available steam exceeds the design capacity of the reboiler system and, as this is steam that otherwise would have been wasted, using it in conjunction with solvent storage for stored solvent regeneration represents a substantial opportunity. When early steam is utilized, and the methodology detailed in Table 3 implemented, it is estimated that a rich solvent storage capacity of circa 50% of the total solvent inventory (equivalent to 30 minutes of full load flow as per MacKenzie et al. (3)) would be sufficient for all startup types. This compares to circa 350% without early steam (Table 2). When early steam is used, but rich solvent storage limited to the capacity of the absorber sumps, a gross CO_2 capture fraction for the startup (defined as the period before the ST reached 95% load) of just 50 – 52% for all startup types is predicted.

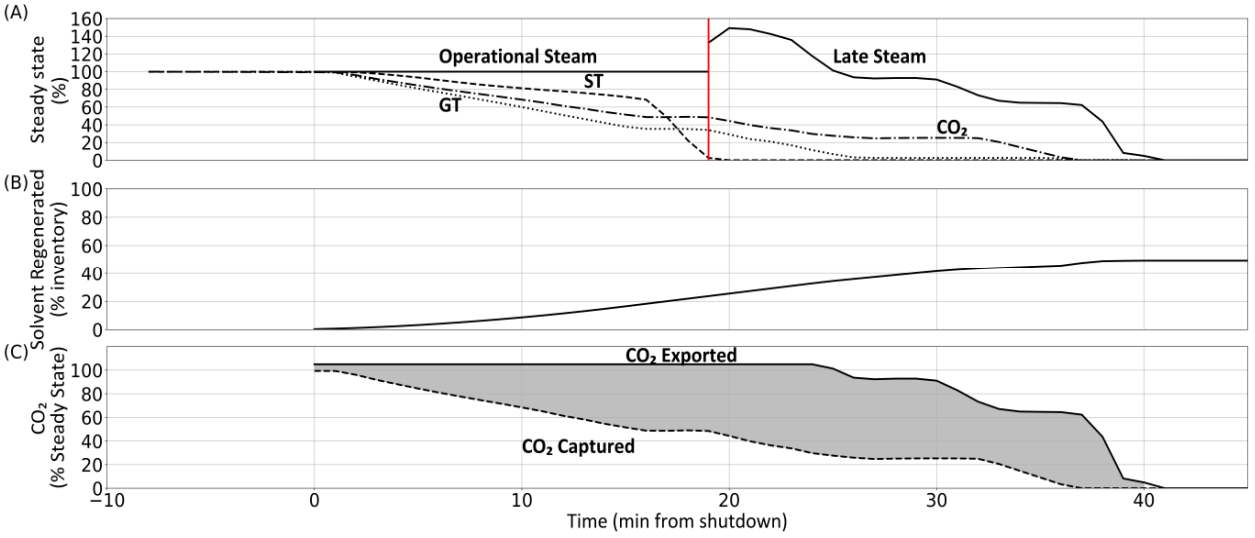


Figure 8: CCGT Shutdown analysis. 100% Solvent inventory set at a standard CCGT without additional solvent for enhanced storage (3)

For cold and warm start sequences, there is sufficient operational time at low GT load and ST bypass to allow the regeneration of all of the stored rich solvent prior to the ST reaching full load. For the hot start sequence, the initial estimates show that the time at GT part load is not long enough to fully regenerate the stored solvent. It was, however,

possible to regenerate the remaining rich solvent within 2hrs of normal operation by utilizing design margins in the regeneration and CO_2 conditioning system. It is worth noting that it may be possible to shorten the duration of additional regeneration at full load, if CO_2 quality is met earlier in the start sequence than what is assumed in this paper. CO_2 quality from the desorber is indeed likely to be higher after a shorter period without operation (hot start) than a longer one (warm or cold start), which we currently don't account for in this analysis due to the unavailability of operational data.

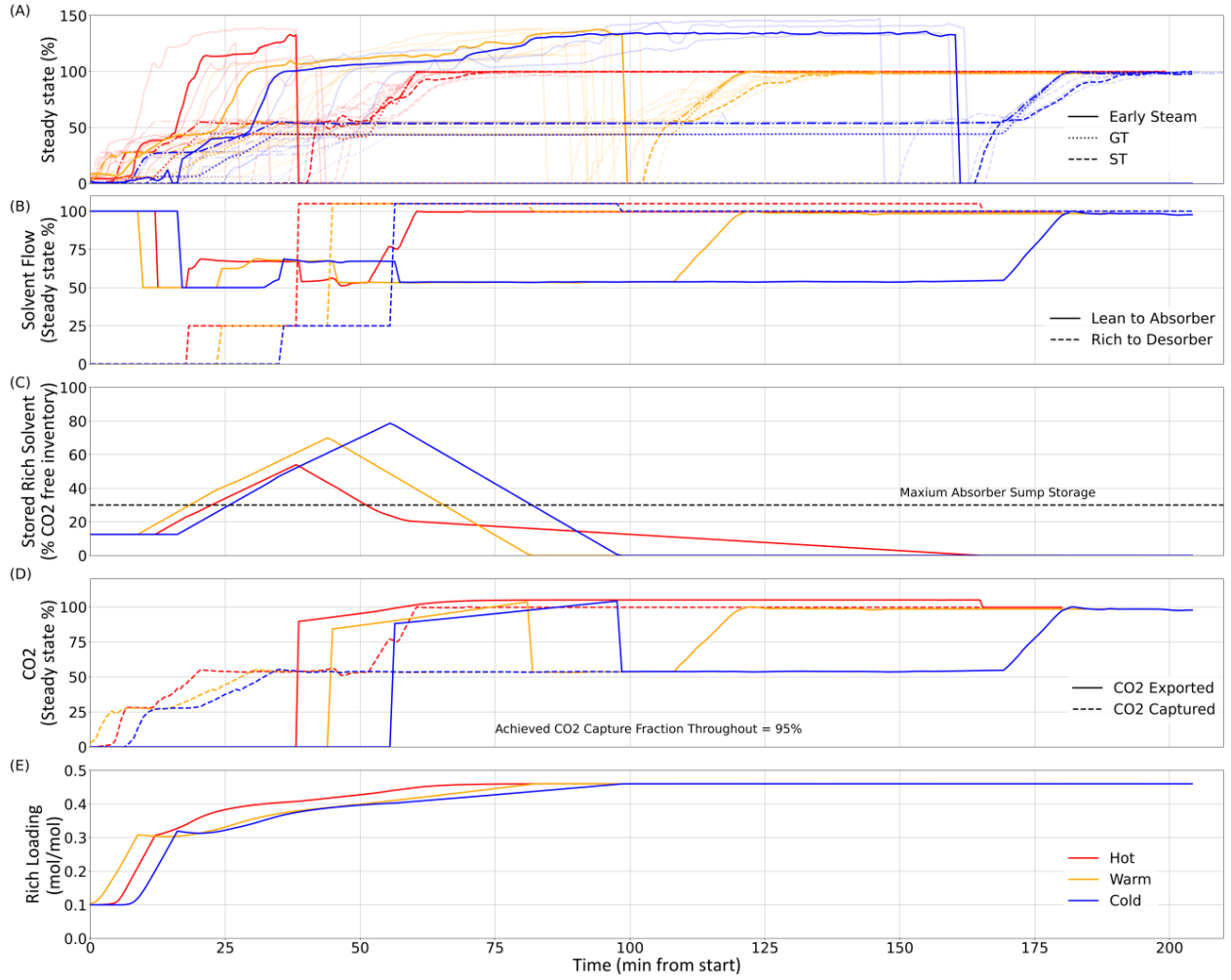


Figure 9: CCGT Start-up analysis, 9(C): storage capacity of the absorber sump (s) shown for comparative purposes, 100% Solvent inventory set at a standard CCGT without additional solvent for enhanced storage (3)

Alternatively, under normal operational circumstances this rich solvent could be maintained as inventory until a shutdown sequence is initiated and "late steam" could be utilized to complete the regeneration, indicating that all CO_2 captured during a complete SUSD sequence may be regenerated within a single sequence, with the caveat that this is very sensitive to the duration necessary to reach acceptable CO_2 quality variable. For the purpose of the analysis, a 20 minute duration from desorber reaching operational conditions was assumed in (Figure 9). For that 20 minutes, CO_2 production from the desorber is assumed conservatively to be 25% of the steady state value and is recirculated to be recaptured in the absorber. It is worth noting that the true magnitude of CO_2 production from the desorber during this 20 minute period is largely unknown, due to lack of operational data, and that additional work is required to further the understanding of this section of a start sequence. With this assumption, any duration above 15 minutes was found to require additional regeneration during operational periods, shutdown, or alternatively, an extension to the duration of the SUSD sequences.

Table 2: Solvent storage requirements with and without the use of early steam, expressed as a percentage of CO_2 free solvent inventory.

Start	Without the use of Early Steam	With the use of Early Steam
Hot	89%	24%
Warm	226%	40%
Cold	344%	49%

Several assumptions and limitations apply to the model detailed in this section. The absorption and desorption systems were modelled on a time stepped mass balance basis, CO_2 purity and the compression train were not modelled, no thermal heat-up rate limitations were placed on the equipment, perfect mixing in column sumps and solvent tanks was assumed and all systems were modelled as plug flow

3.3. Phase 2(A) test program

Installation of the rich solvent storage tanks facilitated the demonstration of a simulated startup sequence (Figure 10) in a second phase of testing, without a ramping up of the gas flow rate representative of GT operation. Building on the learnings from previous tests, the absorber packing was wetted with a flow of lean solvent prior to flue gas being admitted and CO_2 capture fractions above 90% are immediately observed. A 10-minute wait time was employed to simulate the delay in steam production from a CCGT. Maximum heat input to the desorber was then initiated until operational temperature and pressure were reached wherein heat input was modulated to maintain operating conditions. Circa 70 minutes after the test started, the rich solvent previously collected in the rich storage tank was pumped to the desorber and additional regeneration of stored solvent began. CO_2 flow started once the desorber reached operating pressure but was below the low flow limit of the flowmeter from T = circa 50 – 85 minutes. It then increased significantly when rich flow into the absorber commenced.

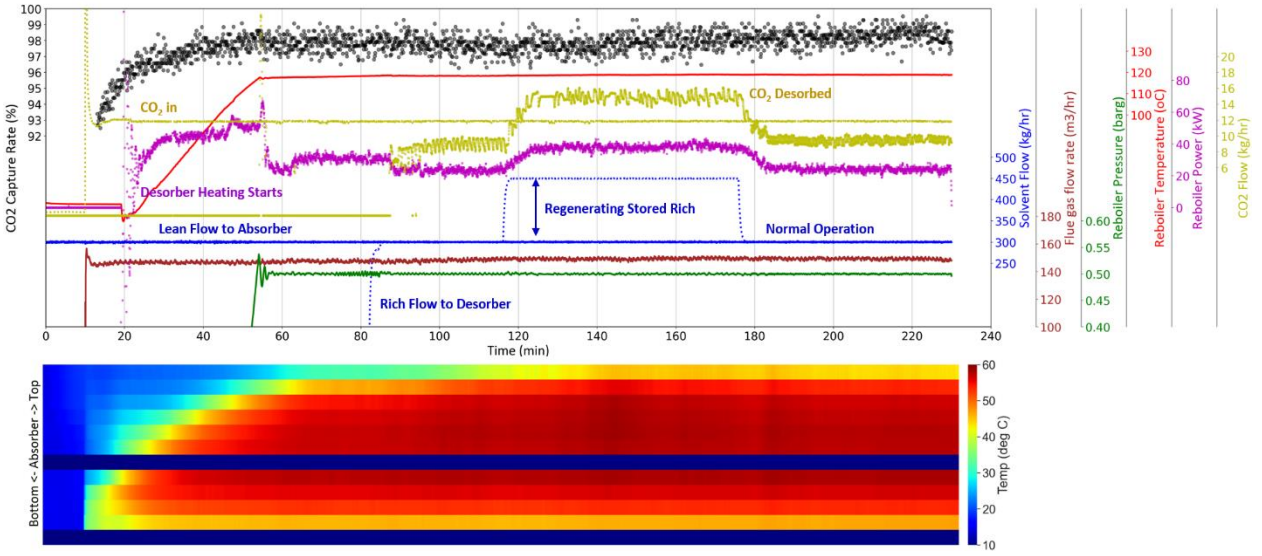


Figure 10: Phase 2 Start Sequence (2 of the temperature probes in the absorber column are non-functional)

After an hold from T = circa 85 to 115 minutes, the flow of rich solvent to the desorber was increased to simulate the regeneration of the inventory produced during the start-up, with an associated increase in reboiler heat input and flow rate of desorbed CO_2. This continues until the rich inventory is reduced to 'normal levels', after which the flow rate of rich solvent to the desorber was reduced to match the production rate in the absorber, simulating the completion of the startup sequence. Throughout this process the CO_2 capture fraction was maintained at very high levels, with a gross CO_2 capture fraction of greater than 97% once the CO_2 injection rate for the synthetic flue gas has stabilized, despite the variable operation of the desorber section.

Figure 10 also presents the temperature profiles of the absorber column throughout the test period which highlights the thermal lag present in the absorber (which may be exacerbated by evaporative cooling as unsaturated flue gas was used) and the resulting slow upward drift in the CO_2 capture fraction.

4. Conclusions & Discussion

This article describes the pilot scale plant upgrades, process modelling and test campaigns completed as part of the Flexibly Operated Capture Using Solvent Storage (FOCUSS) project to date. Two test campaigns simulating the startup of a CCGT were completed, successfully demonstrating a gross CO_2 capture fraction of greater than 97% using a 35% wt. MEA solution and solvent storage. The availability of stored lean solvent at a constant lean loading facilitates the fine control of the flowrate into the absorber that is required to achieve very high levels of CO_2 capture without excessive energy consumption. The availability of both lean and rich storage capacity decouples the absorption and desorption cycles, allowing the CO_2 capture process to be unaffected by operational changes within the desorber, at least while solvent storage capacity remains.

The authors have obtained operational data from a commercial CCGT, provided by SSE Thermal, to investigate steam production in the early and late stages of startup and shutdown. Steam produced during these periods, while the steam turbines heat up, is, in the absence of a CO_2 capture plant, typically dumped to the main condenser and is waste heat from the process. Seventeen (Six hot, seven warm and four cold) startup and three shutdown sequences are analysed to establish the quantity and timing of steam suitable for use in the CO_2 capture plant. The use of "early steam" for equipment heating and solvent regeneration during startup can reduce the rich solvent tank capacity (and the required increase in solvent inventory) required to capture 95% of CO_2 emissions during all SUSD sequences to an additional circa 50% of the solvent inventory (100% solvent inventory is defined as a standard CCGT without additional solvent for enhanced storage (3)), this compares to circa 350% without the use of early steam. When early steam is used, but rich solvent storage limited to the capacity of the absorber sumps, a gross CO_2 capture fraction of just 50 – 52% for all startup types is predicted

For warm and cold starts, the availability of early steam enables the regeneration of all stored rich solvent within the startup sequence by exploiting the unused capacity of the desorber and the compression train. For hot starts, additional solvent regeneration during normal operation or during shutdown may be required, if desorbed CO_2 recirculation is required to meet specifications on CO_2 quality in the transport and storage system.

During shutdown, it is estimated that there is unused desorber and compression capacity and sufficient surplus steam to regenerate circa 50% of the base solvent inventory, facilitating the regeneration of any remaining rich solvent from startup or the intentional delaying of solvent regeneration to maximize power output during a period of high-power prices.

Finally, drawing from the learnings of FOCUSS we propose a detailed SUSD sequence for a full scale plant (Table 3) that ensures greater than 95% CO_2 capture fractions are maintained at all times while maximizing energy efficiency and minimizing capital expenditure. It is worth noting that this work considers a single commercial CCGT and a MEA solvent, similar trends are expected for alternative solvents and CCGT models this they should be specifically investigated during the design phase on a case by case basis.

Table 3 Proposed SUSD sequence for a full scale plant

Step	Action
Pre-Startup	Majority of solvent inventory stored as lean solvent in lean storage tank(s) at or below operational lean loading, the remainder is contained in pipework, heat exchangers and column sumps. Desorber and absorber sumps and rich storage tank at minimum level. Desorber kept warm by electric trace heating and maintained above atmospheric pressure using CO_2 or N_2. Reboiler isolation valves closed. CO_2 compression and conditioning system stored under CO_2.
Instruction to Start	Prior to GT firing, lean solvent flow from lean storage tank(s) to absorber starts at minimum level to wet packing, with lean solvent accumulating in the absorber sump.
GT ramping up to 25% load	Flue gas enters absorber, lean flow from storage tank(s) is stopped. The hold up volume in the absorber is recirculated at full flow to increase rich loading to the point where CO_2 capture fractions begin to drop from > 95% to < 95%. Reduce the quantity of flow recirculated from the absorber sump and restart the flow of solvent from the lean storage tank(s). The aim is now to maintain CO_2 capture fraction while achieving a high rich solvent loading (>0.4mol/mol). Reduce solvent flow rate to the liquid distributor minimum turndown level and gradually reduce the ratio of recirculation from the absorber sump to transition full operation from the lean storage tank(s).
GT ramping from 25 to 50% load Early Steam available	Open reboiler isolation valves, admit maximum levels of steam to reboiler to bring system to operating conditions, recirculate desorber sump contents to the rich solvent liquid distributor. CO_2 capture continues to be achieved using stored lean solvent.

GT @ ~ 50% load	Match lean solvent flow rate to GT flue gas flow rate to maintain CO_2 capture fraction. Rich solvent from absorber sump should be pumped to desorber at a low flow rate and, once at the appropriate lean loading, lean solvent from desorber sump is pumped to the lean storage tank(s). Once CO_2 is being produced from the desorber column, begin recirculation of CO_2 through LP compression and conditioning system and back to the absorber until CO_2 quality is confirmed, utilise minimum steam flow to minimize CO_2 generation rate, and by extension the amount of CO_2 to be recaptured. Operate HP compressor (if present) in full recycle. When CO_2 quality is met, begin export. Increase the drawdown from rich storage to full flow rates, increase reboiler steam flow rate to the maximum and utilize the full CO_2 export capacity. Warming of steam turbines completed, steam bypass gradually reduces, power generation from steam turbines increases
GT @ 100% load	If the full volume of stored rich solvent has not been regenerated during the startup sequence it can continue to be regenerated alongside normal operation using any excess CO_2 export capacity. Absorber and desorber sump should be maintained at minimum levels during normal operation.
Shutdown initiated GT @ > 50% load	If stored rich solvent is available through the intentional delay of regeneration (to maximize power output) or any carryover from startup, operate desorber at full flow, maximizing draw down of rich solvent.
GT @ < 50% load	Shut off flow of rich solvent form the absorber sump to the rich storage tank (s), begin recirculation of the absorber sump contents (should be at a low level), increasing the recirculation flow rate while reducing the flow of additional lean solvent to absorber. The aim is to minimize lean solvent use, maintain > 95% CO_2 capture and maximize absorber sump loading.
GT @ 0% load	Utilize any residual steam to lean out the remaining rich solvent inventory as much as possible, drawing down the absorber sump level if required.
Available Steam Ends	Shut of CO_2 compressors and isolate. Isolate reboiler and if required purge desorber of CO_2 and pressurize with N_2, begin warm keeping.

5. Future Work

Further testing at the TERC ACP is planned for November ’24, while concurrent testing at the Haifeng Power Plant Carbon Capture Test Platform will be completed and demonstrate the solvent storage concept at a 50tpd scale. Upon project completion March ’25 a final report will be published.

Acknowledgements

The Flexible Operated Capture Using Solvent Storage (FOCUSS) project is funded by the UK Department for Energy Security and Net Zero (DESNZ) under the Carbon Capture, Usage and Storage (CCUS) Innovation 2.0 Programme. SSE Thermal, AECOM and the University of Sheffield provided in-kind support. The authors have licensed this work under a Creative Commons Attribution (CC BY) license for open access.

References

1. Global CCS Institute. Global Status of CCS 2023 – Report & Executive Summary [Internet]. [cited 2024 Jun 13]. Available from:https://www.globalccsinstitute.com/resources/publications-reports-research/global-status-of-ccs-2023-executive-summary/
2. Bui, M, Nixon, S, Mac Dowell, N. The prospects of flexible natural gas-fired CCGT within a green taxonomy. iScience 26, 107382, August 18, 2023. 10.1016/ j.isci.2023.107382
3. MacKenzie K, Calvert J. Start up and shut down times of power carbon capture, usage and storage (CCUS) facilities [Internet]. 2020 [cited 2024 Jun 14]. Available from: https://www.gov.uk/government/publications/start-up-and-shut-down-times-of-power-carbon-capture-usage-and-storage-ccus-facilities
4. Gibbins J, Akram M, Mullen D, Pokora M, Pourkashanian M, Samson A. PCC – CARER: Post-Combustion Capture – Cost and Residual Emission Reduction (Flexible Funding 2021) [Internet]. 2021 [cited 2024 Aug 18]. Available from: https://ukccsrc.ac.uk/blog_posts/pcc-carer-post-combustion-capture/
5. Elliott B. Front-End Engineering Design (FEED) Study for a Carbon Capture Plant Retrofit to a Natural Gas-Fired Gas Turbine Combined Cycle Power Plant (2x2x1 Duct-Fired 758-MWe Facility With F Class Turbines) [Internet]. Reston: Bechtel; 2022 Mar. Available from: https://ukccsrc.ac.uk/open-access-sherman-feed/
6. Mullen D, Braakhuis L, Knuutila HK, Gibbins J, Lucquiaud M. Monoethanolamine Degradation Rates in Post-combustion CO_2 Capture Plants with the Capture of 100% of the Added CO 2. Ind Eng Chem Res. 2024 Aug 7;63(31):13677–91.
7. Michailos S, Gibbins J. A Modelling Study of Post-Combustion Capture Plant Process Conditions to Facilitate 95–99% CO2 Capture Levels From Gas Turbine Flue Gases. Front Energy Res [Internet]. 24 May 2022. 2022 May 24;10. Available from: https://www.frontiersin.org/articles/10.3389/fenrg.2022.866838/full

7.1 Conclusion

Two test campaigns simulating the start-up of a CCGT were completed as part the project at the time of writing, these campaigns successfully demonstrated a net CO_2 capture fraction of circa 97% using a 35% wt. monoethanolamine (MEA) solution and solvent storage, providing valuable evidence to the industry on the viability of abating CO_2 emissions from SUSD events

Of particular note is the topic of “early” and “late” steam, which is the authors primary novel contribution. Operational data detailing 17 start-up sequences (6 hot, 7 warm and 4 cold) and 3 shutdown sequences were procured from a commercial CCGT. Through analysis of this data, it was established there is a large quantity of steam that, during a SUSD sequences would be dumped to the condenser as cannot be admitted to the steam turbine, is available for use for equipment heating and solvent regeneration in the PCC. Use of this early and late steam is predicted to accelerate the start-up times of the PCC to the point that all rich solvent generated during the SUSD can be regenerated within said SUSD event, primarily using previously wasted steam. This is estimated to reduce the required rich solvent tank capacity (and additional solvent inventory) to circa 50% of the solvent inventory, this compares to circa 350% without the use of early steam. When early steam is employed but solvent storage is limited to the capacity of the absorber sumps the gross CO_2 capture fraction for a startup (defined as the period before the gas turbine load is above 99%) is predicted to be 72, 80 and 83% for a hot, warm and cold start respectively, a substantial increase over previous assumptions (Calvert and MacKenzie, 2020). However, achieving the ultra-high CO_2 capture fractions required for net zero operation was not possible without increased solvent storage.

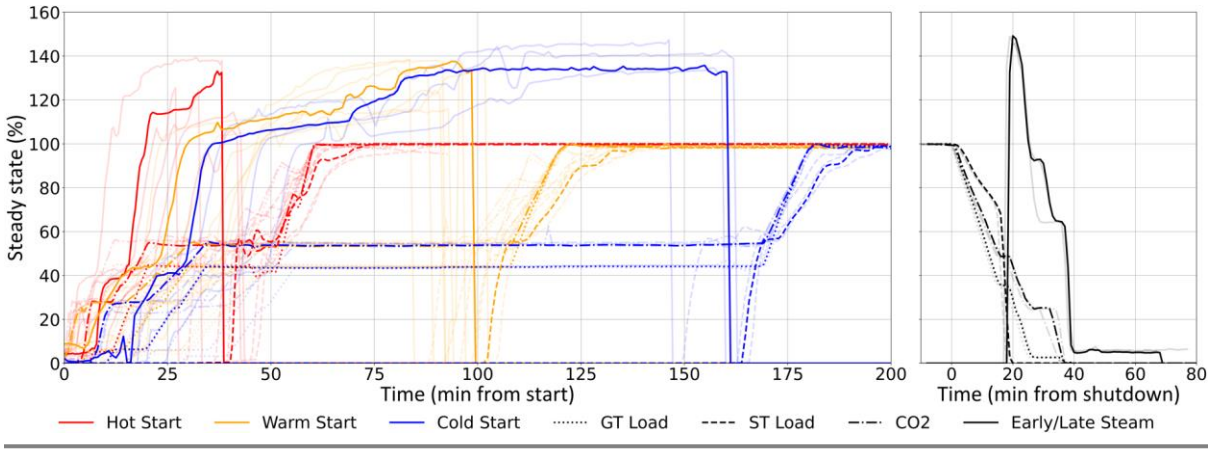


Figure 17: Availability of steam during CCGT Startup and Shutdown Sequences

There may even be scope to intentionally delay the regeneration of operational rich solvent (temporarily maximizing the power output of the plant) until shutdown. This is because there

is the capacity to regenerate an estimated 50% of the solvent inventory using “late” steam, further demonstrating the economic benefits available to flexible CCS plants using solvent storage.

7.2 Highlights

- Pilot plant scale demonstration of net CO_2 capture fractions greater than 95% during simulated start up events using a 35% wt. MEA solution.
- Use of “early” and “late“ steam during start up and shutdown reduces rich solvent storage and additional solvent inventory requirements from 350% to just a 50% increase in the base inventory.
- Rich solvent regeneration predicted to be completed within the start-up and shutdown events, primarily using waste heat.

7.3 Limitations and Future Work

The following limitations were identified for the work described in this chapter; any future work should endeavour to resolve these limitations:

- Absorption and desorption systems were modelled on a time stepped mass balance basis and were not dynamically modelled
- CO_2 conditioning and the compression train were not modelled with the time taken for CO_2 exiting the desorber to meet export quality a key unknown with the results of the modelling study highly sensitive to this variable. Future work should endeavour to close this knowledge gap.
- Although not discussed in this work additional solvent degradation during storage is often considered a potential limitation for the implementation of solvent storage. Chapter 6 of this thesis investigates solvent degradation for an MEA solvent and demonstrates that due to the rapid kinetics of the oxidative degradation reaction equilibrium is reached very rapidly and, assuming no further dissolution of O_2 occurs, effectively ceases. This indicates that if contact with O_2 rich air is limited, though N_2 caping in the storage tank or minimising head space, solvent storage is not expected to notably increase the rate of solvent degradation for an MEA solvent. This should however be further investigated as this may not be the case for alternative, less reactive solvents.

- A technoeconomic assessment to quantify the CO_2 abatement cost of increasing SUSD CO_2 capture fractions using early/late steam and solvent storage was not within the scope of this work and could be investigated in future work.

8. Conclusions & Discussion

This thesis investigates the technical and economic feasibility of post combustion capture plants (PCC) operating under a regime that is compatible with global net zero ambitions, and to the knowledge of the author, represents the most complete body of work on this topic to date.

For PCC to be compatible with Net Zero, just one condition must be met:

All of the greenhouse gases, or the equivalent amount of CO_2, attributed to the lifecycle of the facility must be captured, or recaptured in a timely fashion, and permanently sequestered. Or the equivalent amount of fossil CO_2 emissions avoided if the CO_2 is utilised in a downstream process

The first step in achieving this is to increase the historical target to capture 90% of the CO_2 entering the absorber up to its economic limit. Under the assumption of Net Zero, where no CO_2 emitted from industrial operations can remain in the atmosphere, the economically optimal CO_2 capture fraction is simply the point at which it is more expensive to capture the CO_2 than to recapture it via permanent negative emission technologies (NET). As it stands this point is not easy to define due to the limited deployment of high-quality NETs and in any event is likely to change as the cost of NETs decrease as deployment increases.

For the purpose of this thesis the point at which no additional CO_2 is added to the atmosphere from direct operations, i.e., where the capture of all produced CO_2 is achieved, is chosen as an appropriate placeholder. This is termed as 100% fossil CO_2 capture, all other CO_2 fractions referenced are reported as gross values i.e., CO_2 entering vs CO_2 leaving the absorber.

Chapters 3 and 4 present the first comprehensive techno-economic assessments of a steam methane reformer (SMR) and combined-cycle gas turbine (CCGT), demonstrating that operation at 100% fossil CO_2 capture fractions are not only technically feasible but economically viable. While Chapter 5 presents a novel integration method for the combination of the CCGT and SMR processes into a “Combined Fuel and Power” (CFP) plant also operating at a 100% fossil CO_2 capture fraction.

In all cases increasing CO_2 capture fractions from 90 – 95% gross to 100% fossil rates required three distinct but moderate design modifications[8]:

[8] Results presented are for an open art 35% wt. MEA solvent however are expected to be broadly applicable to alternative solvents, noting that the absolute values will vary.

- **A minimum of 16 – 20m of absorber packing and up to 24m:** Exact value is dependent on the CO_2 concentration in the flue gas and lean loading utilised however this represents an increase of typically circa 4m over "standard designs". This increases the residence time of the solvent with the flue gas to be treated, ensuring sufficient absorption of CO_2 even at very low partial pressures. It's worth noting that this may not represent a substantial CAPEX increase if the same number of absorber beds can be maintained, i.e. 2 X 10m beds vs 2 X 8m.
- **Reduced lean solvent loadings:** Reducing lean loadings from 0.20 – 0.25 mol/mol to circa 0.10 – 0.16 mol/mol, in conjunction with any increased packing hight will ensure increased diving force of absorption in the upper portions of the absorber.
- **Increase Regeneration Pressures:** To efficiently achieve the required decrease in lean loading an increase in the operating pressure of the desorber will be required (210 – 275KPa vs 170 – 190KPa), with an associated and unavoidable increase in reboiler temperatures (125 - 135°C vs 115 – 125°C) which may impact solvent management requirements (ref Chapter 6).

When theses process modifications were implemented the increase in key process indicators; specific reboiler duty (SRD), capital (CAPEX) and operational (OPEX) expenditure, process efficiency and cost of production was found to increase in an approximately (or below) linear rate with increasing CO_2 capture fraction (Table 7), in contrast to the exponential increase that was previously assumed by the existing literature.

Table 7: Impact on key plant indicators from increasing the CO_2 capture fraction from 95% gross to 100% fossil

Process	SRD	CAPEX	OPEX	Process Efficiency	Cost of Production	Marginal Cost of Capture
SMR	+1.6%	+5.3%	+4.3%	-1.9% point (HHV)	LCOH = +3.6%	184 £/tCO_2
CCGT	+4.2%	+3.9%	+0.6%	-0.5% point (LHV)	LCOE = +2.0%	197 £/tCO_2
CFP	+6.1%	+3.1%	+2.8%	-0.5% point (2nd Law)	IRR = +0.3% point	

Likewise, the marginal capture cost (the average cost per ton of additional CO_2 captured) of increasing CO_2 capture fractions from 95% gross up to 100% fossil capture rates is presented in Table 7. At 184 £/tCO_2 for a CCGT and 197 £/tCO_2 for an SMR, this compares favourably to the recent cost estimate for direct air capture of 275 £/tCO_2 (175 – 447 £/tCO_2) (Sievert et al., 2024) assuming a 1 GtCO_2 per year deployment scale. The above process modifications are shown to effectively limit the increase in energy penalty and CAPEX required to achieve 100% fossil CO_2 capture. However, although moderate in nature, represent unexplored process conditions that may result in a change in the observed solvent degradation rate. This is because monoethanolamine (MEA) will degrade when exposed to oxygen-rich atmospheres (oxidative degradation), therefore increase exposure time in the absorber is thought to increase this, and high temperatures (thermal degradation) as the carbamate in the solvent polymerises, however the decreased carbamate concentration in lean solvent solutions may limit the effect somewhat despite the increase in regeneration temperature.

Chapter 6 provides the first body of evidence on this subject by using a newly developed solvent degradation framework (Braakhuis, Høisæter and Knuutila, 2022; Braakhuis and Knuutila, 2023) for MEA to compare the predicted solvent degradation rate for three industrial processes, the SMR, CCGT processes as described in Chapters 3 and 4 and including an Energy from Waste (EfW) plant (Su *et al.*, 2023) to cover the expected range of O_2 (1.2−11.0 vol %) and CO_2 concentrations (4.7−19.5 vol %) relevant in PCC applications.

Over the three processes analysed, increasing CO_2 capture fractions from 95% gross to 100% fossil CO_2 capture increase specific degradation by between 21 and 112%, primarily due to the increased rate of thermal degradation in the regeneration section which is predicted in increase thermal degradation by a factor of 3 to 4. However, as MEA is a low-cost solvent (circa 0.5 – 5£/kg) the effect on plant economics is predicted to be minimal with an estimated increase in OPEX due to additional solvent replacement of between 0.02−0.38 £/tCO_2.

In addition to this first of a kind analysis a number of additional insights are reported:

- Relative insensitivity is observed to flue gas O_2 concentration with similar rates of degradation observed across all 3 flue gases analysed, this is an entirely novel observation as the current view is that high O_2 concentrations in flue gas such as CCGTs will have a detrimental effect on solvent stability. However, due to the low CO_2 concentration in the flue gas a lower average temperature throughout the absorber is observed which limits rate of the oxidative reaction.
- By the same virtue intercooling of the solvent and thus reducing the average temperature of the flue gas in the absorber was found to have a strong dampening effect on the oxidative degradation reaction across all cases with reductions in specific degradation of the order of 30-70% observed.
- Oxidative degradation rates in the absorber sump (or external storage tank) were found to be minimal, however strongly dependant on the degree of continued O_2 exposure, as the dissolved O_2 present in the solvent when leaving the absorber packing is rapidly consumed, reaching equilibrium levels. Reducing the exposure to O_2 in external storage tanks though limited head space or N_2 caping would likely serve to arrest continued degradation

While Chapter 4 of this thesis provides evidence that CCGTs can operate economically at 100% fossil CO2 capture, this analysis is limited to steady state operations. For CCGTs to operate as critical backup and support to intermittent renewable power generation they will be required to operate flexibly, with frequent load changes and start-up and shutdown (SUSD) events while maintaining CO_2 capture fractions similar to that of steady state values.

Capture 7 details the authors contribution to a project that demonstrated a net CO_2 capture fraction of circa 97% using a 35% wt. monoethanolamine (MEA) solution by utilising an advanced solvent storage scheme. Of particular note is the topic of “early” and “late” steam, which is the authors primary novel contribution.

Operational data detailing 17 start-up sequences (6 hot, 7 warm and 4 cold) and 3 shutdown sequences were procured from a commercial CCGT. Through analysis of this data, it was established there is a large quantity of steam that, during a SUSD sequences would be dumped to the condenser as it cannot be admitted to the steam turbine, is available for use for equipment heating and solvent regeneration in the PCC. Use of this early and late steam is predicted to accelerate the start-up times of the PCC to the point that all rich solvent

generated during the SUSD can be regenerated within said SUSD event, primarily using previously wasted steam. This is estimated to reduce required rich solvent tank capacity (and additional solvent inventory) to circa 50% of the solvent inventory, this compares to circa 350% without early steam. When early steam is employed but solvent storage is limited to the capacity of the absorber sumps the gross CO_2 capture fraction for a startup (defined as the period before the gas turbine load is below 99%) is predicted to be 72, 80 and 83% for a hot, warm and cold start respectively, a substantial increase over previous assumptions (Calvert and MacKenzie, 2020). However, achieving the ultra-high CO_2 capture fractions required for net zero operation was not possible without increased solvent storage.

Zero direct CO_2 emissions from operation is not, however net zero. Upstream, downstream and construction emissions, although not dominant, are a non-trivial portion of the lifecycle emissions of energy production facilities, in particular GHG emissions from the natural gas supply chain. And of course, as the facility decarbonises with ever increasing CO_2 capture fractions, they become the dominant component of the remaining lifecycle emissions. This thesis proposes the timely recapture of any remaining lifecycle emissions, using an appropriate NET, once all direct emissions from the facility are captured. For the purpose of the analysis, direct air CO_2 capture and storage (DACCS) with median cost of 300 £/tCO_2 (100 – 1000 £/tCO_2) is assumed as the likely highest cost NET, serving as an upper bound on the estimate.

Greenhouse Gas (GHG) emissions from the natural gas supply chain, CO_2 transport and storage network, and plant construction/decommissioning are estimated from the available literature while a new metric, advocated for using with short lived GHGs like CH_4 by the Intergovernmental Panel on Climate Change (IPCC), GWP* was used to estimate the CO_2e emissions resulting from methane leakage from the natural gas supply chain.

For the CCGT and SMR processes, the cost of recapturing upstream and downstream emissions resulted in a 9% (SMR) and 29% (CCGT) increase in production cost, for the median cost of DACCS and global average natural gas supply chain emission rate of 1.5%, however high degrees of sensitivity was observed for both these variables.

Future Work

"Every milestone in research is but a signpost on a road that stretches on indefinitely."

Anonymous

Throughout this thesis a number of limitations with the competed work has been highlighted, with recommendations made for areas of further development, these are summarised below:

- Operational experience from pilot and/or commercial plants operating at 100% fossil CO_2 capture fractions should be obtained and used to revalidate process models to a wider range of parameters.
- The lifecycle studies for CCGT and SMR processes should be extended to investigate the effect of additional GHG not covered by this work (SF_6, NO_X), the GWP of H_2 leakage, and the effect of establishing a H_2 transport and storage network.
- Long term (greater than 12 months of continuous operation) campaigns with thermal reclaiming should be completed using an MEA solvent at the operation conditions suggested in this thesis. This will provide further validation for the model presented in Chapter 6 and advise the rate of solvent degradation that can be expected when operating at 100% fossil CO_2 capture fractions.
- Further studies should investigate dynamic operations of the CFP configuration to establish the capacity to vary the production rate of each energy vector to match market demands
- A technoeconomic assessment to quantify the CO_2 abatement cost of increasing SUSD CO_2 capture fractions using early/late steam and solvent storage should be completed.
- Chapter 7 identified that the time taken for CO_2 exiting the desorber to meet export quality during start-up as a key unknown. Future work should model the CO_2 compression and conditioning system.

Summary

Prior to commencement of this work a number of key gaps in the state of the field, i.e. utilising CCS as an effective climate change mitigation technology, were identified. These are summarised below:

- There was limited evidence detailing the effective process design for PCC plants operating at 100% fossil CO_2 capture fractions. This led to repeated predictions of rapidly increasing costs as capture fractions increase.
- The economic impacts of a mandate to recapture scope 2 and 3 GHG emissions from energy conversion processes had not been quantified.
- Combined fuel and power plants (CFP) had been proposed but with limited and inefficient integration.
- Increased MEA degradation rates due to the modified regeneration conditions and increased absorber residence time required to efficiently achieve 100% fossil CO_2 capture was often considered a barrier. However, no quantitative analysis had been completed.
- CO_2 capture during start-up and shutdown (SUSD) was considered impractical and costly. This would limit the effectiveness of decarbonised CCGTs to operate in a dynamic energy market while maintaining high net rates of CO_2 abatement.

The work presented in this thesis goes some way towards resolving these knowledge gaps, with a summary of the novel contributions and how they pertain those gaps detailed below:

- First comprehensive body of work detailing the process and economic conditions required to make 100% fossil CO_2 capture economically competitive, demonstrating that 100% fossil CO_2 capture is already economically incentivised in the UK. Provides clear and achievable design recommendations to do so.
- Scope 2 & 3 emissions are quantified and the recapture using direct air CO_2 capture (DACCS) is costed, providing evidence for the development of policy mechanisms to incentivise it.
- Clear process improvements to CFP plants are identified and costed. Demonstrating increased efficiency and profitability over independent generation.
- The effect increasing CO_2 capture fractions has on MEA degradation was predicted. Clear and apparently effective mitigation strategies were identified.
- Demonstrated a commercially available and cost-effective method to achieve high rates of CO_2 capture during SUSD through pilot plant test campaigns. The first body of evidence to propose, and quantify the benefit of, using of previously dumped steam

during the startup and shut down sequences for CO_2 capture, with the scope for substantial cost reductions and increase efficiency.

The analysis contained in this thesis not only provides critical insights into the process conditions required to ensure that 100% fossil CO_2 capture is achieved with a minimal increase in specific energy demand but demonstrate that the impact on the economics of the process is much lower than previous assessments have concluded. Likewise, although high sensitivity to the emission assumptions and economic parameters were observed, this thesis provides a first of a kind analysis on the true cost of producing truly net zero hydrogen and electricity from natural gas with the recapture and permeant storage of all remaining lifecycle GHG emissions.

9. References

ACC (2024) *Aker Carbon Capture*. Available at: https://akercarboncapture.com/ (Accessed: 14 June 2024).

Ajanovic, A., Sayer, M. and Haas, R. (2022) 'The economics and the environmental benignity of different colors of hydrogen', *International Journal of Hydrogen Energy*, 47(57), pp. 24136–24154. Available at: https://doi.org/10.1016/j.ijhydene.2022.02.094.

Allam, R. *et al.* (2017) 'Demonstration of the Allam Cycle: An Update on the Development Status of a High Efficiency Supercritical Carbon Dioxide Power Process Employing Full Carbon Capture', *Energy Procedia*, 114, pp. 5948–5966. Available at: https://doi.org/10.1016/j.egypro.2017.03.1731.

Allen, M.R. *et al.* (2018) 'A solution to the misrepresentations of CO2-equivalent emissions of short-lived climate pollutants under ambitious mitigation', *npj Climate and Atmospheric Science*, 1(1), p. 16. Available at: https://doi.org/10.1038/s41612-018-0026-8.

Aronu, U. E., Gondal, S., Hessen, E. T., Haug-Warberg, T., Hartono, A., Hoff, K. A., & Svendsen, H. F. (2011). Solubility of CO2 in 15, 30, 45 and 60 mass% MEA from 40 to 120 °C and model representation using the extended UNIQUAC framework. Chemical Engineering Science, 66(24), 6393–6406. https://doi.org/10.1016/j.ces.2011.08.042

Arcadis (2020) *International Construction Costs 2020*, *International Construction Costs*. https://connect.arcadis.com/: The Organisation. Available at: https://www.arcadis.com/en/knowledge-hub/perspectives/global/international-construction-costs.

ASPENtech (2022) *ASPEN PLUS V10 [internet]*. The orginisation. Available at: https://www.aspentech.com/en/products/engineering/aspen-plus.

Augustsson, O. *et al.* (2017) 'Chilled Ammonia Process Scale-up and Lessons Learned', *Energy Procedia*, 114, pp. 5593–5615. Available at: https://doi.org/10.1016/j.egypro.2017.03.1699.

Ayittey, F.K. *et al.* (2020) 'Process modifications for a hot potassium carbonate-based CO_2 capture system: a comparative study', *Greenhouse Gases: Science and Technology*, 10(1), pp. 130–146. Available at: https://doi.org/10.1002/ghg.1953.

Balcombe, P. *et al.* (2018) 'Methane emissions: choosing the right climate metric and time horizon', *Environmental Science: Processes & Impacts*, 20(10), pp. 1323–1339. Available at: https://doi.org/10.1039/C8EM00414E.

Basf (2024) *OASE® blue for Flue Gas and Post Combustion CO2 Capture*. Available at: https://energy-resources.basf.com/global/en/gas-treatment/gas-treatment-oase/OASE_blue_for_Flue_gas_industrial_CO2.html (Accessed: 14 June 2024).

Bashir, A., Ali, M., Patil, S., Aljawad, M. S., Mahmoud, M., Al-Shehri, D., Hoteit, H., & Kamal, M. S. (2024). Comprehensive review of CO2 geological storage: Exploring principles, mechanisms, and prospects. *Earth-Science Reviews*, *249*, 104672. Available at: https://doi.org/10.1016/j.earscirev.2023.104672

Bauer, C. *et al.* (2022) 'On the climate impacts of blue hydrogen production', *Sustainable Energy & Fuels*. 19 Nov 2021, 6(1), pp. 66–75. Available at: https://doi.org/10.1039/D1SE01508G.

Booras, G.S. and Smelser, S.C. (1991) 'An engineering and economic evaluation of CO2 removal from fossil-fuel-fired power plants', *Energy*, 16(11–12), pp. 1295–1305. Available at: https://doi.org/10.1016/0360-5442(91)90003-5.

Borhani, T.N.G. *et al.* (2015) 'CO2 capture with potassium carbonate solutions: A state-of-the-art review', *International Journal of Greenhouse Gas Control*, 41, pp. 142–162. Available at: https://doi.org/10.1016/j.ijggc.2015.06.026.

Bouckaert, S. *et al.* (2021) *Net Zero by 2050*. Paris. Available at: https://www.iea.org/reports/net-zero-by-2050.

Braakhuis, L., Høisæter, K.K. and Knuutila, H.K. (2022) 'Modeling the Formation of Degradation Compounds during Thermal Degradation of MEA', *Industrial & Engineering Chemistry Research*. 10 February 2022, 61(7), pp. 2867–2881. Available at: https://doi.org/10.1021/acs.iecr.1c04496.

Braakhuis, L. and Knuutila, H.K. (2023) 'Predicting solvent degradation in absorption–based CO2 capture from industrial flue gases', *Chemical Engineering Science*, 279(118940), p. 118940. Available at: https://doi.org/10.1016/j.ces.2023.118940.

Brandl, P. *et al.* (2021) 'Beyond 90% capture: Possible, but at what cost?', *International Journal of Greenhouse Gas Control*. February 2021, 105, p. 103239. Available at: https://doi.org/10.1016/j.ijggc.2020.103239.

Bukar, A. M., & Asif, M. (2024). Technology readiness level assessment of carbon capture and storage technologies. *Renewable and Sustainable Energy Reviews*, *200*, 114578. Available at: https://doi.org/10.1016/j.rser.2024.114578

Calvert, J. and MacKenzie, K. (2020) *Start up and shut down times of power carbon capture, usage and storage (CCUS) facilities*. Available at: https://www.gov.uk/government/publications/start-up-and-shut-down-times-of-power-carbon-capture-usage-and-storage-ccus-facilities (Accessed: 14 June 2024).

Calvin, K. *et al.* (2023) *IPCC, 2023: Climate Change 2023: Synthesis Report. Contribution of Working Groups I, II and III to the Sixth Assessment Report of the Intergovernmental Panel on Climate Change [Core Writing Team, H. Lee and J. Romero (eds.)]. IPCC, Geneva, Switzerland.* Edited by P. Arias et al. Available at: https://doi.org/10.59327/IPCC/AR6-9789291691647.

Campbell, matthew *et al.* (2022) 'CESAR1 Solvent Degradation and Thermal Reclaiming Results from TCM Testing', *SSRN Electronic Journal* [Preprint]. Available at: https://doi.org/10.2139/ssrn.4286150.

Capros, P. *et al.* (2014) 'European decarbonisation pathways under alternative technological and policy choices: A multi-model analysis', *Energy Strategy Reviews*, 2(3–4), pp. 231–245. Available at: https://doi.org/10.1016/j.esr.2013.12.007.

CCS Institute (2012) *CO2 CAPTURE TECHNOLOGIES*. Available at: https://www.globalccsinstitute.com/archive/hub/publications/29721/co2-capture-technologies-pcc.pdf (Accessed: 14 June 2024).

Chemical Engineering (2022) *THE CHEMICAL ENGINEERING PLANT COST INDEX [Internet]*. chemengonline.com: Chemical Engineering. Available at: https://www.chemengonline.com/pci-home.

Chen, C.-I. and Rochelle, G. (2022) 'Amine Oxidation Catalyzed by NO2', *SSRN Electronic Journal* [Preprint]. Available at: https://doi.org/10.2139/ssrn.4284295.

Chen, Z. (2022) ‘A Review of Pre-combustion Carbon Capture Technology’, in. Available at: https://doi.org/10.2991/aebmr.k.220405.086.

Christensen Larry, P.D. (2005) *COST ESTIMATE CLASSIFICATION SYSTEM – AS APPLIED IN ENGINEERING, PROCUREMENT, AND CONSTRUCTION FOR THE PROCESS INDUSTRIES*, *TCM Framework: 7.3 – Cost Estimating and Budgeting*. AACE.

Climate Watch (2024) *Historical GHG Emissions*. Available at: https://www.climatewatchdata.org/ghg-emissions?end_year=2021&start_year=1990 (Accessed: 13 June 2024).

Collodi, G. *et al.* (2017) ‘Techno-economic Evaluation of Deploying CCS in SMR Based Merchant H2 Production with NG as Feedstock and Fuel’, *Energy Procedia*, 114, pp. 2690–2712. Available at: https://doi.org/10.1016/j.egypro.2017.03.1533.

Danaci, D., Bui, M., Petit, C., Dowell Mac, N., 2021. En Route to zero emissions for power and industry with amine-based post-combustion capture. Environ. Sci. Technol. 55 (15). Available at: https://doi.org/10.1021/acs.est.0c07261.

David Menmuir *et al.* (2022) *Review of next generation carbon capture technology for industrial, waste and power sectors*. Glasgow: Department for Business, Energy & Industrial Strategy. Available at: https://www.gov.uk/government/publications/review-of-next-generation-carbon-capture-technology-for-industrial-waste-and-power-sectors.

DeHart, T.R. *et al.* (1999) ‘Solving corrosion problems at the NEA Bellingham Massachusetts carbon dioxide recovery plant’, in *Corrosion 1999 conference*. San Antonio.

Delmotte, M. *et al.* (2022) ‘Summary for Policymakers’, in *Global Warming of 1.5°C*. Cambridge, UK and New York: Cambridge University Press, pp. 1–24. Available at: https://doi.org/10.1017/9781009157940.001.

Department for Energy Security & Net Zero (2023, March 30). *Cluster sequencing Phase-2: Track-1 project negotiation list, March 2023*. Gov.uk. Retrieved March 9, 25, from https://www.gov.uk/government/publications/cluster-sequencing-phase-2-eligible-projects-power-ccus-hydrogen-and-icc/cluster-se

Dixon, J., Bell, K. and Brush, S. (2022) ‘Which way to net zero? a comparative analysis of seven UK 2050 decarbonisation pathways’, *Renewable and Sustainable Energy Transition*, 2, p. 100016. Available at: https://doi.org/10.1016/j.rset.2021.100016.

Donald, R.W. (2007) ‘Rules of Thumb’, in *Rules of Thumb in Engineering Practice*. Wiley, pp. 1–44. Available at: https://doi.org/10.1002/9783527611119.ch1.

Earth.org (2024) *A Graphical History of Atmospheric CO2 Levels Over Time*. Available at: https://earth.org/data_visualization/a-brief-history-of-co2/ (Accessed: 13 June 2024).

Elliott, B. *et al.* (2018) *Retrofitting an Australian Brown Coal Power Station With Post-Combustion Capture - A Conceptual Study*. Bechtel Infrastructure and Power Corporation.

Elliott, B. (2022) *Front-End Engineering Design (FEED) Study for a Carbon Capture Plant Retrofit to a Natural Gas-Fired Gas Turbine Combined Cycle Power Plant (2x2x1 Duct-Fired 758-MWe Facility With F Class Turbines)*. Reston: Bechtel. Available at: https://ukccsrc.ac.uk/open-access-sherman-feed/.

European Commission (2023) *National long-term strategies*. Available at: https://commission.europa.eu/energy-climate-change-environment/implementation-eu-countries/energy-and-climate-governance-and-reporting/national-long-term-strategies_en (Accessed: 14 June 2024).

Flø, N.E. *et al.* (2017) ‘Results from MEA Degradation and Reclaiming Processes at the CO2 Technology Centre Mongstad’, *Energy Procedia*, 114, pp. 1307–1324. Available at: https://doi.org/10.1016/j.egypro.2017.03.1899.

Fostås, B. *et al.* (2011) ‘Effects of NOx in the flue gas degradation of MEA’, *Energy Procedia*, 4, pp. 1566–1573. Available at: https://doi.org/10.1016/j.egypro.2011.02.026.

Fytianos, G., Vevelstad, S.J. and Knuutila, H.K. (2016) ‘Degradation and corrosion inhibitors for MEA-based CO2 capture plants’, *International Journal of Greenhouse Gas Control*, 50, pp. 240–247. Available at: https://doi.org/10.1016/j.ijggc.2016.05.003.

Gale, J. (2017) *Evaluating the Costs of Retrofitting CO2 Captured in an Integrated Oil Refinery: Technical Design Basis and Economic Assumptions*. IEA Greenhouse Gas R&D Programme. Available at: https://ieaghg.org/publications/technical-reports/reports-list/10-technical-reviews/923-2017-tr5-evaluating-the-costs-of-retrofitting-co2-captured-in-an-integrated-oil-refinery-technical-design-basis-and-economic-assumptions.

Gao, T. and Rochelle, G.T. (2022) ‘Creative absorber design and optimization for CO2 capture with aqueous piperazine’, *International Journal of Greenhouse Gas Control*, 113, p. 103534. Available at: https://doi.org/10.1016/j.ijggc.2021.103534.

General Electric (2016) *9HA.01 Sets Efficiency World Record*.

General Electric (2017) *9HA Power Plants - GEA32927*. GE-Power.

Giannaris, S. *et al.* (2021) 'SaskPower's Boundary Dam Unit 3 Carbon Capture Facility - The Journey to Achieving Reliability', *SSRN Electronic Journal* [Preprint]. Available at: https://doi.org/10.2139/ssrn.3820191.

Gibbions, J. and Lucquiaud, M. (2021) *BAT Review for New-Build and Retrofit Post-Combustion Carbon Dioxide Capture Using Amine-Based Technologies for Power and CHP Plants Fuelled by Gas and Biomass as an Emerging Technology under the IED for the UK*, *Best Available Techniques (BAT) information for CCS technologies*. https://ukccsrc.ac.uk: UKCCSRC. Available at: https://ukccsrc.ac.uk/best-available-techniques-bat-information-for-ccs/.

Global CCS Institute (2023) *Global Status of CCS 2023 – Report & Executive Summary*. Available at: https://www.globalccsinstitute.com/resources/publications-reports-research/global-status-of-ccs-2023-executive-summary/ (Accessed: 13 June 2024).

Goff, G.S. (2005) *Oxidative Degradation of Aqueous Monoethanolamine in CO2 Capture Processes: Iron and Copper Catalysis, Inhibition, and O2 Mass Transfer*. University of Texas. Available at: @inproceedings{Goff2005OxidativeDO, title={Oxidative degradation of aqueous monoethanolamine in CO_2 capture processes: iron and copper catalysis, inhibition, and O_2 mass transfer}, author={George Scott Goff}, year={2005}, url={https://api.semanticscholar.org/CorpusID:93451684} } (Accessed: 18 August 2024).

González Díaz, A. *et al.* (2016) 'Sequential supplementary firing in natural gas combined cycle with carbon capture: A technology option for Mexico for low-carbon electricity generation and CO 2 enhanced oil recovery', *International Journal of Greenhouse Gas Control*, 51, pp. 330–345. Available at: https://doi.org/10.1016/j.ijggc.2016.06.007.

gPROMS (2021) *gPROMS products: gPROMS PROCESSBUILDER [Internet]*. Available at: https://psenterprise.com/products/gproms/processbuilder.

Haldor Topsøe (2007) *BorsodChem MCHZ - 6,000 Nm3/h HTCR Topsoe Hydrogen Plant, A Case Story: 18 Months from Engineering to Operation*. The Organisation. Available at: https://www.readkong.com/page/borsodchem-mchz-czech-republic-6-000-nm3-h-htcr-tops-e-4132361 (Accessed: 18 August 2024).

Heap, R. *et al.* (2016) *Potential Role of Hydrogen in the UK Energy System*. Energy Research Partnership. Available at: https://erpuk.org/wp-content/uploads/2017/01/ERP-hydrogen-report-oct-2016.pdf.

Heidelberg Materials (2024) *Brevik CCS – World's first CO_2-capture facility in the cement industry*. Available at: https://www.brevikccs.com/en (Accessed: 13 June 2024).

Helgesen, L.I. and Gjernes, E. (2016) 'A Way of Qualifying Amine Based Capture Technologies with Respect to Health and Environmental Properties', *Energy Procedia*, 86, pp. 239–251. Available at: https://doi.org/10.1016/j.egypro.2016.01.025.

Herraiz, L. *et al.* (2018) 'Selective exhaust gas recirculation in combined cycle gas turbine power plants with post-combustion CO2 capture', *International Journal of Greenhouse Gas Control*, 71, pp. 303–321. Available at: https://doi.org/10.1016/j.ijggc.2018.01.017.

Herraiz, L. *et al.* (2020) 'Sequential Combustion in Steam Methane Reformers for Hydrogen and Power Production With CCUS in Decarbonized Industrial Clusters', *Frontiers in Energy Research*, 8(180). Available at: https://doi.org/10.3389/fenrg.2020.00180.

Høisæter, K. K., Vevelstad, S. J., Braakhuis, L., & Knuutila, H. K. (2022). Impact of solvent on the thermal stability of amines. *Industrial & Engineering Chemistry Research*. Available at: https://doi.org/10.1021/acs.iecr.2c01934

Intergovernmental Panel on Climate Change (IPCC) (2023a) *Climate Change 2021 – The Physical Science Basis*. Cambridge, United Kingdom and New York: Cambridge University Press. Available at: https://doi.org/10.1017/9781009157896.

Intergovernmental Panel on Climate Change (IPCC) (2023b) *Climate Change 2022 – Impacts, Adaptation and Vulnerability*. Cambridge, UK and New York: Cambridge University Press. Available at: https://doi.org/10.1017/9781009325844.

ION Clean Energy (2024) *How it Works*. Available at: https://www.ioncleanenergy.com/how-it-works (Accessed: 14 June 2024).

J. Murphy and S. Ferguson (2018) *Assessing the Cost Reduction Potential and Competitiveness of Novel (Next Generation) UK Carbon Capture Technology*, *Benchmarking State-of-the-art and Next Generation Technologies*. Amec Foster Wheeler Group. Available at:

https://assets.publishing.service.gov.uk/government/uploads/system/uploads/attachment_data/file/864688/BEIS_Final_Benchmarks_Report_Rev_4A.pdf.

Joffe, D. *et al.* (2018) *Hydrogen in a low-carbon economy*. Committee on Climate Change. Available at: http://www.theccc.org.uk/publications (Accessed: 18 August 2024).

Johnson, N., Parker, N. and Ogden, J. (2014) 'How negative can biofuels with CCS take us and at what cost? Refining the economic potential of biofuel production with CCS using spatially-explicit modeling', *Energy Procedia*, 63, pp. 6770–6791. Available at: https://doi.org/10.1016/j.egypro.2014.11.712.

Khakharia, P. *et al.* (2014) 'Acid Wash Scrubbing as a Countermeasure for Ammonia Emissions from a Postcombustion CO_2 Capture Plant', *Industrial & Engineering Chemistry Research*, 53(33), pp. 13195–13204. Available at: https://doi.org/10.1021/ie502045c.

Knuutila, H.K., Rennemo, R. and Ciftja, A.F. (2019) 'New solvent blends for post-combustion CO2 capture', *Green Energy & Environment*, 4(4), pp. 439–452. Available at: https://doi.org/10.1016/j.gee.2019.01.007.

Lindfeldt, E.G. and Westermark, M.O. (2009) 'Biofuel production with CCS as a strategy for creating a CO2 -neutral road transport sector', *Energy Procedia*, 1(1), pp. 4111–4118. Available at: https://doi.org/10.1016/j.egypro.2009.02.219.

Luterbacher, J. *et al.* (2021) *United in Science 2021*. Geneva. Available at: https://library.wmo.int/idurl/4/57608 (Accessed: 13 June 2024).

Mantripragada, H. C., Zhai, H., & Rubin, E. S. (2019). Boundary Dam or Petra Nova – Which is a better model for CCS energy supply? *International Journal of Greenhouse Gas Control*, *82*, 59–68. Available at: https://doi.org/10.1016/j.ijggc.2019.01.004

Martin, S. *et al.* (2012) 'New Amines for CO_2 Capture. IV. Degradation, Corrosion, and Quantitative Structure Property Relationship Model', *Industrial & Engineering Chemistry Research*, 51(18), pp. 6283–6289. Available at: https://doi.org/10.1021/ie2029877.

Matta, R.K., Mercer, G.D. and Tuthill, R.S. (2000) *Power Systems for the 21st Century - 'H' Gas Turbine Combined-Cycles, GER-3935B*. Schenectady: GE Power Systems.

Mayer, P. *et al.* (2023) 'Blue and green ammonia production: A techno-economic and life cycle assessment perspective', *iScience*, 26(8), p. 107389. Available at: https://doi.org/10.1016/j.isci.2023.107389.

MHI (2024) *CO_2 Capture Technology for Exhaust Gas KM CDR Process^{TM}*. Available at: https://solutions.mhi.com/ccus/co2-capture-technology-for-exhaust-gas-kmcdr-process/ (Accessed: 14 June 2024).

Michailos, S. and Gibbins, J. (2022) 'A Modelling Study of Post-Combustion Capture Plant Process Conditions to Facilitate 95–99% CO2 Capture Levels From Gas Turbine Flue Gases', *Frontiers in Energy Research*. 24 May 2022, 10. Available at: https://doi.org/10.3389/fenrg.2022.866838.

Moioli, S. *et al.* (2017) 'Pre-combustion CO2 Removal in IGCC Plant by MDEA Scrubbing: Modifications to the Process Flowsheet for Energy Saving', *Energy Procedia*, 114, pp. 2136–2145. Available at: https://doi.org/10.1016/j.egypro.2017.03.1349.

Morgan, J.C. *et al.* (2020) 'Development of a framework for sequential Bayesian design of experiments: Application to a pilot-scale solvent-based CO2 capture process', *Applied Energy*. March 2020, 262, p. 114533. Available at*: https://doi.org/10.1016/j.apenergy.2020.114533*.

Morgan, J. C., Chinen, A. S., Omell, B., Bhattacharyya, D., Tong, C., Miller, D. C., Buschle, B., & Lucquiaud, M. (2018). Development of a Rigorous Modeling Framework for Solvent-Based CO2 Capture. Part 2: Steady-State Validation and Uncertainty Quantification with Pilot Plant Data. *Industrial & Engineering Chemistry Research*, *57*(31), 10464–10481. Available at: https://doi.org/10.1021/acs.iecr.8b01472

Morken, A.K. *et al.* (2014) 'Emission Results of Amine Plant Operations from MEA Testing at the CO2 Technology Centre Mongstad', *Energy Procedia*, 63, pp. 6023–6038. Available at: https://doi.org/10.1016/j.egypro.2014.11.636.

Morken, A.K. *et al.* (2019) 'CO2 capture with monoethanolamine: Solvent management and environmental impacts during long term operation at the Technology Centre Mongstad (TCM)', *International Journal of Greenhouse Gas Control*, 82, pp. 175–183. Available at: https://doi.org/10.1016/j.ijggc.2018.12.018.

Moser, P., Wiechers, G., Van Os, P., Figueiredo, R. V., & Pinto, D. (2024). Demonstration of Highest Capture Rates for Deep Removal - Pilot Plant Test with CO2 Capture Rates from 98% to >99.9% with an AMP/PZ-Based Solvent. SSRN Electronic Journal. Available at: https://doi.org/10.2139/ssrn.5016144

Mukherjee, A., Bruijnincx, P. and Junginger, M. (2020) 'A Perspective on Biofuels Use and CCS for GHG Mitigation in the Marine Sector', *iScience*, 23(11), p. 101758. Available at: https://doi.org/10.1016/j.isci.2020.101758.

Mullen, D. *et al.* (2023) 'On the cost of zero carbon hydrogen: A techno-economic analysis of steam methane reforming with carbon capture and storage', *International Journal of Greenhouse Gas Control*. 10 May 2023, 126(103904), p. 103904. Available at: https://doi.org/10.1016/j.ijggc.2023.103904.

Mullen, D. and Lucquiaud, M. (2024) 'On the cost of zero carbon electricity: A techno-economic analysis of combined cycle gas turbines with post-combustion CO2 capture', *Energy Reports*. June 2024, 11, pp. 5104–5124. Available at: https://doi.org/10.1016/j.egyr.2024.04.067.

N.Borhani, T. and Wang, M. (2019a) 'Role of solvents in CO2 capture processes: The review of selection and design methods', *Renewable and Sustainable Energy Reviews*, 114, p. 109299. Available at: https://doi.org/10.1016/j.rser.2019.109299.

N.Borhani, T. and Wang, M. (2019b) 'Role of solvents in CO2 capture processes: The review of selection and design methods', *Renewable and Sustainable Energy Reviews*, 114, p. 109299. Available at: https://doi.org/10.1016/j.rser.2019.109299.

NZT (2024) *Net Zero Teesside Power*. Available at: https://www.netzeroteesside.co.uk/project/ (Accessed: 13 June 2024).

Olav Falk-Pedersen, M. *et al.* (2019) *CO2 Capture Facility at Kårstø, Norway: Front-End Engineering and Design (FEED) Study Report*. 1st edn. GASSNOVA.

Our world in data (2024) *Carbon dioxide concentrations in the atmosphere*. Available at: https://ourworldindata.org/grapher/co2-long-term-concentration?time=-63097..latest (Accessed: 13 June 2024).

Our World in Data (2024) *Electricity Mix*. Available at: https://ourworldindata.org/electricity-mix (Accessed: 13 June 2024).

Pathak, M. *et al.* (2023) 'Technical Summary', in *Climate Change 2022 - Mitigation of Climate Change*. Cambridge, UK and New York: Cambridge University Press, pp. 51–148. Available at: https://doi.org/10.1017/9781009157926.002.

Paulillo, A. *et al.* (2024) 'Decarbonising waste-to-energy: A life cycle assessment study', *Resources, Conservation and Recycling*, 209, p. 107812. Available at: https://doi.org/10.1016/j.resconrec.2024.107812.

Poynting, M. (2024) *BBC News - World's first year-long breach of key 1.5C warming limit*. Available at: https://www.bbc.co.uk/news/science-environment-68110310 (Accessed: 13 June 2024).

PubChem (2024) *N-Nitrosodimethylamine*. Available at: https://pubchem.ncbi.nlm.nih.gov/compound/n-nitrosodimethylamine (Accessed: 13 June 2024).

Rates, E. (2020) *US Dollar to British Pound Spot Exchange Rates for 2020 [Internet]*. Exchange Rates. Available at: https://www.exchangerates.org.uk/USD-GBP-spot-exchange-rates-history-2020.html.

Romano, M.C., Chiesa, P. and Lozza, G. (2010) 'Pre-combustion CO2 capture from natural gas power plants, with ATR and MDEA processes', *International Journal of Greenhouse Gas Control*, 4(5), pp. 785–797. Available at: https://doi.org/10.1016/j.ijggc.2010.04.015.

Sander, M.T. and Mariz, C.L. (1992) 'The Fluor Daniel® econamine FG process: Past experience and present day focus', *Energy Conversion and Management*, 33(5–8), pp. 341–348. Available at: https://doi.org/10.1016/0196-8904(92)90029-V.

Shell (2024) *CANSOLV CO_2 Capture System*. Available at: https://www.shell.com/business-customers/catalysts-technologies/licensed-technologies/emissions-standards/tail-gas-treatment-unit/cansolv-co2.html (Accessed: 14 June 2024).

Sinnott, R. and Towler, G. (2020) *Chemical Engineering Design*. 6th edn, *Chemical Engineering*. 6th edn. Elsevier. Available at: https://doi.org/10.1016/C2017-0-01555-0.

Sievert, K., Schmidt, T. S., & Steffen, B. (2024). Considering technology characteristics to project future costs of direct air capture. *Joule*, *8*(4), 979–999. Available at: https://doi.org/10.1016/j.joule.2024.02.005

Smith, R.W. *et al.* (2000) *Advanced Technology Combined Cycles, GER-3936A*. Schenectady: GE Power Systems. Available at: https://www.gevernova.com/content/dam/gepower-new/global/en_US/downloads/gas-new-

site/resources/reference/ger-3936a-advanced-technology-combined-cycles.pdf (Accessed: 18 August 2024).

Spath, P.L. and Mann, M.K. (2000) *Life Cycle Assessment of a Natural Gas Combined Cycle Power Generation System*. Golden, CO (United States): National Renewable Energy Laboratory. Available at: https://doi.org/10.2172/776930.

Spath, P.L. and Mann, M.K. (2001) *Life Cycle Assessment of Hydrogen Production via Natural Gas Steam Reforming*. Colorado: National Renewable Energy Laboratory. Available at: https://www.energy.gov/sites/default/files/2014/03/f12/27637.pdf.

Stark, C. *et al.* (2020) *The Sixth Carbon Budget: The UK's Path to Net Zero*, *UK Carbon Budgets*. Committee on Climate Change. Available at: https://www.theccc.org.uk/publication/sixth-carbon-budget/.

Su, D. *et al.* (2023) 'Thermal integration of waste to energy plants with Post-combustion CO2 capture', *Fuel*. 15 January 2023, 332, p. 126004. Available at: https://doi.org/10.1016/j.fuel.2022.126004.

Tata Chemicals (2024) 'Tata Chemicals Europe to build UK's first industrial scale carbon capture and utilisation plant with £16.7m investment'. Available at: https://www.tatachemicals.com/Europe/News-room/Press-release/tata-chemicals-europe-to-build-uk (Accessed: 13 June 2024).

Tian, S. *et al.* (2018) 'Inherent potential of steelmaking to contribute to decarbonisation targets via industrial carbon capture and storage', *Nature Communications*, 9(1), p. 4422. Available at: https://doi.org/10.1038/s41467-018-06886-8.

Udayappan, B. and Veawab, A. (2022) 'Performance analysis of methionine as an environmentally friendly corrosion inhibitor for carbon steel in the amine based carbon capture process', *International Journal of Greenhouse Gas Control*, 114, p. 103565. Available at: https://doi.org/10.1016/j.ijggc.2021.103565.

UK Gov (B) (2021a) *Hydrogen production costs 2021*. Department for Business, Energy & Industrial Strategy. Available at: https://www.gov.uk/government/publications/hydrogen-production-costs-2021.

UK Gov (C) (2021b) *Net Zero Strategy: Build Back Greener*. Available at: https://www.gov.uk/government/publications/net-zero-strategy#full-publication-update-history (Accessed: 18 August 2024).

UK Gov (D) (2021c) *UK Hydrogen Strategy*. London: Department for Business, Energy & Industrial Strategy. Available at: https://www.gov.uk/government/publications/uk-hydrogen-strategy.

UK Gov (A) (2022a) *Dispatchable Power Agreement business model summary*. Edited by E. and I.S. Department for Business. Department for Energy Security and Net Zero. Available at: https://assets.publishing.service.gov.uk/government/uploads/system/uploads/attachment_data/file/1117566/ccus-dispatchable-power-agreement-business-model-summary.pdf.

UK Gov (C) (2022b) *UK Low Carbon Hydrogen Standard*. Edited by E.& I.S. Department for Business. London: Crown copyright. Available at: https://www.gov.uk/government/publications/uk-low-carbon-hydrogen-standard-emissions-reporting-and-sustainability-criteria (Accessed: 30 May 2024).

UK Gov (D) (2023) *Carbon Capture, Usage and Storage: A Vision to Establish a Competitive Market*. Available at: https://www.gov.uk/government/publications/carbon-capture-usage-and-storage-a-vision-to-establish-a-competitive-market (Accessed: 13 June 2024).

UOP Honeywell (2024) *A PATH TO CARBON NEUTRALITY STARTS TODAY*. Available at: https://uop.honeywell.com/en/energy-transition/carbon-capture (Accessed: 14 June 2024).

Valente, A., Iribarren, D. and Dufour, J. (2017) 'Harmonised life-cycle global warming impact of renewable hydrogen', *Journal of Cleaner Production*, 149, pp. 762–772. Available at: https://doi.org/10.1016/j.jclepro.2017.02.163.

Vega, F. *et al.* (2020) 'Current status of CO2 chemical absorption research applied to CCS: Towards full deployment at industrial scale', *Applied Energy*, 260, p. 114313. Available at: https://doi.org/10.1016/j.apenergy.2019.114313.

Wanderley, R.R., Pinto, D.D.D. and Knuutila, H.K. (2021) 'From hybrid solvents to water-lean solvents – A critical and historical review', *Separation and Purification Technology*, 260, p. 118193. Available at: https://doi.org/10.1016/j.seppur.2020.118193.

Weir, H. *et al.* (2023) 'Impact of high capture rates and solvent and emission management strategies on the costs of full-scale post-combustion CO2 capture plants using long-term pilot

plant data', *International Journal of Greenhouse Gas Control*. 27 May 2023, 126, p. 103914. Available at: https://doi.org/10.1016/j.ijggc.2023.103914.

Yedinak, E.M. (2022) 'The Curious Case of Geologic Hydrogen: Assessing its Potential as a Near-Term Clean Energy Source', *Joule*, 6(3), pp. 503–508. Available at: https://doi.org/10.1016/j.joule.2022.01.005.

10. Appendix A – Chapter 5 Supporting information

gPROMs Model Parameters

Parameter	*Unit*	*Value*
GT		
Thermal efficiency	*%*	43.1
Compressor pressure ratio	-	1:23.5
Air flow rate	*kg/s*	783
Air/Fuel ratio	-	35.2
Fine filter ΔP	*Pa*	1000
Fuel inlet temperature	*^oC*	120
Fuel inlet pressure	*Bar*	42
Turbine inlet temperature (TIT)	*^oC*	1440
Turbine isentropic efficiency	*%*	90
Compressor isentropic efficiency	*%*	90
Mechanical Efficiency	*%*	99.9
Combustor ΔP	*%*	5
First stage Nozzle ΔT	*^oC*	44
First stage Turbine pressure ratio	-	2.1:1
Second stage Nozzle ΔT	*^oC*	13
Second stage Turbine pressure ratio	-	2.3:1
Third stage Nozzle ΔT	*^oC*	6
GT Exhaust pressure	*Bar*	1.033
GT Exhaust temperature	*^oC*	629
Flue Gas Heat Recovery		
HP Steam temperature	*^oC*	600
HP Turbine Inlet Pressure	*Bar*	186
Reheat Steam temperature	*^oC*	585
IP Turbine Inlet Pressure	*Bar*	41
LP Steam temperature	*^oC*	277
LP Turbine Inlet Pressure	*Bar*	3.7
Condenser pressure	*Bar*	0.045
CW water supply temperature	*^oC*	8
CW return temperature	*^oC*	25
CW supply pressure to condenser	*Bar*	3

HP, IP & LP Turbine isentropic efficiency	*%*	85
Pump isentropic efficiency	*%*	70
Generator efficiency	*%*	99
Condenser thermal efficiency	*%*	80
HRSG thermal efficiency	*%*	99.7
Economizer steam side ΔP	*%*	2
Superheat steam side ΔP	*%*	1
HRSG gas side ΔP (per tube bank)	*%*	0.11
Mechanical efficiency (Turbine)	*%*	99.7
Mechanical efficiency (Pump & Fan)	*%*	95
Minimum Pinch Temp	*^oC*	10
Booster fan Isentropic efficiency	*%*	85
Reforming Cycle		
Inlet Pressure	*Bar*	31
Steam temperature	*^oC*	500
PSA efficiency	*%*	90
Steam to Carbon Ratio	-	2.5
Reformer 1 T_{react}	*^oC*	913
WGSR T_{react}	*^oC*	420
Pre-Reformer T_{react}	*^oC*	500
Reformer unit ΔP	*%*	10
Natural Gas		
Methane	*% vol*	89.00
Ethane	*% vol*	7.00
Carbon Dioxide	*% vol*	2.00
Propane	*% vol*	1.00
Nitrogen	*% vol*	0.89
Butane	*% vol*	0.11

Economic Model Parameters

Parameter	Unit	Value
Discount rate (David Menmuir *et al.*, 2022)	%	7.8
Interest Rate (Elliott, 2022)	%	4.0
Productive lifetime (Collodi *et al.*, 2017)	Years	25
Base year	-	2023
Year operational	-	2026
Build Time (David Menmuir *et al.*, 2022)	Years	3 Years
CAPEX expenditure curve (Collodi *et al.*, 2017)	%	20/45/35
Load Factor (David Menmuir *et al.*, 2022)	%	85%
Transport and storage cost (J. Murphy and S. Ferguson, 2018)	£/tCO_2	19
Natural Gas Fuel price (David Menmuir *et al.*, 2022)	£/MWh	28
Chemical Engineering Plant Index (CEPCI) (Chemical Engineering, 2022)	-	816.3
International Construction Cost Index [Netherlands/UK/Texas] (Arcadis, 2020)	-	100/138/97
USD to GBP exchange rate (2023) (Rates, 2020)	£/$	0.82
Equipment Tax/Insurance/Freight (Donald, 2007; Elliott, 2022)	-	1.10
Civil Works factorial cost (Elliott *et al.*, 2018; Olav Falk-Pedersen *et al.*, 2019; Elliott, 2022)	-	1.21
Utilities factorial cost (Elliott *et al.*, 2018; Olav Falk-Pedersen *et al.*, 2019; Elliott, 2022)	-	1.18
Electrical factorial cost (Elliott *et al.*, 2018; Olav Falk-Pedersen *et al.*, 2019; Elliott, 2022)	-	1.30

Project management (Elliott *et al.*, 2018; Olav Falk-Pedersen *et al.*, 2019; Elliott, 2022)	-	1.21
Contractor Fee (Donald, 2007)	-	1.03
Project Contingency (Elliott *et al.*, 2018; Olav Falk-Pedersen *et al.*, 2019; Elliott, 2022)	-	1.10
Owners Costs (David Menmuir *et al.*, 2022)	-	1.07
Start-up & Spares (David Menmuir *et al.*, 2022)	-	1.05
Utility Connections (David Menmuir *et al.*, 2022)	-	1.01
Consulting Fee (David Menmuir *et al.*, 2022)	-	1.01
Maintenance (CCS) (J. Murphy and S. Ferguson, 2018)	%/Year	1.50
Labour (J. Murphy and S. Ferguson, 2018)	£/Employee/Year	69,810
Insurance/Tax/Admin (David Menmuir *et al.*, 2022)	%/Year	1.50
Regulatory (David Menmuir *et al.*, 2022)	-	1.02
MEA (Michailos and Gibbins, 2022)	£/t	940
Caustic (Gale, 2017)	£/t	34
Reclaimer disposal (Michailos and Gibbins, 2022)	£/t	500
Working Capital (J. Murphy and S. Ferguson, 2018)	-	1 Months Consumables

Performance of the CO_2 Capture plant

		95% Gross			100% Fossil		
Parameter	***Unit***	**SMR**	**CCGT**	**CCP**	**SMR**	**CCGT**	**CCP**
Flue Gas	Kg/s	525	792	848	550	792	848
CO_2 Concentration	% vol	19.9	4.9	16.3	19.4	4.9	16.3
O_2 Concentration	% vol	1	11	1	1	11	1
Absorber(s)	#	1	2	2	1	2	2
Diameter	*m*	17.0	11.3	14.0	17.0	11.4	14.0
Packing Stages	#	2	2	2	2	2	2
Packed Height	*m*	14	20	20	20	24	20
Stripper	#	1	1	1	1	1	1
Diameter	*m*	12.0	7.2	12.6	12.7	7.4	13.4
Packing Stages	#	2	2	2	2	2	2
Packed Height	*m*	16	20	20	16	20	20
Lean Loading	mol CO_2/mol MEA	0.16	0.10	0.10	0.16	0.10	0.10
Rich Loading	mol CO_2/mol MEA	0.47	0.46	0.49	0.47	0.44	0.46
Reboiler Temp	^oC	125	136	136	125	136	136
Reboiler Pressure	Kpa	210	275	275	210	275	275
CO_2 Captured	Kg/s	143	57.0	192	154	59.0	202
Specific Reboiler Duty	GJ/tCO_2	3.62	3.52	3.27	3.67	3.67	3.47
Reboiler Duty	MJ	516	200	628	566	217	701
L/G	Kg/kg	3.52	0.80	2.35	3.81	0.88	2.62